SEMI-DISTRIBUTED HYDROLOGIC MODELING STUDIES
IN
YUVACIK BASIN

A THESIS SUBMITTED TO
THE GRADUATE SCHOOL OF NATURAL AND APPLIED SCIENCES
OF
MIDDLE EAST TECHNICAL UNIVERSITY

BY

MUSTAFA KEMAL YENER

IN PARTIAL FULFILLMENT OF THE REQUIREMENTS FOR THE
DEGREE OF
MASTER OF SCIENCE
IN
CIVIL ENGINEERING

SEPTEMBER 2006

Approval of the Graduate School of Natural and Applied Sciences

Prof. Dr. Canan Özgen
Director

I certify that this thesis satisfies all the requirements as a thesis for the degree of Master of Science.

Prof. Dr. Erdal Çokça
Head of Department

This is to certify that we have read this thesis and that in our opinion it is fully adequate, in scope and quality, as a thesis for the degree of Master of Science.

Asist. Prof. Dr. Zuhal Akyürek	Prof. Dr. Ali Ünal Şorman
Co-Supervisor	Supervisor

Examining Committee Members

Assoc. Prof. Dr. Nuri Merzi (Chairman) (METU, CE)

Prof. Dr. Ali Ünal Şorman (METU, CE)

Prof. Dr. Vedat Toprak (METU, GE)

Assist. Prof. Dr. Zuhal Akyürek (METU, CE)

Assist. Prof. Dr. Aynur Şensoy (Anadolu Unv., CE)

I hereby declare that all information in this document has been obtained and presented in accordance with academic rules and ethical conduct. I also declare that, as required by these rules and conduct, I have fully cited and referenced all material and results that are not original to this work.

Name, Last name : Mustafa Kemal Yener

Signature :

ABSTRACT

SEMI-DISTRIBUTED HYDROLOGIC MODELING STUDIES IN YUVACIK BASIN

YENER, Mustafa Kemal
M. Sc., Department of Civil Engineering
Supervisor: Prof. Dr. Ali Ünal Şorman
Co-Supervisor: Asist. Prof. Dr. Zuhal Akyürek

September 2006, 178 pages

In this study, Yuvacık Basin, which is located in southeastern part of Marmara Region of Türkiye, is selected as the application basin and hydrologic modeling studies are performed for the basin. Basin is divided into three subbasins such as: Kirazdere, Kazandere, and Serindere and each subbasin is modeled with its own parameters. In subbasin and stream network delineation HEC-GeoHMS software is used and for the hydrologic modeling studies the new version of HEC-HMS hydrologic modeling software released in April 2006 is used.

Modeling studies consist of four items: event-based hourly simulations, snow period daily simulations, daily runoff forecast using numerical weather prediction data, and runoff scenarios using intensity-duration-frequency curves.

As a result of modeling studies, infiltration loss and baseflow parameters of each subbasin are calibrated with both hourly and daily simulations. Hourly parameters are used in spring, summer and fall seasons; daily parameters are used in late fall, winter and early spring (snowfall and snowmelt period) to predict runoff. Observed runoffs are compared with the forecasted runoffs that are obtained using MM5 grid data (precipitation and temperature) in the model. Goodness-of-fit between forecasted and observed runoffs is promising. Hence, the model can be used in real time runoff forecast studies. At last, runoffs that correspond to different return periods and probable maximum precipitation are predicted using intensity-duration-frequency data as input and frequency storm method of HEC-HMS. These runoffs can be used for flood control and flood damage estimation studies.

Keywords: HEC-HMS, HEC-GeoHMS, hydrologic modeling, MM5, snow modeling

ÖZ

YUVACIK HAVZASINDA
YARI-DAĞILIMLI HİDROLOJİK MODELLEME ÇALIŞMALARI

YENER, Mustafa Kemal
Yüksek Lisans, İnşaat Mühendisliği Bölümü
Tez Yöneticisi: Prof. Dr. Ali Ünal Şorman
Ortak Tez Yöneticisi: Yrd. Doç. Dr. Zuhal Akyürek

Eylül 2006, 178 sayfa

Bu çalışmada, uygulama havzası olarak Marmara Bölgesi'nin kuzeydoğusunda yer alan Yuvacık Havzası seçilmiş ve havza için hidrolojik modelleme çalışmaları gerçekleştirilmiştir. Havza Kirazdere, Kazandere ve Serindere gibi üç alt havzaya bölünmüş ve her bir alt havza kendi parametreleriyle modellenmiştir. Havza sınırlarının ve nehir hatlarının belirlenmesinde HEC-GeoHMS yazılımı kullanılmış ve hidrolojik modelleme çalışmalarında da Nisan 2006'da yeni sürümü çıkan HEC-HMS yazılımı kullanılmıştır.

Modelleme çalışmaları dört ana kısımdan oluşmaktadır: olay-temelli saatlik benzetimler, kar dönemi günlük benzetimler (simülasyonlar), sayısal hava tahmin verilerini kullanarak günlük akış tahminleri ve yağış-şiddet-tekerrür eğrilerinin kullanımıyla akış senaryolarının oluşturulması.

Modelleme çalışmalarının sonucunda, her bir alt havzanın sızma ve taban suyu parametreleri saatlik ve günlük benzetimler ile kalibre edilmiştir. Saatlik parametreler ilkbahar, yaz ve sonbahar mevsimlerinde; günlük parametreler ise sonbaharın sonu, kış ve ilkbahar başı gibi kar yağışı ve kar erimesinin gözlendiği dönemlerde akımın belirlenmesinde kullanılabilir. Modelde MM5 verisinin (yağış ve sıcaklık) girdi olarak kullanılmasıyla elde edilen tahmini akımlarla gözlenen akım değerleri karşılaştırılmıştır. Tahmini akımlarla gözlenen akımlar arasındaki uyum ümit vericidir. Bu nedenle, model gerçek zamanlı akım tahmin çalışmalarında kullanılabilir. Son olarak, değişik dönüş aralıklarına ve olası maksimum yağışa karşılık gelen akımlar, HEC-HMS programının “frequency storm” metodunda yağış-şiddet-tekerrür verileri girdi olarak kullanılarak bulunmuştur. Bu akımlar taşkın kontrolünde ve taşkın zararı tahminlerinde kullanılabilir.

Keywords: HEC-HMS, HEC-GeoHMS, hidrolojik modelleme, MM5, kar modellemesi

To my grandfather: Mustafa The Orphan,

My uncle: Kemal The Shoemaker,

and

My father: Kamil The Tailor…

ACKNOWLEDGEMENTS

I would especially like to thank to my mother, Perihan, whose love gave me the strength to cope with all kinds of difficulties that I faced throughout this thesis study.

I wish to express my deepest gratitude to Prof. Dr. Ali Ünal Şorman, my supervisor, for his invaluable encouragement and support. Without his guidance I could not have completed this thesis work.

I also wish my deepest gratitude to Assist. Prof. Dr. Zuhal Akyürek, my co-supervisor, for her continuous guidance.

I owe special thanks to Assist. Prof. Dr. Aynur Şensoy, my HEC-HMS modeling supervisor, for her kind helping, supervision and valuable suggestions.

I also owe special thanks to Assist. Prof. Dr. Ali Arda Şorman, my academic advisor, for his guidance during not only my thesis study period but also my undergraduate study period.

In addition, I would like to thank to my colleagues: Musa, for his endless support especially on geographic information systems softwares; and Gençer, for his kind advices.

The thanks are extended to Thames Water Türkiye personnel, especially to Mr. Hasan Akdemir, Mr. Tolga Gezgin, Mr. Sinan Çelebci and Mr. Türker Akgün, who provided data used in this study and organized the site trips to Yuvacık Basin.

Moreover, sincere thanks are extended to Government Organizations: General Directorate of State Hydraulic Works (DSI) for Hacıosman gage data, and State Meteorological Service (DMI) for Kocaeli gage data.

Finally, I would like to thank Prof. Dr. William Schaffenberg from US Army Corps of Engineers - Hydrologic Engineering Center, who supplied detailed information especially on snow module of the software via his emails.

TABLE OF CONTENTS

LIST OF TABLES

LIST OF FIGURES

CHAPTER 1

INTRODUCTION

1.1. Definition of the Problem

Water in the life of human beings is like a two sided medallion. In one side of the medallion the demand for water lies which includes domestic, industrial, agricultural and recreational use of water resources. The better these demands are satisfied (in both quantity and quality); the better a life on earth will a human being has. The problem about the first side of the medallion is that water is not always available in the desired quantity (e.g. droughts) and quality (e.g. pollutants). In the other side of the medallion, the undesired abundance of water (floods) lies. The problem about the second side of the medallion is that when water is uncontrollably abundant especially for short time periods, it causes loss of human lives and great damage to properties (cities, agricultural lands, etc.).

In today's world, it is the main objective of water resources engineers to produce feasible (practically, economically, etc.) solutions to these problems. From the dawn of ancient civilizations till today, water resources engineers have produced different solutions to overcome these problems (like wells, primitive conveyance systems, etc.), but only for the last couple of centuries these solutions are well-documented. The major part of the solutions of water resources engineering consists of appropriate management of basin and river systems.

Basin and river systems management include rainfall-runoff modeling studies. Rainfall-runoff models have been widely used through the last century to formulate a reliable relationship between the rainfall (input of the model) and runoff (output of the model). Engineers seek the answer to two important questions using rainfall-runoff models: what is the amount of water for a particular basin and when that amount of water will be available?

Türkiye, which is one of the most populated countries in Europe, deeply faces the two problems defined above (droughts and floods). Cities like İstanbul and İzmit are rapidly growing and water demand and disastrous effects of abundant water in these cities are increasing. Therefore, basin and river management systems including rainfall-runoff modeling has become a very important study area in Türkiye.

1.2. Purpose and Scope of the Study

Main purpose of this study is to apply a hydrologic model (i.e. rainfall-runoff model) to Yuvacık Basin and to calibrate model parameters. The calibrated model is then to be used as a decision support tool in the operation and management of Yuvacık Dam (located in the southeastern part of Marmara Region).

In the present study, HEC-HMS version 3.0.1, released by US Army Corps of Engineers, Hydrologic Engineering Center (USACE-HEC) in April 2006 is applied to Yuvacık Basin. The basin is not considered in a lumped form in modeling studies, in contrast, model parameters are distributed to three different subbasins: Kirazdere, Kazandere, and Serindere. Since gridded precipitation and parameter data is not used in the modeling studies, naming the model as "distributed" would not be correct; therefore, the model is named as "semi-distributed".

This study includes only hydrologic model application steps; operation and management studies of Yuvacık Dam are beyond the scope.

1.3. Organization of the Thesis

This thesis includes 8 chapters. The subject matter of chapters except “Introduction” is given as follows:

In Chapter 2, a brief literature survey on hydrologic modeling and some of the most popular hydrologic modeling software that are widely used in the recent years is given.

In Chapter 3, description of the two major software used in the study HEC-GeoHMS and HEC-HMS is given. Only introductory information is presented in this chapter. For further details, one may refer to the user’s manuals of this software.

Chapter 4 describes Yuvacık Basin in full details: its location, available hydrometeorological data in the basin, topography, etc. the preliminary work performed prior to modeling studies. Subbasin and river network delineation and subbasin characteristics determination are given in this chapter. In addition, classification of storm events is included in Chapter 4.

The subject of Chapter 5 is model simulations: event-based hourly simulations and snow-period daily simulations. Selected rainfall events for each subbasin are simulated to obtain runoff hydrographs at an hourly simulation time step. The detailed information about basin model, meteorologic model and control specifications of HEC-HMS software is given and model parameter calibrations are discussed in this chapter. Snow period daily simulation details are provided in this chapter. HEC-HMS snowmelt method input parameters; calibration and validation results are presented in this chapter.

Use of Numerical Weather Prediction data (MM5 data) in the model is presented in Chapter 6. For the year 2006, observed runoff data and runoff obtained from the model when MM5 data is used as input to the model are compared.

Chapter 7 mainly includes the performance evaluation of the constructed HEC-HMS model based on subcatchments of Yuvacık Basin under a given frequency storm. Intensity-duration-frequency data available for the basin and frequency storm method of HEC-HMS are presented in Section 7.2 and Section 7.3, respectively. Section 7.4 includes frequency storm simulation methodology and detailed simulation results.

Chapter 8, the last chapter of this thesis, lists the final discussions and conclusions about this study and recommendations for future studies.

CHAPTER 2

LITERATURE SURVEY

The main problem of applied hydrology is the determination of river flows given certain physical parameters such as rainfall, temperature, wind and catchment parameters. These flows are not only required for flood forecasting but also for prediction of the effects of proposed changes of the catchment and, in general, for water resources management. The processes which link rainfall with river flows are essentially deterministic, governed by physical laws which are reasonably well-known, but the boundary conditions (i.e., the physical description of the catchment and the initial conditions and distributions) make solution based on the direct application of the laws of physics impracticable. As a consequence the hydrologists have turned to empirical and analytical modeling of catchments (Raudkivi, 1979).

Hydrologic modeling goes back to the time of ancient Egyptians who measured river stages of Nile and made mathematical computations using sand box and pebbles. During the period of 1500-1800 AD, hydrologic computations based on experiments (e.g. Kepler, Bernoulli) and measurement techniques developed. In the nineteenth century, using improved calculation techniques theories developed (e.g. time of concentration concept and the rational method, groundwater flow theory). In the first part of twentieth century, new theories like Sherman's unit hydrograph theory (1932), Horton's infiltration theory (1933) is introduced in hydrological sciences. For a detailed historical review of hydrological computations one may refer to "Computer Simulation Techniques in Hydrology, (Fleming, 1975)".

The second part of twentieth century witnessed the advent of computer which revolutionized hydrology and made hydrologic analysis possible on a larger scale. Complex theories describing hydrologic processes become applicable using computer simulations, and vast quantities of observed data are reduced to summary statistics for better understanding of hydrologic phenomena (Chow, 1988).

Models take a variety of forms. ***Physical models*** are reduced-dimension representations of real world systems. A physical model of a watershed is a large surface with overhead sprinkling devices that simulate the precipitation input. The surface can be altered to simulate various land uses, soil types, surface slopes, and so on; and the rainfall rate can be controlled. The runoff can be measured, as the system is closed. ***Analog models*** represent the flow of water with the flow of electricity in a circuit. With those methods, the input is controlled by adjusting the amperage, and the output is measured with a voltmeter. ***Mathematical models*** includes an equation or a set of equations that represents the response of a hydrologic system component to a change in hydrometeorological conditions (USACE-HEC, March 2000).

Mathematical models may further be categorized as follows (Ford and Hamilton, 1996):

- *Event or continuous models* - an event model simulates a single storm. The duration of the storm may range from a few hours to a few days. A continuous model simulates a longer period (upto several years), predicting watershed response both during and between precipitation events.
- *Lumped or distributed models* - a distributed model is one in which spatial (geographic) variations of characteristics and processes are considered explicitly, while in a lumped model, these spatial variations are averaged or totally ignored.

- *Conceptual or empirical models* - a conceptual model is built upon a base of knowledge of the pertinent physical, chemical, and biological processes that act on the input to produce the output. An empirical model, on the other hand, is built upon observation of input and output.
- *Deterministic or stochastic model* - if all input, parameters, and processes in a model are considered free of random variation and known with certainty, then the model is a deterministic model. If instead the model describes the random variation and incorporates the description in the predictions of the output, the model is a stochastic model.
- *Measured-parameter or fitted-parameter models* - this distinction is critical in selecting models for application when observations of input and output are unavailable. A measured-parameter model is one in which model parameters can be determined from system properties, either by direct measurement or by indirect methods that are based upon the measurements. A fitted-parameter model, on the other hand, includes parameters that can not be measured. Instead, the parameters must be found by fitting the model with observed values of the input and the output.

There are many different reasons why we need to model the rainfall-runoff processes of hydrology. The main reason is, however, a result of the limitations of hydrological measurement techniques. We are not able to measure everything we would like to know about hydrological systems. We have, in fact, only a limited range of measurement techniques and a limited range of measurements in space and time. We therefore need a means of extrapolating from those available measurements in both space and time, particularly to ungaged catchments (where measurements are not available) and into the future (where measurements are not possible) to asses the likely impact of future hydrological change. Models of different types provide a means of quantitative extrapolation or prediction that will hopefully be helpful in decision-making (Beven, 2000).

The earliest of the computer-based hydrologic models was the Stanford Watershed Model (SWM) (Crawford and Linsley, 1966), cited commonly in hydrologic documents). Since 1960s till today, a large number of computer-based hydrologic models has been proposed. It would be impossible to list all the hydrologic models that are reported in the literature. Haan (1982) lists 75 models used for different purposes in “Hydrologic Modeling of Small Watersheds”, and Fleming (1975) lists 19 models in “Computer Simulation Techniques in Hydrology”.

In the last two decades, five of the most popular hydrologic modeling softwares are worth mentioning here:

- Watershed Modeling System (WMS): It is a comprehensive environment for hydrological analysis. It was developed by the Environmental Modeling Research Laboratory of Brigham Young University in cooperation with the US Army Corps of Engineers Waterways Experiment Station (WMS, User Manual, 2000).
- Snowmelt Runoff Model (SRM): It is referred to in the literature as the “Martinec Model”. It is developed by Martinec (1975), and is designed to simulate and forecast daily streamflow in mountain basins where snowmelt is a major runoff factor (SRM, User Manual, 1994).
- HBV model: It is developed in Sweeden (Bergström, 1976) and is a rainfall-runoff model, which includes conceptual numerical descriptions of hydrological processes at the catchment scale.
- MIKE model: It is a versatile and modular engineering tool for modeling conditions in rivers, lakes/reservoirs, irrigation canals and other inland water systems. It is designed by Danish Hydraulic Institute (DHI)(Mike 11 User’s Manual, 2004).
- HEC-HMS: It is a software package designed by US Army Corps of Engineers, Hydrologic Engineers Center (USACE-HEC) to simulate the precipitation-runoff processes of dendritic watershed systems. The new version of the program (HEC-HMS Version 3.0.1) is released in April

2006, and features a completely integrated work environment including a database, data entry utilities, computation engine, and results reporting tools. HEC-HMS is widely used in the world in rainfall-runoff modeling studies from HEC-1 to new versions: HEC-HMS 2x and 3x. For example, Şensoy (2003) applied HEC-1 package to Upper Karasu Basin in the eastern part of Türkiye. Daly et al. (2000) used HEC-HMS in a spatially distributed snow modeling study performed for Sacramento and San Joaquin basins in California. Anderson et al. (2002) coupled HEC-HMS with atmospheric models for prediction of watershed runoff in Calaveras River watershed in Northern California. HEC-HMS is used by Fleming and Neary (2004) in a continuous modeling study that is performed using the soil moisture accounting method. Cunderlik and Simonovic (2004) applied HEC-HMS in the Upper Thames River Basin study area. Hu et al. (2006) used HEC-HMS in a gridded snowmelt and rainfall-runoff hydrologic modeling study performed in Red River of the North Basin, USA.

CHAPTER 3

SOFTWARE USED IN THIS STUDY

3.1. Introduction

Mainly two software are used in this study. The first software is HEC-GeoHMS and the second one is HEC-HMS. HEC-GeoHMS is actually not a standalone computer software, rather it is a GIS add-in used in ARC View version 3.x software. However, HEC-HMS version 3.0.1 is a standalone hydrologic modeling computer software; written in Java programming language and released in April 2006 (the previous version 3.0.0 was released in November 2005).

The following two sections give only introductory information about this software. The author of this thesis does not intend to give all the details about the programs because such an effort would most probably end with a perfect copy of the user's manuals of the programs. Therefore, for those who are interested in the detailed explanations, please refer to the corresponding user's manuals.

Since some of the information given in the next two sections are partially -or sometimes unavoidably fully- compiled from the user's manuals, it would be better to give the full references here rather than attaching the reference information at the end of each paragraph. Finally, for HEC-GeoHMS software (Section 3.2) refer to "*Geospatial Hydrologic Modeling Extension HEC-GeoHMS Version 1.1 User's Manual*, USACE, Davis CA, December 2003"; for HEC-HMS software (Section 3.3) refer to "W. A. Scharffenberg and M. J. Fleming, *Hydrologic Modeling System Version 3.0.1 User's Manual,* USACE, Davis CA, April 2006".

3.2. Geospatial Hydrologic Modeling Extension (HEC-GeoHMS)

3.2.1 Overview

In recent years, advances in the Geographic Information Systems (GIS) have provided many opportunities for enhancing hydrologic modeling of watershed systems. The ability to perform spatial analysis for the development of lumped hydrologic parameters can not only save time and effort but also improve accuracy over traditional methods. In addition, hydrologic modeling has evolved to consider radar rainfall and advanced techniques for modeling the watershed on a grid level. Rainfall and infiltration are computed cell by cell providing greater detail than traditional lumped methods.

These advanced modeling techniques have become feasible because many time consuming data manipulations can now be generated efficiently with GIS spatial operations. For example, the ability to perform spatial overlays of information to compute lumped or grid-based parameters is crucial for computing basin parameters.

HEC-GeoHMS has been developed as a geospatial hydrology tool kit for engineers and hydrologists with limited GIS experience. The program allows users to visualize spatial information, document watershed conditions, perform spatial analysis, delineate subbasins and streams, construct inputs to hydrologic models, and assist with report preparation. Working with HEC-GeoHMS through its interfaces, menus, tools, buttons, and context-sensitive online help, in a windows environment, allows the user to expediently create hydrologic inputs that can be used directly with the Hydrologic Modeling System, HEC-HMS.

3.2.2. Technical Capabilities of HEC-GeoHMS

Version 1.1 of HEC-GeoHMS operates on digital elevation model (DEM) to derive subbasin delineation, stream segments, and to prepare a number of hydrologic inputs to HEC-HMS. The schematic representation of HEC-GeoHMS technical capabilities is shown in Figure 3.1.

3.2.2.1. Data management

GeoHMS performs a number of administrative tasks that help the user manage GIS data derived from the program. The data management feature tracks thematic GIS data layers and their names in a manner largely transparent to the user. Prior to performing a particular operation, the data manager will offer the appropriate thematic data inputs for operation, and prompt the user for confirmation. Other times, the data management feature manages the locations of various projects and also performs error checking and detection.

3.2.2.2. Terrain preprocessing

Using the terrain data (e.g. digital elevation model (DEM)) as input, the terrain preprocessing is a series of steps to derive the drainage networks. The steps consist of computing the flow direction, flow accumulation, stream definition, watershed delineation, watershed polygon processing, stream processing, and watershed aggregation. These steps can be done step by step or in a batch manner. Once these data sets are developed, they are used in later steps for subbasin and stream delineation. It is important to recognize that the watershed and stream delineation developed in the terrain preprocessing steps is preliminary. In the next step -basin processing- the user has the capability to delineate and edit basins in accordance with project specifications.

3.2.2.3. Basin processing

In this step, the user is provided with a variety of interactive and batch mode tools. Using these menu items and tools, it is possible to merge small subbasins into bigger subbasins, or vice versa, divide bigger subbasins into smaller ones. In addition, river segments can be merged into bigger segments and profiles of the rivers can be extracted.

3.2.2.4. Stream and watershed characteristics

When the stream and subbasins delineation have been finalized, their physical characteristics can be extracted. The stream physical characteristics, such as length, upstream and downstream elevations, and slope are extracted from the terrain data and stored as attributes in the stream table. Similarly, subbasin physical characteristics, such as centroid, longest flow lengths, centroidal flow lengths, and slopes are extracted from terrain data and stored as attributes in the watershed table.

3.2.2.5. Hydrologic parameter estimation

In addition to extracting stream and subbasin physical characteristics, the user has the option to estimate initial values of various hydrologic parameters. The estimated hydrologic parameters are subbasin curve number (for lumped models), ModClark grid curve number (for gridded models), Muskingum-Cunge routing parameters, subbasin time of concentration, and subbasin lag time. The other steps and parameters, such as ModClark Processing, Rainfall 2 Year, TR55 Flow Path Segments, TR55 Flow Path Segment Parameters, TR55 Export Tt to Excel, and Basin Slope, are intermediate steps for computing hydrologic parameters.

3.2.2.6. Hydrologic modeling system

HEC-GeoHMS develops a number of hydrologic inputs for HEC-HMS: background map file, lumped basin schematic file, grid cell parameter file, and distributed basin schematic model file. The steps GeoHMS follows to crate these files include automatic naming of reaches and subbasins, checking for errors in the basin and stream connectivity, and producing an HMS schematic.

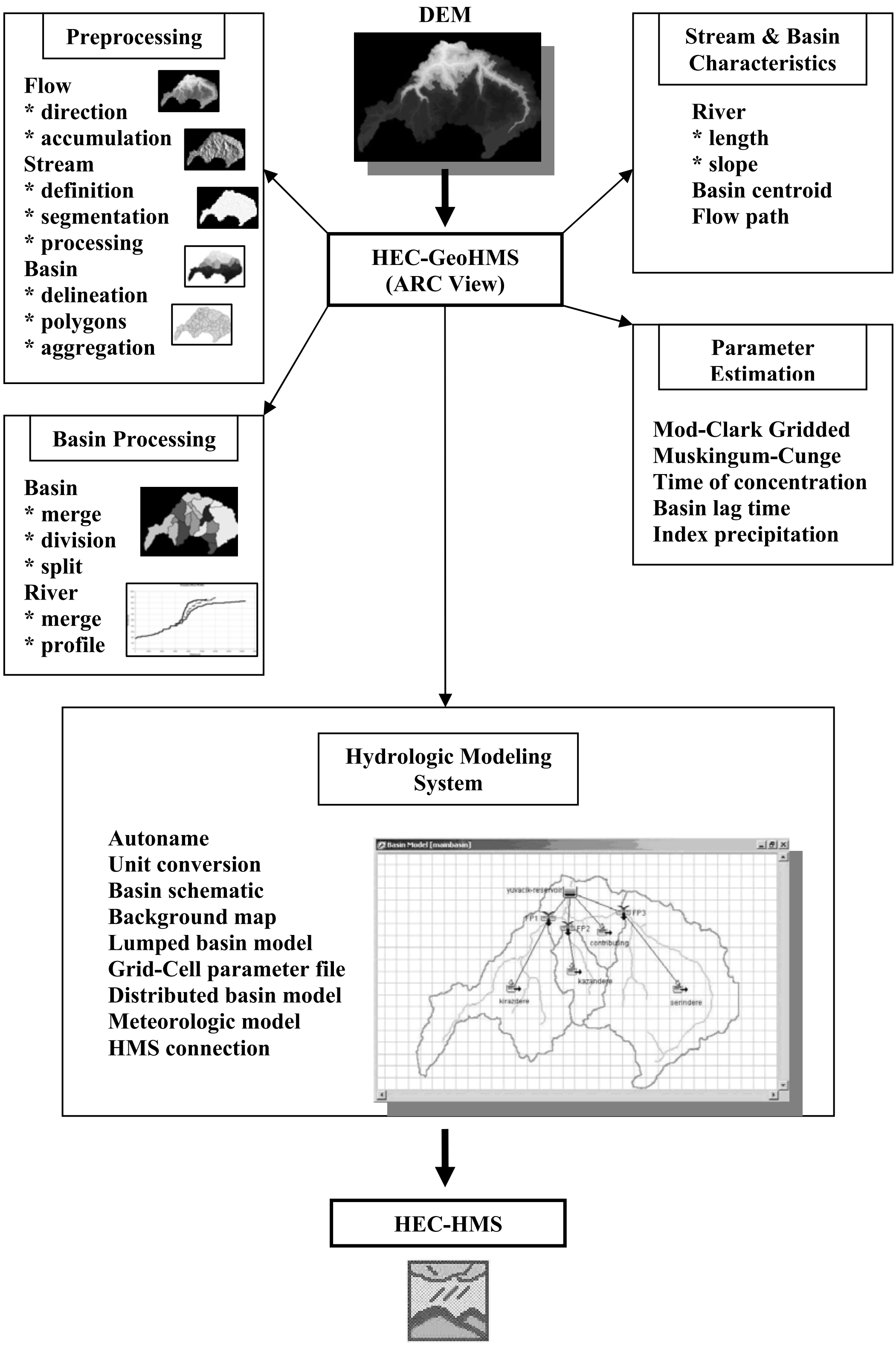

Figure 3.1. Schematic representation of HEC-GeoHMS capabilities

3.3. Hydrologic Modeling System (HEC-HMS)

3.3.1. Description

HEC-HMS (Hydrologic Modeling System) is a hydrologic modeling computer software developed by U.S. Army Corps of Engineers Hydrologic Engineering Center. It is designed to simulate the precipitation-runoff processes of dendritic (i.e. river network of the watershed is of a tree-like, branching form) watershed systems. It can either be used for large river watersheds or for small urban watersheds. Hydrographs that are produced by the program can be used for water availability, urban drainage, flow forecasting, future urbanization impact, reservoir spillway design, flood damage reduction, floodplain regulation, and systems operation studies.

3.3.2. History

The computation engine draws on over 30 years experience with hydrologic simulation software. Many algorithms from HEC-1 (HEC, 1998), HEC-1F (HEC, 1989), PRECIP (HEC, 1989), and HEC-IFH (HEC, 1992) have been modernized and combined with new algorithms to form a comprehensive library of simulation routines. Version 1.0 and Version 2.0 of the program were the two previous major releases of the program. These versions were written in C++ language, and the graphical libraries used in these versions are sold so they became publicly unavailable. To solve this problem (since U.S. Army Corps of Engineers Hydrologic Engineering Center publishes HEC-HMS software and its related documents without any charge) the design team developed new graphical libraries and a user interface and adapted old computation engine in the Java programming environment. Hence, the last major release Version 3.0 is created (Figure 3.2). The final release of the new version is issued in November 2005 but with oncoming bug reports from the beta testers of the software version 3.0.1 is released after a couple of months in April 2006. The author of this thesis was also a beta tester under the supervision of Prof. Dr. Ali Ünal Şorman, Dr. Aynur Şensoy, and Dr. Arda Şorman.

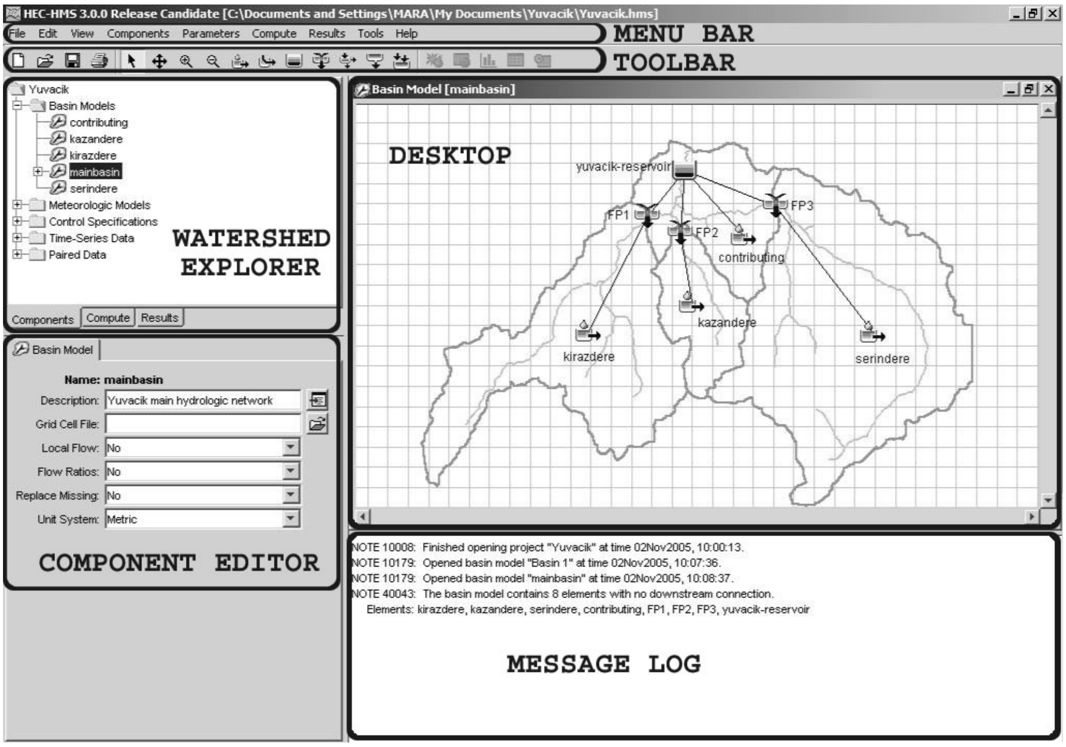

Figure 3.2. HEC-HMS 3.0.0 graphical user interface (GUI)

3.3.3. Capabilities

The program includes many of the well-known and well-applicable hydrologic methods to be used to simulate rainfall-runoff processes (Figure 3.3) in dendritic watersheds. The user of the program doesn't need to make cumbersome calculations but tries to select the most suitable methods for the watershed in consideration.

3.3.4. Watershed physical description (Basin model)

A dendritic network is set up by the user by using the available hydrologic elements (Table 3.1) such as subbasin, reach, junction, reservoir, diversion, source, and sink in the basin model to represent the related watershed physically. Runoff simulation computations proceed from upstream towards downstream direction.

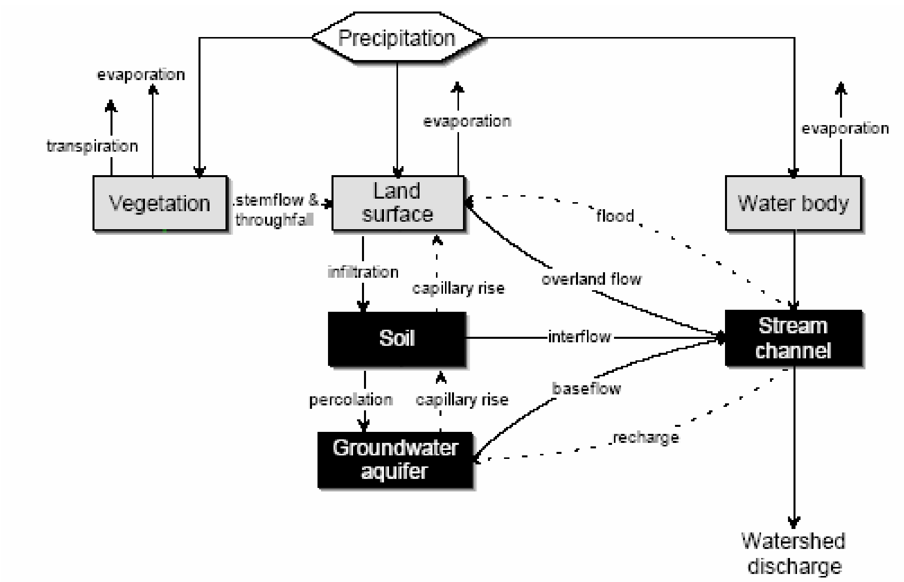

Figure 3.3. Systems diagram of the runoff process at local scale (after Ward, 1975)

Table 3.1. Available hydrologic elements in HEC-HMS

Hydrologic Element	Description
Subbasin	The subbasin element is used to represent the physical watershed. Given precipitation, outflow from the subbasin element is calculated by subtracting precipitation losses, transforming excess precipitation to stream flow at the subbasin outlet, and adding baseflow.
Reach	The reach element is used to convey stream flow downstream in the basin model. Inflow into the reach element can come from one or many upstream hydrologic elements. Outflow from the reach is calculated by accounting for translation and attenuation of the inflow hydrograph.
Junction	The junction element is used to combine stream flow from hydrologic elements located upstream of the junction element. Inflow into the junction element can come from one or many upstream elements. Outflow is simply calculated by summing all inflows and assuming no storage at the junction.
Source	The source element is used to introduce flow into the basin model. The source element has no inflow. Outflow from the source element is defined by the user.
Sink	The sink element is used to represent the outlet of the physical watershed. Inflow into the sink element can come from one or many upstream hydrologic elements. There is no outflow from the sink element.
Reservoir	The reservoir element is used to model the detention and attenuation of a hydrograph caused by a reservoir or detention pond. Inflow into the reservoir element can come from one or many upstream hydrologic elements. Outflow from the reservoir element can be calculated two ways. The user can enter a storage-outflow, elevation-storage-outflow, or elevation-area-outflow relationship, or the user can enter an elevation-storage or elevation-area relationship and define one or more outlet structures.
Diversion	The diversion element is used for modeling stream flow leaving the main channel. Inflow into the diversion element can come from one or many upstream hydrologic elements. Outflow from the diversion element consists of diverted flow and non-diverted flow. Diverted flow is calculated using input from the user. Both diverted and non-diverted flows can be connected to hydrologic elements downstream of the diversion element.

For infiltration loss computations the following methods are available: initial and constant, SCS curve number, gridded SCS curve number, exponential, Green and Ampt, one-layer deficit, five-layer soil moisture accounting, gridded deficit and constant, gridded SCS curve number and gridded soil moisture accounting.

For excess precipitation transformation computations the following methods are available: Clark, Snyder, and SCS unit hydrograph methods; user-specified unit hydrograph or s-graph ordinates; ModClark (with gridded meteorologic data), kinematic wave method (with multiple planes and channels).

For baseflow contribution to subbasin discharge computations the following methods are available: bounded recession, recession, constant monthly and linear reservoir.

For simulating flow in open channels the following hydrologic routing methods are available: kinematic wave lag, modified Puls, Muskingum-Cunge, and straddle stagger. Refer to Table 3.2 for available methods that are used for subbasin and reach elements.

Lakes are usually described by a user-entered storage-discharge relationship. Reservoirs can be simulated by describing the physical spillway and outlet structures. Pumps can also be included as necessary to simulate interior flood area. Control of the pumps can be linked to water depth in the collection pond and, optionally, the stage in the main channel.

Table 3.2. Available methods for subbasin and reach elements

Hydrologic Element	Calculation Type	Method
Subbasin	Runoff volume	Deficit and constant rate (DC)
		Exponential
		Green and Ampt
		Gridded DC
		Gridded SCS CN
		Gridded SMA
		Initial and constant rate
		SCS curve number (CN)
		Soil moisture accounting (SMA)
	Direct runoff	Clark's UH
		Kinematic wave
		ModClark
		SCS UH
		Snyder's UH
		User-specified s-graph
		User-specified unit hydrograph (UH)
	Baseflow	Bounded recession
		Constant monthly
		Linear reservoir
		Recession
Reach	Routing	Kinematic wave
		Lag
		Modified Puls
		Muskingum
		Muskingum-Cunge

3.3.5. Meteorology description (Meteorologic model)

Meteorologic data analysis is performed by the meteorologic model and includes precipitation, evapotranspiration, and snowmelt. Refer to Table 3.3 for available meteorological methods.

3.3.6. Control specifications

The time span of a hydrologic simulation in HEC-HMS is controlled by control specifications. Control specifications include a starting date and time, ending date and time, and a time interval. A simulation run is created by combining a basin model, meteorologic model, and control specifications. HEC-HMS presents the simulation results in the form of printable global and element summary tables that include peak flow, total volume and graphs.

Table 3.3. Meteorological methods available for describing meteorology

Meteorological Methods	Description
Precipitation	
Frequency storm	Used to develop a precipitation event where depths for various durations within the storm have a consistent exceedance probability.
Gage weights	User specified weights applied to precipitation gages.
Gridded precipitation	Allows the use of gridded precipitation products, such as NEXRAD radar.
Inverse distance	Calculates subbasin average precipitation by applying an inverse distance squared weighting with gages.
SCS storm	Applies a user specified SCS time distribution to a 24-hour total storm depth.
Specified hyetograph	Applies a user defined hyetograph to a specified subbasin element.
Standard project storm	Uses a time distribution to an index precipitation depth.
Evapotranspiration	
Gridded Priestley-Taylor	Evapotranspiration method that works with the gridded ModClark transform method
Monthly Average	Works with measured pan evaporation data
Priestley-Taylor	Implements the Priestley-Taylor equation for computing evapotranspiration
Snowmelt	
Gridded Temperature Index	Snowmelt method that works with the gridded ModClark transform method
Temperature Index	An extension of the degree-day approach to modeling a snowpack

3.3.7. Input data components

Time-series data, paired data, and gridded data (Table 3.4) are often required as parameter or boundary conditions in a basin and meteorologic modeling methods.

3.3.8. Parameter estimation

Most parameters for methods included in subbasin and reach elements can be estimated automatically using optimization trials. Observed discharge must be available for at least one element before optimization can begin. Parameters at any element upstream of the observed flow location can be estimated. Six different objective functions are available to estimate the goodness-of-fit between the computed results and observed discharge such as: peak weighted RMS error, percent error peak, percent error volume, sum absolute residuals, sum squared residuals, and time-weighted error. Two different search methods can be used to minimize the objective function such as: Nelder Mead and Univariate Gradient.

Table 3.4. Input data components

Time-Series Data	Paired Data	Gridded Data
Precipitation	Storage-outflow	Precipitation
Discharge	Elevation-storage	Temperature
Temperature	Elevation-area	Solar radiation
Solar radiation	Elevation-discharge	Crop coefficient
Crop coefficient	Inflow-diversion	Storage capacity
	Cross sections	Percolation rate
	Unit hydrograph curves	Storage coefficients
	Percentage curves	Moisture deficit
	ATI-meltrate functions	Impervious area
	ATI-coldrate functions	SCS curve number
	Groundmelt patterns	Elevation
	Evaporation patterns	Cold content
	Meltrate patterns	Cold content ATI
		Meltrate ATI
		Liquid water content
		Snow water equivalent

3.3.9. Analyzing simulations

Analysis tools are designed to work with simulation runs to provide additional information or processing. Currently the only tool is the depth-area analysis tool. It works with simulation runs that have a meteorologic model using the frequency storm precipitation method. Given a selection of elements, the tool automatically adjusts the storm area and generates peak flows represented by the correct storm areas.

3.3.10. GIS connection

The power and speed of the program make it possible to represent watersheds with hundreds of hydrologic elements. Traditionally these elements would be identified by inspecting a topographic map and manually identifying drainage boundaries. While this method is effective, it is prohibitively time consuming when the watershed will be represented with many elements. A geographic information system (GIS) can use elevation data and geometric algorithms to perform the same task much more quickly. A GIS companion product has been developed to aid in the creation of basin models for such projects. It is called the

Geospatial Hydrologic Modeling Extension (HEC-GeoHMS) and can be used to create basin and meteorologic models for use with the program.

3.3.11. Limitations

Every simulation system has limitations due to the choices made in the design and development of the software. The limitations that arise in this program are due to two aspects of the design: simplified model formulation, and simplified flow representation.

All of the mathematical models included in the program are deterministic. This means that the boundary conditions, initial conditions, and parameters of the models are assumed to be exactly known. All of the mathematical models included in the program use constant parameter values, that is, they are assumed to be time stationary. All of the mathematical models included in the program are uncoupled. The program first computes evapotranspiration and then computes infiltration. In the physical world, the amount of evapotranspiration depends on the amount of soil water. The amount of infiltration also depends on the amount of soil water. However, evapotranspiration removes water from the soil at the same time infiltration adds water to the soil.

CHAPTER 4

STUDY AREA AND PRELIMINARY DATA ANALYSIS

4.1. Description of study area

4.1.1. Location

Yuvacık basin is located in the east part of Marmara region of Türkiye, and approximately 20 km southeast of Kocaeli city center (Figure 4.1). The basin is in between 40º 30’ - 40º 41’ northern latitudes and 29º 48’ - 30º 08’ eastern longitudes. The basin, which has a drainage area of 257.86 km², is surrounded by the following settlements: İzmit and Gölcük towns in the north; Hacıosman village and İznik town in the southwest; Pamukova in the southeast and Kartepe (a famous ski center) in the northeast.

Yuvacık basin is a south to north oriented basin; streams originate from the southern parts of the basin and join together in the reservoir lake in the north of the basin. The reservoir lake has a 1.70 km² area and is about 12 km away from Kocaeli city.

4.1.2. Meteorological and streamflow data

Yuvacık Basin is still under development when data collection business is considered. Currently, there are a total number of 15 meteorological gages and 4 streamflow gages (i.e. flow plants) (Table 4.1), and the data of all these gages are used in this study.

Until the beginning of the new millennium governmental organizations like DSI and DMI, collected meteorological and streamflow data in the basin (actually, around the basin). For example, DSI operated a streamflow gage named as

Kirazdere (02-06) in the period of 1963-1992 in the outlet of the basin. In this gage, average daily runoff values were recorded, but this gage is no longer operational due to construction of Yuvacık Dam. DSI has a meteorologic gage at the southwestern part of the basin. This gage is named as Hacıosman (HO) taking its name from the village it is located in and daily precipitation and snow depth values have been recorded since 1980s and it is still operational (Figure 4.2). DMI operates one of the oldest meteorologic gages in the region: Kocaeli gage, located in Kocaeli city center and it has been in operation since 1930s. It collects daily precipitation, snow depth and temperature data (not shown in Figure 4.2).

After the year 1999, Thames Water Türkiye (TWT) private company undertook the operation of Yuvacık Dam and water treatment plant, and then installed new meteorological and streamflow gages in the basin (Figure 4.2) (Table 4.1). Starting from 2001 TWT has been collecting streamflow data every 5 minutes at 4 different locations (FP1 to FP4) in the basin, one of which is just at the entrance site of the reservoir lake, and the other three are at the outlets of three major stream branches of the basin. FP1 and FP3 have 2 different measurement devices, flow radar and ultrasonic. In addition, TWT has been collecting precipitation data at 6 different locations (from RG1 to RG6), again every 5 minutes.

In spring 2005, TWT started a study with the researchers from two universities (Middle East Technical University (METU), Anadolu University (AU)) on the subject “Hydrologic-Atmospheric Model Integration and Applications in Yuvacık Basin”. In the preliminary steps of the studies it is decided that six precipitation gages (RG1 to RG6) were far away from representing the spatial distribution of precipitation of the whole basin due to their locations and elevations (refer to Figure 4.2). Also these six gages (named as “old stations”) were incapable of recording snow depths. Therefore, it is decided to install new gages, new meteorologic stations that are capable of recording both precipitation data and snow depth data.

Figure 4.1. Location of Yuvacık Basin

Table 4.1. Summary station information of Yuvacık Basin

Organization *	Operation Start Year	Station ID	Station Name	Data Type **	Data Interval	Data Transmission ***	Elevation (m)
TWT	2001	FP1	Flow Plant 1	S	5 minutes	RF	185
TWT	2001	FP2	Flow Plant 2	S	5 minutes	RF	180
TWT	2001	FP3	Flow Plant 3	S	5 minutes	RF	200
TWT	2001	FP4	Flow Plant 4	S	5 minutes	RF	188
TWT	2001	RG1	Rain Gage 1	P	5 minutes	RF	188
TWT	2001	RG2	Rain Gage 2	P	5 minutes	RF	320
TWT	2001	RG3	Rain Gage 3	P	5 minutes	RF	460
TWT	2001	RG4	Rain Gage 4	P	5 minutes	RF	520
TWT	2001	RG5	Rain Gage 5	P	5 minutes	RF	265
TWT	2001	RG6	Rain Gage 6	P	5 minutes	RF	173
TWT	2006	RG7	Tepecik	P, SD, T, RH	5 minutes Daily	GSM	700
TWT	2006	RG8	Aytepe	P, SD, T, RH	5 minutes Daily	GSM	953
TWT	2006	RG9	Kartepe	P, SD, T, RH	5 minutes Daily	GSM	1487
TWT	2006	RG10	Çilekli	P, SD, T, RH	5 minutes Daily	GSM	805
TWT	2006	M1	Kazandere	P, SD, T, RH	5 minutes Daily	M	732
TWT	2006	M2	Menekşe Yaylası	P, SD, T, RH	5 minutes Daily	M	915
TWT	2006	M3	Arif Tarı	P, SD, T, RH	5 minutes Daily	M	546
DSI	1980s	HO	Hacıosman	P, SD	Daily	M	900
DMI	1930s	KE	Kocaeli	P, SD, T	Daily	M	76

* TWT: Thames Water Türkiye, DSI: State Hydraulic Works, DMI: State Meteorological Service
** S: streamflow depth, P: precipitation, SD: snow depth, T: temperature, RH: relative humidity
*** RF: Radio frequency, GSM: cellular phone communication network, M: Manual

At the end of 2005 seven "new stations" comprising of four "fixed" stations (RG7 to RG10) that transmit the collected data using GSM network, and three "mobile" stations (M1, M2, and M3) that can not transmit data automatically, but the operator has to go to site and download the data from the data logger of the station. These seven stations started operation at the very beginning of 2006. In near future (at least after one water year), some of the "mobile" stations may be turned into "fixed" stations if they are found to be representative of the basin. Some of the "old stations" will be disassembled from their current places and moved out of the basin and reassembled in several of the northwest settlements like İzmit, Gölcük. These reassembled gages may be used to detect the storms coming from The Balkans (northwest of Türkiye) in order to take action before the storm reaches the basin.

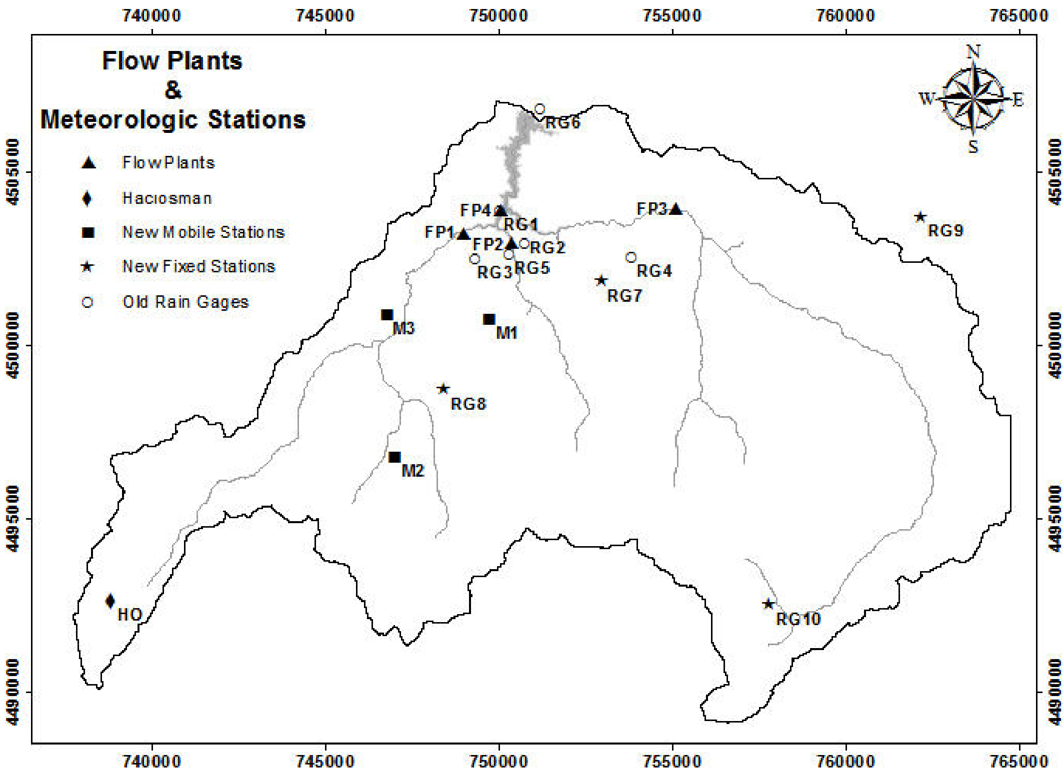

Figure 4.2. Stream gages and meteorologic stations in Yuvacık Basin

4.1.3. Topography

Yuvacık Basin is mainly composed of deep valleys originating in the south and with almost parallel flowing streams ending up in the north regions of the basin. There are three major valleys, and correspondingly, three major stream branches which can be named as Kirazdere, Kazandere, and Serindere, respectively from west to east of the basin. The northern parts of the basin (around the reservoir lake) have the smaller elevations than the southern parts as can be seen from the digital elevation model (DEM) of the basin (Figure 4.3). The DEM of the basin is generated using 1/25000 scale topographical maps with 10x10 meters grid size. The minimum elevation of the basin is 75.5 meters, the maximum elevation is 1547 meters and the mean elevation is 848 meters. Elevation classes (per 200 meters) and corresponding percent areas of the basin are given in Table 4.2. The lower (75-200 meters) and the upper (1400-1547) elevation classes contain only very little portion of the basin: 1.14 % and 0.47 %, respectively. The majority of the basin (73.4%) is within 600 to 1200 meters.

To give a better idea about the elevation of the basin, hypsometric curve of the basin is given in Figure 4.4. *Hypsometric mean elevation* of the basin, that is to say, median elevation of the basin is 889 meters and it is not much different from the mean elevation.

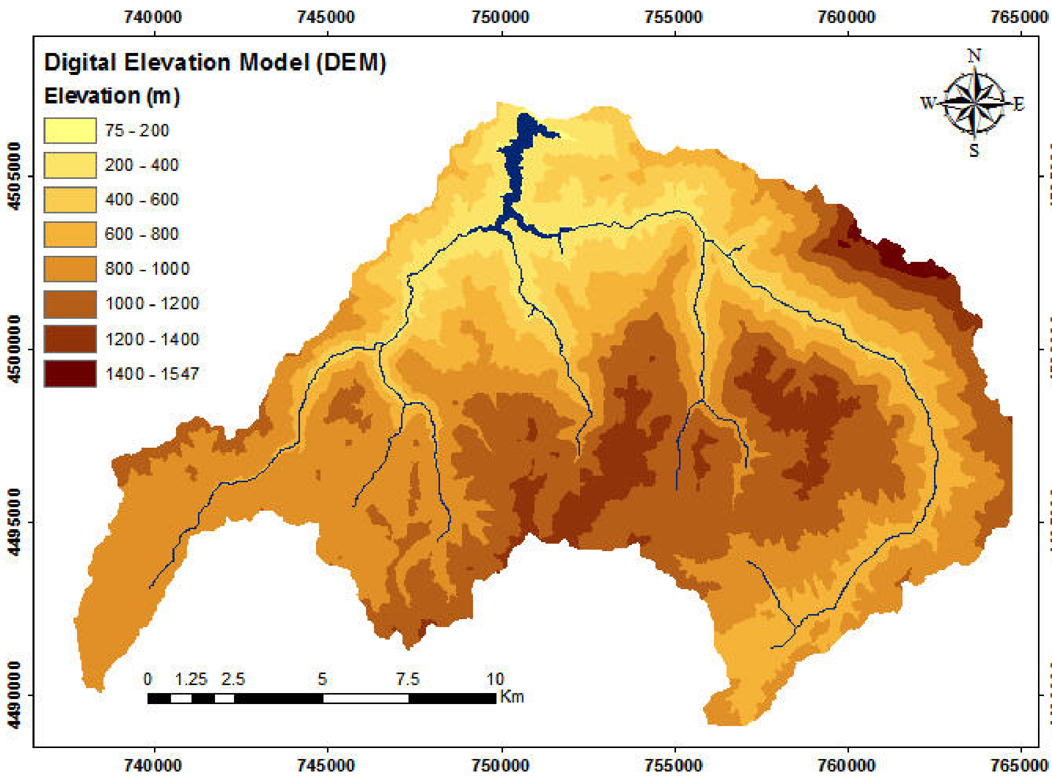

Figure 4.3. Digital elevation model (DEM) of Yuvacık Basin

Table 4.2. Yuvacık Basin elevation classes and corresponding areas

Elevation (m)	Area (km²)	Area (%)
75 - 200	2.939	1.14
200 - 400	18.092	7.02
400 - 600	29.493	11.44
600 - 800	45.049	17.47
800 - 1000	81.692	31.68
1000 - 1200	62.580	24.27
1200 - 1400	16.810	6.52
1400 - 1547	1.204	0.47
Total	**257.86**	**100.0**

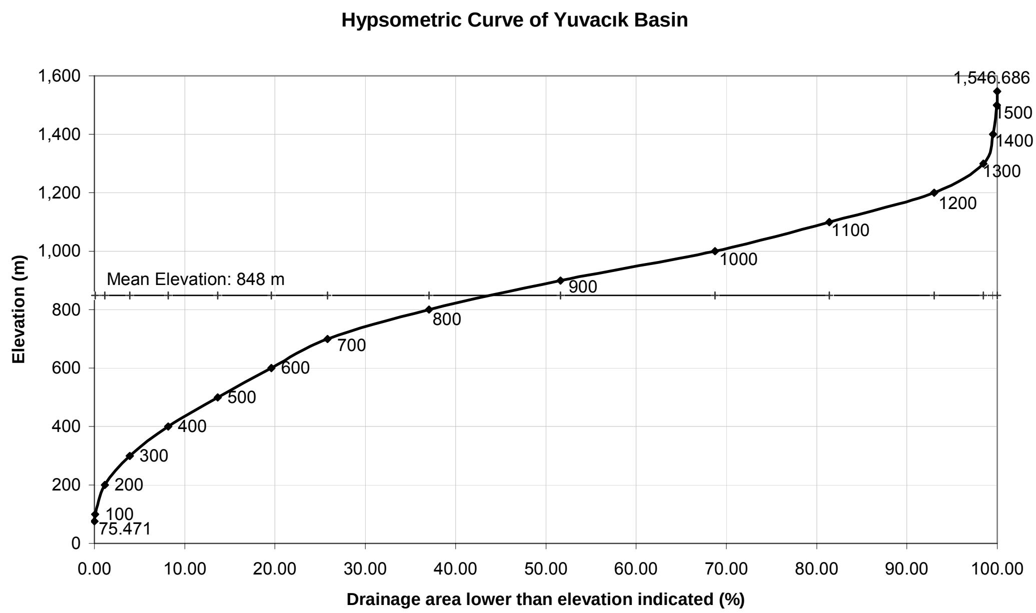

Figure 4.4. Hypsometric curve of Yuvacık Basin

Almost 70% of Yuvacık Basin has a slope greater than 15 degrees, and more than 15% of the basin has slopes greater than 30 degrees (Table 4.3). Nearly one third of the basin has slopes between 0 and 15 degrees. Steep regions (slopes more than 15 degrees) are generally accumulated around the stream branches (Figure 4.5).

Table 4.3. Yuvacık Basin slope classes and corresponding areas

Slope (degrees)	Area (km^2)	Area (%)
0 - 15	82.098	31.84
15 - 30	133.600	51.81
30 - 45	39.153	15.18
45 - 60	2.984	1.16
60 - 64.5	0.025	0.01
Total	**257.86**	**100.0**

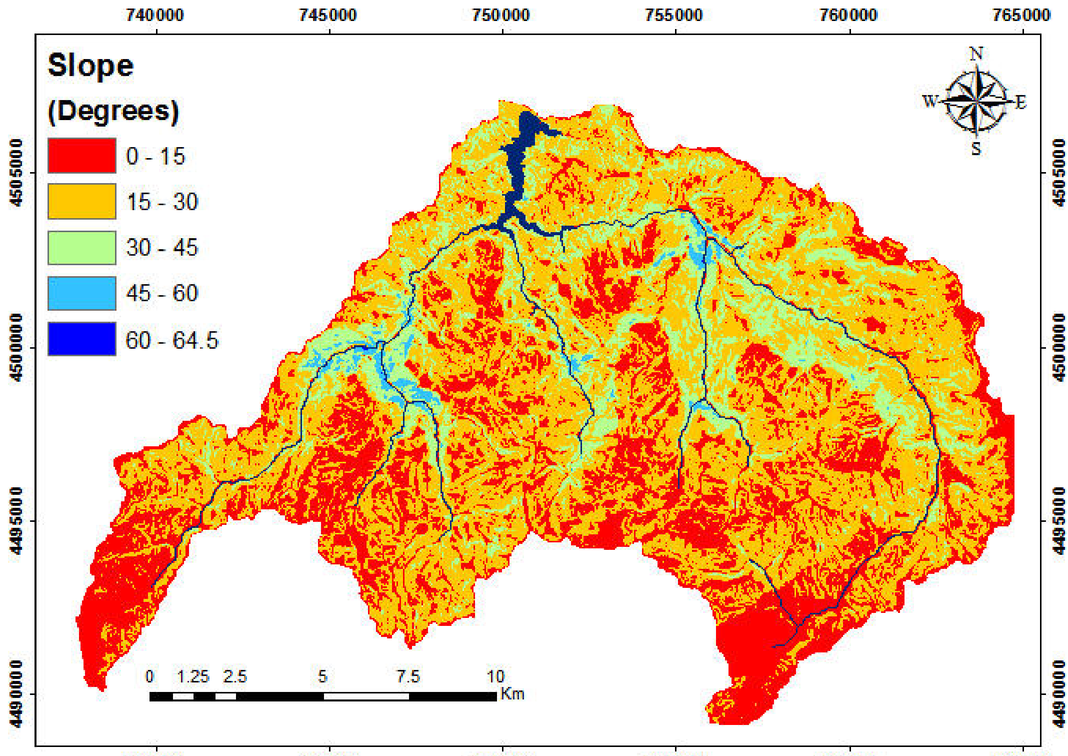

Figure 4.5. Slope map of Yuvacık Basin

In Table 4.4 aspect classes of Yuvacık Basin and the areas corresponding to each aspect class are given. As can be observed from the given table, 10.38% of the basin faces north and 11% of the basin faces south. The portion of the basin facing west is 14.22% and facing east is 13.1%. The aspect map of the basin is given in Figure 4.6.

Table 4.4. Yuvacık Basin aspect classes and corresponding areas

Aspect	Area (km²)	Area (%)
North (0 - 22.5)	13.63	5.28
Northeast (22.5 - 67.5)	33.78	13.10
East (67.5 - 112.5)	33.62	13.04
Southeast (112.5 - 157.5)	30.56	11.85
South (157.5 - 202.5)	28.32	10.98
Southwest (202.5 - 247.5)	34.99	13.57
West (247.5 - 292.5)	36.66	14.22
Northwest (292.5 - 337.5)	33.17	12.86
North (337.5 - 360)	13.14	5.10
Total	**257.86**	**100.0**

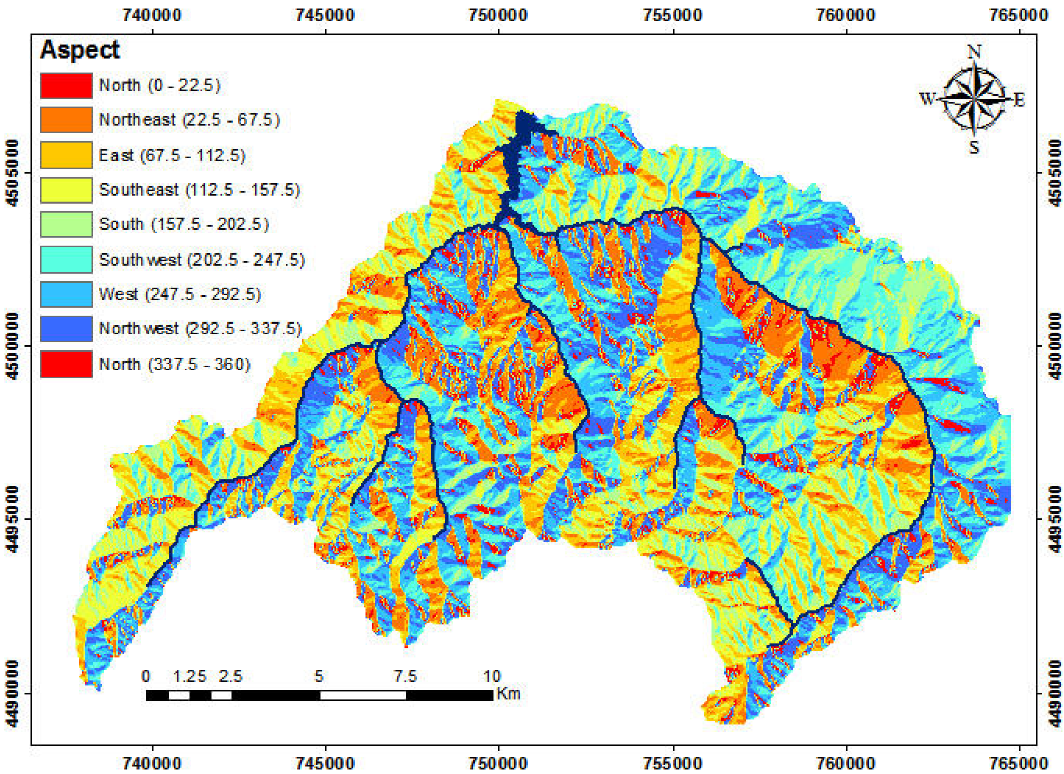

Figure 4.6. Aspect map of Yuvacık Basin

4.1.4. Rock Units

Yuvacık Basin is mainly composed of shale (31% of the basin) and andesite and basalt rock types (20.38%) (Table 4.5). Also, there are a number of marble areas (14.2%) spread to different parts of the basin as shown in Figure 4.7.

Table 4.5. Yuvacık Basin geologic formation classes and corresponding areas

Geologic Formations	Area (km²)	Area (%)
Alluvium	5.89	2.28
Andesite-Basalt	52.56	20.38
Dolomite-Limestone	8.88	3.44
Limestone-Marl	23.19	8.99
Marble	36.63	14.20
Ophiolite	15.08	5.85
Melange	11.89	4.61
Shale	79.80	30.95
Schist-Marble	23.94	9.28
Total	**257.86**	**100.0**

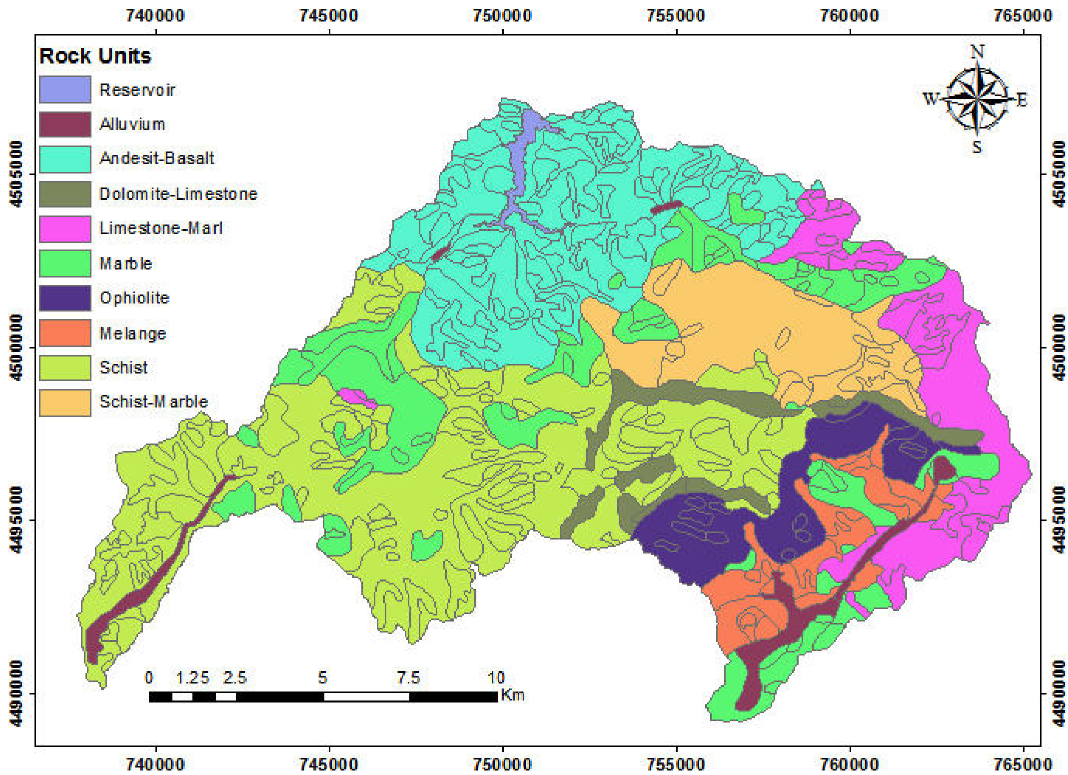

Figure 4.7. Geology map of Yuvacık Basin (Source: PRI, 2005)

4.1.5. Land use

Three major land use classes are present for Yuvacık Basin: forests, agricultural lands, and pasture lands. Forests form 78.45% of the basin, and are sub-classified as "bad" and "good" forests (Table 4.6). Agricultural lands form 16.85% of the basin and 70% of total agricultural lands are cultivated. Pasture lands constitute 3.57% of the basin. In addition, in a very little portion of the basin (only 0.47%) poplar and nut trees are grown. Reservoir is also shown as a land use class in land use map of the basin constituting 0.60% of the basin (Figure 4.8).

Table 4.6. Yuvacık Basin land use classes and corresponding areas

Land use classes	Area (km^2)	Area (%)
Bad Forest (10-40% Closed)	36.56	14.18
Good Forest (40-70% Closed)	64.23	24.91
Good Forest (70-100% Closed)	101.51	39.37
Cultivated	30.57	11.86
Not Cultivated	12.88	4.99
Good Pasture	7.38	2.86
Bad Pasture	1.82	0.71
Poplar - Nut	1.21	0.47
Reservoir	1.70	0.66
Total	**257.86**	**100.0**

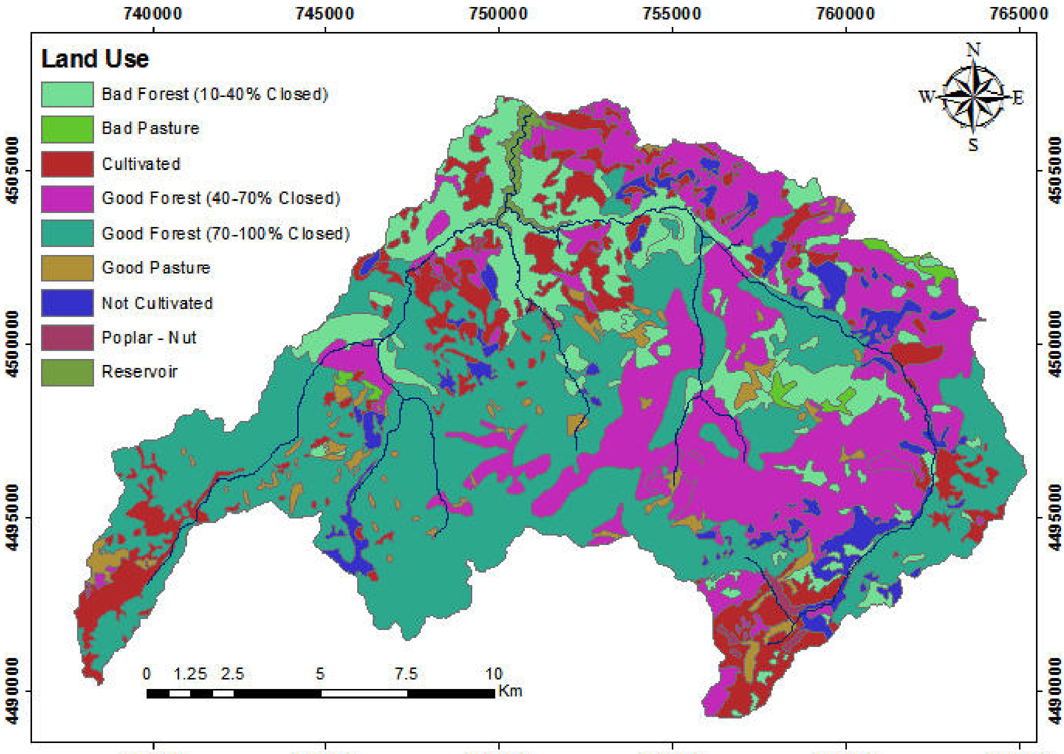

Figure 4.8. Land use map of Yuvacık Basin (Source: PRI, 2005)

4.2. Basin preprocessing

Using the digital elevation model (DEM) (Figure 4.3) of the basin as input, the terrain preprocessing is a series of steps performed in HEC-GeoHMS to derive the drainage networks. The steps consist of computing the flow direction, flow accumulation, stream definition, watershed delineation, watershed polygon processing, stream processing, and watershed aggregation. Once these data sets are developed, they are used in later steps for subbasin and stream delineation. Terrain preprocessing is performed in the ***MainView*** document.

4.2.1. Depressionless DEM (Fill sinks)

The depressionless DEM is created by filling the depressions or pits by increasing the elevation of the pit cells to the level of the surrounding terrain in order to determine flow directions. The steps to fill the depressions are shown below:

- Select **Terrain Preprocessing → Fill Sinks**
- Input of the **RawDEM** should be **DEM of the basin**, the output of the **HydroDEM** is the **fillgrid (Figure 4.9)**.

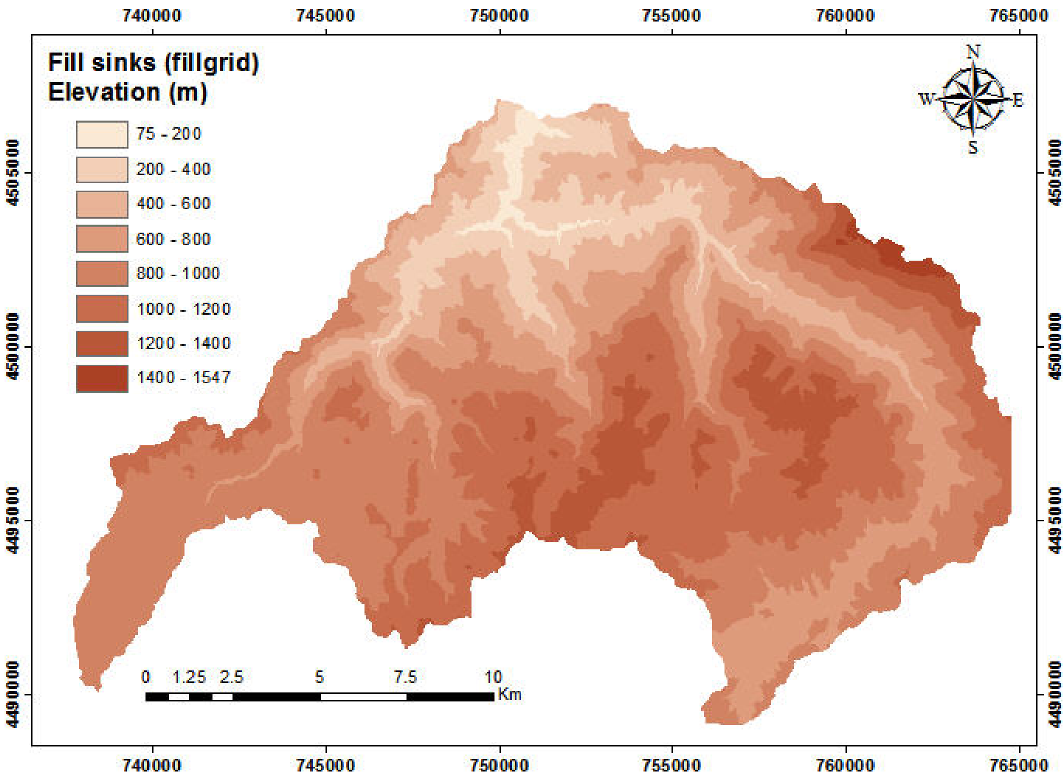

Figure 4.9. Fill sinks

4.2.2. Flow direction

This step defines the direction of the steepest descent for each terrain cell. Similar to a compass, the eight-point pour algorithm specifies the following eight possible directions such as: 1(east), 2(southeast), 4(south), 8(southwest), 16(west), 32(northwest), 64(north), and 128(northeast). The steps to compute flow directions are shown below:

- Select **Terrain Preprocessing → Flow Direction**
- Input of the **HydroDEM** is **fillgrid.**
- Output of the **FlowDirGrid** is **fdirgrid (Figure 4.10).**

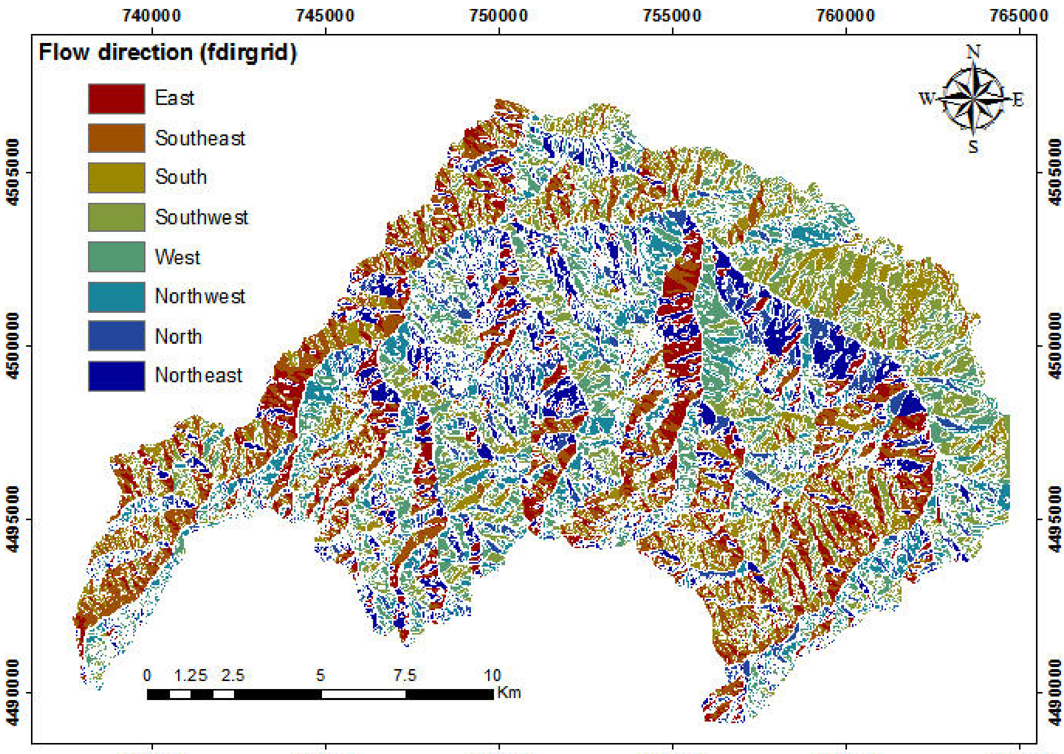

Figure 4.10. Flow direction

4.2.3. Flow accumulation

This step determines the number of upstream cells draining to a given cell. Upstream drainage area at a given cell can be calculated by multiplying the flow accumulation value by the cell area. The steps to compute flow accumulation are shown below:

- Select **Terrain Preprocessing → Flow Accumulation**.
- Input of the **FlowDirGrid** is **fdirgrid**, the output of the **FlowAccGrid** is **faccgrid (Figure 4.11)**.

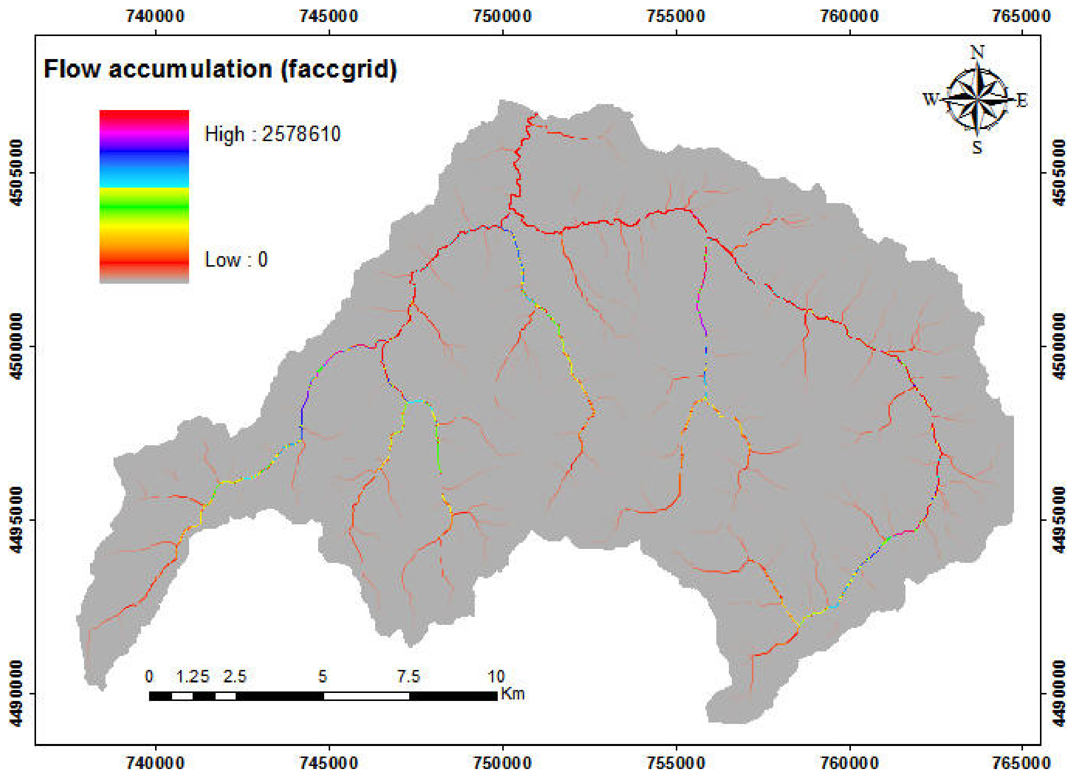

Figure 4.11. Flow accumulation

4.2.4. Stream definition

This step classifies all cells with flow accumulation greater than the user-defined threshold as cells belonging to the stream network. Typically, cells with high flow accumulation, greater than a user-defined threshold value, are considered part of a stream network. The user-specified threshold may be specified as an area in distance units squared, e.g., square miles, or as a number of cells. The flow accumulation for a particular cell must exceed the user defined threshold for a stream to be initiated. The default is one percent (1%) of the largest drainage area in the entire basin. The smaller the threshold chosen, the greater the number of subbasins delineated by Geo-HMS.

The steps to compute stream definition are shown below:

- Select **View → Properties**

- Specify the **Map Units** as **meters**
- Specify the **Distance Units** as **kilometers**
- Select **Terrain Preprocessing → Stream Definition**
- Input of the **FlowAccGrid** is **faccgrid**, the output of the **StreamGrid** is **strgrid** **(Figure 4.12).**
- Select the **threshold type** as **Area in Distance Units squared.**
- Enter the threshold for stream initiation at **1** square kilometers

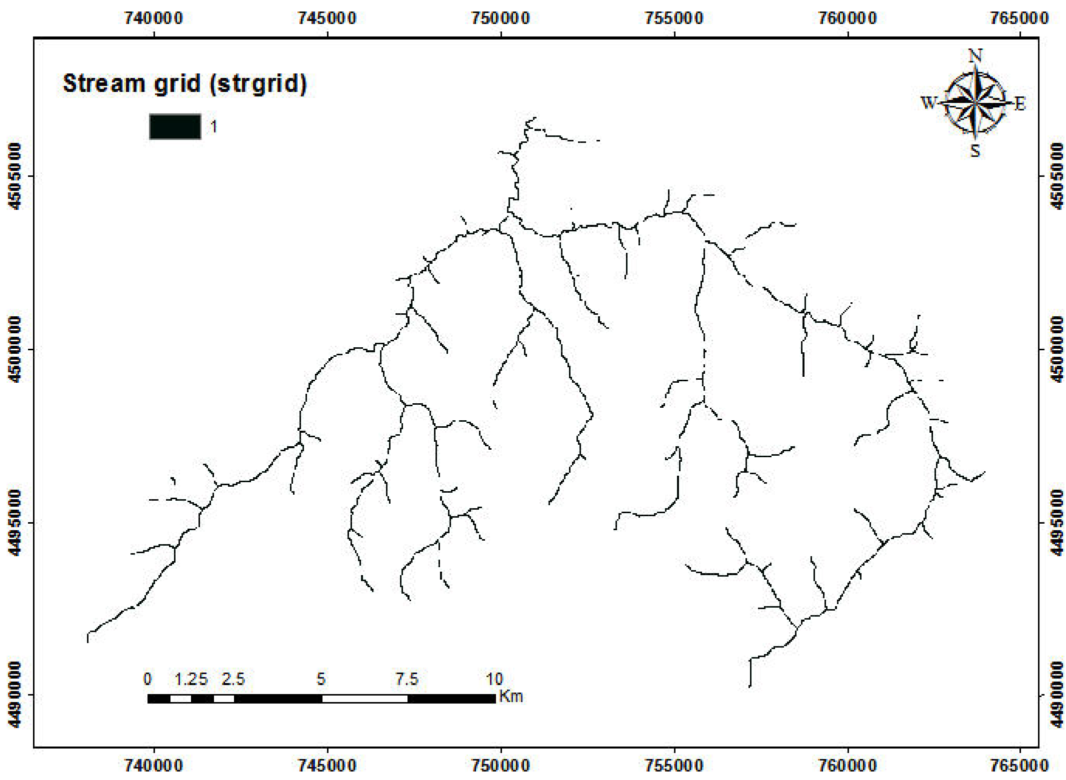

Figure 4.12. Stream definition

4.2.5. Stream segmentation

This step divides the stream into segments. Stream segments or links are the sections of a stream that connect two successive junctions, a junction and an outlet, or a junction and the drainage divide. The steps to compute flow segmentation are shown below:

- Select **Terrain Preprocessing → Stream Segmentation**
- Input of the **FlowDirGrid** is **fdirgrid**, and the output of the **LinkGrid** is **strlnkgrid (Figure 4.13).**

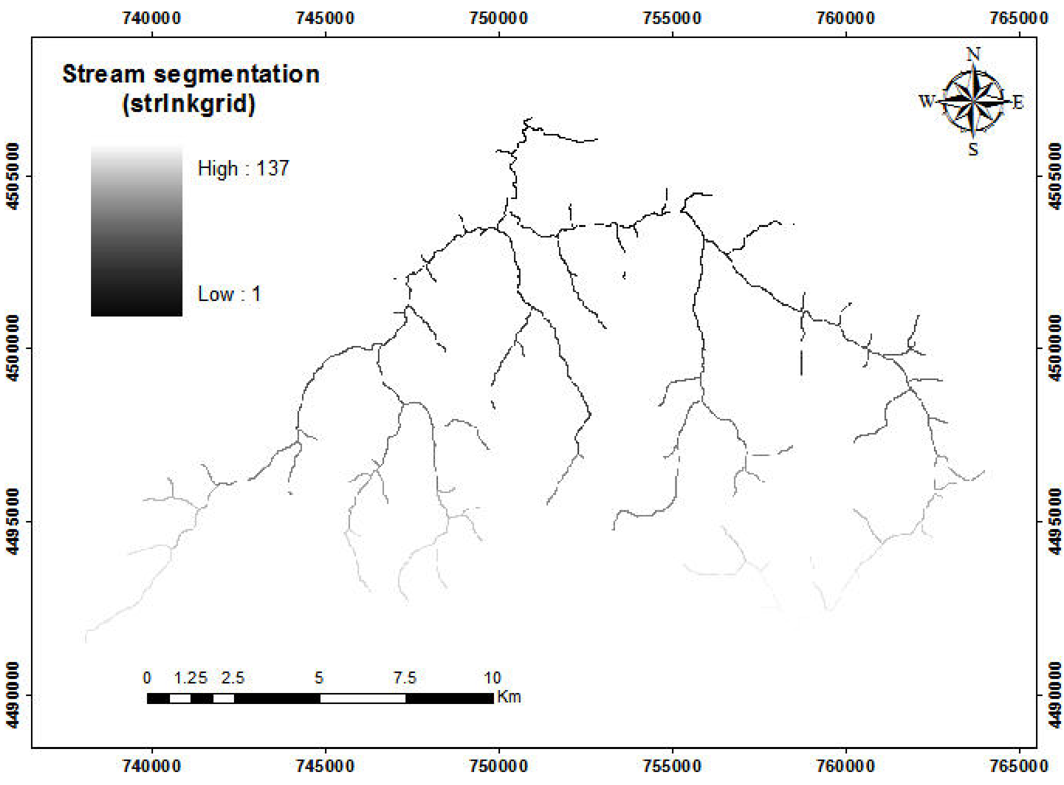

Figure 4.13. Stream segmentation

4.2.6. Watershed delineation

This step delineates a subbasin or watershed for every stream segment. The steps to delineate watersheds are shown below:

- Select **Terrain Preprocessing → Watershed Delineation**
- Input of the **FlowDirGrid** is **fdirgrid** and **LinkGrid** is **strlnkgrid**. The output of the **WaterGrid** is **wshedgrid (Figure 4.14).**

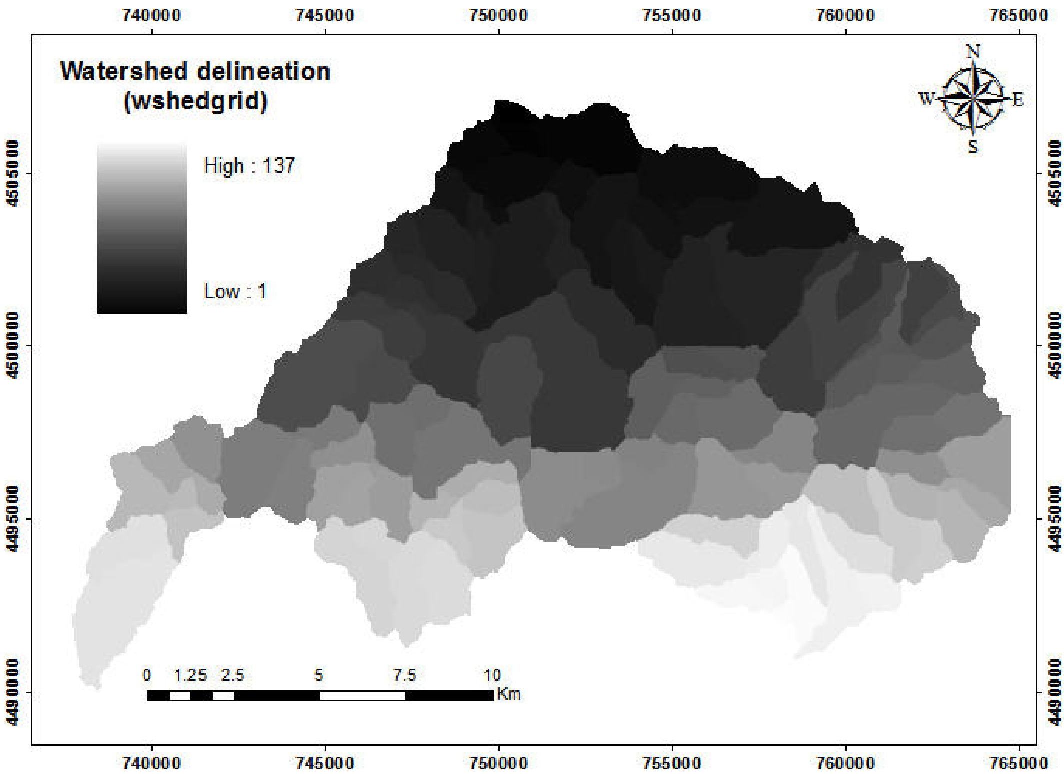

Figure 4.14. Watershed delineation

4.2.7. Watershed polygon processing

This step converts subbasins in the grid representation into a vector representation. The steps to vectorize a grid-based watershed are shown below:

- Select **Terrain Preprocessing → Watershed Polygon Processing**
- Input of the **WaterGrid** is **wshedgrid**, and the output of the **Watershed** is **wshedshp.shp (Figure 4.15).**

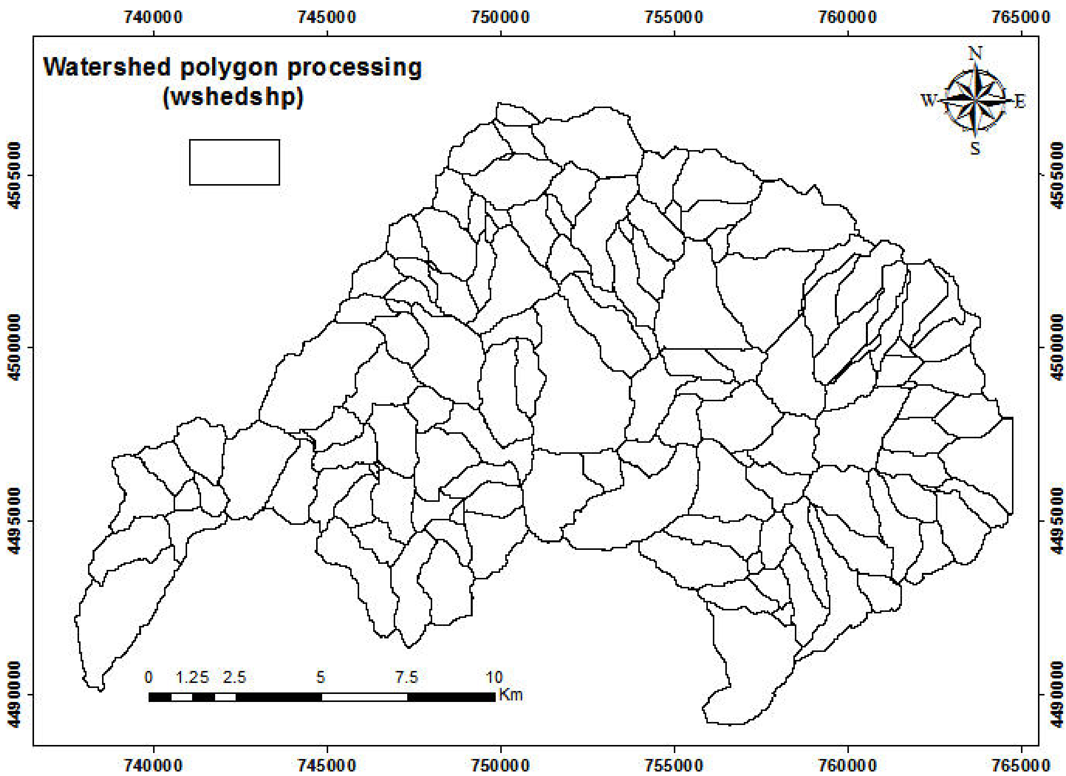

Figure 4.15. Watershed polygon processing

4.2.8. Stream segment processing

This step converts streams in the grid representation into a vector representation. The steps to vectorize stream segments are shown below:

- Select **Terrain Preprocessing → Stream Segment Processing**
- Input of the **LinkGrid** is **strlnkgrid** and **FlowDirGrid** is **fdirgrid**. The output of the **River** is **River.shp (Figure 4.16).**

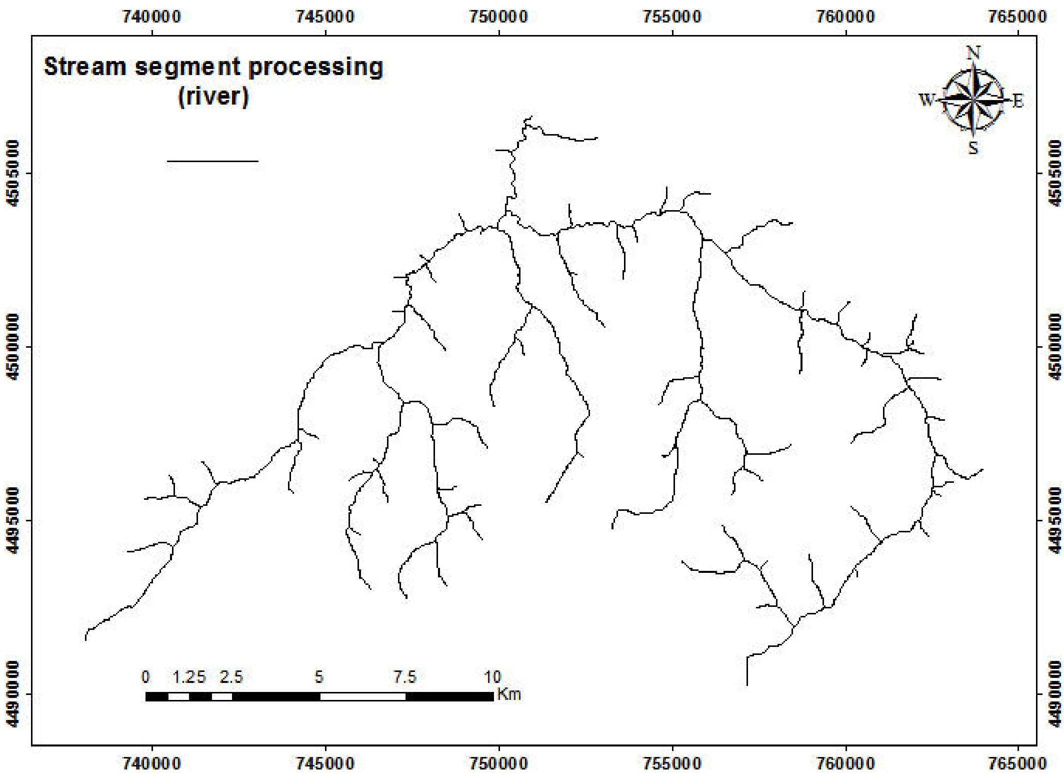

Figure 4.16. Stream segment processing

4.2.9. Watershed aggregation

This step aggregates the upstream subbasins at every stream confluence. This is a required step and is performed to improve computational performance for interactively delineating subbasins and to enhance data extraction. The number of aggregated watersheds depends on the stream definition threshold. The steps to aggregate watersheds are shown below:

- Select **Terrain Preprocessing → Watershed Aggregation**
- Input of the **River** is **river.shp** and **Watershed** is **wshedshp.shp**. The output of the **Aggregated Watershed** is **wshedmg.shp (Figure 4.17)**.

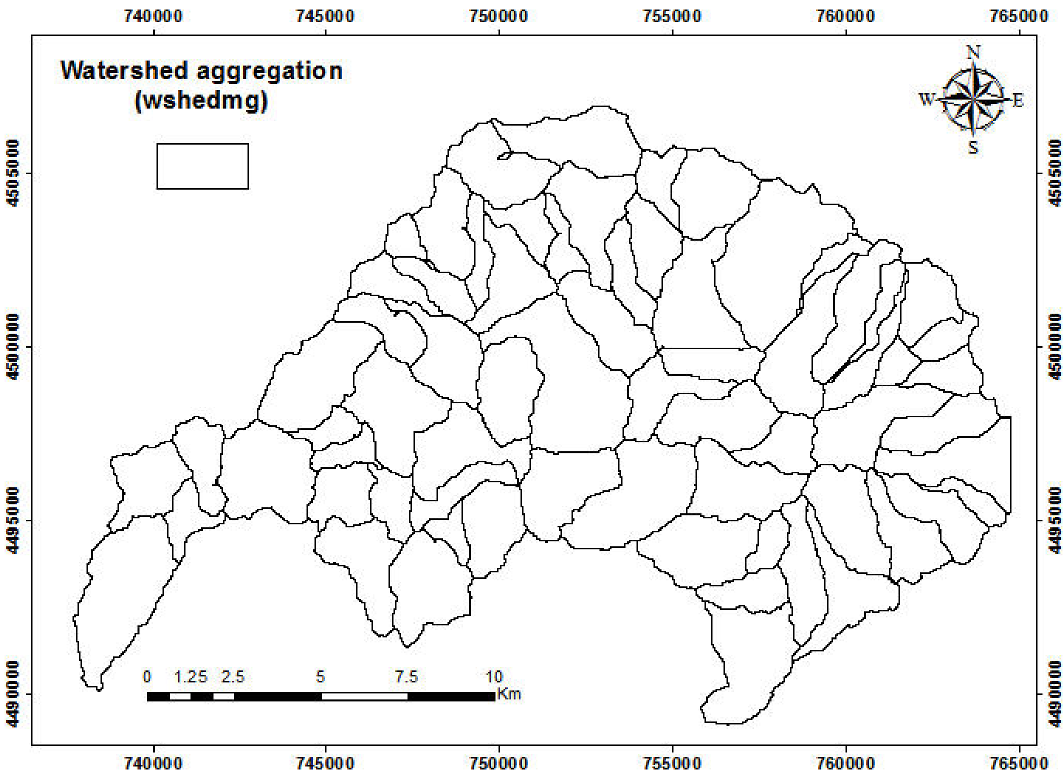

Figure 4.17. Watershed aggregation

4.3. Basin processing

4.3.1. Defining project areas to generate subbasins

The number of aggregated subbasins in HEC-GeoHMS at the end of basin preprocessing steps varies depending on the stream definition threshold given in Section 4.2.4. The more detailed the stream network of the basin is defined (i.e. the lower the threshold), the more number of subbasins are produced automatically by GeoHMS. As can be seen from Figure 4.17, the number of produced subbasins is 137 for Yuvacık Basin.

Obviously, not all of these subbasins are used in hydrologic modeling studies, because one would need the corresponding flow and precipitation data for each of the subbasins, collection of which is practically impossible. Therefore, 137 subbasins are further processed using the available *basin processing* tools of GeoHMS.

First of all, three project areas are defined in GeoHMS. In **MainView** document, a new HMS project is created using **HMS Project Setup** menu **Start New Project** item. Using the **Specify Outlet Point** tool, an outlet point for flow plant 1 (FP1) is defined by clicking on stream grid that has the same coordinate data as FP1. To be able to click to the correct position, a point shape file of FP1 may be created at the beginning to use as a guide layer. FP1 as a specified outlet point is given in Figure 4.18 together with FP2 and FP3. Under **HMS Project Setup** menu use **Generate Project** after the outlet point specification. In this step, GeoHMS once more asks for the basin creation threshold. Either the previously defined stream threshold may be used here or a new threshold may be defined. Then, the project area of FP1 is created. All the points in the basin that contributes flow to FP1 stream gage are considered in the project area of FP1.

GeoHMS extracts the following themes into a new **ProjView** document with the creation of the project area: watershed shape file, river shape file, small stream grid, flow accumulation grid, and flow direction grid. Unfortunately, digital elevation grid is not automatically extracted; it is clipped from the DEM of the whole basin using Arc Toolbox functions.

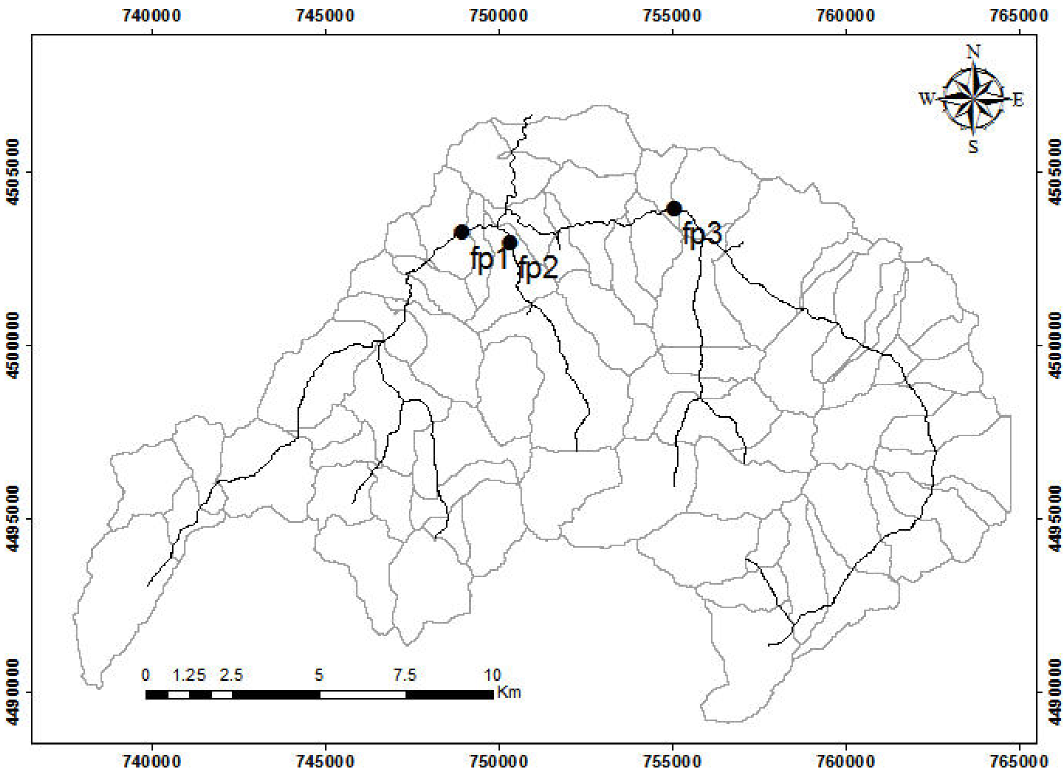

Figure 4.18. Specified outlet points (FP1, FP2, FP3) in Yuvacık Basin

Watershed shape file that is extracted using the project area of FP1 from the whole basin is named as Kirazdere Subbasin. Similarly, project areas for FP2 and FP3 are generated, and watershed shape files for those project areas are extracted. Kazandere and Serindere Subbasins are then formed. All together representation of project areas of FP1, FP2, and FP3 are given in Figure 4.19.

The remaining northern part of Yuvacık Basin is accepted as the fourth subbasin and it is named as Contributing Subbasin.

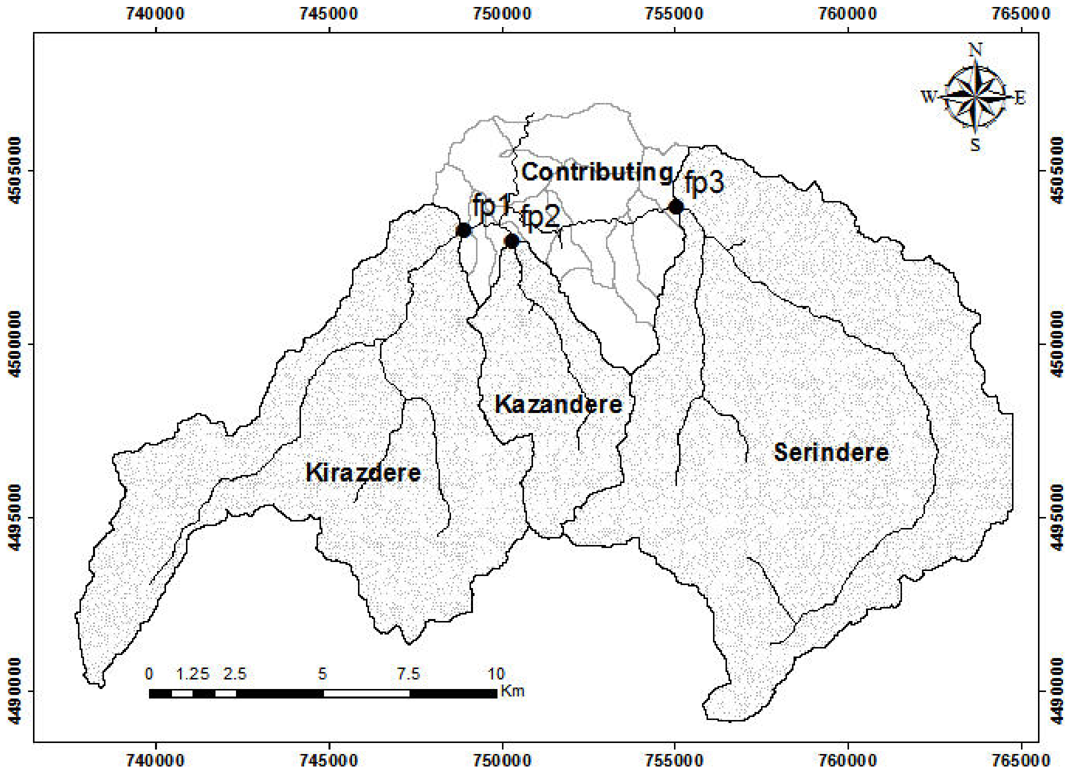

Figure 4.19. Project areas for FP1, FP2 and FP3

4.3.2. Subbasin characteristics

The next step after the generation of subbasins in GIS environment is to determine subbasin characteristics. Area (A) and perimeter (P) can directly be found from the watershed shape files of each subbasin and elevation information can be presented using the DEM of each subbasin, whereas slope and aspect information of subbasins is generated from their DEMs.

In **ProjView** document of GeoHMS, using the **Basin Characteristics** menu items, longest flow path, basin centroid (via flow path method), and centroidal flow path are determined. Longest flow path attribute data gives the longest main channel length (L) of the basin from its outlet to the farthest point in the basin that is contributing to runoff, channel slopes, S_e and S_{1085}, where S_e is the slope between the endpoints of the longest flow path and S_{1085} is the slope between 10% and 85% of the longest main channel length. From centroidal flow path attribute data, the length of the main channel from the outlet point to the centroid measured on the main channel (L_c) is determined.

Basin length (L_h) and basin width (W_h) are computed externally; they can not be determined in GeoHMS. Basin length is the bird's eye view distance from the outlet point of the basin to the farthest point in the basin that contributes to runoff. Basin width is then found as;

$$W_h = \frac{A}{L_h} \tag{4.1}$$

Maybe, the simplest shape factor that can be used for the analysis of a basin's shape is the division of basin length to basin width which is given as:

$$SI = \frac{L_h}{W_h} \tag{4.2}$$

Another shape factor that can be used is the circularity ratio that is given as:

$$R_c = \frac{4\pi A}{P^2} \tag{4.3}$$

One of the mostly used shape factors in hydrology is the Gravelius Index (coefficient of compactness) that is given as:

$$K_c = 0.28\frac{P}{\sqrt{A}} \tag{4.4}$$

Time of concentration values (t_c) for each subbasin are also computed using Kirpich's Equation. This equation is given in Equation 4.5, and is suitable for rural areas where slope is high (>10%) and land cover is timber in more than 59% of the area.

$$t_c = 0.0078\left(\frac{L^{0.77}}{S^{0.385}}\right) \tag{4.5}$$

All of the aforementioned subbasin characteristics are summarized in Tables 4.7 and 4.8. In addition, geology and land use characteristics of the subbasins together with the whole basin are given in Tables 4.9 and 4.10.

Table 4.7. Subbasin characteristics of Yuvacık

YUVACIK BASIN	Flow Plants			Basin Characteristics							
	ID	X	Y	Area (km²)	Perimeter (km)	Elevation (m)			Slope (degrees)		
						Min	Mean	Max	Min	Mean	Max
Subbasin1 Kirazdere	**FP1**	748952	4503260	79.536	72.840	179.0	871.5	1312.0	0.02	19.73	64.47
Subbasin2 Kazandere	**FP2**	750342	4502930	23.100	30.640	187.0	893.0	1347.0	0.02	21.92	58.24
Subbasin3 Serindere	**FP3**	755102	4503960	120.534	68.700	272.0	935.8	1547.0	0.00	19.75	61.30
Subbasin4 Contributing Subbasin	-	-	-	34.692	38.940	75.5	470.1	1231.0	0.04	23.03	52.80
WHOLE BASIN	-	-	-	**257.862**	**123.860**	**75.5**	**848.0**	**1547.0**	**0.00**	**20.27**	**64.47**

	Basin Characteristics										
	Longest Flow Path Slopes		Length Factors				Shape factors			Time of Concentration (Kirpich, 1940)	
	S_e (%)	S_{1085} (%)	L (km)	L_c (km)	L_h (km)	W_h (km)	SI	R_c	K_c	t_c (min)	t_c (hr)
Subbasin1 Kirazdere	3.60	3.80	21.10	10.55	16.30	4.88	3.34	0.19	2.29	149.57	2.49
Subbasin2 Kazandere	10.10	10.40	10.81	5.41	8.60	2.69	3.20	0.31	1.79	89.39	1.49
Subbasin3 Serindere	3.70	2.40	25.87	12.94	9.65	12.49	0.77	0.32	1.75	175.03	2.92
Subbasin4 Contributing Subbasin	-	-	-	-	-	-	-	-	-	-	-
WHOLE BASIN	-	-	-	-	-	-	-	-	-	-	-

Table 4.8. Aspect information of Yuvacık and its subbasins

Aspect	Yuvacık		Kirazdere		Kazandere		Serindere		Contributing	
	Area (km^2)	**Area (%)**	**Area (km^2)**	**Area (%)**	**Area (km^2)**	**Area (%)**	**Area (km^2)**	**Area (%)**	**Area (km^2)**	**Area (%)**
North (0 - 22.5)	13.63	5.28	3.69	4.65	1.76	7.62	5.45	4.52	2.39	6.88
Northeast (22.5 - 67.5)	33.78	13.10	9.56	12.03	4.80	20.79	14.47	12.00	4.92	14.20
East (67.5 - 112.5)	33.62	13.04	10.94	13.75	3.25	14.08	16.16	13.41	3.32	9.58
Southeast (112.5 - 157.5)	30.56	11.85	11.87	14.92	1.16	5.03	13.96	11.58	3.63	10.48
South (157.5 - 202.5)	28.32	10.98	7.90	9.93	0.61	2.62	16.48	13.67	3.43	9.88
Southwest (202.5 - 247.5)	34.99	13.57	8.33	10.47	2.70	11.70	20.20	16.76	3.94	11.35
West (247.5 - 292.5)	36.66	14.22	11.46	14.41	3.76	16.26	16.56	13.74	4.87	14.03
Northwest (292.5 - 337.5)	33.17	12.86	11.57	14.55	3.54	15.34	12.36	10.25	5.48	15.79
North (337.5 - 360)	13.14	5.10	4.20	5.28	1.51	6.55	4.89	4.06	2.71	7.82
Total	**257.86**	**100.0**	**79.54**	**100.0**	**23.10**	**100.0**	**120.53**	**100.0**	**34.69**	**100.0**

Table 4.9. Geologic information of Yuvacık and its subbasins

	Yuvacık		Kirazdere		Kazandere		Serindere		Contributing	
Geologic Formations	**Area (km^2)**	**Area (%)**	**Area (km^2)**	**Area (%)**	**Area (km^2)**	**Area (%)**	**Area (km^2)**	**Area (%)**	**Area (km^2)**	**Area (%)**
Alluvion	5.89	2.28	1.84	2.31	0.00	0.00	3.96	3.29	0.17	0.52
Andesit-Basalt	52.56	20.38	8.44	10.61	6.97	30.19	6.68	5.55	27.72	84.10
Dolomite-Limestone	8.88	3.44	0.00	0.00	1.60	6.91	7.40	6.14	0.00	0.00
Limestone-Marn	23.19	8.99	0.37	0.46	0.00	0.00	22.22	18.43	0.00	0.00
Marble	36.63	14.20	14.32	18.00	3.48	15.07	16.68	13.84	2.25	6.83
Ophiolitic Shale	15.08	5.85	0.00	0.00	0.00	0.00	15.30	12.69	0.00	0.00
Sedimentary	11.89	4.61	0.00	0.00	0.00	0.00	12.07	10.01	0.00	0.00
Shale	79.80	30.95	54.58	68.62	11.01	47.65	14.79	12.27	0.04	0.12
Shale-Marble	23.94	9.28	0.00	0.00	0.04	0.17	21.44	17.78	2.78	8.43
Total	**257.86**	**100.00**	**79.54**	**100.00**	**23.10**	**100.00**	**120.53**	**100.00**	**32.96**	**100.00**

Table 4.10. Land use information of Yuvacık and its subbasins

	Yuvacık		Kirazdere		Kazandere		Serindere		Contributing	
Land use classes	**Area (km^2)**	**Area (%)**	**Area (km^2)**	**Area (%)**	**Area (km^2)**	**Area (%)**	**Area (km^2)**	**Area (%)**	**Area (km^2)**	**Area (%)**
Bad Forest (10-40% Closed)	36.56	14.18	5.22	6.56	3.50	15.17	13.48	11.19	13.12	37.83
Good Forest (40-70% Closed)	64.23	24.91	4.83	6.07	3.18	13.78	50.28	41.71	6.19	17.85
Good Forest (70-100% Closed)	101.51	39.37	54.53	68.56	13.56	58.71	31.03	25.74	3.23	9.31
Cultivated	30.57	11.86	9.45	11.89	1.45	6.26	11.27	9.35	8.52	24.57
Not Cultivated	12.88	4.99	2.31	2.91	0.72	3.13	9.01	7.47	0.98	2.83
Good Pasture	7.38	2.86	2.62	3.29	0.59	2.56	3.35	2.78	0.81	2.34
Bad Pasture	1.82	0.71	0.36	0.45	0.00	0.00	1.33	1.10	0.00	0.00
Poplar - Nut	1.20	0.47	0.21	0.27	0.09	0.39	0.79	0.65	0.13	0.37
Reservoir	1.71	0.66	0.00	0.00	0.00	0.00	0.00	0.00	1.70	4.90
Total	**257.86**	**100.0**	**79.54**	**100.0**	**23.10**	**100.0**	**120.53**	**100.0**	**34.68**	**100.0**

4.3.3. Subbasin background maps

The last operation that is performed in HEC-GeoHMS is the generation of subbasin maps. These maps are used as background layers in HEC-HMS. Since hydrologic model is not set up in GeoHMS in this study, the background maps do not posses any hydrologic meaning, only they show the basin boundaries and river branches of the basin.

In GeoHMS, in the **ProjView** document, using the **Background Map File** item in **HMS** menu, background maps of each subbasin is created. Background maps of Kirazdere, Kazandere, and Serindere subbasins are given in Figures 4.20, 4.21, and 4.22, respectively.

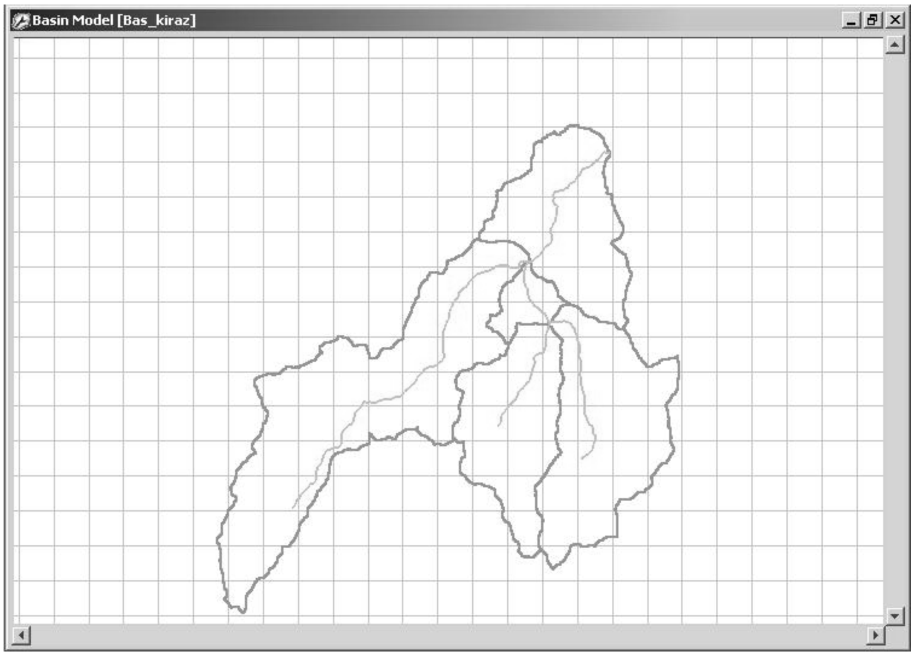

Figure 4.20. Background map of Kirazdere subbasin

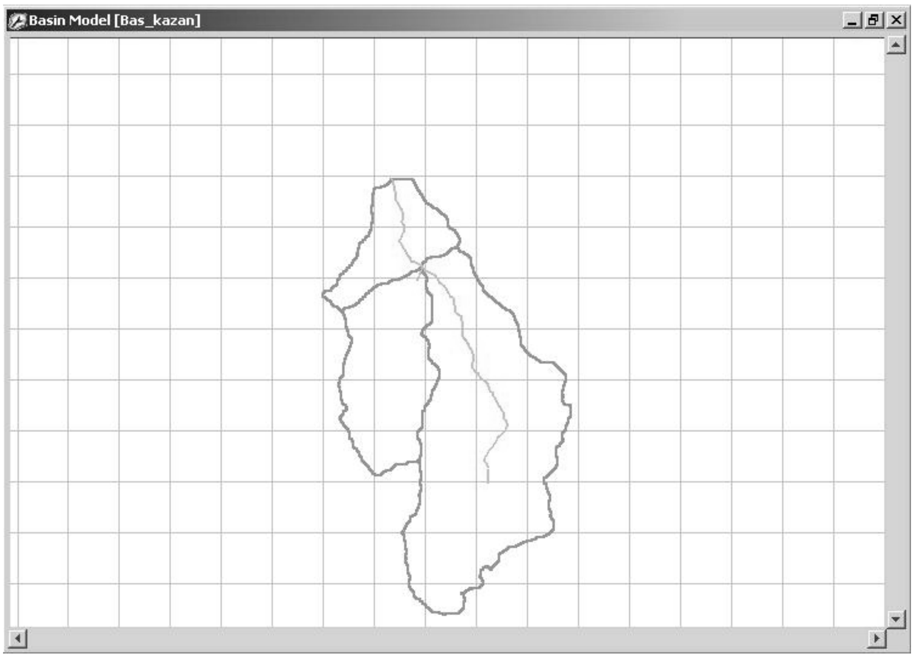

Figure 4.21. Background map of Kazandere subbasin

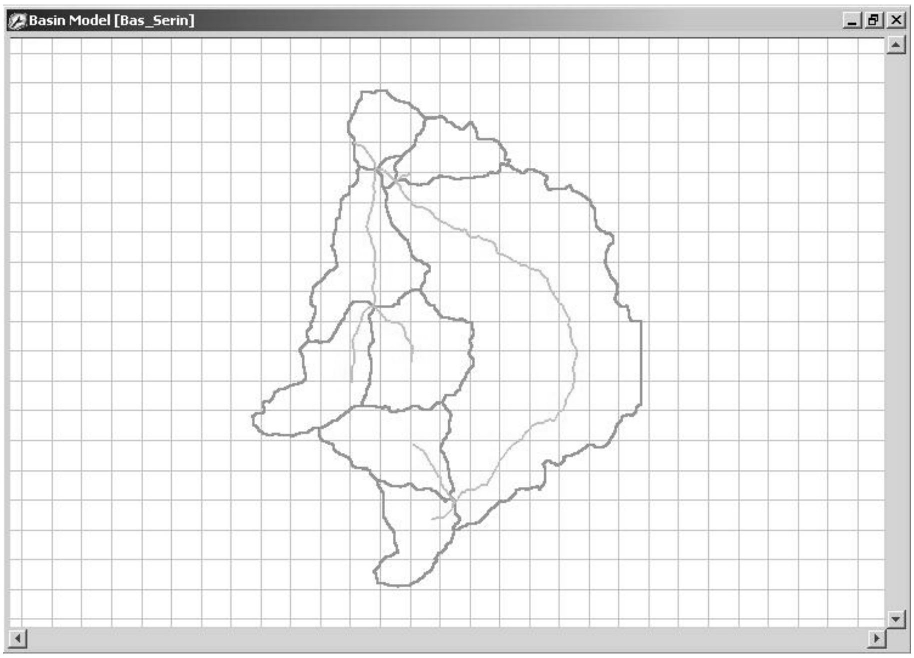

Figure 4.22. Background map of Serindere subbasin

4.4. Classification of events

Through the analysis of observed hydrographs and rainfall hyetographs 44 events are selected to be used in the simulation studies in HEC-HMS. The thresholds that are used in the event selection process were 500,000 and 1,250,000 m^3 for a total daily reservoir inflow (TDRI) and 15 and 30 mm for a total daily precipitation (TDP). Storms primarily classified in 7 groups:

Group 1: TDP ≥ 30 mm and TDRI ≥ 1,250,000 m^3
Group 2: 15 ≤ TDP < 30 mm and TDRI ≥ 1,250,000 m^3
Group 3: TDP ≥ 30 mm and 750,000 < TDRI < 1,250,000 m^3
Group 4: 15 ≤ TDP < 30 mm and 750,000 < TDRI < 1,250,000 m^3
Group 5: TDP ≥ 30 mm and 500,000 < TDRI < 750,000 m^3
Group 6: 15 ≤ TDP < 30 mm and 500,000 < TDRI < 750,000 m^3
Group 7: TDP ≥ 30 mm and TDRI < 500,000 m^3

According to the upper criteria 44 storm events are selected from October 2001 to April 2006. After that, selected events are classified according to the precipitation type. Storm events that are due only to rainfall constitute the first class (Class 1); storm events that are due both to rainfall and snowfall constitute the second class (Class 2); storm events that are due both to snowfall and snowmelt constitute the third class (Class 3); storm events that are due only to snowmelt constitute the fourth class (Class 4) and storm events that are classified in one of the given seven groups but that do not have any peak at all constitute the seventh class (Class 7) (Table 4.11).

Events may be rearranged and further classified into three categories as given in Table 4.12. This classification is helpful for the determination of model parameters during calibration stage for different periods of the year. These categories are rainfall events (Category 1), rainfall with snow accumulation events (Category 2) and rainfall with snowmelt or pure snowmelt events (Category 3).

Table 4.11. General list of selected storm events

NO	PERIOD	CLASS ID	EVENT TYPE
1a	20-23 NOV 2001	2	RAIN+SNOWFALL
1b	24-26 NOV 2001	3	RAIN+SNOWMELT
2	01-10 DEC 2001	2	RAIN+SNOWFALL
3	20-27 DEC 2001	3	RAIN+SNOWMELT
4	16-20 JAN 2002	4	SNOWMELT
5	21-23 MAR 2002	1	RAIN
6a	29-31 MAR 2002	3	RAIN+SNOWMELT
6b	01-04 APR 2002	3	RAIN+SNOWMELT
7	05-09 APR 2002	1	RAIN
8	16-19 APR 2002	1	RAIN
9	13-15 MAY 2002	7	NO PEAK
10	11-15 JUL 2002	1	RAIN
11	01-04 JAN 2003	3	RAIN+SNOWMELT
12-13	02-14 FEB 2003	3	RAIN+SNOWMELT
14	3-7 MAR 2003	3	RAIN+SNOWMELT
15	12-16 MAR 2003	3	RAIN+SNOWMELT
16	13-18 APR 2003	1	RAIN
17	02-06 SEP 2003	1	RAIN
18	23-30 OCT 2003	1	RAIN
19	06-09 NOV 2003	1	RAIN
20	09-11 NOV 2003	3	RAIN+SNOWMELT
21	01-12 DEC 2003	7	NO PEAK
22	15-20 DEC 2003	2	RAIN+SNOWFALL
23	24-29 DEC 2003	3	RAIN+SNOWMELT
24	04-07 JAN 2004	1	RAIN
25	21-23 JAN 2004	2	RAIN+SNOWFALL
26	25-29 FEB 2004	4	SNOWMELT
27	01-09 MAR 2004	3	RAIN+SNOWMELT
28	13-18 APR 2004	1	RAIN
29	25 APR-01 MAY 2004	1	RAIN
30	15-19 MAY 2004	7	NO PEAK
31	09-11 JUN 2004	1	RAIN
32	13-19 JAN 2005	3	RAIN+SNOWMELT
33	27 JAN-02 FEB 2005	1	RAIN
34	04-05 FEB 2005	2	RAIN+SNOWFALL
35	25 FEB-03 MAR 2005	2	RAIN+SNOWFALL
36	31 MAY-06 JUN 2005	1	RAIN
37	04-09 JUL 2005	1	RAIN
38	19-21 JUN 2004	1	RAIN
39	23-25 JUN 2004	1	RAIN
40	15-19 NOV 2004	1	RAIN
41	5-10 MAR 2005	1	RAIN
42	1-5 MAR 2006	3	RAIN+SNOWMELT
43	18-22 JAN 2006	3	RAIN+SNOWMELT
44	08-13 FEB 2006	3	RAIN+SNOWMELT

This categorization of events also includes a sub-categorization for different seasons in a year. Since snow data is scarce in the region for the previous years (snow data are only available at Hacıosman (900 m) and Kocaeli (76 m) gages) the model calibration studies have been taken start with rainfall (Category 1) events which do not require snow component of the model (Section 5.1). Model calibration of events including snow has been studied with the help of recently collected snow measurement records and is presented in Section 5.2. Thus, Class 1, rainfall events are calibrated in hourly time steps for each subbasin and results are presented in Section 5.1, however Class 2 and Class 3, mixed events are calibrated on daily time steps and they are the main focus of Section 5.2.

Table 4.12. Categorization of selected storm events

Rainfall Events (Category 1)			
Sep-Dec	Jan-Feb	Mar-Apr	Jun-Jul
	24 (FP1, FP2, FP3)	5 (FP1)	10 (FP1)
	33 (FP1, FP2, FP3)	7 (FP1)	31 (FP1, FP3(?))
		8 (FP1)	36 (FP1, FP2, FP3)
17 (FP1(?), FP2, FP3)		16 (FP1(?), FP3)	37 (FP1, FP2, FP3)
18 (FP1(?), FP2)		28 (FP1, FP2)	38 (FP1, FP2, FP3)
19 (FP1(?), FP2, FP3)		29 (FP1(?), FP2)	39 (FP1, FP2, FP3)
40 (FP1, FP2, FP3)		41 (FP1(?), FP2)	

Rainfall and Snow Accumulation (Category 2)			
Sep-Dec	Jan-Feb	Mar-Apr	Jun-Jul
1a (FP1, FP3)	25 (FP1, FP2)		
2 (FP1)	34 (FP1, FP2, FP3)		
22 (FP1(?), FP2, FP3)	35 (FP1(?), FP2, FP3)		

Table 4.12. Categorization of selected storm events (continued…)

Rain and Snowmelt (Category 3)			
Sep-Dec	Jan-Feb	Mar-Apr	Only snowmelt
1b (FP1, FP3)	11 (FP1)	6a (FP1)	26 (FP1, FP2)
3 (FP1(?))	12-13 (FP1, FP3(?))	6b (FP1)	
20 (FP1(?), FP2, FP3)	32 (FP1, FP2, FP3)	14 (FP1, FP3 (?))	
23 (FP1(?), FP2, FP3)	43 (FP1, FP2, FP3)	15 (FP1, FP2, FP3)	
	44 (FP1, FP2, FP3)	27 (FP1, FP2)	
		42 (FP1, FP2, FP3)	

In Table 4.12, the available flow plant (stream flow) data is shown in the parenthesis with the flow plant codes under the event numbers. Obviously, in some of the events one or more of the flow plant data is not available (e.g. Event 11), and in some of the events flow plant data has mistakes (e.g. Event 17). A question mark is put next to the flow plant code to show that flow data has inconsistency.

Model parameters of the events listed above are calibrated for Kirazdere, Kazandere and Serindere subbasins. However, the model parameter calibrations were only carried out for the events except for the ones having small peaks, missing data or inconsistent levels. The analysis and final evaluation of events are given in Table 4.13.

Table 4.13. Analysis and evaluations of storm events

	Kirazdere	**Kazandere**	**Serindere**
Calibrated with Event Based Hourly Simulations	5, 7, 8, 10, 24, 31, 33, 36 - 41	24, 33, 36 - 41	16, 24, 33, 36 - 41
Calibrated or Validated with Snow Period Daily Simulations	1 - 3, 5 - 7, 11 - 16, 23, 24, 26, 27, 32 - 35, 41	16, 23, 24, 26, 27, 32 – 35, 41	11 - 13, 23, 24, 32 - 35, 41
Not processed due to missing data / small peaks / mistaken data	17 - 22, 25, 28 - 30	1 -15, 17 – 22, 25, 28 – 31	1 -10, 14, 15, 17 - 22, 25 - 31
Events with no peak	4, 9	4, 9	4, 9

CHAPTER 5

MODEL SIMULATIONS

5.1. Event-based hourly simulations

5.1.1. Basin model

To set up the basin model of the subbasins Kirazdere, Kazandere, and Serindere only two hydrologic elements are used from the available elements (Table 3.1): subbasin and junction element. Subbasin element handles the infiltration loss and baseflow computations, and rainfall runoff transformation process. Junction element handles the observed flow data and is mainly used for the comparison of the observed flow hydrographs with the simulated flow hydrographs. No reach element is used; therefore no routing procedures are taken into account in the basin model of each subbasin.

For the subbasin element in basin model, a suitable method among the available ones (Table 3.2) for each of the loss, transformation and baseflow methods is selected as given in following sections.

5.1.1.1. Loss method selection

While a subbasin element conceptually represents infiltration, surface runoff, and subsurface processes interacting together, the actual infiltration calculations are performed by a loss method contained within the subbasin. A total of nine different loss methods are provided in HEC-HMS such as: deficit and constant loss, exponential loss, Green and Ampt loss, gridded deficit constant loss, gridded SCS curve number loss, gridded soil moisture accounting, initial constant loss, SCS curve number loss, and soil moisture accounting loss. Some of the methods are designed primarily for simulating events while others are intended for continuous simulation. All of the methods conserve mass; that is, the sum of infiltration and precipitation left on the surface will always be equal to total incoming precipitation.

Gridded Loss Methods (Gridded Deficit Constant, Gridded SCS Curve Number, and Gridded Soil Moisture Accounting) and Soil Moisture Accounting Loss Method are not preferred for the simulation studies because they require a high number of parameters (e.g. Gridded Soil Moisture Accounting loss method requires 17 parameters, and 12 of these parameters are gridded data sets).

Among the remaining loss methods the simplest one "Initial and Constant Loss" method is selected for the initial event based hourly simulation studies. The method is simple and practical because it requires only three input parameters such as initial loss (mm), constant rate (mm/hr), and impervious area (%).

As the number of simulated events increased, the disadvantage of the Initial and Constant Loss method has been realized since the method can not catch sequential peaks. Referring to Figure 5.1, it can easily be observed that the second peak (at time 14:00) of the observed flow has been suppressed by the high constant rate of loss (12.5 mm), because all the precipitation is lost, and there is no excess rainfall to create the second peak. From the graph it is obvious that the constant loss rate should not be greater than 4 mm, so that there will be excess rain, and correspondingly in the simulation hydrograph a second peak will be observed. But when constant loss rate is decreased to 4 mm, the first peak of the simulation increases above 10 m^3/s (observed peak = 2.4 m^3/s). In addition, a significant volumetric increase in the simulation hydrograph is observed. Table 5.1 summarizes the simulation results, and Figure 5.2 represents the simulation graph.

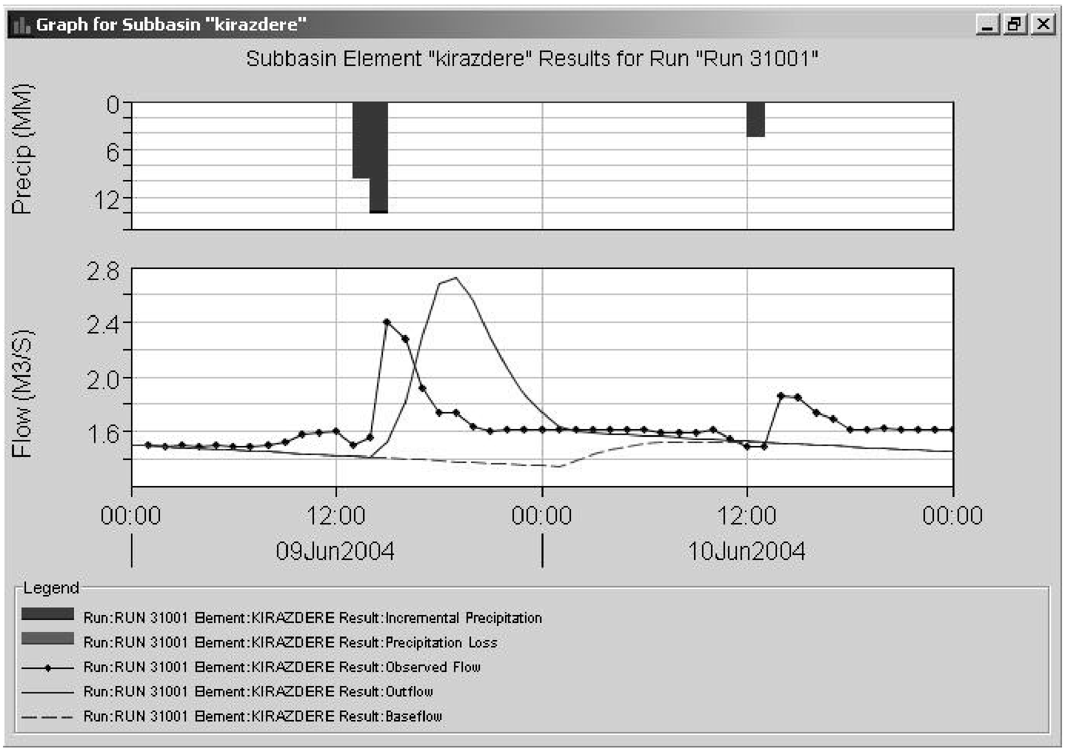

Figure 5.1. Simulation Graph of Event 31, using Initial and Constant Loss method (Constant Loss Rate = 12.5 mm)

Due to the mentioned disadvantage of Initial and Constant Loss Method, another loss method, Exponential Loss, is selected. In Exponential Loss method, which relates loss rate to rainfall intensity and accumulated losses, loss rate is represented by a logarithmic decaying function. Since loss rate is not constant, the method shows better performance in catching the sequential peaks, as shown in Figure 5.3.

Table 5.1. Percent Errors in Peak and Volume when Constant Loss Rate is decreased to 4 mm/hr

Event 31	**Observed**	**Simulated**
Total Precipitation (mm)	28.11	
Total Loss (mm)		25.16
Total Baseflow (mm)		3.10
Peak Discharge (m^3/s)	2.4	10.06
Total Q (mm)	3.55	5.95
Time of Peak Discharge	15:00 (9 Jun)	19:00 (9 Jun)
Avg Abs Residual (m^3/s)		1.14
Total Residual (mm)		2.40
Peak Difference (%)		-319.17
Volume Difference (%)		-67.61

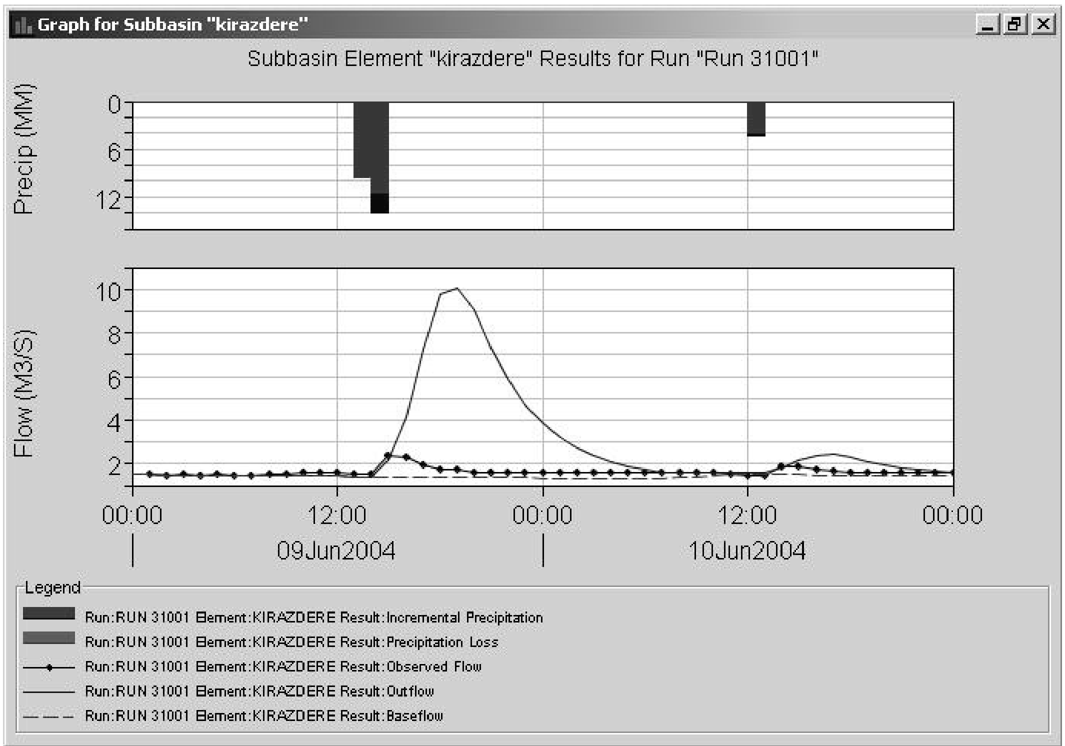

Figure 5.2. Simulation Graph of Event 31, using Initial and Constant Loss method (Constant Loss Rate = 4 mm)

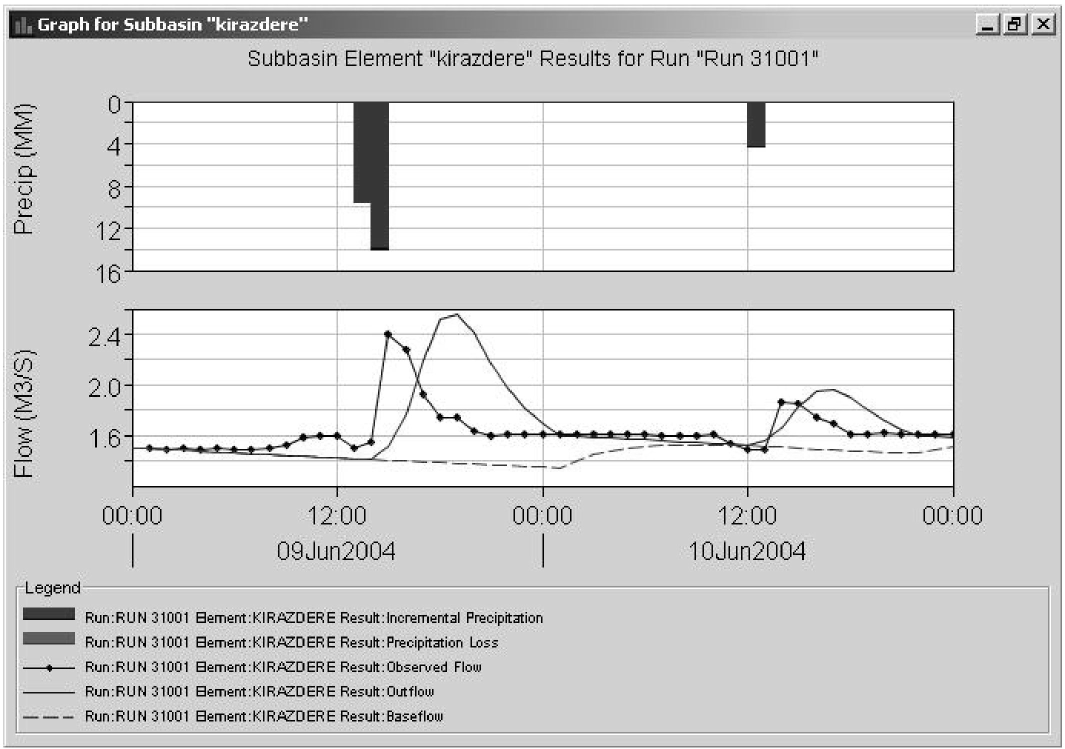

Figure 5.3. Simulation Graph of Event 31, using Exponential Loss method

5.1.1.2. Transform method selection

HEC-HMS has seven different transform methods to perform the surface runoff calculations: Clark's Unit Hydrograph, Kinematic Wave, ModClark, SCS Unit Hydrograph, Snyder's Unit Hydrograph, user-specified S-graph, and user-specified Unit Hydrograph.

There are several different unit hydrographs available to be used in rainfall-runoff transformation process for Yuvacık basin. For example State Hydraulic Works (DSI) derived three different unit hydrographs for the basin from historical storm data. These are DSI Synthetic Unit Hydrograph, Mocus Unit Hydrograph and Snyder Unit Hydrograph. Also, two unit hydrographs were derived for the basin from the storm events observed in December 1987 and Nov 1989 for 1 hour and 7 hours excess rainfall durations, respectively (Table 5.2).

Table 5.2. Available unit hydrographs for Yuvacık Basin

DSI SYNTHETIC UNIT HYDROGRAPH			
Time (hr)	Serindere Discharge (m³/s/mm) (151 km²)	Duzlukdere Discharge (m³/s/mm) (107 km²)	Serindere+Duzlukdere Discharge (m³/s/mm) (258 km²)
0	0.00	0.00	0.00
1	0.40	0.50	0.90
2	1.50	1.80	3.30
3	3.35	3.80	7.15
4	5.10	5.10	10.20
5	5.90	4.70	10.60
6	5.55	3.80	9.35
7	4.65	2.60	7.25
8	3.65	1.90	5.55
9	2.70	1.40	4.10
10	2.05	1.00	3.05
11	1.60	0.70	2.30
12	1.20	0.50	1.70
13	0.90	0.35	1.25
14	0.65	0.25	0.90
15	0.50	0.20	0.70
16	0.35	0.15	0.50
17	0.25	0.10	0.35
18	0.20	0.07	0.27
19	0.15	0.05	0.20
20	0.10	0.03	0.13
21	0.07	0.02	0.09
22	0.05	0.01	0.06
23	0.02	0.00	0.02
24	0.00	0.00	0.00

MOCKUS UH	
Time (hr)	Yuvacik Discharge (m³/s/mm)
0	0.00
1	3.10
2	6.20
3	9.20
4	10.90
5	9.90
6	8.50
7	7.20
8	5.90
9	4.50
10	3.10
11	2.10
12	1.40
13	0.70
14	0.00
15	-
16	-
17	-
18	-
19	-
20	-
21	-
22	-
23	-
24	-

SNYDER UH	
Time (hr)	Yuvacik Discharge (m³/s/mm)
0	0.00
1	1.10
2	2.80
3	6.00
4	8.40
5	9.04
6	9.06
7	7.80
8	6.60
9	5.60
10	4.60
11	4.00
12	3.40
13	3.20
14	2.80
15	2.60
16	2.50
17	2.32
18	2.20
19	2.10
20	2.00
21	1.94
22	1.84
23	1.76
24	1.68

9-11 DEC 1987	
Time (hr)	Yuvacik Discharge (m³/s/mm)
0	0.00
1	4.20
2	5.80
3	9.00
4	10.00
5	11.00
6	9.00
7	7.00
8	5.20
9	4.80
10	4.00
11	3.00
12	2.00
13	1.00
14	0.00
15	-
16	-
17	-
18	-
19	-
20	-
21	-
22	-
23	-
24	-

13-14 NOV 1989	
Time (hr)	Yuvacik Discharge (m³/s/mm)
0	0.00
1	4.00
2	6.00
3	9.00
4	10.00
5	11.00
6	9.00
7	7.00
8	5.00
9	4.00
10	3.00
11	2.00
12	2.00
13	1.00
14	0.00
15	-
16	-
17	-
18	-
19	-
20	-
21	-
22	-
23	-
24	-

In the simulation studies DSI Synthetic Unit Hydrograph data is input in the user-specified unit hydrograph transform method. Originally, the synthetic unit hydrograph was developed for two subbasins in Yuvacık (DSI, Bursa 1983) namely Duzlukdere (107 km²) and Serindere (151 km²). The sum of two given hydrographs is the unit hydrograph for the whole basin. However, due to the presence of FP stations, Yuvacık basin is divided into three subbasins and also there is a contributing subbasin as given in Section 4.3.2. Then, there is a need to distribute the total unit hydrograph to the defined subbasins, because all of the subbasins (Kirazdere, Kazandere, and Serindere) are simulated separately. The distribution is simply done to these subbasins according to their area ratios as given in Table 5.3.

Table 5.3. Unit hydrographs of each subbasin

DISTRIBUTED UNIT HYDROGRAPHS			
Kirazdere Discharge (m^3/s/mm) (79.536 km²)	**Kazandere Discharge (m^3/s/mm) (23.1 km²)**	**Serindere Discharge (m^3/s/mm) (120.534 km²)**	**Contributing Discharge (m^3/s/mm) (34.692 km²)**
0.0000	0.0000	0.0000	0.0000
0.2775	0.0806	0.4205	0.1210
1.0173	0.2955	1.5417	0.4437
2.2042	0.6402	3.3404	0.9614
3.1444	0.9133	4.7653	1.3715
3.2678	0.9491	4.9522	1.4253
2.8824	0.8372	4.3682	1.2572
2.2350	0.6491	3.3871	0.9749
1.7109	0.4969	2.5929	0.7463
1.2639	0.3671	1.9155	0.5513
0.9403	0.2731	1.4249	0.4101
0.7090	0.2059	1.0745	0.3093
0.5241	0.1522	0.7942	0.2286
0.3853	0.1119	0.5840	0.1681
0.2775	0.0806	0.4205	0.1210
0.2158	0.0627	0.3270	0.0941
0.1541	0.0448	0.2336	0.0672
0.1079	0.0313	0.1635	0.0471
0.0832	0.0242	0.1261	0.0363
0.0617	0.0179	0.0934	0.0269
0.0401	0.0116	0.0607	0.0175
0.0277	0.0081	0.0420	0.0121
0.0185	0.0054	0.0280	0.0081
0.0062	0.0018	0.0093	0.0027
0.0000	0.0000	0.0000	0.0000

5.1.1.3. Baseflow method selection

The actual subsurface calculations in a subbasin element in basin model are performed with a baseflow method. There are four baseflow methods available in HEC-HMS: bounded recession baseflow, constant monthly baseflow, linear reservoir baseflow, recession baseflow.

Recession baseflow method is selected among the available methods. This method is designed to approximate the typical behavior observed in watersheds when channel flow recedes exponentially after an event. It is intended primarily for event simulation. However, it does have the ability to automatically reset after each storm event and consequently may be used for continuous simulation.

5.1.2. Meteorologic model

Meteorologic model is one of the major components of a HEC-HMS project. It defines the meteorologic boundary conditions for subbasins, i.e. it specifies how the precipitation is generated for each of the subbasins in the project.

Meteorologic model has three components such as: *precipitation*, *evapotranspiration* and *snowmelt* to be used during simulations. There are different methods available in each of the meteorologic model components (Table 3.3). For example, for precipitation component, frequency storm, gage weights, gridded precipitation, inverse distance, SCS storm, specified hyetograph, standard project storm methods are available; for evapotranspiration component, gridded Priestley-Taylor, monthly average, and Priestley-Taylor methods are available; and the snowmelt component, temperature index and gridded temperature index methods are available.

In event based hourly simulations, precipitation component of meteorologic model is used, but snowmelt and evapotranspiration components are not used.

Snowmelt component is used in the daily simulations where snowfall, and snowmelt periods are considered. Evapotranspiration component is used in continuous simulations with any of the following loss methods: deficit constant, gridded deficit constant, soil moisture accounting, gridded soil moisture accounting. Since in this study exponential loss method is selected to be used, evapotranspiration component is not used either in hourly simulations or in daily simulations.

5.1.2.1. Selection of precipitation method

The precipitation records are available from rain gages in Yuvacık Basin from RG1 to RG6 that are operated by Thames Water Türkiye (TWT), Kocaeli (KE) rain gage operated by DMI and Hacıosman (HO) rain gage operated by DSI. RG rain gages are recording rain gages, i.e. they record the rainfall every 5 minutes. On the other hand KE and HO rain gages have daily cumulative records (they are non-recording). In the study, a kind of partitioning between the rain gages and subbasins is considered to be appropriate. As a result:

- RG3 is used in Kirazdere simulations,
- RG2 and RG5 are used in Kazandere simulations,
- RG4 is reserved for Serindere subbasin (although RG4 is not always working at the time periods of selected events),
- KE and HO gages are used in the simulations of all the three subbasins. Since, KE (76 m) represents the lowest elevation in the whole basin, and HO (900 m) represents the mean elevation of the whole basin.

21 peak rainfalls are selected from the available classified events and the gage data are compared with each other to see the relationship between the TWT gages, KE, and HO. The results are presented in Table 5.4.

In Table 5.4 some records (strikethrough records) are accepted as outliers and they are not considered in the average ratio computation, e.g. the records that give ratios less than 0.5 and ratios more than 3.0, because in a small basin like Yuvacık, it is not likely for the ratios to be outside of the upper stated values.

As it can be seen from the table, TWT gage ratios are very close to “1”, which means TWT rain gages have high correlation since both their elevations and locations are close to each other. More specifically, using RG2 instead of RG5 for a subbasin will not affect the results of the simulations much. Similarly, using all the 3 rain gages (RG2, RG3, and RG5) for a subbasin will not yield more significant results than using only one of them. Therefore, RG3 is reserved for Kirazdere simulations, and RG2 and RG5 gages are reserved to be used for Kazandere simulations.

Table 5.4. Comparison of precipitation gage data for Yuvacık Basin

DATE	RAINGAGE DAILY PEAK RAINFALLS					RATIOS OF RAIN GAGES							
	KE DMI (76 m)	RG2 TWT (320 m)	RG3 TWT (460 m)	RG5 TWT (264 m)	HO DSI (900 m)	RG2/KE	RG3/RG2	RG3/KE	HO/RG3	HO/RG2	HO/KE	RG2/RG5	RG3/RG5
20-Nov-01	31.5	44.2	43	43.6	33.8	1.40	0.97	1.37	0.79	0.76	1.07	1.01	0.99
24-Nov-01	3	25.4	32	21.6	36.5	~~8.47~~	1.26	~~10.67~~	1.14	1.44	~~12.17~~	1.18	1.48
21-Mar-02	3.3	17	18.2	18.4	3.5	~~5.15~~	1.07	~~5.52~~	~~0.19~~	~~0.21~~	1.06	0.92	0.99
5-Apr-02	21.9	16	18	15.8	60	0.73	1.13	0.82	~~3.33~~	~~3.75~~	2.74	1.01	1.14
16-Apr-02	10.2	18	17.8	17.8	29	1.76	0.99	1.75	1.63	1.61	2.84	1.01	1.00
13-Jul-02	0.7	37.4	32.2	39.6	35	~~53.43~~	0.86	~~46.00~~	1.09	0.94	~~50.00~~	0.94	0.81
4-Jan-03	15.7	19.4	22.2	19.6	26.5	1.24	1.14	1.41	1.19	1.37	1.69	0.99	1.13
2-Feb-03	9.2	15.4	13.6	17.6	23.5	1.67	0.88	1.48	1.73	1.53	2.55	0.88	0.77
7-Feb-03	45.6	24	12.6	24.2	73	0.53	0.53	~~0.28~~	~~5.79~~	~~3.04~~	1.60	0.99	0.52
13-Apr-03	18.1	21.4	22	20.4	17	1.18	1.03	1.22	0.77	0.79	0.94	1.05	1.08
4-Sep-03	24.3	43.4	40.6	46.4	25	1.79	0.94	1.67	0.62	0.58	1.03	0.94	0.88
25-Oct-03	11.2	37.8	37.2	38.2	25	~~3.38~~	0.98	~~3.32~~	0.67	0.66	2.23	0.99	0.97
5-Nov-03	4.1	15.8	15.4	17.4	4	~~3.85~~	0.97	~~3.76~~	~~0.26~~	~~0.25~~	0.98	0.91	0.89
4-Jan-04	19.4	20.8	18	20.4	15.5	1.07	0.87	0.93	0.86	0.75	0.80	1.02	0.88
15-Apr-04	6.9	18.4	19	19	30	2.67	1.03	2.75	1.58	1.63	~~4.35~~	0.97	1.00
27-Apr-04	13.9	14	11.8	14.2	15	1.01	0.84	0.85	1.27	1.07	1.08	0.99	0.83
16-Jan-05	14.6	36.6	48.6	33.6	18.4	2.51	1.33	~~3.33~~	~~0.38~~	~~0.50~~	1.26	1.09	1.45
28-Jan-05	35.1	32.4	42.6	35	30.5	0.92	1.31	1.21	0.72	0.94	0.87	0.93	1.22
27-Feb-05	20.8	14.8	18.2	14.6	23.4	0.71	1.23	0.88	1.29	1.58	1.13	1.01	1.25
31-May-05	10.7	6.8	37.6	17.6	21	0.64	~~5.53~~	~~3.51~~	0.56	~~3.09~~	1.96	~~0.39~~	2.14
4-Jul-05	47.8	65	60.8	70.4	50.4	1.36	0.94	1.27	0.83	0.78	1.05	0.92	0.86
			AVERAGE RATIO			**1.32**	**1.02**	**1.35**	**1.05**	**1.09**	**1.49**	**0.99**	**1.11**
			LAPSE RATE (per 100 m)			**0.133**	**0.011**	**0.092**	**0.010**	**0.016**	**0.060**	**0.023**	**0.058**

The relationship between TWT rain gages and KE is meaningful. On the average, peak rainfalls of TWT gages are 30% more than KE peak rainfalls as expected due to elevation difference. However, the relationship between HO and TWT gages is not so satisfying. Even HO is located in a level that is twice the elevation of RG3, only 5% of peak rainfall increase is observed in HO. In a mountainous region, the percent peak rainfall increase with altitude, or in other words *rainfall lapse rate*, would be much higher than its current values. This phenomenon can be explained with the primary type of precipitation in HO region. The peak rainfalls generally are observed less than the expected values due to snow accumulation at the station. Even if you add 10% of the accumulated snow (which is done in the preparation of Table 5.4) to the peak rainfall in HO gage, it will not yield satisfactory ratios.

In a gaged basin like Yuvacık the two most suitable precipitation methods to be used in the meteorologic model are gage weights and inverse distance methods. In inverse distance precipitation method one or more *nodes* together with their *search distances* are specified in each subbasin and the *closeness* of each gage to the specified node(s) is determined from the latitude and longitude data of the gages. Search distance is specified in terms of kilometers or miles around each node, and the gages within this distance are considered in weight calculations. The gage weights are then determined from the distances of the gages to the specified node(s). The weight of gage *i* will be the inverse distance square of gage *i* divided by the sum of inverse distance squares of all the gages.

$$w_i = \frac{\dfrac{1}{d_i^{\,2}}}{\displaystyle\sum_{i=1}^{n} \frac{1}{d_i^{\,2}}} \tag{5.1}$$

where, w_i : weight of i^{th} rain gage,

d_i : distance of the i^{th} gage to the selected node,

n : number of rain gages within the search distance.

Inverse distance method may become an effective tool to be used in continuous simulations especially when one or more of the gages stop recording in the simulation period, because in such a case the method automatically neglects the stopped gages and assigns new weights to the working gages according to their inverse distance squares. The method has its drawback: it takes into account all the gages within the specified search distance. Are all the gages really necessary? The answer to this question will be a simple "No" after the discussion made on Table 5.4. Therefore, the method is applied explicitly with the model.

Gage weights precipitation method is used in the meteorologic models of Kirazdere, Kazandere and Serindere subbasin simulations. The weight of each gage (Table 5.5) is computed externally by using inverse distance weight formula (Equation 5.1). The distance of each gage to the *specified node* is used in the computations. *Centroid* of each subbasin is selected as the specified node.

Centroids of the subbasins are determined using HEC-GeoHMS add-in under ARC-View GIS program. HEC-GeoHMS finds three types of centroids for a given subbasin, namely Bounding Box Centroid, Longest Flow Path Centroid, and Ellipse Centroid. For example, all the three types of centroids for Kirazdere are shown graphically in Figure 5.4, and the related centroid data is given in Table 5.6.

Table 5.5. Gages and their weights for each subbasin

Kirazdere		Kazandere		Serindere	
Gage	**Weight**	**Gage**	**Weight**	**Gage**	**Weight**
RG3	0.5163	RG2	0.4423	RG4	0.8356
HO	0.4243	RG5	0.4925	HO	0.0922
KE	0.0595	HO	0.0428	KE	0.0722
		KE	0.0224		

The mean elevation of the subbasin will be the criterion to be used in selecting the centroid. The centroid that has the closest elevation to the mean elevation will better represent the hypsometry of the subbasin. From the comparison of centroid elevations (Table 5.6), one can conclude that ellipse centroid elevation is the closest to the mean elevation of subbasin in Kirazdere subbasin (Table 4.7) and for Kazandere and Serindere subbasins there is almost not any difference between the elevations of ellipse centroid and bounding box centroid. Therefore, ellipse centroid is chosen as the nodes for the subbasins. Longest flow path centroids for all the three subbasins have very low elevations compared to the mean elevations of subbasins, so they are not taken into consideration.

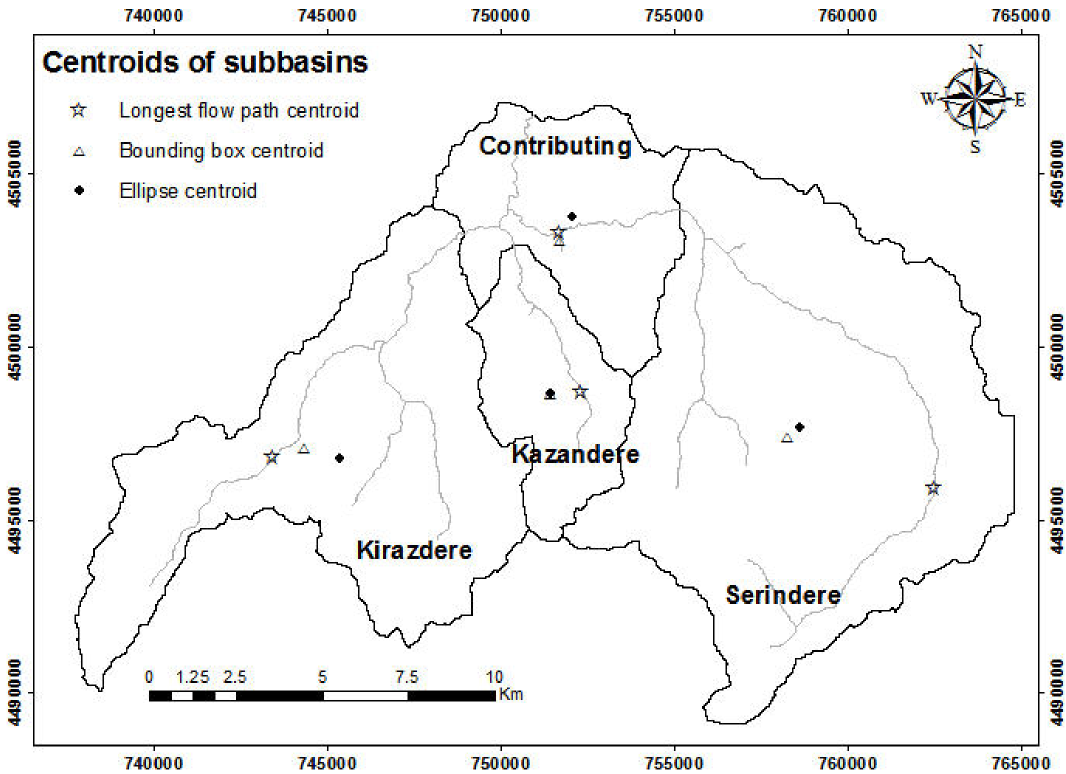

Figure 5.4. Subbasin centroids found in HEC-GeoHMS

Table 5.6. Coordinate and elevation information of subbasin centroids

Subbasin	Centroid	Xcoord (m)	Ycoord (m)	Elevation (m)
Kirazdere	Ellipse	745332	4496767	910
	Bounding Box	744225	4497062	819
	Longest Flow Path	743414	4496840	769
Kazandere	Ellipse	751417	4498647	907
	Bounding Box	751417	4498684	907
	Longest Flow Path	752339	4498721	704
Serindere	Ellipse	758571	4497688	1205
	Bounding Box	758203	4497467	1192
	Longest Flow Path	762554	4495918	667
Contributing	Ellipse	752007	4503774	231
	Bounding Box	751675	4503110	190
	Longest Flow Path	751638	4503368	165

5.1.2.2. Preparation of rainfall input files

TWT rain gages are recording rain gages and they record rainfall every 5 minutes. For all the selected events the rainfall records are summed into 1 hour records since the model will be calibrated in an hourly time interval and then hourly data is used in the rainfall gage data.

On the other hand, KE and HO gages are non-recording rain gages and they have daily cumulative rainfall data. These data are transformed into hourly rainfall data with a kind of fractioning approach; in the transformation process *double mass curve analysis* is used.

Double mass curve analysis is used in hydrometeorology as a test of the consistency of the rainfall at a given station by comparing its accumulated annual record with that of the accumulated annual, or seasonal mean values of several other nearby stations. Actually, the daily cumulative records of HO and KE stations are compared with the average daily rainfall of the TWT gages.

The average rainfall is named as DMS, which is computed from the sum of the rainfalls in working gages divided by the number of working gages. The hourly rainfall pattern in HO and KE is assumed to have the same temporal pattern of DMS. The cumulative rainfall in HO and KE is distributed throughout the day according to this pattern. In Table 5.7 a sample distribution of HO and KE rainfall according to DMS pattern is shown.

Besides rainfall, runoff data which is also collected at every 5 minutes is converted into 1 hour data by taking the averages of 5 minutes data in one hour.

5.1.3. Control specifications

Control specifications are one of the main components in a HEC-HMS project, even though they do not contain much parameter data (USACE-HEC, April 2006). They specify when the simulations start and end, and also the simulation time step (from 1 minute to 24 hours). As the name implies, in event based hourly simulations, the simulation time step is selected as 1 hour.

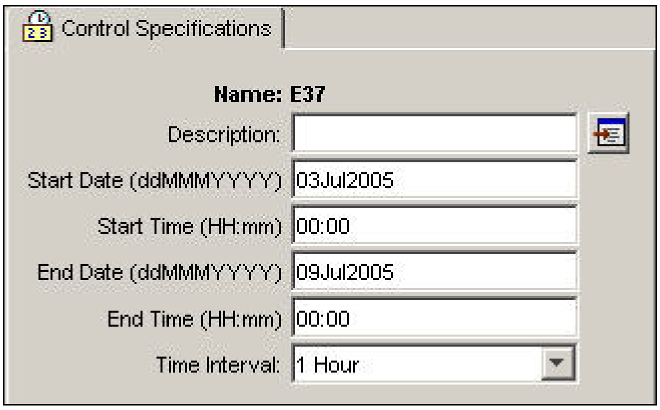

Figure 5.5. Control Specifications inputs table

Table 5.7. Hourly rainfall distribution of HO and KE gages based on the rainfall pattern of DMS average rainfall

(Rainfall is in mm)

DATE	RG1	RG2	RG3	RG4	RG5	RG6	DMS (Average of RG gages)	DMS HOURLY PERCENTS	KE HOURLY PATTERN	HO HOURLY PATTERN	DMS CUMUL.	KE CUMUL.	HO CUMUL.
7/12/2002 0:00													
7/12/2002 1:00													
7/12/2002 2:00													
7/12/2002 3:00													
7/12/2002 4:00													
7/12/2002 5:00													
7/12/2002 6:00													
7/12/2002 7:00													
7/12/2002 8:00						1,80	1,80	0,05	0,04	1,88	1,80	0,04	1,88
7/12/2002 9:00	12,80	21,60	14,60		22,20	13,00	16,84	0,50	0,35	17,57	18,64	0,39	19,45
7/12/2002 10:00											18,64	0,39	19,45
7/12/2002 11:00	4,40	0,60	2,40		0,80	0,20	1,68	0,05	0,04	1,75	20,32	0,42	21,20
7/12/2002 12:00											20,32	0,42	21,20
7/12/2002 13:00											20,32	0,42	21,20
7/12/2002 14:00											20,32	0,42	21,20
7/12/2002 15:00											20,32	0,42	21,20
7/12/2002 16:00						0,80	0,80	0,02	0,02	0,83	21,12	0,44	22,03
7/12/2002 17:00	7,00	9,80	10,40		10,60	1,60	7,88	0,23	0,16	8,22	29,00	0,61	30,25
7/12/2002 18:00	2,00	5,40	4,80		6,00		4,55	0,14	0,09	4,75	33,55	0,70	35,00
7/12/2002 19:00											33,55	0,70	35,00
7/12/2002 20:00											33,55	0,70	35,00
7/12/2002 21:00											33,55	0,70	35,00
7/12/2002 22:00											33,55	0,70	35,00
7/12/2002 23:00											33,55	0,70	35,00
7/13/2002 0:00											33,55	0,70	35,00
	26,20	**37,40**	**32,20**		**39,60**	**17,40**	**33,55**	**1,00**	**0,70**	**35,00**	33,55	0,70	35,00

5.1.4. Summary of calibration procedure

Each method in HEC-HMS has parameters. The values of these parameters should be entered as input to the model to obtain the simulated runoff hydrographs. Some of the parameters may be estimated by observation and measurements of stream and basin characteristics, but some of them can not be estimated. When the required parameters can not be estimated accurately, the model parameters are *calibrated,* i.e. in the presence of rainfall and runoff data the *optimum* parameters are found as a result of a systematic search process that yield the best fit between the observed runoff and the computed runoff. This systematic search process is called as *optimization.* Optimization begins from initial parameter estimates and adjusts them so that the simulated results match the observed streamflow as closely as possible. Two different search algorithms are provided that move from the initial estimates to the final best estimates: Nelder and Mead search algorithm and Univariate Gradient search algorithm. A variety of objective functions are provided to measure the goodness of fit between the simulated and observed streamflow in different ways such as: peak weighted RMS error, percent error peak, percent error volume, sum absolute residuals, sum squared residuals, and time-weighted error. Calibration procedure of HEC-HMS is summarized schematically in Figure 5.6.

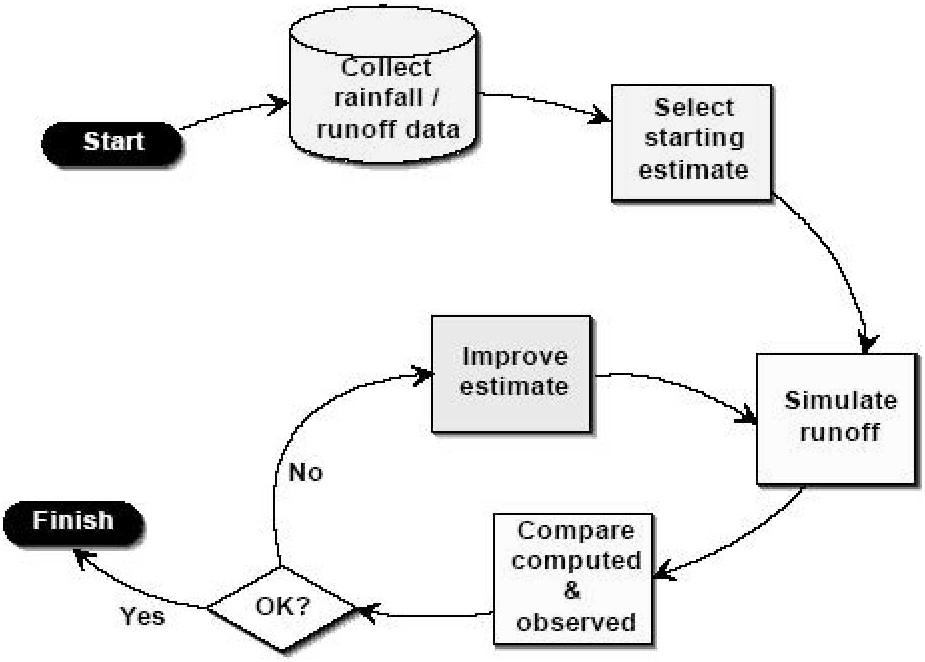

Figure 5.6. Schematic representation of calibration procedure (USACE-HEC, March 2000)

As can be seen from Figure 5.6, calibration procedure begins with data collection (rainfall and runoff data). The next step is to select initial estimates of the parameters. As with any search, the better these initial estimates are given (the starting point of the search), the quicker the search will yield a solution. Given these initial estimates of the parameters, the models of HEC-HMS can be used with the observed boundary conditions (rainfall) to compute the output, the watershed runoff hydrograph. At this point, HEC-HMS compares the computed hydrograph to the observed hydrograph. The goal of this comparison is to judge how well the model "fits" the real hydrologic system. If the fit is not satisfactory, HEC-HMS systematically adjusts the parameters and reiterates.

5.1.5. Goodness-of-fit indices in optimization process

To compare a computed hydrograph to an observed hydrograph, HEC-HMS computes an index of the goodness-of-fit. The quantitative measure of goodness of fit between the computed result from the model and the observed flow is called the objective function. An objective function measures the degree of variation between computed and observed hydrographs. It is equal to zero if the hydrographs are exactly identical. In HEC-HMS, one of six objective functions can be used in optimization procedure, depending upon the needs of the analysis. The goal of all optimization schemes is to find reasonable parameters that yield the minimum value of the objective function.

The first objective function that is to be mentioned is **sum of absolute errors.** This objective function compares each ordinate of the computed hydrograph with the observed, weighting each equally. The index of comparison, in this case, is the difference in the ordinates. However, as differences may be positive or negative, a simple sum would allow positive and negative differences to offset each other. In hydrologic modeling, both positive and negative differences are undesirable, as overestimates and underestimates as equally undesirable. To reflect this, the function sums the absolute differences. Thus, this function implicitly is a measure of fit of the magnitudes of the peaks, volumes, and times of peak of the two hydrographs.

The second objective function is **percent error in peak.** This measures only the goodness-of-fit of the computed hydrograph peak to the observed peak. It quantifies the fit as the absolute value of the difference, expressed as a percentage, thus treating overestimates and underestimates as equally undesirable. It does not reflect errors in volume or peak timing. This objective function is a logical choice if the information needed for designing or planning is limited to peak flow or peak stages. This might be the case for a floodplain management study that seeks to limit development in areas subject to inundation.

The third objective function is **percent error in volume.** This function measures only the goodness-of-fit of the computed hydrograph volume to the observed volume. The peak and the timing of the peak are of no concern. This function is a logical choice where the subject of the hydrologic study is primarily the total volume of discharges, e.g. reservoir operation studies.

The fourth objective function is **peak-weighted root mean square error.** It compares all ordinates, squaring differences, and it weights the squared differences. The weight assigned to each ordinate is proportional to the magnitude of the ordinate. Ordinates greater than the mean of the observed hydrograph are assigned a weight greater than a unity and those smaller, a weight less than unity. The peak observed ordinate is assigned the maximum weight. The sum of the weighted, squared differences is divided by the number of computed hydrograph ordinates; thus, yielding the mean squared error. Taking the square root yields the root mean squared error. This function is an implicit measure of comparison of the magnitudes of the peaks, volumes, and times of peak of the two hydrographs.

The fifth objective function is **sum of squared residuals.** This is a commonly-used objective function for model calibration. It too compares all ordinates, but uses the squared differences as the measure of fit. Thus a difference of 10 m^3/sec "scores" 100 times worse than a difference of 1 m^3/sec. Squaring the differences also treats overestimates and underestimates as undesirable. This function too is implicitly a measure of the comparison of the magnitudes of the peaks, volumes, and times of peak of the two hydrographs.

Finally, the sixth objective function is **time-weighted error.** It too compares all ordinates, but gives greater weight to errors near the end of the optimization time window and less weight to errors early in the window.

5.1.6. Simulation runs and optimization trials

After creating basin model, meteorologic model and control specifications for each of the three subbasins (Kirazdere, Kazandere, and Serindere) as specified in the upper sections, **simulation runs** are created in HEC-HMS to compute the output (runoff hydrograph) with the initial parameter estimates. Simulation runs produce a graph to visually compare observed hydrograph with the computed (simulated) hydrograph and several tables such as summary results table (where peak discharges, total discharge volumes, total precipitation, baseflow, loss, direct runoff, average absolute residuals, and total residuals can be seen), and time series results table (where the results can be seen at each time step). According to the obtained results, initial parameter estimates are refined.

After that, the iterative optimization process starts with the creation of **optimization trials** in HEC-HMS. Optimization trials require the simulation start and end times and simulation time step. This information can not be beyond the range of previously defined temporal information in control specifications.

In an optimization trial not every parameter specified in loss or baseflow methods can be optimized. For example, gridded data and meteorologic model data like gage weights, snow module data can not be optimized. A full list of all the parameters that can be optimized in an optimization trial is given in User's Manual of HEC-HMS (USACE-HEC, April 2006).

All the parameters of exponential loss method (initial range, initial coefficient, exponent, and coefficient ratio) and baseflow recession method (initial discharge, recession constant, and recession threshold flow) can be optimized. However, only the parameters of exponential loss method except coefficient ratio (which is taken as equal to "1" in all of the events) are optimized in this study. Recession parameters are determined from observed flow hydrographs for each event; and these parameters are locked in optimization trials.

Optimization trials give several different output tables and graphs some of which are worth mentioning here:

- Objective function table: Peak flow and total flow volume values of observed and simulated hydrographs and the percent differences between these values are given in this table. Also, time to peak and basin lag information is given.
- Optimized parameters table: Parameters names, initial parameter values and optimized parameters together with objective function sensitivity are presented in this table.
- Element summary table: Presents similar information as the summary results table of a simulation run.
- Hydrograph comparison graph: Observed hydrograph is plotted in the same time scale with simulated hydrograph to supply a visual comparison.

5.1.7. Model performance measures

Simulated (predicted) flow and the observed flow relationship is the main tool used in hydrology to asses the performance of a hydrologic model. In general, the differences between the simulated and observed flow data are computed using several different mathematical expressions, i.e. goodness-of-fit criteria, to show whether the model yields satisfactory predictions.

In this chapter, graphical evaluation of the goodness-of-fit between the predicted and the observed hydrographs of the event-based hourly simulations of all the three subbasins, Kirazdere, Kazandere, and Serindere is given. Then, the goodness-of-fit criteria supplied by HEC-HMS software such as average absolute residuals and total residuals, percent errors (differences) in peak and volume are presented. Later on, two widely used statistical criteria for the model performance evaluation in hydrology are given, namely, Pearson's coefficient of determination (R^2) and Nash and Sutcliffe model efficiency (NSE).

At the last section of the chapter, all the model performance evaluation criteria that are found for the event-based hourly simulations are summarized in tabular form.

5.1.7.1. Graphical evaluation

A hydrologic modeling study, most probably, can not be performed without the extensive use of graphical comparisons of predicted and observed flows and hydrologic modeling software which does not have such graphical comparison tools will not be of use to a hydrologist dealing with a modeling study. With the advances in computer technology, in both hardware and software, modeling software graphical representation tools have developed in favor of the hydrologist that uses the software.

HEC-HMS software has powerful graphical tools to represent different simulation and optimization results, such as hydrograph comparison graphs, flow comparison graphs, precipitation, temperature graphs, snow water equivalent graphs, etc. The capability to show the results in graphical form enables the hydrologist (modeler) to make his/her first evaluation about the simulation results. Hydrologist decides on whether the peaks, shapes of the hydrographs are consistent or something is going wrong. Then continues with optimization of the parameters if predicted and observed hydrographs seem to fit well, or changes the model parameters as required if the visual fit is not satisfactory.

In this thesis study, to visually evaluate the results of the event-based hourly simulations three categories are determined as: Good, Moderate, and Poor according to the visual fit between predicted and observed flows. In Tables 5.8 to 5.10, the graphical evaluation category for each event is given for the three subbasins. Obviously, this graphical evaluation is subjective. One event that is categorized here as “Good” may be evaluated as “Moderate” by a different hydrologist, or vice versa.

5.1.7.2. Performance criteria supplied in HEC-HMS

Residuals

HEC-HMS presents two different residual values in the simulation result tables: average absolute residuals and total residuals. As their names imply, average absolute residual is the average of absolute values of the differences between predicted hydrograph ordinates and observed hydrograph ordinates. This value is given in m^3/s. The lesser this value the better the model performance is. Total residual given in millimeters, is the sum of the differences between the hydrograph ordinates multiplied by the time increment of the hydrographs and divided by the subbasin area. Usually, a value of total residual close to "0" may not mean a good fit, because negative and positive residuals may cancel each other. Residual values of each event simulation are given in Tables 5.8 to 5.10.

Percent peak and volume differences

HEC-HMS demonstrates the percent differences (errors) between the predicted and observed flow peak and volumes in "objective function" results table in an optimization trial result. The computation principle is very simple when determining these percent differences as given in Equation 5.2 and 5.3.

$$\%\ \text{Peak Error} = [\ (Opt_{peak} - Obs_{peak}) / Obs_{peak}\ ] \times 100 \qquad (5.2)$$

$$\%\ \text{Volume Error} = [(Opt_{vol} - Obs_{vol}) / Obs_{vol}\ ] \times 100 \qquad (5.3)$$

where, Opt_{peak} and Obs_{peak} are optimized and observed flow peaks, respectively; and Opt_{vol} and Obs_{vol} are optimized and observed flow volumes, respectively.

These percent differences are not given in the summary result tables of simulation runs in HEC-HMS, so these values have to be computed manually using Equations 5.2 and 5.3 after a simulation.

Percent error in peak does not give any information about hydrograph shape, volume and peak timing, so it must be used only when peak flow is taken into consideration. Similarly, percent error in volume is an index showing only the volume difference between predicted and observed flows, so it must be used in a performance evaluation only when flow volume is of primary concern.

5.1.7.3. Statistical performance criteria

Coefficient of determination (R^2)

The coefficient of determination is the square of the Pearson's Product Moment Correlation Coefficient (Pearson, 1932) and describes the proportion of the total variance in the observed data that can be explained by the model. It is defined with the ratio of explained variation to the total variation (EV/TV) (McCuen, 1993). It ranges from 0.0 (poor model) to 1.0 (perfect model) and is given by:

$$R^2 = \left[\frac{\sum_{i=1}^{N} \left(O_i - \overline{O}\right)\left(P_i - \overline{P}\right)}{\left[\sum_{i=1}^{N} \left(O_i - \overline{O}\right)^2\right]^{0.5} \left[\sum_{i=1}^{N} \left(P_i - \overline{P}\right)^2\right]^{0.5}} \right] \tag{5.4}$$

where, P: predicted data and O: observed data, and the overbar denotes the mean for the entire period of the evaluation.

The correlation based coefficient of determination have been widely used to evaluate the goodness-of-fit of hydrologic and hydroclimatic models. It is oversensitive to extreme values (outliers) and is insensitive to additive and proportional differences between model predictions and observations (Legates, 1999). These limitations are well documented in the literature (Willmott, 1981; Moore, 1991; Kessler and Neas, 1994). However, coefficient of determination is still widely used in hydrological model performance evaluation.

Computed coefficient of determination values for each of the events for each of the subbasins are given in Tables 5.8 to 5.10.

Nash and Sutcliffe model efficiency (NSE)

NSE is widely used to evaluate the performance of hydrologic models (e.g. Şorman, A. A., 2005; Wilcox et al., 1990). NSE is defined by Nash and Sutcliffe (1970) which ranges from minus infinity (poor model) to 1.0 (perfect model) as:

$$\mathrm{NSE} = 1 - \frac{\sum_{i=1}^{N} (O_i - P_i)^2}{\sum_{i=1}^{N} (O_i - \overline{O})^2} \qquad (5.5)$$

where, P: predicted data and O: observed data, and the overbar denotes the mean for the entire period of the evaluation. If the value of NSE is less than "0", then the observed mean flow is better than the model prediction. If the value of NSE is equal to "0", then the observed mean is as good as the model prediction. Values of NSE from "0" approaching to "1" show the increasing improvement obtained by the model prediction over the observed mean flow. NSE is an improved evaluation index compared to R^2 because it is sensitive to differences in the observed and simulated means and variances (Legates, 1999). But NSE is oversensitive to outliers, too. Computed NSE values for each event are given in Tables 5.8 to 5.10.

5.1.8. Parameter calibration results

The model calibration studies started with a user defined unit hydrograph and exponential loss method. The selected storm events from Category 1 (Section 4.4), are simulated first, and then the simulation parameters are used as initial values in model optimization stage. The available search algorithms can only find local optimum values of calibrated parameters; therefore, the calibrated parameters are not global optimum values. The detailed results of model simulations and optimizations with respect to each of the objective functions are presented with summary tables and simulation and optimization graphs for Kirazdere, Kazandere and Serindere subbasins in Appendix A (only one Event is given as an example for each of the subbasins). Also, observed and simulated flow graphs of all events are given in Appendix B. The model calibration studies are carried out with one hour data and run time step.

All of the goodness of fit criteria discussed in Section 5.1.5 is taken into account and model parameters are optimized for each criterion separately. At the end of each model calibration stage, observed and simulated peak discharge values (m^3/s), hydrograph volumes (mm), and time to peak (hr) values are compared. The computed average absolute and total residuals of each event calibration are evaluated together with the percent error in volume and percent error in peak of simulated and observed hydrographs to decide on the appropriate model parameter set for that specific event.

Kirazdere, Kazandere and Serindere subbasins were optimized for 14, 8 and 9 rainfall events, respectively. The summary tables (Table 5.8 - 5.10) present the selected model parameters at the end of each optimization together with computed statistics related with model calibration and general information about the event for each subbasin. In these tables two statistical criteria that are not given by HEC-HMS but computed externally are given: Coefficient of Determination (R^2) and Nash and Sutcliffe model efficiency (NSE, or E) (Nash and Sutcliffe, 1970). In the model calibration stage, exponential loss method, parameters of initial range, initial coefficient and exponent are optimized, other parameters are provided to the model within their physical ranges from the observed hydrograph (base flow parameters) or computed values (unit hydrograph).

Visual comparisons of optimized and observed hydrographs are used besides the statistical criteria to evaluate the results and decide on the optimum model parameter set. Rainfall events are further grouped into fall (A), winter (B), spring (C) and summer seasons (D). Most of the events occur during spring including rainfall, snow accumulation and snowmelt, and summer periods with rainfall only. Model parameters are expected to be consistent and changed in a range within each season, Table 5.11 - 5.13 can be referred for the average parameter values of events in each period and minimum and maximum range of model parameters for each sub-basin, respectively. The model parameter set is chosen based on a kind of multi-variable criteria including both the minimum percent peak difference and minimum percent volume difference as a result of optimization scheme of each objective function. The objective function that provides best estimates of model parameters in terms of both peak and volume difference between optimized and observed hydrographs is selected at the end of each model calibration stage. Generally, percent error peak, described in Section 5.1.5, is found as the most effective objective function to find the local optimum parameter set for both peak discharge and total discharge.

Table 5.8. Kirazdere optimization parameters summary table

	Seasons	Fall (Sep.-Oct.-Nov.)	Winter (Dec.-Jan.-Feb.)		Spring (Mar.-Apr.-May)				
	Event ID	E40	E24	E33	E5	E7	E8	E16	E41
	Period	15-19Nov2004	4-7Jan2004	27Jan-2Feb2005	21-23Mar2002	5-9Apr2002	16-19Apr2002	13-18Apr2003	5-10Mar2005
	Selected Objective Function	Percent Error Peak	Percent Error Peak	Percent Error Peak	Percent Error Peak	Percent Error Peak	Percent Error Peak	Percent Error Peak	Percent Error Peak
Exponential Loss	**Initial Range (mm)**	15.70	15.00	21.23	17.84	23.52	21.41	17.93	11.76
	Initial Coef ((mm/hr)^(1-x))	0.93	0.95	0.89	0.94	0.56	0.89	0.91	0.78
	Coef Ratio	1.00	1.00	1.00	1.00	1.00	1.00	1.00	1.00
	Exponent	0.94	0.96	0.93	0.96	1.00	0.97	0.90	0.88
Recession	**Initial Discharge (m^3/s)**	0.40	2.00	2.50	2.44	4.50	2.60	4.50	3.60
	Recession Constant	0.70	0.80	0.80	0.90	0.80	0.85	0.80	0.70
	Threshold Flow (m^3/s)	0.50	3.00	6.00	2.50	6.60	4.20	5.00	10.00
Summary Results	**Total Precipitation (mm)**	16.82	28.50	102.61	14.34	48.88	24.52	25.72	36.23
	Total Loss (mm)	16.41	27.32	87.43	14.06	29.58	22.88	23.26	27.04
	Total Baseflow (mm)	0.93	6.77	24.19	5.06	19.42	8.43	19.07	26.22
	Peak Discharge (m^3/s)	1.06	4.00	14.63	3.23	21.60	4.79	9.43	20.76
	Total Discharge (mm)	1.33	7.92	39.01	5.38	38.16	10.03	21.47	35
	Avg Absolute Residual (m^3/s)	0.09	0.40	1.69	0.11	2.84	0.15	0.45	1.12
	Total Residual (mm)	0.00	-0.60	-7.70	-0.10	-0.20	-0.40	-2	-1.10
	Peak Difference (%)	0.00	-1.48	0.00	0.00	-0.05	-0.21	0.00	0.39
	Volume Difference (%)	-0.75	-9.07	-16.41	-1.31	-0.42	-3.65	-8.44	-3.07
	R^2	0.63	0.46	0.64	0.74	0.37	0.93	0.90	0.80
	NSE	0.62	0.36	0.52	0.66	0.10	0.88	0.83	0.79
	Graphical	Moderate	Moderate	Poor	Moderate	Poor	Good	Good	Good

Table 5.8. Kirazdere optimization parameters summary table (continued…)

Seasons		Summer (Jun.-Jul.-Aug.)					
Event ID		E10	E31	E36	E37	E38	E39
Period		11-15Jul2002	9-11Jun2004	31May-6Jun2005	4-9Jul2005	19-21Jun2004	23-25Jun2004
Selected Objective Function		Percent Error Peak	Percent Error Peak	Percent Error Volume	Percent Error Peak	Percent Error Peak	Sum Absolute Residuals
Exponential Loss	**Initial Range (mm)**	18.12	16.00	19.59	15.37	23.91	21.16
	Initial Coef ((mm/hr)^(1-x))	0.94	0.98	0.93	0.94	0.97	0.96
	Coef Ratio	1.00	1.00	1.00	1.00	1.00	1.00
	Exponent	0.96	0.99	0.96	0.97	0.98	0.97
Recession	**Initial Discharge (m^3/s)**	0.37	1.50	1.15	1.13	1.40	1.37
	Recession Constant	0.75	0.90	0.75	0.70	0.80	0.90
	Threshold Flow (m^3/s)	1.20	1.60	5.60	3.00	1.60	1.80
Summary Results	**Total Precipitation (mm)**	37.43	28.11	56.91	51.66	22.14	21.24
	Total Loss (mm)	34.46	27.60	52.84	46.98	21.87	20.75
	Total Baseflow (mm)	2.93	3.16	20.00	7.08	2.88	3.04
	Peak Discharge (m^3/s)	8.43	2.56	9.00	8.75	2.08	2.45
	Total Discharge (mm)	5.83	3.64	23.96	11.63	3.14	3.52
	Avg Absolute Residual (m^3/s)	0.28	0.17	0.82	0.42	0.10	0.15
	Total Residual (mm)	0.60	0.10	1.00	-0.40	-0.10	-0.10
	Peak Difference (%)	0.00	6.67	-1.96	0.00	0.00	0.41
	Volume Difference (%)	11.05	2.54	4.36	-3.00	-3.68	-3.83
	R^2	0.83	0.10	0.65	0.86	0.56	0.60
	NSE	0.63	-1.64	0.64	0.84	-0.31	0.48
	Graphical	Good	Poor	Poor	Good	Poor	Poor

Table 5.9. Kazandere optimization parameters summary table

	Seasons	Fall (Sep.-Oct.-Nov.)	Winter (Dec.-Jan.-Feb.)		Spring (Mar.-Apr.-May)	Summer (Jun.-Jul.-Aug.)			
	Event ID	E40	E24	E33	E41	E36	E37	E38	E39
	Period	16-19Nov2004	4-7Jan2004	27Jan-2Feb2005	5-10Mar2005	31May-6Jun2005	5-9Jul2005	19-21Jun2004	23-25Jun2004
	Selected Objective Function	Percent Error Peak	Percent Error Peak	Percent Error Peak	Percent Error Peak	Percent Error Peak	Percent Error Peak	Percent Error Peak	Percent Error Peak
Exponential Loss	Initial Range (mm)	15.70	13.52	12.73	11.76	18.73	16.00	16.00	12.00
	Initial Coef ((mm/hr)^(1-x))	0.95	0.88	0.81	0.81	0.82	0.92	0.96	0.80
	Coef Ratio	1.00	1.00	1.00	1.00	1.00	1.00	1.00	1.00
	Exponent	0.97	0.91	0.91	0.92	0.93	0.95	0.98	0.90
Recession	Initial Discharge (m^3/s)	0.09	2.00	0.65	1.00	0.13	0.45	0.16	0.23
	Recession Constant	0.70	0.80	0.80	0.80	0.75	0.70	0.70	0.70
	Threshold Flow (m^3/s)	0.15	3.00	2.00	1.75	1.60	2.00	0.24	0.25
Summary Results	Total Precipitation (mm)	26.45	33.36	80.77	38.02	47.12	72.83	17.43	6.67
	Total Loss (mm)	25.49	29.69	62.55	30.20	37.12	61.34	16.97	5.83
	Total Baseflow (mm)	0.82	15.85	26.59	22.77	19.26	14.66	1.21	1.36
	Peak Discharge (m^3/s)	0.48	3.80	5.04	5.02	4.75	6.20	0.57	0.74
	Total Discharge (mm)	1.76	23.31	44.35	30.38	29.02	25.87	1.67	2.17
	Avg Absolute Residual (m^3/s)	0.05	0.38	0.85	0.71	0.40	0.59	0.05	0.04
	Total Residual (mm)	0.00	-3.30	-14.50	-10.40	0.00	-1.70	0.00	0.20
	Peak Difference (%)	0.00	0.26	0.80	0.80	0.00	0.20	0.00	0.00
	Volume Difference (%)	2.92	-13.94	-24.59	-25.52	-0.07	-6.00	-2.34	9.05
	R^2	0.67	0.68	0.45	0.26	0.62	0.72	0.21	0.70
	NSE	0.56	0.54	0.21	-0.05	0.61	0.66	-0.19	0.50
	Graphical	Moderate	Moderate	Poor	Poor	Poor	Moderate	Poor	Good

Table 5.10. Serindere optimization parameters summary table

Seasons		Fall (Sep.-Oct.-Nov.)	Winter (Dec.-Jan.-Feb.)		Spring (Mar.-Apr.-May)		Summer (Jun.-Jul.-Aug.)			
Event ID		E40	E24	E33	E16	E41	E36	E37	E38	E39
Period		15-19Nov2004	4-7Jan2004	27Jan-2Feb2005	12-18Apr2003	5-10Mar2005	31May-6Jun2005	4-9Jul2005	19-21Jun2004	23-25Jun2004
Selected Objective Function		Percent Error Peak	Percent Error Peak	Percent Error Peak	Percent Error Peak	Percent Error Peak	Percent Error Peak	Percent Error Peak	Percent Error Peak	Percent Error Peak
Exponential Loss	**Initial Range (mm)**	26.46	7.03	16.60	8.01	8.84	23.52	9.40	5.99	6.82
	Initial Coef ((mm/hr)^(1-x))	0.98	0.94	0.91	0.90	0.82	0.94	0.95	0.90	0.96
	Coef Ratio	1.00	1.00	1.00	1.00	1.00	1.00	1.00	1.00	1.00
	Exponent	0.99	0.97	0.94	0.93	0.85	0.98	0.98	0.88	0.97
Recession	**Initial Discharge (m^3/s)**	0.20	4.00	1.30	8.20	3.00	1.00	0.75	1.20	1.02
	Recession Constant	0.80	0.80	0.80	0.80	0.80	0.80	0.70	0.70	0.80
	Threshold Flow (m^3/s)	0.50	5.00	5.00	10.00	5.00	3.00	4.00	1.20	1.00
Summary Results	**Total Precipitation (mm)**	41.03	35.72	78.49	27.09	37.28	55.32	118.89	4.54	4.08
	Total Loss (mm)	40.57	33.31	70.09	23.84	28.59	51.90	108.55	4.29	3.99
	Total Baseflow (mm)	0.63	7.24	14.90	24.55	13.99	6.34	6.84	1.41	1.24
	Peak Discharge (m^3/s)	1.22	9.57	12.95	14.52	28.53	9.97	19.01	1.61	1.21
	Total Discharge (mm)	1.07	9.58	23.10	27.72	22.40	9.68	16.92	1.65	1.33
	Avg Absolute Residual (m^3/s)	0.17	0.51	0.95	0.87	1.40	0.74	1.45	0.13	0.09
	Total Residual (mm)	-0.30	-0.80	0.90	-2.7	-0.70	-1.80	4.50	0.00	-0.10
	Peak Difference (%)	0.83	0.00	1.33	0.00	0.04	1.63	0.00	0.00	0.00
	Volume Difference (%)	-24.11	-8.15	3.91	-8.76	-3.07	-15.97	36.01	2.48	-5.67
	R^2	0.53	0.84	0.62	0.90	0.85	0.74	0.59	0.08	0.05
	NSE	0.49	0.78	0.56	0.78	0.85	0.64	0.31	-0.29	-0.98
	Graphical	Poor	Good	Moderate	Good	Good	Moderate	Poor	Poor	Poor

Table 5.11. Kirazdere optimization parameters summary statistics

Season				Fall (Sep.-Oct.-Nov.)	Winter (Dec.-Jan.-Feb.)	Spring (Mar.-Apr.-May)	Summer (Jun.-Jul.-Aug.)				
ID (Seasonal)				A	B	C	D				
Number of Events				1	2	5	6	14			
Parameter Statistics		Minimum		Seasonal Average				Overall Average	Maximum		Range
Exponential Loss	**Initial Range (mm)**	11.76	C	15.70	18.12	18.49	19.02	18.47	23.91	D	0.001 - 500
	Initial Coef ((mm/hr)^(1-x))	0.56	C	0.93	0.92	0.82	0.95	0.90	0.98	D	0.001 - 100
	Coef Ratio	1.00	All	1.00	1.00	1.00	1.00	1.00	1.00	All	0.275 - 1
	Exponent	0.88	C	0.94	0.95	0.94	0.97	0.95	1.00	C	0.001 - 1
Recession	**Initial Discharge (m^3/s)**	0.37	D	0.40	2.25	3.53	1.15	2.10	4.50	C	0.001 - 100000
	Recession Constant	0.70	A,C,D	0.70	0.80	0.81	0.80	0.80	0.90	C,D	0.00001 - 1
	Threshold Flow (m^3/s)	0.50	A	0.50	4.50	5.66	2.47	3.76	10.00	C	0.001 - 100000
Summary Results	**Total Precipitation (mm)**	14.34	C	16.82	65.56	29.94	36.25	36.79	102.61	B	-
	Total Loss (mm)	14.06	C	16.41	57.38	23.36	34.08	32.32	87.43	B	-
	Total Baseflow (mm)	0.93	A	0.93	15.48	15.64	6.52	10.66	26.22	C	-
	Peak Discharge (m^3/s)	1.06	A	1.06	9.32	11.96	5.55	8.06	21.60	C	-
	Total Discharge (mm)	1.33	A	1.33	23.47	22.01	8.62	15.00	39.01	B	-
	Avg Absolute Residual (m^3/s)	0.09	A	0.09	1.05	0.93	0.32	0.63	2.84	C	-
	Total Residual (mm)	-7.70	B	0.00	-4.15	-0.76	0.18	-0.79	1.00	D	-
	Peak Difference (%)	-1.96	D	0.00	-0.74	0.03	0.85	0.27	6.67	D	-
	Volume Difference (%)	-16.41	B	-0.75	-12.74	-3.38	1.24	-2.55	11.05	D	-

Table 5.12. Kazandere optimization parameters summary statistics

Season				Fall (Sep.-Oct.-Nov.)	Winter (Dec.-Jan.-Feb.)	Spring (Mar.-Apr.-May)	Summer (Jun.-Jul.-Aug.)				
ID (Seasonal)				A	B	C	D				
Number of Events				1	2	1	4	8			
Parameter Statistics		Minimum		Seasonal Average				Overall Average	Maximum		Range
Exponential Loss	**Initial Range (mm)**	11.76	C	15.70	13.13	11.76	15.68	14.56	18.73	D	0.001 - 500
	Initial Coef ((mm/hr)^(1-x))	0.80	D	0.95	0.85	0.81	0.87	0.87	0.96	D	0.001 - 100
	Coef Ratio	1.00	All	1.00	1.00	1.00	1.00	1.00	1.00	All	0.275 - 1
	Exponent	0.90	D	0.97	0.91	0.92	0.94	0.93	0.98	D	0.001 - 1
Recession	**Initial Discharge (m^3/s)**	0.09	A	0.09	1.33	1.00	0.24	0.59	2.00	B	0.001 - 100000
	Recession Constant	0.70	A, D	0.70	0.80	0.80	0.71	0.74	0.80	B,C	0.00001 - 1
	Threshold Flow (m^3/s)	0.15	A	0.15	2.50	1.75	1.02	1.37	3.00	B	0.001 - 100000
Summary Results	**Total Precipitation (mm)**	6.67	D	26.45	57.07	38.02	36.01	40.33	80.77	D	-
	Total Loss (mm)	5.83	D	25.49	46.12	30.20	30.32	33.65	62.55	D	-
	Total Baseflow (mm)	0.82	A	0.82	21.22	22.77	9.12	12.82	26.59	B	-
	Peak Discharge (m^3/s)	0.48	A	0.48	4.42	5.02	3.07	3.33	6.20	B	-
	Total Discharge (mm)	1.67	D	1.76	33.83	30.38	14.68	19.82	44.35	B	-
	Avg Absolute Residual (m^3/s)	0.04	D	0.05	0.62	0.71	0.27	0.38	0.85	D	-
	Total Residual (mm)	-14.50	B	0.00	-8.90	-10.40	-0.38	-3.71	0.20	D	-
	Peak Difference (%)	0.00	D	0.00	0.53	0.80	0.05	0.26	0.80	All	-
	Volume Difference (%)	-25.52	C	2.92	-19.27	-25.52	0.16	-7.56	9.05	D	-

Table 5.13. Serindere optimization parameters summary statistics

Season				Fall (Sep.-Oct.-Nov.)	Winter (Dec.-Jan.-Feb.)	Spring (Mar.-Apr.-May)	Summer (Jun.-Jul.-Aug.)				
ID (Seasonal)				A	B	C	D				
Number of Events				1	2	2	4	9			
Parameter Statistics		Minimum		Seasonal Average				Overall Average	Maximum		Range
Exponential Loss	**Initial Range (mm)**	5.99	D	26.46	11.82	8.42	11.43	12.52	26.46	A	0.001 - 500
	Initial Coef ((mm/hr)^(1-x))	0.82	C	0.98	0.93	0.86	0.94	0.92	0.98	A	0.001 - 100
	Coef Ratio	1.00	All	1.00	1.00	1.00	1.00	1.00	1.00	All	0.275 - 1
	Exponent	0.85	C	0.99	0.96	0.89	0.95	0.94	0.99	A	0.001 - 1
Recession	**Initial Discharge (m^3/s)**	0.20	A	0.20	2.65	5.60	0.99	2.30	8.20	C	0.001 - 100000
	Recession Constant	0.70	D	0.80	0.80	0.80	0.75	0.78	0.80	All	0.00001 - 1
	Threshold Flow (m^3/s)	0.50	A	0.50	5.00	7.50	2.30	3.86	10.00	C	0.001 - 100000
Summary Results	**Total Precipitation (mm)**	4.08	D	41.03	57.11	32.19	45.71	44.72	118.89	D	-
	Total Loss (mm)	3.99	D	40.57	51.70	26.22	42.18	40.57	108.55	D	-
	Total Baseflow (mm)	0.63	A	0.63	11.07	19.27	3.96	8.57	24.55	C	-
	Peak Discharge (m^3/s)	1.21	D	1.22	11.26	21.53	7.95	10.95	28.53	C	-
	Total Discharge (mm)	1.07	A	1.07	16.34	25.06	7.40	12.61	27.72	C	-
	Avg Absolute Residual (m^3/s)	0.09	D	0.17	0.73	1.14	0.60	0.70	1.45	D	-
	Total Residual (mm)	-2.70	C	-0.30	0.05	-1.70	0.65	-0.11	4.50	D	-
	Peak Difference (%)	0.00	B,C,D	0.83	0.67	0.02	0.41	0.42	1.63	D	-
	Volume Difference (%)	-24.11	A	-24.11	-2.12	-5.91	4.21	-2.59	36.01	D	-

5.1.9. Discussion of results

The first simulation studies began with rainfall events in Kirazdere subbasin due to FP1's relatively high performance for the selected events. According to model calibration for Kirazdere subbasin two events resulted in different values for initial coefficient and exponent parameters (Table 5.8); these are Event 7 and Event 41 in which peak discharges (21.60 and 20.76 m^3/s, respectively) and thus, excess precipitation values after subtracting the losses are high compared to that of other events. Initial coefficient of loss method is reduced to 0.56 and 0.78 for these specific events, and model parameter for exponent reaches to its highest (1.0) and lowest values (0.88), respectively. Comparable high rainfall amount recorded at Hacıosman station might have led to unexpectedly high flows in the observed hydrograph of Event 7.

Model calibration studies for Kazandere subbasin includes comparatively less number of events due to the fact that FP2 had not recorded properly during most of the rainfall events. The optimized model parameter set seems more scattered compared to that of Kirazdere subbasin (Table 5.9 and 5.10), however, due to relatively small peaks (0.5-5.0 m^3/s), these parameters are not as sensitive as in Kirazdere calibration. Since the characteristics of observed hydrographs of events 33, 37 and 41 are different than that of the other hydrographs characteristics, the percent volume difference values are slightly larger for these events.

Model calibration studies for Serindere subbasin also includes comparatively less number of events due to the fact that FP3 had not recorded properly during most of the rainfall events. Since the peaks of storm events are relatively high compared to Kazandere peak runoffs, model parameters are less scattered as in the case of Kazandere.

At the end of the overall model calibration, one may refer to Table 5.11 - 5.13 for the range of model parameter sets corresponding to different seasons of the water year. The average values of model parameters, especially for that of exponential loss method are close to each other. Initial coefficient is 0.90, 0.87, and 0.92 for Kirazdere, Kazandere and Serindere, respectively. Exponent is 0.95, 0.94, and 0.94 for Kirazdere, Kazandere and Serindere, respectively. Performance criteria given in Tables 5.8 - 5.10 indicate that both the percent volume and peak differences are less than 15% except for 1, 2 and 3 events for Kirazdere, Kazandere and Serindere subbasins. Overall evaluation for the percent error in peak and volume shows that the average values are well below five percent.

All of the criteria mentioned in the previous sections should be considered together for the evaluation of the simulation results of HEC-HMS. Simulation graphics (Appendix B) should be examined carefully together with the residuals, percent errors and statistical indices. Depending primarily on one of the evaluation criteria may mislead the modeler. For example, for Event 7 of Kirazdere subbasin, percent peak and volume errors are almost zero, however, it is classified as “poor” if visual evaluation is considered (Appendix B, Figure B.5) and computed R^2 and NSE values are 0.37 and 0.1, respectively (Table 5.8). The decrease in these indices is due to the unexpected peaks (outliers) simulated by the model (e.g. peaks at the second part of the simulation period), because as previously said these indices are oversensitive to outliers.

In Event 40 of Serindere, R^2 and NSE values are found as 0.53 and 0.49, respectively, which can be accepted as satisfactory, but visual evaluation of the event is made as “poor”, and also percent volume error is nearly 25% (underestimation) (Table 5.10).

In all of the events percent peak errors are less than 6.67% in all of the subbasins. Percent volume error goes as much as 36% (Event 37 of Serindere) but in generally stays less than 20% which is very satisfactory. In general poor results are obtained for all of the subbasins (except Event 39 of Kazandere and Event 40 for Kirazdere) when peak flows are less than 5 m^3/s and total volumes are less than 4 mm (Tables 5.8 to 5.10).

5.2. Snow-period daily simulations

5.2.1. Snowmelt component of HEC-HMS

Snowmelt is one of the three meteorologic components available in HEC-HMS. It has two snowmelt methods such as: gridded temperature index and temperature index. In this study *temperature index method* is used.

Snowmelt component considers the previously computed precipitation data by the precipitation method (in this study, *gage weights*) and according to the temperature data that is specified by a temperature gage determines whether the precipitation is liquid rain or frozen snow. The accumulation and melt of the snowpack can be simulated using snowmelt component. The result of the computations done by this component is the liquid water available at the soil surface, which then becomes the hyetograph for the subbasin.

The temperature index method is an extension of the degree-day approach to modeling a snowpack. A typical approach to the degree day is to have a fixed amount of snowmelt for each degree above freezing. This method includes a conceptual representation of the cold energy stored in the pack along with a limited memory of past conditions and other factors to compute the amount of melt for each degree above freezing. As the snowpack internal conditions and atmospheric conditions change dynamically, the melt coefficient also changes (USACE-HEC, April 2006). Temperature index method requires different parameter inputs which are the same for all of the subbasins (Figure 5.7).

The *PX temperature* is used to discriminate between precipitation falling as rain or snow. When the air temperature is less than the specified temperature, any precipitation is assumed to be snow.

The difference between the *base temperature* and the air temperature defines the temperature index used in calculating snowmelt; the melt rate is multiplied by the difference between the air temperature and the base temperature to estimate the snowmelt amount. If the air temperature is less than the base temperature, then the amount of melt is assumed to be zero. It should be 0 ºC or close to it.

The *wet meltrate* is used during time periods of precipitation when the precipitation is falling as rain at rates greater than the rain rate limit. It represents the rate at which the snowpack melts when it is raining on the pack. The rain on snow is a special case for snowmelt process, rainfall causes a faster melting compared to normal conditions, therefore this value should be slightly higher then the melt rates defined for pure snowmelt.

The *rain rate limit* discriminates between dry melt and wet melt. The wet meltrate is applied as the meltrate when it is raining at rates greater than the rain rate limit. If the rain rate is less than the rain rate limit, the meltrate is computed as if there were no precipitation.

The *antecedent temperature index meltrate function* (ATI meltrate) is used to calculate a meltrate from the current meltrate index. The function must be specified separately in the Paired Data Manager before it can be used in the snow melt method. The function should define appropriate melt rates to use over the range of meltrate index values that can be encountered during a simulation. Optionally, one may adjust the meltrate computed from the index meltrate function. A *meltrate pattern* may be specified that defines the percentage adjustment as a function of the time of the year. In this study the former one is selected during the model application.

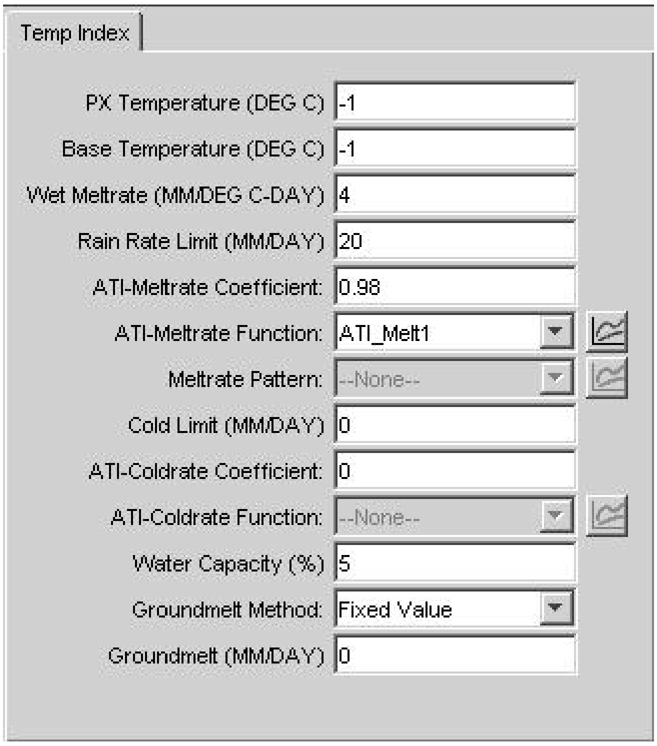

Figure 5.7. Temperature index snowmelt inputs for all subbasins in a meteorologic model.

The *maximum liquid water capacity* specifies the amount of melted water that must accumulate in the snowpack before liquid water becomes available at the soil surface for infiltration or runoff. Typically, the maximum liquid water held in the snowpack is on the order of 3-5% of the snow water equivalent, although it can be higher.

The other parameters as the *cold limit*, *cold content antecedent temperature index coefficient*, *antecedent temperature index cold content function*, *heat from the ground* are set to zero since they are unknown. The necessary information about these parameters can be read from the HEC's User Manual (USACE-HEC, April 2006).

Each subbasin is broken into one or more elevation bands; each band has its own parameter data. One elevation band may be used to represent a subbasin with very little terrain variation. Subbasins with large elevation variations should use multiple elevation bands.

One must specify the percentage of the subbasin that each elevation band composes (Figure 5.8). An elevation band is not required to be contiguous. The percentage specified for each elevation band will automatically be normalized if the sum of the percentages across all subbasins does not equal to hundred percent. There is no limit to the number of elevation bands that can be used, but at least one is required. Typically only one band is used in watersheds with small elevation differences. Mountainous watersheds usually require several bands for each subbasin. Typically the specified elevation will be either the area-weighted elevation of the band, or the average of the highest and lowest point in the band.

The *initial snow water equivalent* that exists at the beginning of the simulation must be entered. This information is usually determined by interpolating from actual measurements of snow water equivalent. This value can be set to zero if there is no snow.

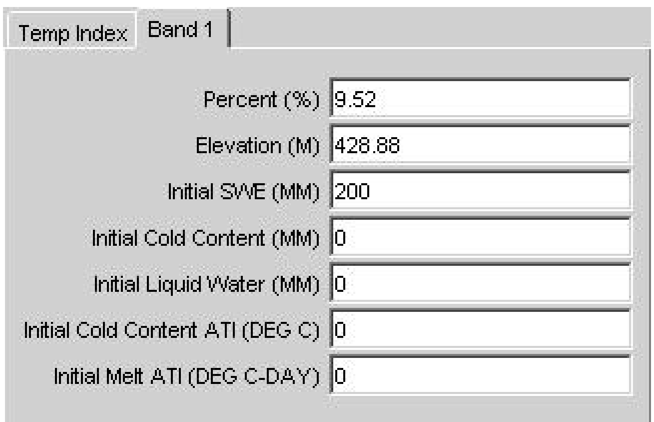

Figure 5.8. Inputs properties of an elevation band

The *initial cold content* represents the heat required to raise the temperature of the snow pack to 0 ºC and is expressed as a number equivalent to mm of frozen water. Generally this value is not known at the start of simulation unless there is no snow, in which case it can be set to zero. If the value is not known it can be set to zero. The error in doing this may be small for relatively shallow ephemeral snow covers.

For any melt or precipitation to get though the snowpack, the *liquid water holding capacity* of the snow first be satisfied. The liquid water held within the snowpack at the beginning of the simulation must be entered. Generally this value is not known at the start of simulation unless there is no snow, in which case it can be set to zero.

The *initial cold content antecedent temperature index* is an index to the snow temperature near the surface of the snowpack. It should be set to the approximate snowpack temperature at the beginning of the simulation, if the initial temperature is not known; it can be set to 0 ºC.

5.2.2 Subbasin elevation bands

The subbasins were subdivided into elevation bands by the help of Geographic Information System Technologies. The Digital Elevation Model of each subbasin is used as an input in ARC GIS to derive the elevation bands.

The recommended range of an elevation band was 1000 ft in the previous version of HEC-HMS (HEC-1). Therefore, any value close to 350 m can be chosen for elevation band discrimination. Analysis showed that this recommended value lead to the creation of three elevation bands for Kirazdere Subbasin. The elevation range, corresponding area (both in terms of km^2 and %) and average elevations of each elevation band is given in Table 5.14 for Kirazdere.

Table 5.14. Kirazdere subbasin elevation bands information

Band ID	Elevation Range	Average Elev. (m)	Area (km²)	Area (%)
1	179 - 550	~350 (428.872)	7.570	9.52
2	550 - 900	~725 (820.23)	27.839	35.00
3	900 - 1312	~1106 (978.272)	44.126	55.48
		Total Basin Area	**79.535**	**100.00**

The average elevation of an elevation band can be considered as the mean altitude of that elevation band; however the hypsometric mean altitude is more representative for an average elevation since it includes the area factor in it. Therefore, the hypsometric curve of the each elevation band is derived and the elevation corresponding to 50% area is found by linear interpolation). These values are provided in Table 5.14 within the parenthesis. Elevation bands of Kirazdere are shown in Figure 5.9.

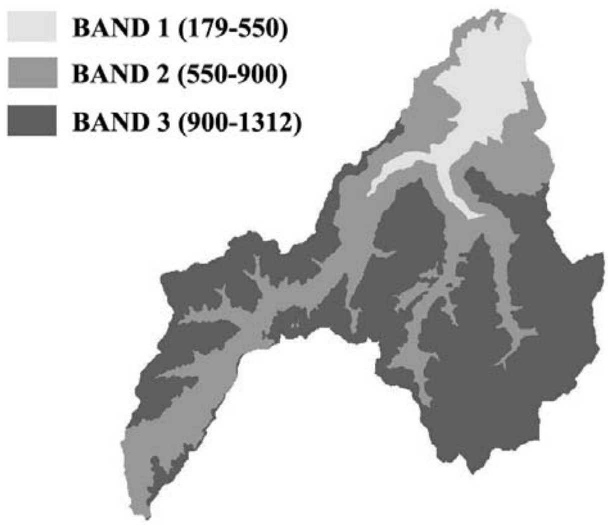

Figure 5.9. Kirazdere subbasin elevation bands

Analysis showed that three elevation bands are appropriate for Kazandere subbasin similar to Kirazdere. The elevation range, corresponding area (both in terms of km² and %) and average elevations of each elevation band is given in Table 5.15. The values provided within the parenthesis in Table 5.15 are hypsometric mean elevations. Figure 5.10 presents the general view of elevation bands.

Table 5.15. Kazandere subbasin elevation bands information

Band ID	Elevation Range	Average Elev. (m)	Area (km²)	Area (%)
1	186.4 - 600	~393 (441.462)	4.589	19.87
2	600 - 1000	~800 (800)	8.103	35.08
3	1000 – 1347.1	~1173 (1157.221)	10.407	45.05
		Total Basin Area	**23.099**	**100.00**

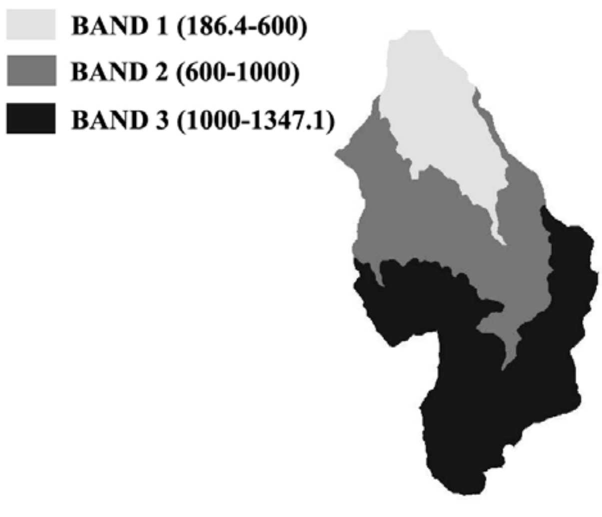

Figure 5.10. Kazandere subbasin elevation bands

Like the other two subbasins, three elevation bands are specified for Serindere Subbasin. The elevation range, corresponding area (both in terms of km² and %) and average elevations of each elevation band is given in Table 5.16. The values provided within the parenthesis in table are hypsometric mean elevations. Figure 5.11 presents the general view of elevation bands.

Table 5.16. Serindere subbasin elevation bands information

Band ID	Elevation Range	Average Elev. (m)	Area (km²)	Area (%)
1	272.2 - 700	~486 (579.779)	16.762	13.91
2	700 - 1100	~900 (884.659)	69.275	57.48
3	1100 – 1546.7	~1323 (1181.806)	34.474	28.61
		Total Basin Area	**120.511**	**100.00**

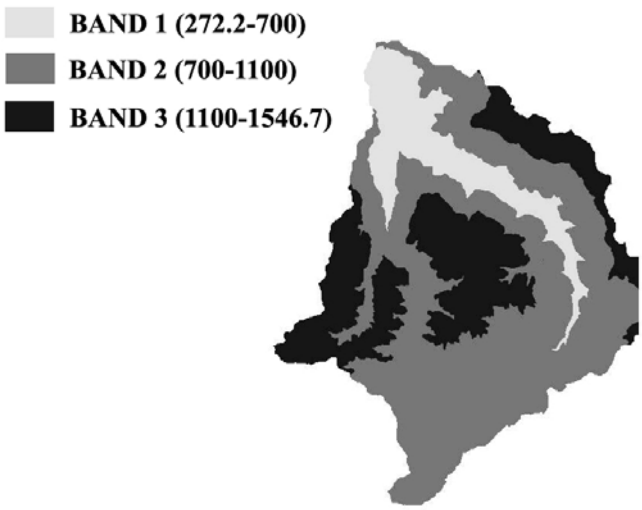

Figure 5.11. Serindere subbasin elevation bands

5.2.3. Determination of temperature lapse rate

Yuvacık basin is a mountainous basin and the elevation ranges between 176 m and 1546 m. The subbasins are divided into three elevation zones due to the high elevation difference as explained in the previous section. The temperature measurements were not available in the basin before the installation of the new stations. The temperature data were only available at Kocaeli Station, (KE, 76 m) that is operated by DMI for the period 2001-2005. After the installation of seven new stations, temperature is started to be measured in the basin. Since the snowmelt is effective between the months December and April, availability of temperature records is important in this period. The model require the temperature difference with altitude, in other words, temperature lapse rate as an input, therefore temperature lapse rate among the new installed stations and Kocaeli gage is found for the period between January 06, 2006 and April 24, 2006 and the results of the study are presented in Table 5.17. Temperature lapse rates are found using the following equation:

$$\text{Lapse rate} = [(\Delta T) / (\Delta E)] * 100 \qquad (5.6)$$

where, ΔT is the daily temperature difference between two stations in ºC, and ΔE is the elevation difference in meters. Lapse rate is found in ºC per 100 meters.

Table 5.17. Temperature lapse rates for 100 m elevation increase

Station (Altitude)	**Kartepe (1487 m)**	**Aytepe (953 m)**	**M2 (915 m)**	**Çilekli (805 m)**	**M1 (732 m)**	**Tepecik (700 m)**	**M3 (546 m)**
Kocaeli	-0.63	-0.61	-0.69	-0.68	-0.58	-0.49	-0.5
M3	-0.69	-0.74	-0.95	-1	-0.8	-0.47	**0**
Tepecik	-0.74	-0.9	-1.29	-1.79	-2.35	**0**	0.47
M1	-0.67	-0.69	-1.11	-1.54	**0**	2.35	0.8
Çilekli	-0.57	-0.27	**0.35**	**0**	1.54	1.79	1
M2	-0.53	**1.29**	**0**	0.35	1.11	1.29	0.95
Aytepe	-0.57	**0**	1.29	0.27	0.69	0.9	0.74
Kartepe	**0**	0.57	0.53	0.57	0.67	0.74	0.69

As seen from the table, the lapse rate values are negative with the elevation increase as expected, except for two stations (M2 and Aytepe). The general consistency indicates that the lapse rate value computed at Kocaeli Station with respect to the other stations is around -0.49 and -0.68 ^{o}C/100 m. The lapse rate ranges between -0.53 to -0.74 ^{o}C/100 m for Kartepe. The overall average of the lapse rate values for each station is calculated and this value is found to be -0.60 ^{o}C/100 m, -0.63 ^{o}C/100 m for Kocaeli and Kartepe stations, respectively.

5.2.4. Model inputs

5.2.4.1. Precipitation

Between the period 2001 and 2005, the gage weights of the old stations (RG1 to RG6, KE, and HO) are found using inverse distance square weights approach as mentioned in Section 5.1.2.1. For daily simulation periods that are in 2006, the weights of the stations are found by Thiessen polygons method. The stations that are used for each subbasin and corresponding station weights are given in Table 5.18 for daily simulations in 2006.

Table 5.18. Gages and their weights within each subbasin for the year 2006

Kirazdere		Kazandere		Serindere	
Gage	**Weight**	**Gage**	**Weight**	**Gage**	**Weight**
HO	0.211	M1	0.30	RG4	0.34
M1	0.020	RG5	0.11	RG7	0.07
M2	0.476	RG7	0.21	RG10	0.59
M3	0.148	RG8	0.38		
RG3	0.043				
RG8	0.102				

5.2.4.2. Temperature

In daily simulations, daily temperature data is input to the snowmelt component of HEC-HMS via a base temperature gage. Threshold temperature value is used to determine whether the falling precipitation will be rain or snow, and also it is used to compute snowmelt amount by the help of temperature index method. Base temperature gage data is used to compute temperature values in each elevation zone of the subbasin by means of a predefined lapse rate. The base temperature station was selected as Kocaeli Station for 2001-2005 periods since it is the only station that can provide temperature values. Then, the most representative stations were selected for different subbasins for the year 2006.

The M1, M2 and M3 stations are mobile stations and Kartepe (RG9) station has harsh weather conditions in winter, therefore Aytepe (RG8), Tepecik (RG7) and Cilekli (RG10) are selected as the base temperature station for Kirazdere, Kazandere and Serindere basins, respectively.

5.2.4.3. Temperature lapse rate

For the period 2001-2005 temperature lapse rate is used as -0.5 ºC/100 m and for the year 2006 as -0.6 ºC/100 m in the daily model calibration and validation simulations. These lapse rate values are within physical ranges and close to average values given in Table 5.17.

5.2.4.4. Threshold and base temperatures

The threshold temperature that discriminates between rain and snow precipitation is found to be -1 ºC for almost all the daily simulations, and the base temperature that specifies the melt or no melt condition changes between 0 and -1 ºC and these values are found by trial and errors.

5.2.4.5. Initial snow water equivalent

The initial snow water equivalent (SWE) values must be provided for each elevation band in the subbasins. SWE values are used to evaluate the snowpack conditions at the beginning of the simulation period. Most of the time, snow measurements are not available for the catchments at the western part of Turkey. Thus, it is a troublesome issue to input snow water equivalent values to each elevation zone of a basin.

HO snow depth values were the only available data source from the site for 2001-2005 simulation periods. These valuable records were used to evaluate the snow accumulation and melting conditions in the basin. Snow density values (0.10-0.40 gr/cm^3 from accumulation to snowmelt) are used to convert snow depths to snow water equivalent values.

SWE values must be distributed though the elevation zones of each subbasin. The measurements for the new stations at the year 2006 gave an insight for the distribution methodology. HO snow depths are compared with the snow depths of new stations for the year 2006 as given in Figure 5.12. From the analysis of these snow depths the following distribution is accepted:

- HO snow depths are used to determine the SWE values of the first elevation band.
- The average of Çilekli and Tepecik snow depths are used in second band,
- Finally, the average of Kartepe and Aytepe snow depths are used in the third band.

5.2.4.6. Melt rate

The melt rate or the degree day coefficient (in mm/ ºC/ day) is the main parameter for temperature index method since the method uses this parameter to compute snowmelt amount. It is an empirical coefficient and can be computed using snow density values. The melt rate has an increasing pattern with the season since it represents the effect of sun radiation, albedo, snow grain size, snow density, etc. This coefficient is described with Antecedent Temperature Index (ATI) or Accumulated Thawing Temperatures in HEC-HMS. Therefore, one can describe the melt rate according to cumulative positive temperatures.

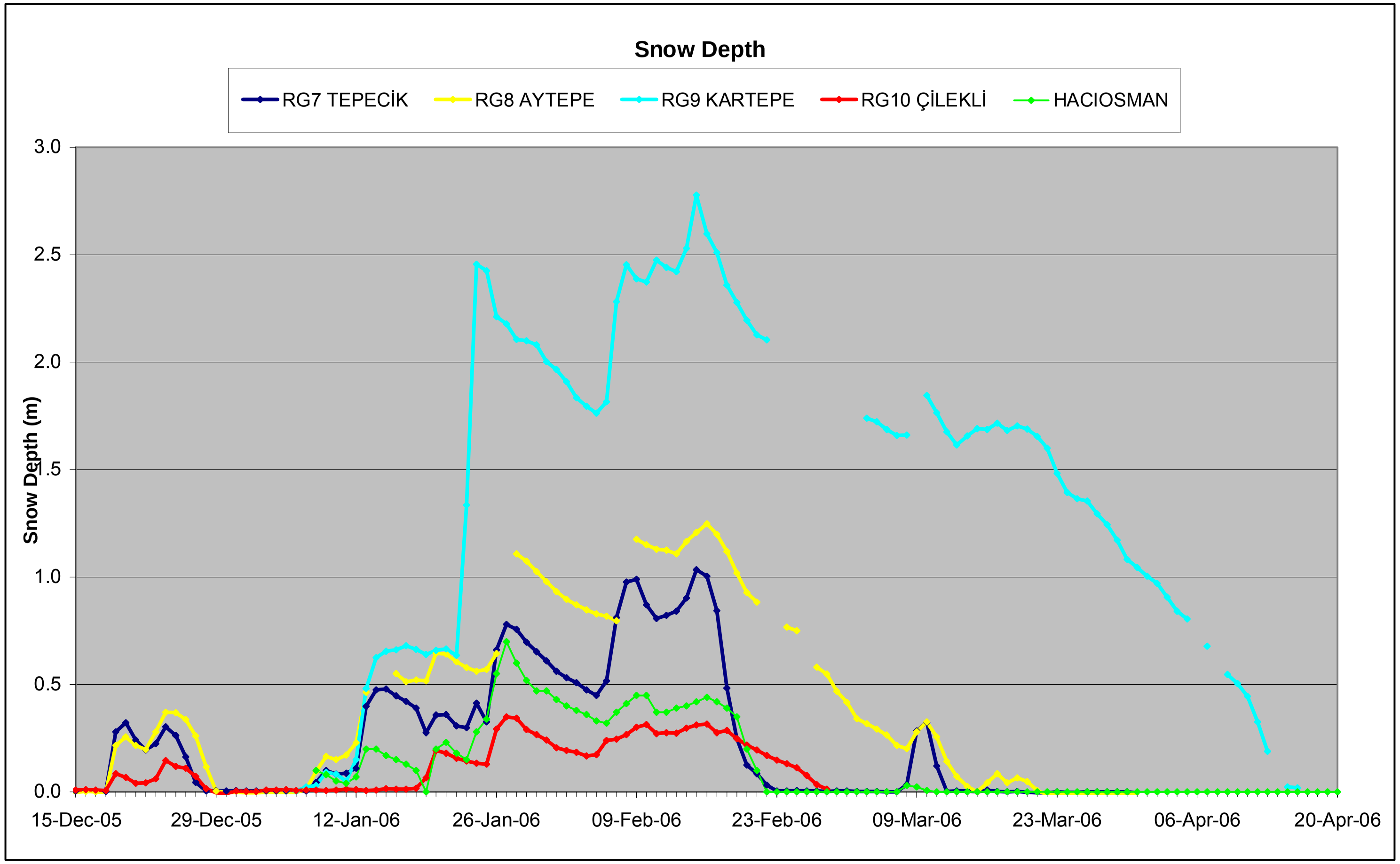

Figure 5.12. Observed snow depths for the year 2006

5.2.5. Calibration and validation of model parameters

Daily simulations are performed for the calibration of model parameters (loss and baseflow parameters). As the name implies the simulation time step is chosen to be 24 hours due to various reasons; the past records of temperature at KE station have been available only in daily time steps and since the temperature is one of the main inputs to the models, uncertainty in the temporal distribution of temperature data would be very effective on the model results, and the model computes the snowmelt with temperature index which is not sensitive to hourly fluctuations in snowpack.

The total number of periods used for the calibration/validation procedure is 13 (10/3) for Kirazdere Subasin, 7 (6/1) for Kazandere Subbasin, 8 (7/1) for Serindere Subbasin. The main reason of reduced number of periods for Kazandere and Serindere is the non or erroneous working Flow Plants until the period Dec 2002 and Mar 2003, respectively, as shown in Table 5.19.

Table 5.19. Periods of daily snowmelt simulations

Period	Kirazdere	Kazandere	Serindere
2001-2002	20/11/01-10/12/01 09/12/01-15/01/02 15/01/02-15/03/02 15/03/02-15/04/02		
2002-2003	**20/12/02-16/01/03** **15/01/03-16/03/03** **15/03/03-22/04/03**	20/03/03-18/04/03	20/12/02-15/01/03 **03/02/03-20/02/03** 20/03/03-22/04/03
2003-2004	21/12/03-09/01/04 19/02/04-15/03/04	21/12/03-09/01/04 19/02/04-15/03/04	21/12/03-09/01/04
2004-2005	15/01/05-13/02/05 13/02/05-15/03/05	**16/01/05-13/02/05** 13/02/05-15/03/05	16/01/05-13/02/05 13/02/05-15/03/05
2005-2006	01/02/06-10/03/06 10/03/06-10/04/06	01/02/06-10/03/06 10/03/06-10/04/06	01/02/06-10/03/06 10/03/06-10/04/06

The model parameters of Kirazdere subbasin are calibrated for the periods 2001-02, 2003-04, 2004-05 and 2005-06. Then, the model parameters are verified for the three periods in 2002-2003 water year. Since the model calibration periods are limited for Kazandere and Serindere subbasins, only one period from the year 2004 and the year 2003 are selected for model validation for these subbasins, respectively. These validation periods are shown in bold letters in Table 5.19.

Sample graphs are presented in Figures 5.13 to 5.18 to give an idea of the comparison of computed daily simulation results with the observed runoff. One sample for calibration results and one sample for validation results are given for each of the three subbasins.

Calibrated model parameters are presented in Tables 5.13 to 5.15 for each subbasin. ATI values and corresponding melt rates are given in the same tables.

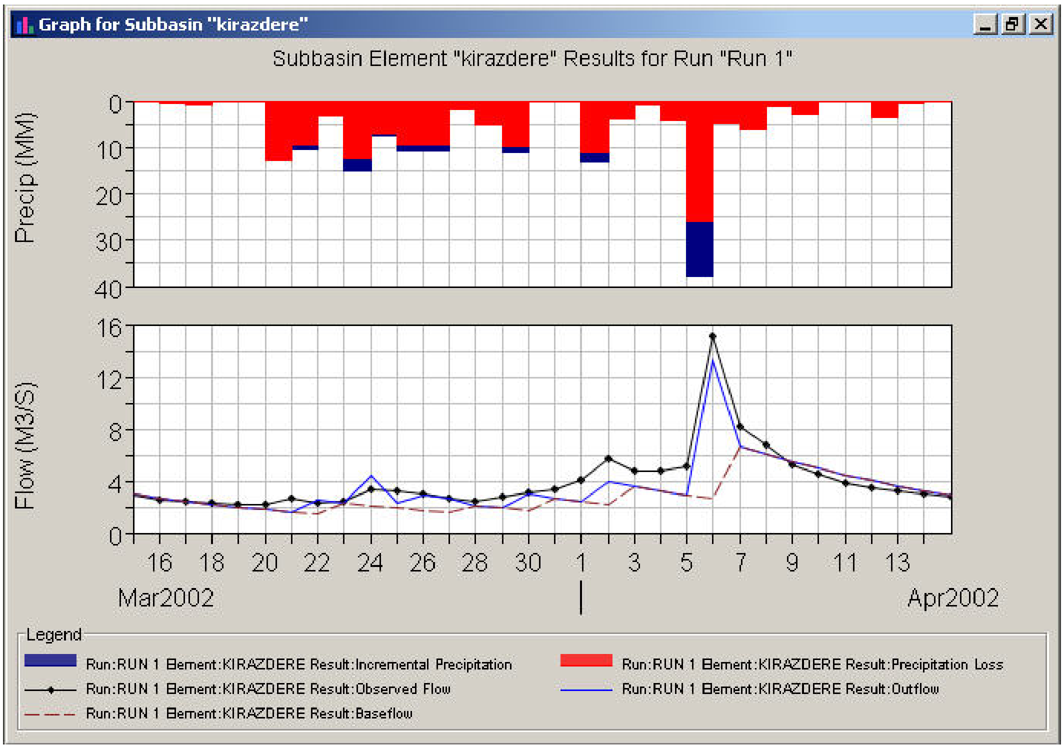

Figure 5.13. Kirazdere daily model calibration results graph

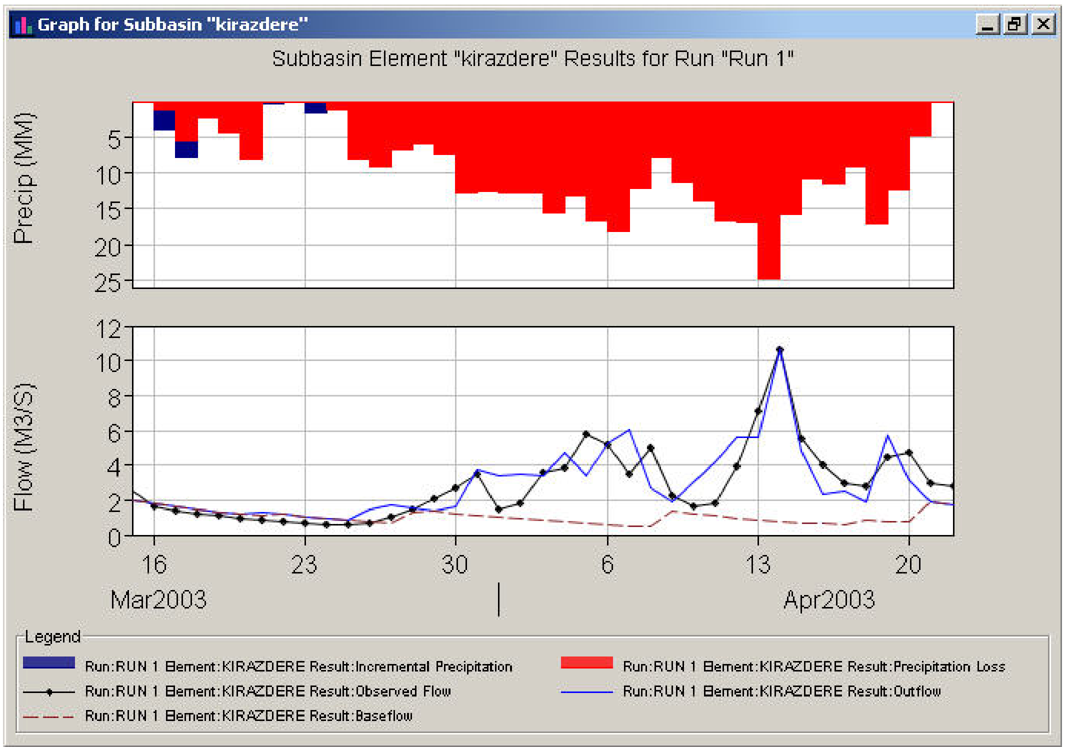

Figure 5.14. Kirazdere daily model validation results graph

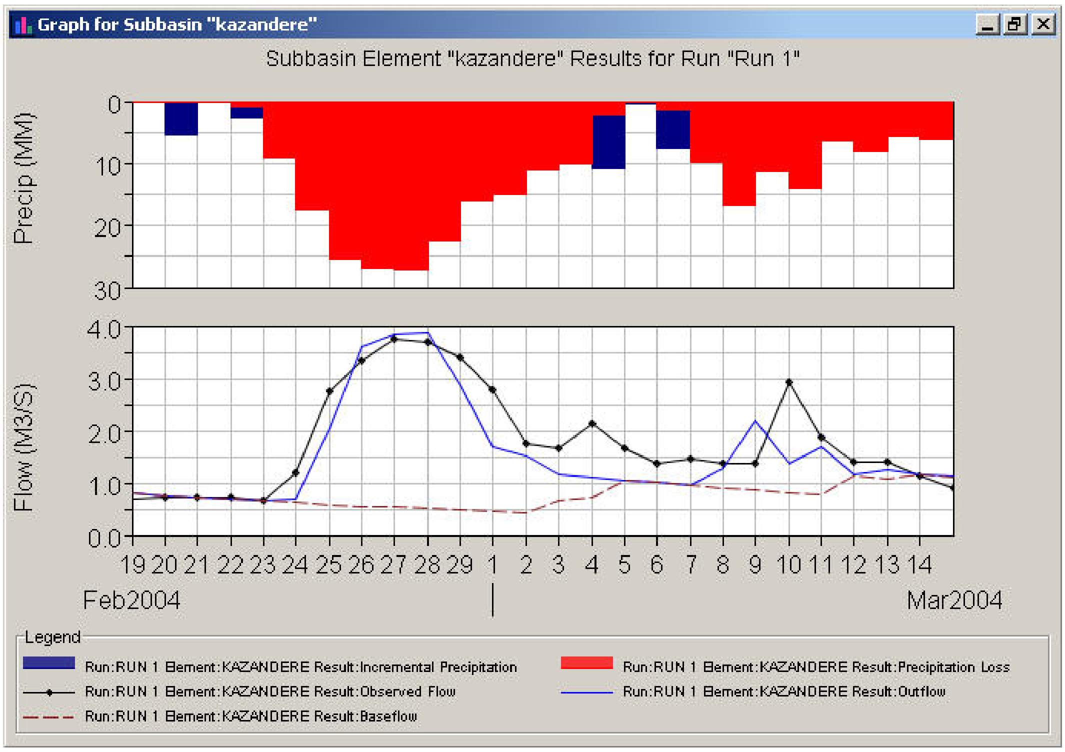

Figure 5.15. Kazandere daily model calibration results graph

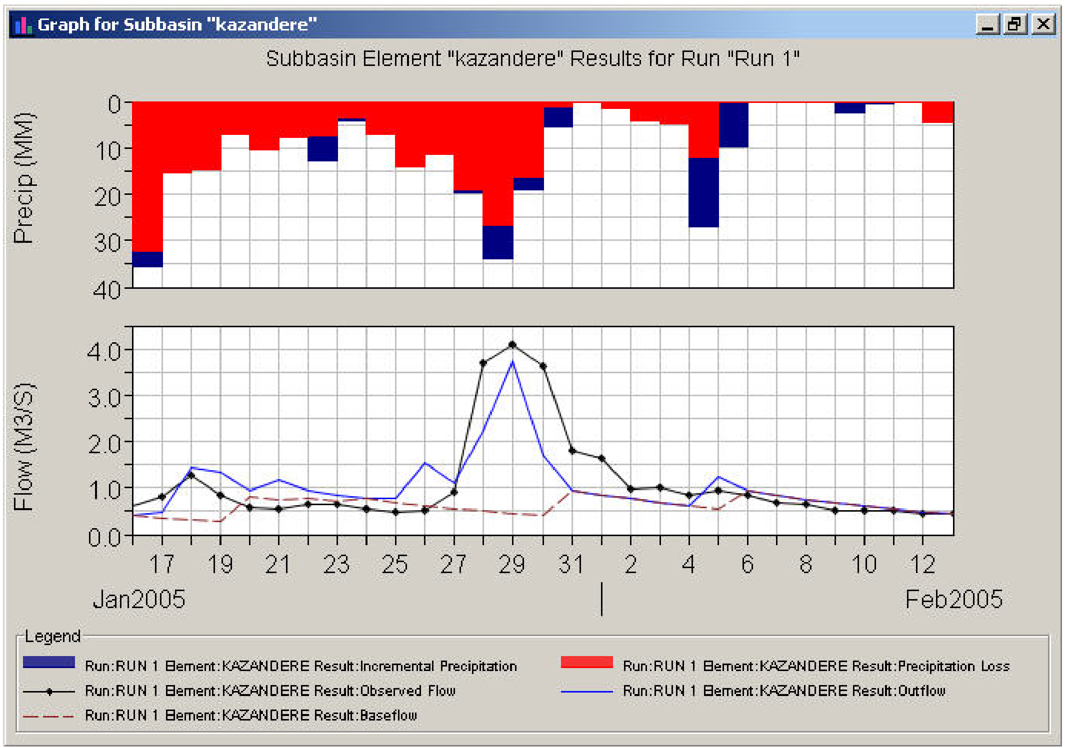

Figure 5.16. Kazandere daily model validation results graph

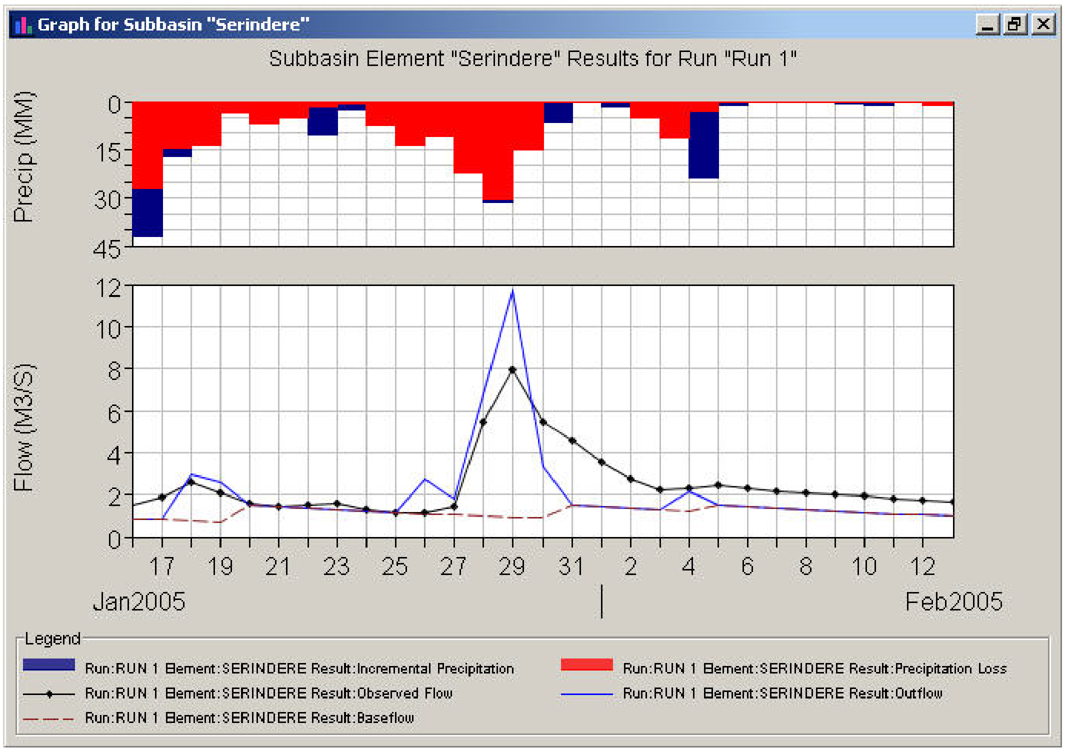

Figure 5.17. Serindere daily model calibration results graph

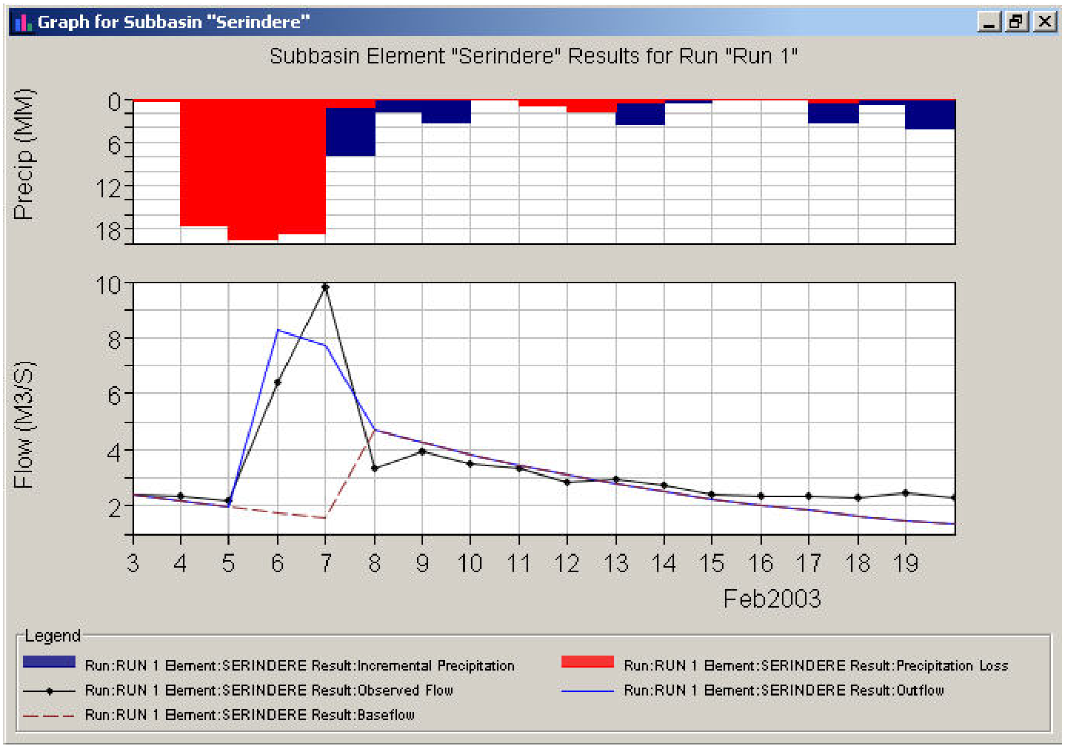

Figure 5.18. Serindere daily model validation results graph

Table 5.20. Kirazdere daily simulations input and statistical results

	BASIN:	**KIRAZDERE**	**KIRAZDERE**	**KIRAZDERE**	**KIRAZDERE**	**KIRAZDERE**	**KIRAZDERE**	**KIRAZDERE**
	START:	**20-Nov-2001**	**9-Dec-2001**	**15-Jan-2002**	**15-Mar-2002**	**20-Dec-2002**	**15-Jan-2003**	**15-Mar-2003**
	END:	**10-Dec-2001**	**15-Jan-2002**	**15-Mar-2002**	**15-Apr-2002**	**15-Jan-2003**	**16-Mar-2003**	**22-Apr-2003**
LOSS	**Initial Range (mm)**	20	20	15	15	20	20	20
	Initial Coef ((mm/hr)^(1-x))	0.75	0.8	0.75	0.75	0.85	0.75	0.75
	Coef Ratio	1	1	1	1	1	1	1
	Exponent	0.8	0.85	0.8	0.8	0.85	0.85	0.8
	Impervious (%)	0	0	0	0	0	0	0
BASEFLOW	**Initial Discharge (m^3/s)**	1.5	4	3	3	0.2	0.5	2
	Recession Constant	0.92	0.92	0.9	0.9	0.9	0.9	0.9
	Threshold Flow(m^3/s)	3	8	8	7	2	2	2
SNOW	**Px Temp**	-1	-1	-1	-1	-1	-1	-1
	Base Temp	-1	0	-1	-1	0	-1	-1
	Wet Meltrate	4	4	4	4	4	4	4
	Rainrate Limit	20	20	20	20	20	20	20
	ATI Coefficient	0.98	0.98	0.98	0.98	0.98	0.98	0.98
	Water Content	0.05	0.05	0.05	0.05	0.05	0.05	0.05
	Lapse Rate (ºC/100m)	-0.5	-0.5	-0.5	-0.5	-0.5	-0.5	-0.5
	Snow Depth at HO (mm)	0	150	620	0	550	0	420
	SWE at each zone (mm)	0,0,0	45, 75, 125	200, 320, 560	0, 0, 0	165, 275, 460	0, 0, 0	150, 240, 410
MODEL RELIABILITY	**Avg Abs Residual (m^3/s)**	2.14	1.46	1.02	0.68	0.5	0.27	0.89
	Total Residual (mm)	-15.8	-32	-28.5	-14.2	6	-4.9	3.4
	Peak Difference (%)	-8.1	9.4	-10.5	-12.2	28.7	-12.8	-0.3
	Volume Difference (%)	-15.7	-18.3	-10.9	-10.6	14.8	-7.0	2.1
	R^2	0.700	0.787	0.774	0.893	0.937	0.894	0.706
	NSE	0.672	0.745	0.567	0.861	0.845	0.792	0.693

ATI	0	1	1	1.5	2	1	1.5	2
ATI	35	1	1	1.5	2.5	1	2	3
ATI	50	1	1	2	2.5	2	2	3
ATI	70	1	2.5	2.5	3	2	3	3
ATI	90	1	2.5	2.5	3	2	3	3
ATI	100	1	2.5	2.5	3	2	3	3.5
ATI	150	1	2.5	2.5	4	2	3	3.5
ATI	200	1	3	2.5	4.5	2	3	3.5

Table 5.20. Kirazdere daily simulations input and statistical results (continued…)

	BASIN:	KIRAZDERE	KIRAZDERE	KIRAZDERE	KIRAZDERE	KIRAZDERE	KIRAZDERE
	START:	21-Dec-2003	19-Feb-2004	16-Jan-2005	13-Feb-2005	1-Feb-2006	10-Mar-2006
	END:	9-Jan-2004	15-Mar-2004	13-Feb-2005	15-Mar-2005	10-Mar-2006	10-Apr-2006
LOSS	Initial Range (mm)	18	20	20	20	8	8
	Initial Coef ((mm/hr)^(1-x))	0.85	0.85	0.8	0.75	0.75	0.75
	Coef Ratio	1	1	1	1	1	1
	Exponent	0.85	0.85	0.85	0.8	0.8	0.8
	Impervious (%)	0	0	0	0	0	0
BASEFLOW	Initial Discharge (m^3/s)	2	2.2	2.2	4	3	7
	Recession Constant	0.92	0.95	0.92	0.93	0.95	0.95
	Threshold Flow(m^3/s)	2.4	3	4	4	7	7
SNOW	Px Temp	-1	-1	-1	-1	-1	-1
	Base Temp	0	0	0	0	-1	-1
	Wet Meltrate	4	4	4	4	4	4
	Rainrate Limit	20	20	20	20	20	20
	ATI Coefficient	0.98	0.98	0.98	0.98	0.98	0.98
	Water Content	0.05	0.05	0.05	0.05	0.05	0.05
	Lapse Rate (ºC/100m)	-0.5	-0.6	-0.5	-0.5	-0.6	-0.6
	Snow Depth at HO (mm)	620	700	200	500	430	7
	SWE at each zone (mm)	185, 310, 520	210, 350, 525	60, 100, 160	165, 270, 450	150, 260, 440	70,110, 180
MODEL RELIABILITY	Avg Abs Residual (m^3/s)	0.39	0.38	1.18	1.35	1.4	0.91
	Total Residual (mm)	-4.8	-5.3	7.4	-10.8	-36.4	-11.9
	Peak Difference (%)	33.1	11.8	10.2	5.4	-3.4	-2.4
	Volume Difference (%)	-9.6	-6.3	6.1	-5.1	-12.3	-5.3
	R^2	0.417	0.895	0.810	0.676	0.877	0.909
	NSE	-0.581	0.627	0.634	0.328	0.719	0.784

ATI	0	1	2	1.5	2.5	2.5	3
ATI	35	1	2	2	2.5	3.5	3
ATI	50	1	2	2	2.5	3.5	3.5
ATI	70	1	2.5	2	2.5	3.5	3.5
ATI	90	1.5	2.5	2	2.5	3.5	3.5
ATI	100	1.5	2.5	2	2.5	3.5	3.5
ATI	150	2	3	2.5	3	3.5	4
ATI	200	3	3.5	2.5	3	4.5	4.5

Table 5.21. Kazandere daily simulations input and statistical results

	BASIN:	KAZANDERE	KAZANDERE	KAZANDERE	KAZANDERE	KAZANDERE	KAZANDERE	KAZANDERE
	START:	20-Mar-2003	21-Dec-2003	19-Feb-2004	16-Jan-2005	13-Feb-2005	1-Feb-2006	10-Mar-2006
	END:	18-Apr-2003	9-Jan-2004	15-Mar-2004	13-Feb-2005	15-Mar-2005	10-Mar-2006	5-Apr-2006
LOSS	Initial Range (mm)	10	15	5	20	5	5	5
	Initial Coef ((mm/hr)^(1-x))	0.75	0.85	0.75	0.75	0.75	0.75	0.75
	Coef Ratio	1	1	1	1	1	1	1
	Exponent	0.8	0.85	0.8	0.8	0.85	0.85	0.8
	Impervious (%)	0	0	0	0	0	0	0
BF	Initial Discharge (m^3/s)	0.5	2	0.8	0.4	0.5	0.35	2
	Recession Constant	0.93	0.9	0.95	0.9	0.93	0.95	0.95
	Threshold Flow(m^3/s)	1.5	1	1.2	1	1	1.5	1
SNOW	Px Temp	-1	-1	-1	0	-1	-1	-1
	Base Temp	-1	0	-1	-1	0	-1	-1
	Wet Meltrate	4	4	4	4	4	4	4
	Rainrate Limit	20	20	20	20	20	20	20
	ATI Coefficient	0.98	0.98	0.98	0.98	0.98	0.98	0.98
	Water Content	0.05	0.05	0.05	0.05	0.05	0.05	0.05
	Lapse Rate (ºC/100m)	-0.5	-0.5	-0.5	-0.5	-0.5	-0.6	-0.5
	Snow Depth at HO (mm)	480	620	700	200	500	430	7
	SWE at each zone (mm)	170, 275, 470	185, 310, 520	210, 350, 525	60, 100, 160	165, 270, 450	150, 260, 440	70, 110, 190
MODEL RELIABILITY	Avg Abs Residual (m^3/s)	0.47	0.49	0.38	0.4	0.42	0.89	0.91
	Total Residual (mm)	-28.4	-30.6	-24.9	-5.9	-30.9	-61.4	-11.9
	Peak Difference (%)	12.9	-3.7	3.3	-9.1	-19.2	-15.7	-16.1
	Volume Difference (%)	-17.5	-28.4	-13.9	-5.4	-19.0	-22.9	-21.5
	R^2	0.693	0.435	0.875	0.817	0.541	0.653	0.871
	NSE	0.610	0.100	0.687	0.641	0.069	0.342	0.604

ATI	0	4	1	2.75	1.5	2.5	3.5	3.5
ATI	35	4	1.5	2.75	2	2.5	3.5	3.5
ATI	50	4	1.5	2.75	2	2.5	3.5	3.5
ATI	70	4	1.5	2.75	2.5	2.5	3.5	3.5
ATI	90	4	2	2.75	2.5	2.5	3.5	3.5
ATI	100	4	2	2.75	2.5	2.5	3.5	3.5
ATI	150	4	2	3	2.5	3	4	4
ATI	200	4	3	3.5	2.5	3	4	4

Table 5.22. Serindere daily simulations input and statistical results

	BASIN:	SERINDERE	SERINDERE	SERINDERE	SERINDERE	SERINDERE	SERINDERE	SERINDERE	SERINDERE
	START:	20-Dec-2002	3-Feb-2003	20-Mar-2003	21-Dec-2003	16-Jan-2005	13-Feb-2005	1-Feb-2006	10-Mar-2006
	END:	15-Jan-2003	20-Feb-2003	22-Apr-2003	6-Jan-2004	13-Feb-2005	15-Mar-2005	10-Mar-2006	5-Apr-2006
LOSS	Initial Range (mm)	20	20	20	15	20	20	8	20
	Initial Coef ((mm/hr)^(1-x))	0.8	0.8	0.8	0.85	0.85	0.85	0.8	0.85
	Coef Ratio	1	1	1	1	1	1	1	1
	Exponent	0.85	0.85	0.85	0.85	0.85	0.85	0.85	0.85
	Impervious (%)	0	0.8	0	0	0	0	0	0
BF	Initial Discharge (m^3/s)	1.22	2.4	2	2.5	0.85	2	4	3.8
	Recession Constant	0.9	0.9	0.9	0.92	0.95	0.92	0.95	0.95
	Threshold Flow(m^3/s)	5	5	2	3	1.5	3.5	4	4
SNOW	Px Temp	-1	-1	-1	-1	-1	-1	-1	-1
	Base Temp	-1	-1	-1	0	0	0	-1	-1
	Wet Meltrate	4	4	4	4	4	4	4	4
	Rainrate Limit	20	20	20	20	20	20	20	20
	ATI Coefficient	0.98	0.98	0.98	0.98	0.98	0.98	0.98	0.98
	Water Content	0.05	0.05	0.05	0.05	0.05	5%	5%	5%
	Lapse Rate (ºC/100m)	-0.5	-0.5	-0.5	-0.5	-0.6	-0.5	-0.6	-0.6
	Snow Depth at HO (mm)	550	120	480	620	200	500	430	7
	SWE at each zone (mm)	165, 275, 460	40, 65, 110	170, 285, 470	185, 310, 520	60, 100, 160	165, 270, 450	150, 260, 440	70, 110, 180
MODEL RELIABILITY	Avg Abs Residual (m^3/s)	0.89	0.67	1.64	0.81	0.940	1.15	1.48	0.7
	Total Residual (mm)	-2.5	-6.6	-17.9	-4.5	-7.800	-4.6	-10.6	-7.2
	Peak Difference (%)	-10.6	-15.6	22.0	25.0	46.8	-8.8	16.2	0.2
	Volume Difference (%)	-2.3	-3.7	-13.2	-10.5	-16.2	-4.7	-7.7	-9.7
	R^2	0.918	0.901	0.562	0.521	0.832	0.534	0.779	0.907
	NSE	0.917	0.787	0.427	0.160	0.289	0.107	0.552	0.791

ATI	0	1	1.5	2.5	1	1.5	2.5	3	3
ATI	35	2	2	2.5	1.5	1.5	2.5	3.5	3.5
ATI	50	2	2	2.5	1.5	2	2.5	3.5	3.5
ATI	70	2.5	3	2.5	1.5	2	2.5	4	3.5
ATI	90	2.5	3.5	2.5	2	2.5	2.5	4	3.5
ATI	100	2.5	3.5	2.5	2	2.5	2.5	4	3.5
ATI	150	2.5	3.5	3	2	2.5	3	4	4
ATI	200	2.5	3.5	3	3	3	3	4.5	4

5.2.6. Discussion of daily simulation results

The precipitation data are limited with the measurements at RG1-RG6 (at lower altitudes as 170 m – 530 m) collected by TWT, Kocaeli Station, KE (76 m) operated by State Meteorological Service, DMI and Haciosman Station, HO (900 m) operated by State Hydraulic Works, DSI for the period between November 2001- November 2005, therefore these data sets were used during the calibration and validation parts. Then, the new mobile and permanent station (RG7-10 located at higher elevations) measurements are used in the modeling of 2006 year events. Since the stations were concentrated on the lower parts of the basin except for HO Station, model simulations, concerning the snow accumulations have not ended up with satisfying results. The precipitation gages were not sufficient to measure snowfall. On the other hand, since HO is located at the south west part of Kirazdere basin, its effect on Kazandere and Serindere subbasins is not well enough to represent spatial distribution of precipitation during the study periods until the year 2006.

The snow measurements at new stations during the year 2006 yield very interesting results for comparisons; the amount of snow depths observed at HO (900 m) is almost half of the snow depths at Aytepe station (953 m) even they have only 50 m elevation difference (Figure 5.12).

The modeling results give melt rate of 1 mm/ ºC/day for November and December, 2-2.5 mm/ ºC/day for January, 2.5-3 mm/ ºC/day for February, 2.5-3.5 mm/ ºC/day for March and 3.5-4 mm/ ºC/day for April if the snow cover exists at the site. ATI values and the corresponding melt rates are provided within the same tables as model parameters are presented (Tables 5.20 to 5.22)

The model performance is better in Kirazdere than that in Kazandere and Serindere, the possible reason is the availability of appropriate modeling data. Statistical analysis yields high goodness of fit for Kirazdere subbasin except for two events one of which includes level corrections and the other has runoff values less than 5 m^3/s. The model efficiencies are higher than 0.5 at least for half of the events for Kazandere and Serindere. The model efficiency reduces with low flows which is the main issue for Kazandere subbasin. Either the percent peak and volume percent difference or model efficiency is in the acceptable ranges for almost all simulations.

The main issue is related with the number of periods that are available for model calibration and validation, historical records are not available for the desired period of time and/or some of the records are not appropriate for the reliable calibration/validation of the model. The model performance is highly correlated with the quantity and the quality of data. The goodness of fit values are decreased for all of the subbasins for the same time periods (Tables 5.20 to 5.22).

CHAPTER 6

RUNOFF FORECASTS USING NUMERICAL WEATHER PREDICTION DATA

6.1. Introduction

A common source of spatially and temporarily varying meteorological data is the outputs of numerical weather prediction models. Numerical weather prediction (NWP) is the name given to the technique used to forecast the weather by computer from its present, measured state up to several days ahead. Hydrological forecast analyses are highly dependent on the forecasted meteorological data. As the accuracy of the meteorological forecast data increase, better results of the hydrological analysis can be derived. Such accurate hydrological analyses enable better optimization of water supply, flood control and hydropower production. Thus, future weather situations are the key interest of hydrological and meteorological model forecasts.

In this respect, rain and snowmelt runoff forecasting is conducted in Yuvacık Basin during the 2006 snowmelt season. Daily average temperature and total precipitation products of 5^{th} Generation Mesoscale Model (MM5) data are used as input data for the calibrated HEC-HMS model in all subbasins. As being a pioneer study in the region, this work could not be conducted in a real time form during its first application.

6.2. Model application for daily runoff forecasting

The two simulation periods that are used in daily snowmelt simulations as given in Section 5.2 are used in runoff forecast studies. These periods are 01 February 2006 - 10 March 2006 and 10 Mar 2006 - 10 Apr 2006. These two periods are used for all of the three subbasins: Kirazdere, Kazandere, and Serindere.

The HEC-HMS model structure used in daily simulations is not changed in forecast simulations. Hence, simulation time step remained constant (1 day) since MM5 data is available daily. Exponential loss method and recession baseflow method are used. The parameter set that is calibrated in daily simulations for the year 2006 is used in the loss and baseflow methods.

The precipitation data and temperature data is required by the model for each subbasin. Precipitation data is input to the model by a single precipitation gage. Therefore, depth weight of this gage is simply "1". Temperature data is input to the model by a base temperature gage. The data of both precipitation and temperature gages are obtained from the average values of selected MM5 grid data. MM5 grid points that fall in or around Yuvacık Basin are shown in Figure 6.1, grid points are referred as "pixels" in this figure. The following grids are selected to be used for each subbasin since these grid combinations yield better results: grids (pixels) 2, 3, 7, and 8 for Kirazdere; grids 8, and 9 for Kazandere; grids 4, 9, 10, and 14 for Serindere subbasin.

The summary results of the simulations done using MM5 data are given in Table 6.1. If percent errors in peak flows and total volumes are considered, the worst value of percent peak error is obtained as 22.53 (underestimation) for Kirazdere subbasin for the first simulation period. The best value of percent peak error is obtained as 0.4 (underestimation) again for Kirazdere subbasin, but this time for the second simulation period. The worst percent volume error is obtained as 15.14 (overestimation) both for Kirazdere and Serindere subbasins, but for Kirazdere subbasin it is in the second simulation period, whereas for Serindere, it is in the first period. The percent volume errors obtained for Kazandere is very close to the worst values, but there is an underestimation in Kazandere. The best value of percent volume error is obtained as 1.76 (overestimation) for Kirazdere subbasin for the first simulation period (Table 6.1).

Besides percent peak and volume errors, coefficient of determination (R^2) and Nash and Sutcliffe model efficiency (NSE) values are given in Table 6.1. In general the results obtained for Serindere subbasin are not very satisfactory. Graphical comparisons of observed and simulated flows are presented in Appendix C. These graphs may be compared with the calibration results graphs that are given in Section 5.2.5 for the same periods.

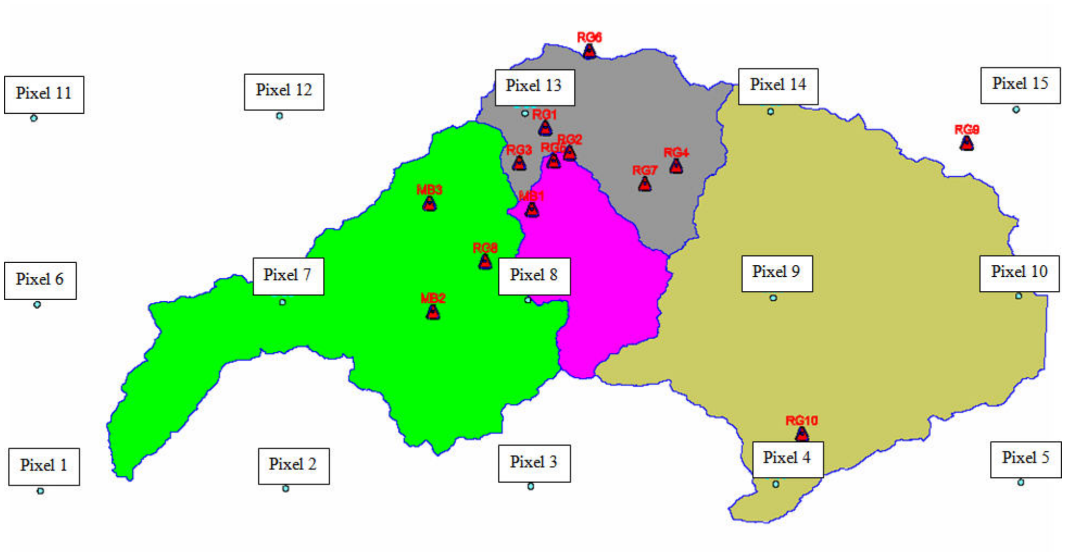

Figure 6.1. MM5 grid points in or around Yuvacık Basin

Table 6.1. Simulation results when MM5 grid data is used in the model

Period	**01Feb06 - 10Mar06**			**10Mar06 - 10Apr06**		
Subbasins	**Kirazdere**	**Kazandere**	**Serindere**	**Kirazdere**	**Kazandere**	**Serindere**
Observed peak (m^3/s)	19.98	5.53	14.12	14.74	5.81	10.27
Simulated peak (m^3/s)	15.48	4.79	14.43	14.68	4.73	10.4
Observed volume (mm)	291.42	264.68	128.04	222.84	223.46	73.24
Simulated volume (mm)	296.55	230.03	147.42	256.57	190.32	81.18
% Error peak	-22.53	-13.38	2.2	-0.4	-18.6	1.27
% Error volume	1.76	-13.09	15.14	15.14	-14.83	10.84
R^2	0.55	0.56	0.34	0.5	0.68	0.07
NSE	0.51	0.53	0.14	0.31	0.6	0.47

CHAPTER 7

RUNOFF SCENARIOS USING IDF CURVES

7.1. Introduction

This chapter mainly includes the performance evaluation of the constructed HEC-HMS hydrologic model based on subcatchments of Yuvacık Basin under a given frequency storm. The source of the frequency storm is the intensity-duration-frequency (IDF) curves which are prepared based on long records of precipitation data at Kocaeli station. The model results, obviously frequency hydrographs, may be used for flooding studies, water intake structure capacity analysis, and probable future design discharge estimates.

7.2. IDF data

In this study several different flood scenarios are generated using IDF curves of Kocaeli meteorology station. Currently there are three IDF curve sets available for the station. One of the sets is prepared by General Directorate of State Hydraulic Works (DSI, Bursa 1983) and the remaining two are prepared by Turkish State Meteorological Service (DMI). The maximum rainfall depth (mm/standard time), storm duration (hr) and frequency (yrs) is given in Table 7.1. Among the three available curve sets, the one prepared by DMI for the period 1945-2004 is selected as presented in Figure 7.1 to be used in model computations. Not all the available storm durations are considered in the study, three durations are selected among the available ones: 1 hr, 6 hrs, and 24 hrs.

Table 7.1. Maximum rainfall depth (mm/standard time), storm duration (hrs) and frequency (yrs) at Kocaeli Meteorology Station

		Storm duration (hr)						
Return Period		1	2	4	6	12	18	24
2	a	22.8	28.5	35.9	39.3	46.2	51.3	57
	b	19.55	22.9	29.6	34.8	43.5	47.6	51.8
	c	19.8	23.4	30.2	34.5	43.8	47.6	52.2
10	a	40	50.1	63.1	69.1	81.1	90.1	100.1
	b	40.45	46.36	58.6	66.1	77.3	88.7	103.3
	c	43.7	51.7	61.6	69.5	79.9	90.2	104.1
25	a	49.8	62.3	78.5	86	100.9	112.1	124.6
	b	54.12	62.45	73.7	83.7	95.4	112.7	131.6
	c	60.8	68.2	80	92.3	99.6	115.9	132.3
50	a	57.1	71.4	90	98	115.7	128.5	142.8
	b	65.83	76.61	84.8	97.4	109.2	131.9	152.9
	c	76.2	80.9	94.7	111.9	114.8	137	153.4
100	a	64.3	80.4	101.3	111	130.2	144.7	160.8
	b	78.87	92.8	95.8	111.6	123.4	152.5	174.5
	c	94.2	93.8	110.2	133.7	130.5	159.6	174.5

a) IDF values (mm) from DSI Report (DSI, Bursa 1983)
b) IDF values (mm) (1945-2000) DMI
c) IDF values (mm) (1945-2004) DMI

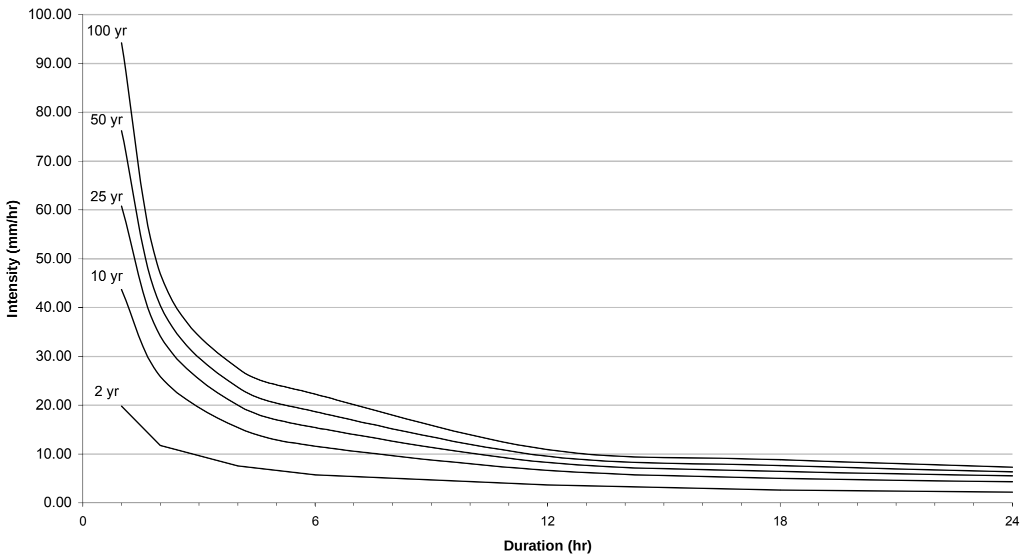

Figure 7.1. Selected IDF curves (DMI, 1945-2004)

7.3. Frequency Storm Method

The frequency storm method is a meteorologic method used in meteorologic model to produce a frequency storm from given statistical precipitation data. The method requires the following inputs: *probability*, *output type*, *intensity duration*, *storm duration*, *intensity position*, *storm area*, and *precipitation depth* values.

Probability is the exceedance probability of the selected storm. The available probabilities range from 0.2% to 50%, with the intermediate values: 0.4, 1, 2, 4, 10, and 20 percents.

The intensity duration specifies the shortest time period of the storm. Usually the duration should be set equal to the time step of the simulation. It must be less than the total storm duration.

Storm duration determines how long the precipitation will last. It must be longer than the intensity duration. If the simulation duration is longer than the storm duration, all time periods after the storm duration will have zero precipitation.

The intensity position determines where in the storm the period of peak intensity will occur. Changing the position does not change the total depth of the storm; it only changes how the total depth is distributed in time during the storm. The list of intensity positions consists of 25%, 33%, 50%, 67% and 75%.

The storm area is used to automatically compute the depth-area reduction factor. In most cases the specified storm area should be equal to the watershed drainage area at the point of evaluation. The same hyetograph is used for all subbasins in the study. Optionally the storm area may be left blank. In this case, each subbasin will have a different hyetograph computed using the subbasin area as the storm area.

Precipitation depth values must be entered for all durations from the peak intensity to the total storm length. Values for durations less than the peak intensity duration, or greater than the total storm duration cannot be entered. Figure 7.2. shows the precipitation editor of frequency storm method.

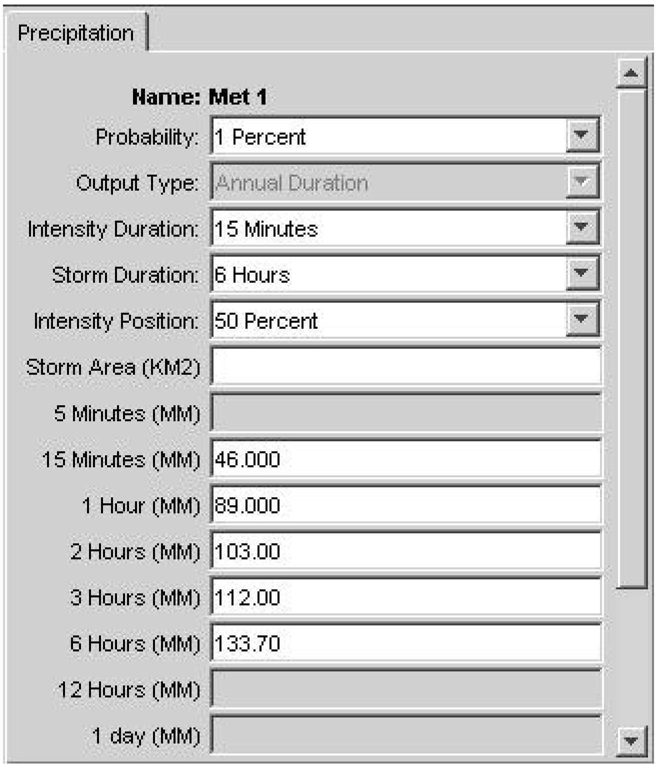

Figure 7.2. Frequency storm method inputs

7.4. Frequency storm simulations

7.4.1. Basin model inputs

A general basin model consisting of Kirazdere, Kazandere, Serindere, and Contributing subbasins is set up in HEC-HMS software for this study. In addition to 4 subbasins, a lake element is used in the basin model to observe the total outflow of the subbasins.

Exponential loss method is used for loss method; user-specified unit hydrograph is used for transform method; and recession is used as baseflow method.

Two sets of exponential loss and recession method parameters are used in the simulations. The first set is the minimum (MIN) parameters set. The minimum parameters for exponential loss method and recession baseflow method that are obtained from the model calibrations are used for Kirazdere, Kazandere and Serindere subbasins. For Contributing subbasin the average of the minimum parameters is used. Only for Kirazdere subbasin, initial coefficient of Event 41 (0.78) is used in the loss method, since the minimum value of that parameter (0.56), which belongs to Event 7, is unacceptably small. The second set is the average (MEAN) parameters set. The average parameters obtained from event-based simulations are used for Kirazdere, Kazandere, and Serindere subbasins. Again the average of the average parameters is used for the Contributing subbasin.

Finally, in the rainfall-runoff transform method, unit hydrographs of each subbasin is used.

7.4.2. Frequency storm method inputs

Hydrologic model simulations are performed for the following return periods: 2, 10, 25, 50 and 100 years, corresponding to 50, 10, 4, 2, 1 percent exceedance probabilities, respectively. Annual output, the default choice for the output type, is selected for the probabilities of 4, 2, and 1 percent. As for the probabilities of 50 and 10 percents, partial-duration output is selected. The intensity position is selected as 50% from the available list of choices.

The storm durations of 1 hour, 6 hours and 24 hours are used in the simulations. The intensity duration is selected to be 15 minutes (the same with the simulation time step) for 1 hour and 6 hours storms, and 1 hour for 24 hours storm.

Storm area is not defined, so that the area of each subbasin is separately used in the model computations.

HEC-HMS requires precipitation depths for the following predefined time values: 15-min and 1-hr depth for 1-hr storm duration, 15-min, 1-hr, 2-hrs, 3-hrs, and 6-hrs depth for 6 hr storm duration, and 1-hr, 2-hrs, 3-hrs, 6-hrs, 12-hrs, and 1-day (24-hrs) depths for a 1-day storm. To satisfy this input requirement, a temporal storm pattern should be defined for each of the three storm types (1-hr, 6-hrs, and 1-day).

Besides the spatial distribution of rainfall, the temporal distribution pattern has always been a major problem in hydrologic studies. There are several different methods suggested for the temporal distribution of rainfall in a specified period. A general classification of these methods is given by Veneziano and Villani (1999):

- A single rainfall intensity value from an IDF curve may be used together with a rectangular hyetograph (the single value is then accepted as the average rainfall during the storm) or the single value may be used with a triangular hyetograph as given by Yen and Chow (1980).
- Alternatively, the entire IDF curve intensities for particular durations and frequencies may be used for the definition of the rainfall temporal pattern. Keifer and Chu (1957) proposed a method to compute the peak intensity from the entire IDF curve, and redistribute the rainfall before and after the peak with appropriate equations.
- As a third approach, standardized mass curves like Huff's mass rainfall distribution curves (Huff, 1967) or SCS mass distribution curves (SCS, 1986) may be used in the determination of rainfall temporal pattern.

In this study, the second approach, i.e. using the entire IDF curve(s) to obtain the rainfall temporal pattern, is used. The total rainfall depths expected for the specified rainfall durations are computed from IDF curves and already given in

Table 7.1. Sample rainfall hyetographs that are input to *frequency storm method* of HEC-HMS are given in Figure 7.3.

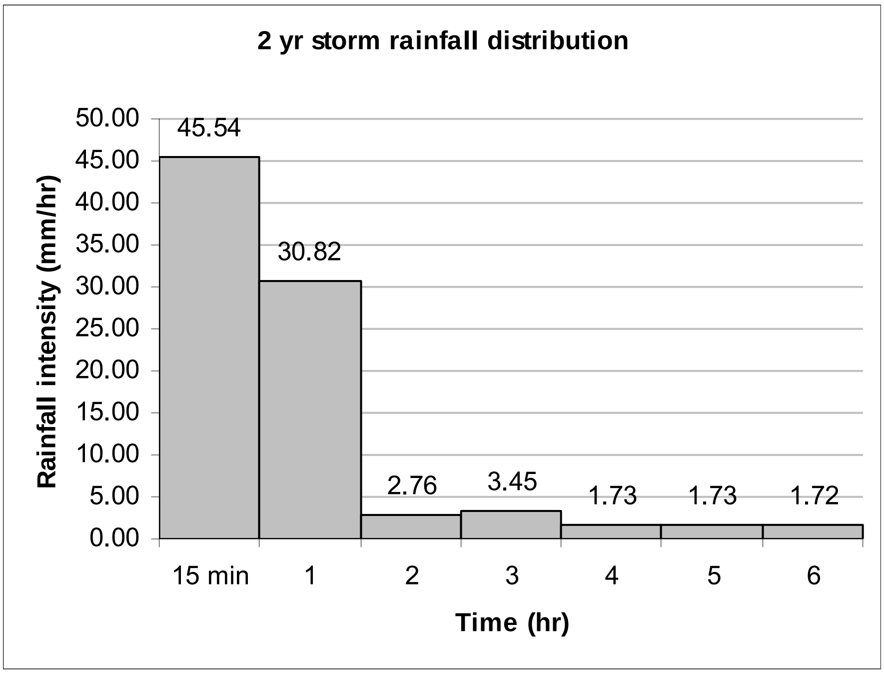

(a)

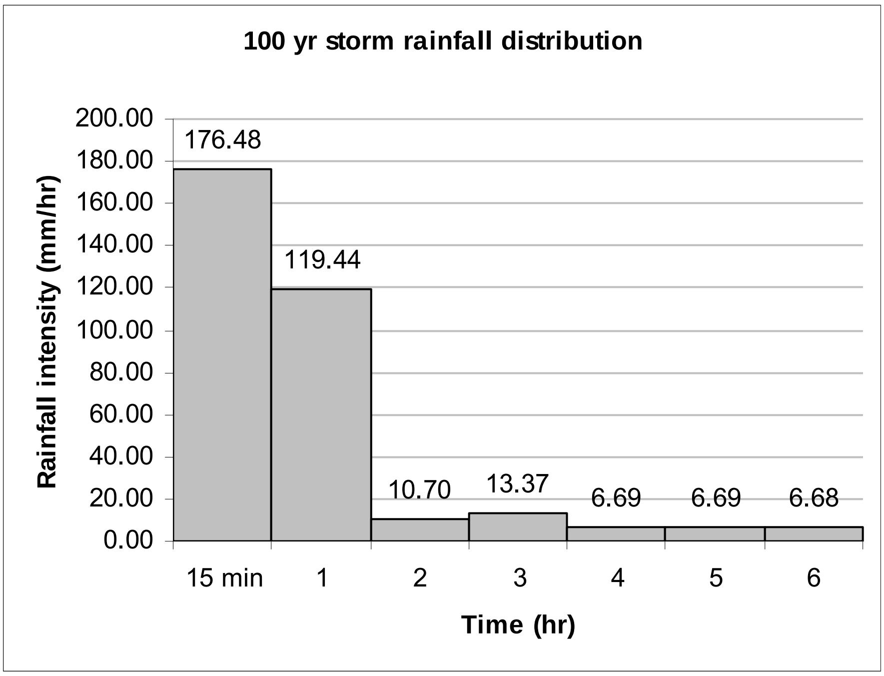

(b)

Figure 7.3. Rainfall distribution pattern for a 6-hrs duration storm

It is important to note here that HEC-HMS redistributes the given rainfall hyetograph according to the peak position. For example if the peak is positioned to the 50% of the storm duration, the redistribution is performed as given in Figure 7.4.

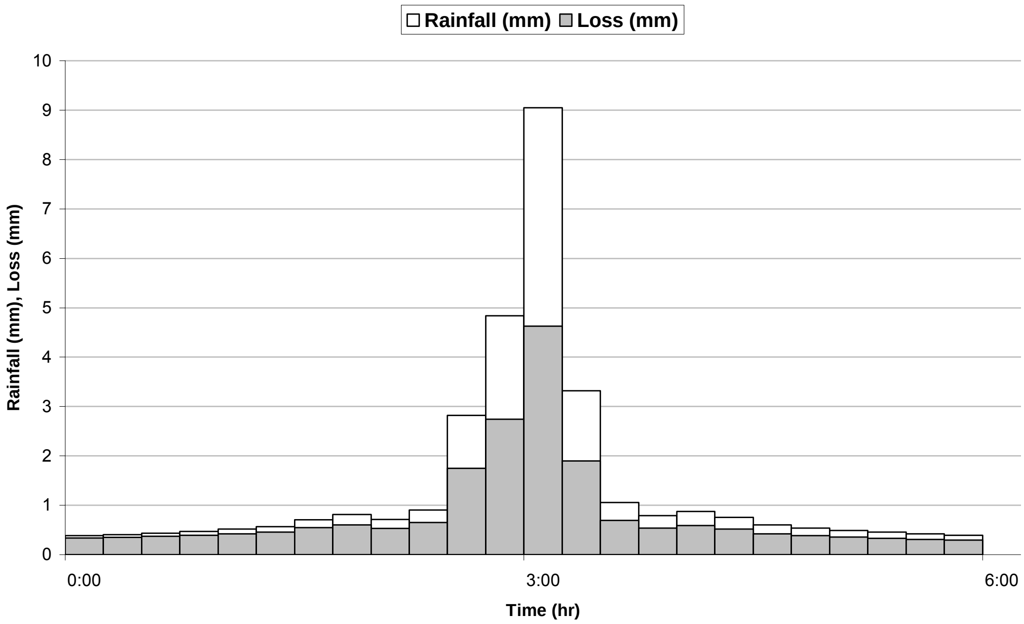

Figure 7.4. Redistributed rainfall pattern in HEC-HMS (Kirazdere subbasin, 6-hrs storm with 2 yrs frequency)

7.4.3. Simulation results

The tables presented here (Tables 7.2 to 7.7) give the detailed results of model simulations. The following results are concluded:

- Subbasins gave runoff proportional to their areas: larger subbasins having bigger peaks and smaller subbasins having smaller peaks. The biggest peaks occurred in Serindere (120.534 km²) and the smallest peaks occurred in Kazandere (23.1 km²).

- When the minimum loss parameters are used, runoff peaks increased with respect to the runoffs obtained from average loss parameters.
- When the return period increased (exceedance probability of the storm decreased), bigger peaks are obtained.
- Average time to peak is found out to be 7.5 hours with 50% intensity position, but it reduces to 6.0 hours with 25% intensity position.
- The minimum peak flow for Yuvacık Basin is 79.77 m^3/s and obtained from a 1-hr storm with 2 year frequency when the **minimum loss parameters** are used; and the maximum peak flow is 618.29 m^3/s and obtained from a 6-hrs storm with 100 years frequency.
- The minimum peak flow for Yuvacık Basin is 38.32 m^3/s and obtained from a 1-hr storm with 2 years frequency when the **average loss parameters** are used; and the maximum peak flow is 330.71 m^3/s and obtained from a 24-hrs storm with 100 years frequency.
- HEC-HMS uses an area reduction factor when the subbasins get larger than 25 km^2 and reduces the given rainfall depths to find the average rainfall of the subbasin. Hence, larger subbasins have smaller rainfall depths, and smaller subbasins have larger rainfall depths. A similar relationship is observed in total loss.

Table 7.2. Simulation results for minimum loss parameters and 1-hr storm

Storm duration 1 hr	Return Period (yr)	2	10	25	50	100
	IDF Prec. (mm)	19.8	43.7	60.8	76.2	94.2
Qp (m^3/s)	Kirazdere	23.69	60.79	89.35	115.71	147.18
	Kazandere	6.85	17.7	26.07	33.76	42.88
	Serindere	37.87	95.82	139.28	178.94	226.7
	Contributing	11.36	28.87	42.23	54.42	68.92
	Yuvacık	79.77*	203.18*	296.93	382.83	485.68
Precipitation (mm) & Loss (mm)	Kirazdere	17.24	38.05	52.95	66.36	82.03
		10.13	19.64	25.83	31.21	37.3
	Kazandere	18.93	41.78	58.14	72.86	90.07
		11.84	23.32	30.88	37.55	45.2
	Serindere	16.32	36.01	50.11	62.8	77.63
		8.74	16.79	22.14	26.85	32.08
	Contributing	18.54	40.92	56.93	71.35	88.2
		10.75	20.9	27.58	33.49	40.21
Time to peak (hr)	Kirazdere	5	5	5	5	5
	Kazandere	5	5	5	5	5
	Serindere	5	5	5	5	5
	Contributing	5	5	5	5	5

* When the output type is selected as annual-output, peaks decrease to 68.38 and 200.82 m^3/s, respectively.

Table 7.3. Simulation results for minimum loss parameters and 6-hrs storm

Storm duration 6 hr	Return Period (yr)	2	10	25	50	100
	IDF Prec. (mm)	34.5	69.5	92.3	111.9	133.7
Qp (m^3/s)	Kirazdere	38.46	89.31	123.49	154.05	188.68
	Kazandere	10.73	24.86	34.35	42.83	52.46
	Serindere	59.24	137.6	190.7	238.36	292.53
	Contributing	17.44	40.14	55.41	69.09	84.62
	Yuvacık	125.87*	291.91*	403.95	504.33	618.29
Precipitation (mm) & Loss (mm)	Kirazdere	32.34	65.14	86.51	104.88	125.31
		20.09	36.44	46.64	55.1	64.29
	Kazandere	33.77	68.02	90.34	109.52	130.85
		22.06	40.68	52.39	62.16	72.81
	Serindere	31.55	63.56	84.42	102.34	122.28
		19.01	34.21	43.56	51.25	59.54
	Contributing	33.43	67.35	89.44	108.44	129.56
		20.8	37.95	48.66	57.53	67.16
Time to peak (hr)	Kirazdere	7.5	7.5	7.5	7.5	7.5
	Kazandere	7.5	7.5	7.5	7.5	7.5
	Serindere	7.5	7.5	7.5	7.5	7.5
	Contributing	7.5	7.5	7.5	7.5	7.5

* When the output type is selected as annual-output, peaks decrease to 107.53 and 288.52 m^3/s, respectively.

Table 7.4. Simulation results for minimum loss parameters and 24-hrs storm

Storm duration 24 hr	Return Period (yr)	2	10	25	50	100
	IDF Prec. (mm)	52.2	104.1	132.3	153.4	174.5
Qp (m³/s)	Kirazdere	39.81	96.66	124.24	153.73	189.04
	Kazandere	10.99	26.69	34.34	42.57	52.51
	Serindere	59.09	147.16	190.01	236.15	291.25
	Contributing	17.61	42.89	55.21	68.48	84.48
	Yuvacık	127.5*	313.4*	403.8	500.93	617.28
Precipitation (mm) & Loss (mm)	Kirazdere	50.47	100.64	127.9	148.3	168.7
		34.51	61.88	76.31	85.59	94.6
	Kazandere	51.61	102.93	130.81	151.67	172.53
		36.7	66.82	82.77	93.15	103.19
	Serindere	49.84	99.39	126.32	146.46	166.61
		34.31	60.54	74.26	82.81	91.15
	Contributing	51.34	102.39	130.13	150.89	171.64
		35.53	63.81	78.71	88.15	97.27
Time to peak (hr)	Kirazdere	17	17	17	17	17
	Kazandere	17	17	17	17	17
	Serindere	17	17	17	17	17
	Contributing	17	17	17	17	17

* When the output type is selected as annual-output, peaks decrease to 108.99 and 309.76 m³/s, respectively.

Table 7.5. Simulation results for mean loss parameters and 1-hr storm

Storm duration 1 hr	Return Period (yr)	2	10	25	50	100
	IDF Prec. (mm)	19.8	43.7	60.8	76.2	94.2
Qp (m³/s)	Kirazdere	9.97	27.68	42.68	57.08	74.23
	Kazandere	4.52	11.84	17.72	23.16	29.52
	Serindere	17.06	45.93	69.1	90.23	115.23
	Contributing	6.77	16.74	24.84	32.38	41.22
	Yuvacık	38.32*	102.19*	154.34	202.85	260.2
Precipitation (mm) & Loss (mm)	Kirazdere	17.24	38.05	52.95	66.36	82.03
		14.82	30.24	40.56	49.58	60.04
	Kazandere	18.93	41.78	58.14	72.86	90.07
		14.74	29.91	40.1	49.13	59.67
	Serindere	16.32	36.01	50.11	62.8	77.63
		13.33	27.22	36.66	45.1	54.91
	Contributing	18.54	40.92	56.93	71.35	88.2
		14.97	30.39	40.75	49.9	60.59
Time to peak (hr)	Kirazdere	5	5	5	5	5
	Kazandere	5	5	5	5	5
	Serindere	5	5	5	5	5
	Contributing	5	5	5	5	5

* When the output type is selected as annual-output, peaks decrease to 32.89 and 100.9 m³/s, respectively.

Table 7.6. Simulation results for mean loss parameters and 6-hrs storm

Storm duration 6 hr	Return Period (yr)	2	10	25	50	100
	IDF Prec. (mm)	34.5	69.5	92.3	111.9	133.7
Qp (m³/s)	Kirazdere	18.1	44.17	61.86	77.75	95.78
	Kazandere	7.29	16.98	23.5	29.34	35.98
	Serindere	28.42	67.81	94.75	119.09	146.92
	Contributing	10.45	23.72	32.69	40.77	49.96
	Yuvacık	64.26*	152.68*	212.8	266.95	328.64
Precipitation (mm) & Loss (mm)	Kirazdere	32.34	65.14	86.51	104.88	125.31
		27.24	51.73	67.38	80.64	95.26
	Kazandere	33.77	68.02	90.34	109.52	130.85
		26.36	49.95	65.01	77.73	91.72
	Serindere	31.55	63.56	84.42	102.34	122.28
		26.06	49.71	64.77	77.5	91.49
	Contributing	33.43	67.35	89.44	108.44	129.56
		27.05	51.27	66.72	79.78	94.13
Time to peak (hr)	Kirazdere	7.75	7.5	7.5	7.5	7.5
	Kazandere	7.5	7.5	7.5	7.5	7.5
	Serindere	7.5	7.5	7.5	7.5	7.5
	Contributing	7.75	7.5	7.5	7.5	7.5

* When the output type is selected as annual-output, peaks decrease to 54.64 and 150.85 m³/s, respectively.

Table 7.7. Simulation results for mean loss parameters and 24-hrs storm

Storm duration 24 hr	Return Period (yr)	2	10	25	50	100
	IDF Prec. (mm)	52.2	104.1	132.3	153.4	174.5
Qp (m³/s)	Kirazdere	20	49.35	63.55	78.86	97.28
	Kazandere	7.63	18.35	23.6	29.26	36.14
	Serindere	29.36	73.34	95.04	118.69	147.16
	Contributing	10.84	25.53	32.75	40.6	50.13
	Yuvacık	67.83*	166.57*	214.94*	267.41*	330.71*
Precipitation (mm) & Loss (mm)	Kirazdere	50.47	100.64	127.9	148.3	168.7
		43.52	82.49	103.38	118.11	132.55
	Kazandere	51.61	102.93	130.81	151.67	172.53
		42.07	79.17	98.99	112.68	126.05
	Serindere	49.84	99.39	126.32	146.46	166.61
		42.95	81.29	101.75	116.05	130.11
	Contributing	51.34	102.39	130.13	150.89	171.64
		43.27	81.57	102.03	116.17	130
Time to peak (hr)	Kirazdere	17	17	17	17	17
	Kazandere	17	17	17	17	17
	Serindere	17	17	17	17	17
	Contributing	17	17	17	17	17

* When the output type is selected as annual-output, peaks decrease to 57.92 and 164.64 m³/s, respectively.

7.4.4. Comparison of flood hydrographs with various return periods (DSI) with model results (HEC-HMS)

In this section the hydrographs obtained from HEC-HMS model simulations using frequency storm method and the hydrographs that are obtained by DSI (DSI, Bursa 1983) using statistical techniques are compared. In addition to graphical comparisons, corresponding peak values and volumes of each hydrograph are also presented.

DSI hydrographs are found as follows: From the statistical analysis of the annual maximum peak records of (2-6) Kirazdere Yuvaköy station operated by DSI (1963-1993), peak flow values corresponding to 2 yrs, 10 yrs, 25 yrs, 50 yrs and 100 yrs return periods are found. Then, these peak values are multiplied by the ordinates of dimensionless flood hydrograph that is produced for the spillway design using DSI synthetic hydrograph method, and the ordinates of the flood hydrographs for the corresponding return periods are found. These hydrograph ordinates are given in Table 7.8.

In Figure 7.5 DSI flood hydrographs, their peak discharge values (m^3/s) and total flow volumes (m^3) are given; similarly, in Figure 7.6 HEC-HMS simulation hydrographs, their peak discharge values (m^3/s) and total flow volumes (m^3) are given for comparison.

As compared to DSI hydrographs, HEC-HMS overestimates the peak flows of 2-yr and 100-yrs storms; however, it underestimates the peak flows of 10-yrs, 25-yrs and 50-yrs storms. When total volumes of the flows are compared, only the total volume of the 2-yr storm is overestimated in HEC-HMS. Total volumes of all the other storms are underestimated.

The peak time in DSI hydrographs is 6 hours as can be seen from Figure 7.5, whereas the peak time for HEC-HMS hydrographs is 7.5 hours as can be seen from Figure 7.6. The difference of 1.5 hours is simply due to the intensity position which was previously selected as 50% in frequency storm method. If intensity position is selected as 25%, then the peak time of HEC-HMS hydrographs also becomes 6 hours. Total volumes of hydrographs produced with 25% rainfall intensity position do not change; however, the peak values decrease to some extent (Figure 7.7).

Table 7.8. Dimensionless flood hydrograph and flood hydrographs for different return periods (DSI, Bursa 1983)

Time (hr)	Dimensionless Flood Hydrograph (6-hrs storm)	Flood Hydrographs (m^3/s) Return Periods				
		2	10	25	50	100
0	0	0	0	0	0	0
1	0.069	7.6	20.5	28.3	34.9	41.2
2	0.25	27.5	74.3	102.5	126.5	149.2
3	0.57	62.7	196.3	233.7	288.4	340.3
4	0.86	94.6	255.4	352.6	435.2	513.4
5	0.99	108.9	294	405.9	500.9	591
6	1	110	297	410	506	597
7	0.9	99	267.3	369	455.4	537.3
8	0.77	84.7	228.7	315.7	389.6	459.7
9	0.62	68.2	184.1	254.2	313.7	370.1
10	0.48	52.8	142.6	196.8	242.8	286.6
11	0.36	39.6	106.9	147.6	182.1	214.9
12	0.27	29.7	80.2	110.7	136.6	161.2
13	0.2	22	59.4	82	101.2	119.4
14	0.15	16.5	44.5	61.5	75.9	89.5
15	0.11	12.1	32.7	45.1	55.6	65.7
16	0.08	8.8	23.8	32.8	40.5	47.7
17	0.06	6.6	17.8	24.6	30.4	35.8
18	0.04	4.4	11.9	16.4	20.2	23.9
19	0.03	3.3	8.9	12.3	15.2	17.9
20	0.02	2.2	5.9	8.2	10.1	11.9
21	0.016	1.8	4.8	6.15	8.1	9.5
22	0.011	1.2	3.3	4.5	5.5	6.5
23	0.006	0.7	1.8	2.5	3	3.6
24	0.003	0.3	0.9	1.23	1.5	1.8
25	0.0015	0.2	0.4	0.6	0.7	0.9
26	0.0007	0.1	0.2	0.3	0.3	0.4
27	0.0004	0.04	0.1	0.2	0.2	0.2
28	0	0	0	0	0	0

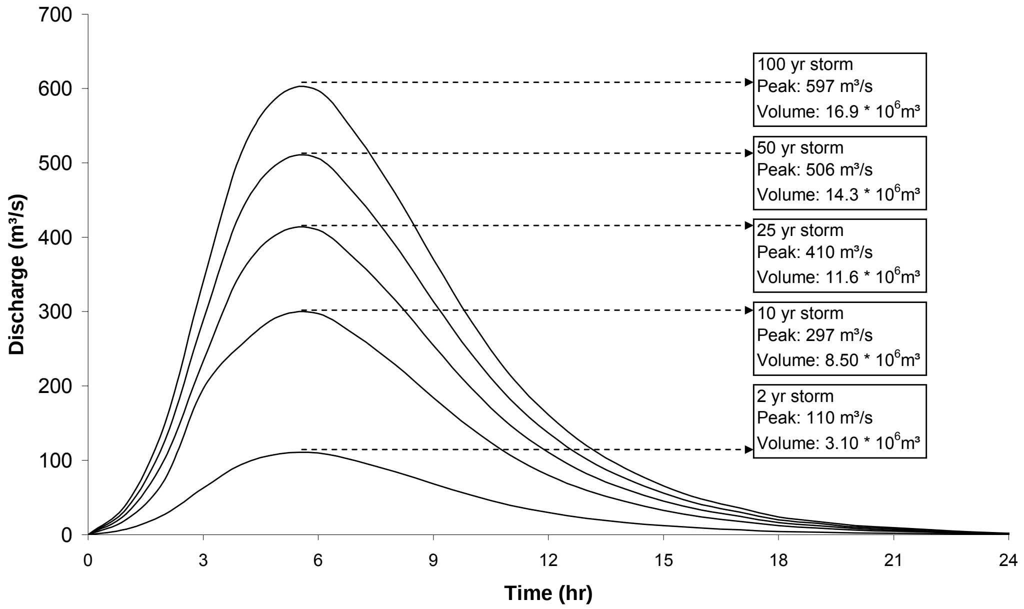

Figure 7.5. DSI hydrographs, peak flows and total volumes (DSI, 1983) (6-hrs storm)

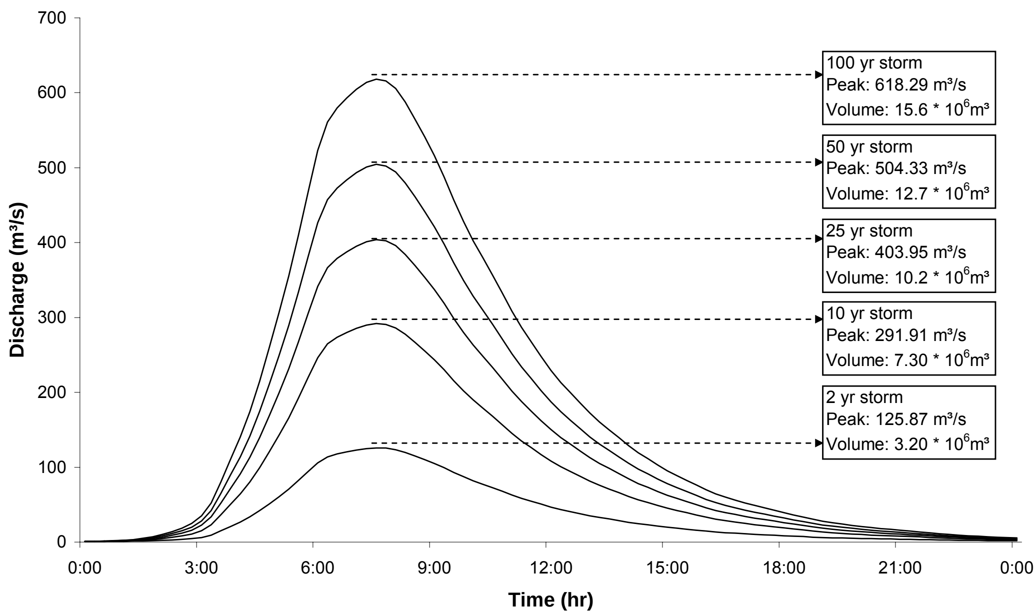

Figure 7.6. HEC-HMS hydrographs, peak flows and total volumes (Frequency storm method, 6-hrs storm)

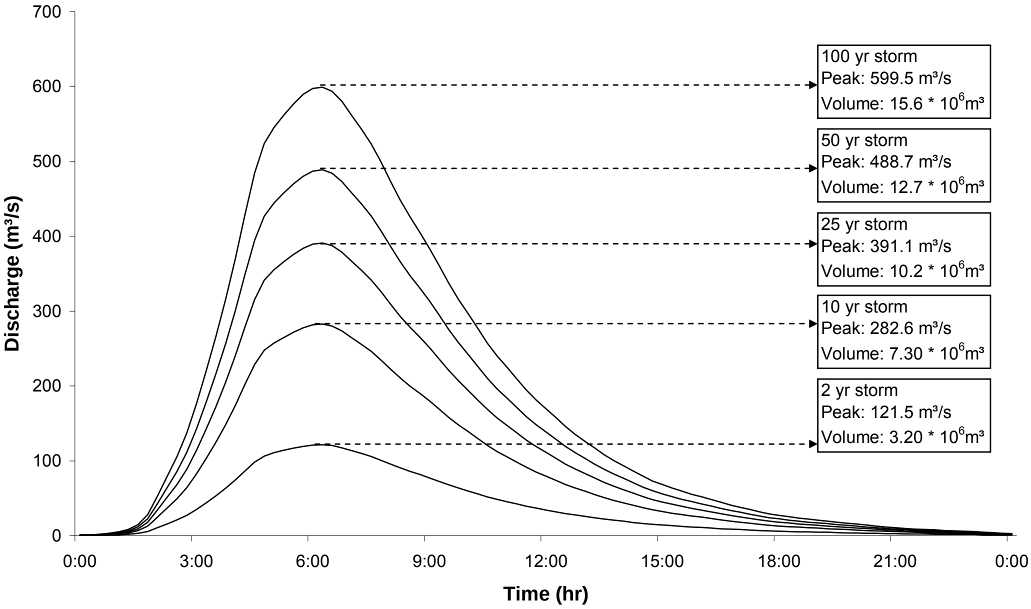

Figure 7.7. HEC-HMS hydrographs, peak flows and total volumes (Frequency storm method, 25% intensity position, 6-hrs storm)

7.4.5. Storm runoff produced from Probable Maximum Precipitation

DSI also performed probable maximum precipitation studies to use in the design flood computations for the spillway of Yuvacık Dam. In this study long record of maximum annual precipitation values of Kocaeli station is used. Table 7.9 shows the probable maximum precipitation values for the given durations (DSI, Bursa 1983).

Table 7.9. Probable maximum precipitation depth values of Kocaeli station (DSI, Bursa 1983)

t (hr)	1	2	4	6	12	18	24
PMP (mm)	126.8	158.5	199.7	218.8	256.7	285.3	317.0

Maximum runoff found out to correspond to 6-hrs storm (218.8 mm depth), and yielded a peak of 1500 m^3/s which is then used in the design of the spillway. By multiplying this peak value with the ordinates of the dimensionless hydrograph prepared for the spillway, the maximum runoff hydrograph is obtained (Figure 7.8). The volume of the hydrograph is 42.5 million cubic meters.

HEC-HMS model runs generate flood hydrographs that have peaks lower than the design flood discharge given by DSI. To generate simulated hydrographs, again frequency storm method is used in HEC-HMS. 6-hrs storm precipitation depth values of Table 7.8 are used, and depth value is distributed in the same temporal pattern with IDF simulations. Two different hydrographs are generated (Figure 7.8): one for 50% intensity position, and the other for 25% intensity position. The volumes of generated hydrographs remained the same (27.1 10^6 m^3) but peak discharges changed slightly. The peak of the hydrograph generated with 50% intensity position is 1074.4 m^3/s, and the second peak is 1041 m^3/s. No matter what the intensity position is, HEC-HMS highly underestimated the design discharge value of DSI method. Nearly, peaks of HEC-HMS hydrographs are two thirds of DSI design hydrograph peak.

The same discussions made on time to peak in the previous section (Section 7.4.4), are still valid here.

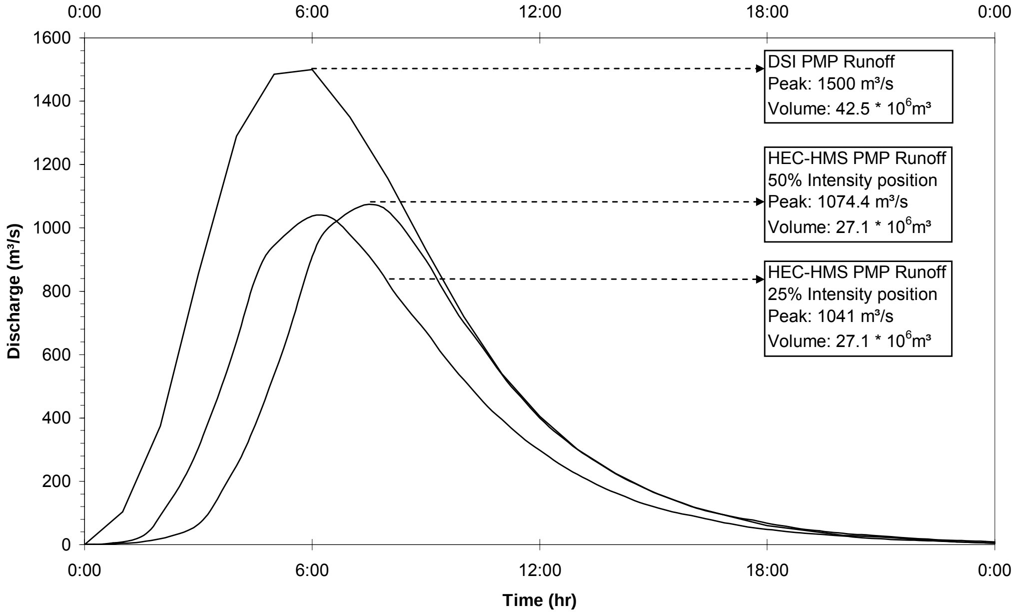

Figure 7.8. Maximum runoff hydrographs obtained by PMP depths, peak flows and total volumes

CHAPTER 8

CONCLUSIONS AND RECOMMENDATIONS

In this study, HEC-HMS version 3.0.1 (April 2006) hydrologic modeling software is applied to Yuvacık Basin and model parameters are calibrated. This calibrated model can be used as a decision support tool in the Yuvacık Dam reservoir operation and management such as: reservoir operation studies that will be performed to supply the domestic and industrial water demand of İzmit city and nearby regions, as well floodplain management and flood damage estimation studies.

The model parameters that are calibrated for event-based hourly simulations can be used for the spring, summer and fall seasons to predict runoff. In the snowfall and snowmelt period (late fall, winter and early spring) the model parameters that are calibrated for daily simulations can be used.

New automatic weather stations (AWOS) (RG7-RG10 and M1-M3) located at higher elevations (550-1500 m) provide more representative precipitation records (rainfall and snow) compared to existing rain gage network (RG1-RG6) which are installed previously by the operator company at elevations (170-520 m). Spatial distribution of the new stations is better than the existing ones, because existing gages were accumulated around the reservoir, whereas, new stations are scattered inside the basin as much a representative way as possible. Besides, new stations provide temperature, wind and humidity data. Especially air temperature data has crucial importance for the snowmelt modeling studies.

In general, Kirazdere subbasin simulations gave better results than the other two subbasins (Kazandere and Serindere). One reason for that was the more number of events available for Kirazdere. Unfortunately, in some periods from 2001 to 2006, streamflow data was not available for Kazandere and Serindere, e.g. for the year 2001. Also, in 2003-2004 water year Kazandere and Serindere flow records have flow level inconsistencies. To avoid missing data and erroneous data, streamflow gages and precipitation stations should be calibrated periodically. These stations should be checked especially after heavy rainfall and snow storms. For example, in a heavy snow storm in 2006, Kartepe station was covered with snow depth up to 3 meters) and the station could not transmit data due to electricity shortages.

The model, especially for snowmelt period, can be used for real time runoff forecasts (e.g. one day ahead forecasts) with the use of MM5 grid data as input to the model. The forecasted daily temperature and precipitation data of the most representative grids for each subbasin were integrated into the model. The same grid combinations may be used for future forecasting studies, but checking the validity of given grid combinations with the future data is necessary.

DSI obtained storm runoff values corresponding to different return periods for the whole basin using IDF data of Kocaeli station (up to 1983) (DSI, Bursa 1983). In this earlier study, DSI used statistical method to obtain frequency runoffs and PMP runoffs. In this study, updated IDF data of Kocaeli station (up to 2004) is input into “frequency storm” method of HEC-HMS. Frequency runoffs are obtained for each subbasin with two sets of calibrated model parameters: minimum and mean parameters. Frequency runoffs with return periods ranging from 2 to 100 years obtained using minimum parameter sets are very close to the runoffs given by DSI, on the other hand, frequency runoffs obtained using average parameter sets are almost half of the runoffs given by DSI. PMP runoff obtained by the model is about two thirds of the PMP runoff given by DSI. The details of PMP runoff computations performed by DSI are not known, so a reliable conclusion can not be made for the difference in PMP results.

The calibrated model parameters should be checked with future water year data, and model should be verified. If necessary, model parameters should be updated for better performance of the model runs considering initial soil moisture distribution in the area. Infiltration and soil moisture tests should be conducted in the basin at various soil textures and land use to better define the initial abstraction and infiltration parameters in the model.

The model can be also used to test fully distributed modeling studies by providing gridded precipitation data and entering necessary parameter data in grid format. The fully distributed modeling ability of the model can be tested in future years and the results can be compared with the subbasin scale simulation results.

Evapotranspiration is not included in the model calibrations. In future, if it is possible, evaporation measurements with different land use characteristics should be performed in the basin, and evapotranspiration component should be added to the model to see how it affects the calibrated parameters.

Channel routing can be added to the model. Using one of the available routing methods (e.g. kinematic wave, Muskingum) routing parameters can be calibrated.

This study is one of the first HEC-HMS (Version 3) applications in Türkiye especially when snowmelt module usage and MM5 data integration into the model are considered. Modeling snowmelt and forecasting runoff especially in the spring season is very important for the operation and management of Yuvacık Dam, since efficient operation of the dam is essential in controlling floods in spring and droughts in summer.

REFERENCES

Anderson, M. L., Chen, Z. Q., Kavvas, M. L., and Feldman, A., *Coupling HEC-HMS with Atmospheric Models for Prediction of Watershed Runoff,* J. Hydrologic Engineering, American Society of Civil Engineers (ASCE), vol. 7, No.4, p312, August 2002.

Bergström, S., *Development and Application of a Cconceptual Runoff Model for Scandinavian Catchments,* SMHI Reports RHO, No. 7, Norrköping, 1976.

Beven, K. J., *Rainfall-Runoff Modelling, The Primer,* John Wiley and Sons Ltd., England, 2000.

Chow, V. T., *Applied Hydrology,* McGraw-Hill Book Company, 1988.

Crawford, N. H. And Linsley, R. K., *Digital Simulation in Hydrology Stanford Watershed Model IV,* T.R. 39, Stanford, Calif. Dept. Of Civil Engineering, Stanford University, 1966.

Cunderlik, J. M. and Simonovic, S. P., *Calibration, Verification and Sensitivity Analysis of the HEC-HMS Hydrologic Model,* CFCAS Project: Assesment of Water Resources Risk and Vulnerability to Changing Climatic Conditions, Project Report IV, 2004.

Daly, S. F., Davis, R., Pangburn, T., Ochs, E., Rosenthal, W., Affleck, R., Baldwin, T., Bryant, E., Hardy, J., Taylor, S., Dotson, H., Evans, T., Dunn, C., and Burham, M., *Spatially Distributed Snow Modeling for a Comprehensive Study of the Sacramento and San Joaquin Basins, California,* 57th Eastern Snow Conference, Syracuse, New York, USA, 2000.

(DSI, 1983), *İzmit-Kirazdere Project, Kirazdere Dam Hydrologic Engineering Planning Report,* General Directorate of State Hydraulic Works (DSI), in Turkish, Bursa, 1983.

Fleming, G., *Computer Simulation Techniques in Hydrology,* Elsevier Environmental Science Series, american Elsevier Publishing Co., 1975.

Fleming, M. and Neary, V., *Continuous Hydrologic Modeling Study with the Hydrologic Modeling System,* J. Hydrologic Engineering, American Society of Civil Engineers (ASCE), Vol. 9, No. 3, p175, 2004.

Ford, D. T. and Hamilton, D., *Computer Models for Water-Excess Management,* Larry W. Mays ed., Water Resources Handbook, McGraw-Hill, NY, 1996.

Haan, C. T., et al., *Hydrologic Modeling of Small Watersheds,* American Society of Agricultural Engineers, 1982.

Horton, R. E., *The Role of Infiltration in the Hydrological Cycle,* Transactions, American Geophysical Union, Vol. 14, 446-460.

Hu, H. H., Kreymborg, L. R., Doeing, B. J., Baron, K. S., and Jutila, S. A., *Gridded Snowmelt and Rainfall-Runoff CWMS Hydrologic Modeling of the Red River of the North Basin,* J. Hydrologic Engineering, American Society of Civil Engineers (ASCE), Vol. 11, No. 2, p91, 2006.

Huff, F. A., *Time Distribution of Rainfall in Heavy Storms,* Water Resources Research, Vol. 3 No.4, p1007, 1967.

Huff, F. A., *Time Distributions of Heavy Storms in Illionis,* Circular 173, State of Illionis, Department of Energy and Natural Resources, 1990.

Keifer, C. J. and Chu, H. H., *Synthetic Storm Pattern for Drainage Design,* ASCE Journal of the Hydraulics Division, 83 (HY4), 1-25, 1957.

Kessler, E. and Neas, B., *On Correlation, with Applications to the Radar and Raingage Measurement of Rainfall,* Atmospheric Research, 34:217-229, 1994.

Legates, D. R., *Evaluating the Use of "Goodness of Fit" Measures in Hydrologic and Hydroclimatic Model Validation,* Water Resources Research, 35:233-241, 1999.

Martinec, J., *Snowmelt-Runoff Model for Streamflow Forecasts,* Nordic Hydrology, Vol. 6 (3), 145-154, 1975.

McCuen, R. H., *Microcomputer Applications in Statistical Hydrology,* Prentice Hall, New Jersey, 1993.

Mike 11, *A modeling System for Rivers and Channels User's Guide*, DHI Software, 2004.

Moore, D. S., *Statistics: Concepts and Controversies,* 3rd Edition, W. H. Freeman and Company, New York, 439pp, 1991.

Nash, J.E. and Sutcliffe, J.V., *River flow forecasting through conceptual models. Part I: A discussion of principles*, Journal of Hydrology, Vol. 10, 282-290, 1970.

Pearson, K., *On a Form of Spurious Correlation Which May Arise When Indices are Used in the Measurements of Organs,* Proceedings, Royal Society of London, Vol. 60, 489-502, 1932.

(PRI, 2005), Republic of Turkey Ministry of Environment and Forestry, Poplar and Fast Growing Forest Trees Research Institute, 2005.

Raudkivi, A. J., *An Advanced Introduction to Hydrological Processes and Modelling,* Pergamon Press, 1979.

Scharffenberg, W. A. and Fleming, M. J., *Hydrologic Modeling System Version 3.0.1 User's Manual,* US Army Corps of Engineers, Hydrologic Engineering Center (USACE-HEC), Davis CA, April 2006.

SCS, *Urban Hydrology for Small Watersheds,* Tech. Rep. 55, Engineering Division, Soil Conservation Service, US Department of Agriculture, Washington, DC, 1986.

Sherman, L. K., *Streamflow from rainfall by the unit-graph method,* Engineering News Record, 108, 501-505, 1932.

Snowmelt Runoff Model (SRM) User's Manual, Department of Geography, University of Bern, 1994.

Şensoy, A., Tekeli, A. E., Şorman, A. A., Şorman, A. U., *Simulation of Event-Based Snowmelt Runoff Hydrographs Based on Snow Depletion Curves and the Degree-day Method,* Canadian Journal of Remote Sensing, 29(6): 693-700, 2003.

Şorman, A. A., *Use of Satellite Observed Seasonal Snow Cover in Hydrological Modeling and Snowmelt Runoff Prediction in Upper Euphrates Basin, Turkey,* Ph. Doc. Thesis, Civil Engineering Department, Middle East Technical University (METU), 2005.

(USACE-HEC, 1981), *HEC-1 Flood Hydrograph Package*, *Users Manual*, U.S. Army Corps of Engineers, Hydrologic Engineering Center, 1981.

(USACE-HEC, December 2002), *HEC-HMS Applications Guide,* US Army Corps of Engineers, Hydrologic Engineering Center, 2002.

(USACE-HEC, March 2000), *HEC-HMS Technical Reference Manual,* U.S. Army Corps of Engineers, Hydrologic Engineering Center, 2000.

(USACE-HEC, December 2003)*, Geospatial Hydrologic Modeling Extension, HEC-GeoHMS v1.1. User's Manual,* US Army Corps of Engineers, Hydrologic Engineering Center, December 2003.

Veneziano, D. and Villani, P., *Best Linear Unbiased Design Hyetograph,* Water Resources Research, Vol. 35, No. 9, p2725, 1999.

Ward, R. C., *Principles of Hydrology,* McGraw-Hill Book Company (UK) Limited, London, 1975.

Watershed Modeling System (WMS) User's Manual, Boss International Inc. and Brigham young University, 2000.

Wilcox, B. P., Rawls, W. J., Brakensiek, D. L., and Wight, J. R., *Predicting Runoff from Rangeland Catchments: A Comparison of Two Models,* Water Resources Research, 26:2401-2410, 1990.

Willmott, C. J., *On the Validation of Models,* Physical Geography, 2:184-194, 1981.

Yen, B. C. and Chow, V. T., *Design Hyetographs for Small Drainage Structures,* ASCE Journal of the Hydraulics Division, 106 (HY6), 1055-1076, 1980.

APPENDIX A. SAMPLE RESULTS FOR HOURLY SIMULATIONS

Table A.1. Event 16 (13-18 Apr 2003) calibration results summary table for Kirazdere

METHOD	PARAMETER	SIMULATION	OPTIMIZATION					
			UNIVARIATE GRADIENT					
			Peak-Weighted RMS Error	Percent Error Peak	Percent Error Volume	Sum Absolute Residuals	Sum Squared Residuals	Time-Weighted Error
EXPONENTIAL LOSS	**Initial Range (mm)**	12	12.185	17.93	17.841	10.584	12.183	13.986
	Initial Coef ((mm/hr)^(1-x))	0.9	0.90169	0.91086	0.81811	0.9	0.90013	0.89097
	Coef Ratio	1	Locked	Locked	Locked	Locked	Locked	Locked
	Exponent	0.9	0.90451	0.9	0.91336	0.9	0.90263	0.90101
	Impervious (%)	0	0	0	0	0	0	0
RECESSION (BASEFLOW)	**Initial Discharge (m^3/s)**	4.5	Locked	Locked	Locked	Locked	Locked	Locked
	Recession Constant	0.8	Locked	Locked	Locked	Locked	Locked	Locked
	Threshold Flow(m^3/s)	5	Locked	Locked	Locked	Locked	Locked	Locked

Event 16			Peak-Weighted RMS Error	Percent Error Peak	Percent Error Volume	Sum Absolute Residuals	Sum Squared Residuals	Time-Weighted Error
	Observed	**Simulated**	**Computed**	**Computed**	**Computed**	**Computed**	**Computed**	**Computed**
Total Precipitation (mm)	25.72							
Total Loss (mm)		22.41	22.54	23.26	21.51	22.28	22.47	22.46
Total Baseflow (mm)		19.09	19.09	19.07	19.35	19.09	19.09	19.1
Peak Discharge (m^3/s)	9.43	10.99	10.74	9.43	12.4	11.18	10.86	10.95
Total Discharge (mm)	23.45	22.32	22.19	21.47	23.45	22.45	22.25	22.27
Time of Peak Discharge	04:00 (14Apr)	03:00 (14Apr)	03:00 (14Apr)	03:00 (14Apr)	03:00 (14Apr)	03:00 (14Apr)	03:00 (14Apr)	03:00 (14Apr)
Avg Abs Residual (m^3/s)		0.4	0.4	0.45	0.47	0.4	0.4	0.41
Total Residual (mm)		-1.1	-1.3	-2	0	-1	-1.2	-1.2
Peak Difference (%)		16.54	13.89	0.00	31.50	18.56	15.16	16.12
Volume Difference (%)		-4.82	-5.37	-8.44	0.00	-4.26	-5.12	-5.03

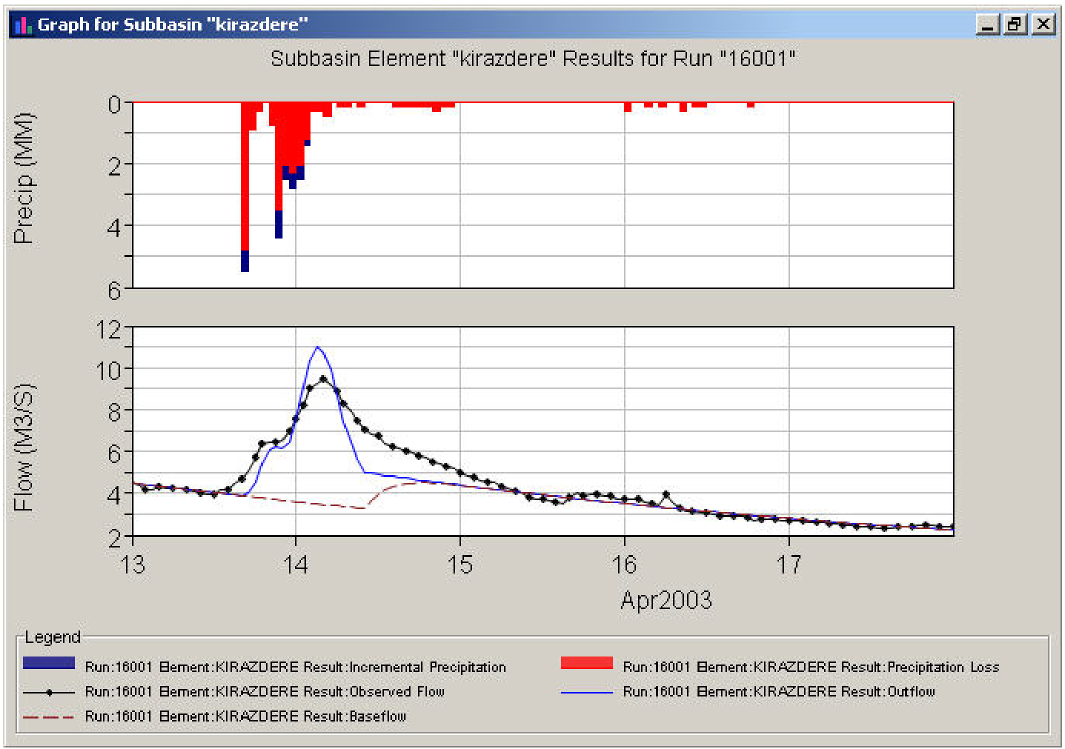

Figure A.1. Event 16 simulation graph for Kirazdere

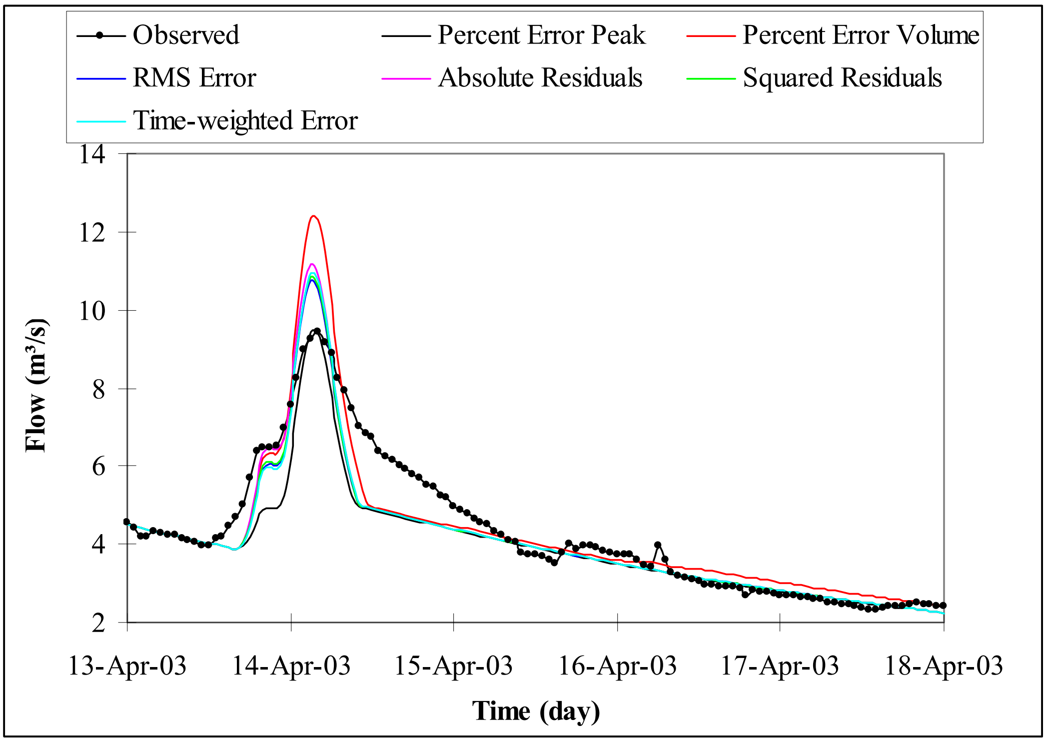

Figure A.2. Event 16 optimization graphs for Kirazdere

Table A.2. Event 39 (23-25 Jun 2004) calibration results summary table for Kazandere

METHOD	PARAMETER	SIMULATION	OPTIMIZATION					
			UNIVARIATE GRADIENT					
			Peak-Weighted RMS Error	Percent Error Peak	Percent Error Volume	Sum Absolute Residuals	Sum Squared Residuals	Time-Weighted Error
EXPONENTIAL LOSS	**Initial Range (mm)**	12	12.279	12	17.64	17.28	12.282	12.285
	Initial Coef ((mm/hr)^(1-x))	0.8	0.81344	0.8	0.784	0.76697	0.82283	0.81683
	Coef Ratio	1	Locked	Locked	Locked	Locked	Locked	Locked
	Exponent	0.9	0.98854	0.9	0.9041	0.92226	0.97933	1
	Impervious (%)	0	0	0	0	0	0	0
RECESSION (BASEFLOW)	**Initial Discharge (m^3/s)**	0.23	Locked	Locked	Locked	Locked	Locked	Locked
	Recession Constant	0.7	Locked	Locked	Locked	Locked	Locked	Locked
	Threshold Flow(m^3/s)	0.25	Locked	Locked	Locked	Locked	Locked	Locked

Event 39			Peak-Weighted RMS Error	Percent Error Peak	Percent Error Volume	Sum Absolute Residuals	Sum Squared Residuals	Time-Weighted Error
	Observed	Simulated	Computed	Computed	Computed	Computed	Computed	Computed
Total Precipitation (mm)	6.67							
Total Loss (mm)		5.83	5.87	5.83	6.05	5.94	5.94	5.88
Total Baseflow (mm)		1.36	1.36	1.36	1.39	1.37	1.37	1.36
Peak Discharge (m^3/s)	0.74	0.74	0.64	0.74	0.58	0.66	0.6	0.62
Total Discharge (mm)	1.99	2.17	2.13	2.17	1.99	2.08	2.07	2.12
Time of Peak Discharge	02:00 (24 Jun)	01:00 (24 Jun)	01:00 (24 Jun)	01:00 (24 Jun)	01:00 (24 Jun)	01:00 (24 Jun)	01:00 (24 Jun)	01:00 (24 Jun)
Avg Abs Residual (m^3/s)		0.04	0.04	0.04	0.04	0.04	0.04	0.04
Total Residual (mm)		0.2	0.1	0.2	0	0.1	0.1	0.1
Peak Difference (%)		0.00	-13.51	0.00	-21.62	-10.81	-18.92	-16.22
Volume Difference (%)		9.05	7.04	9.05	0.00	4.52	4.02	6.53

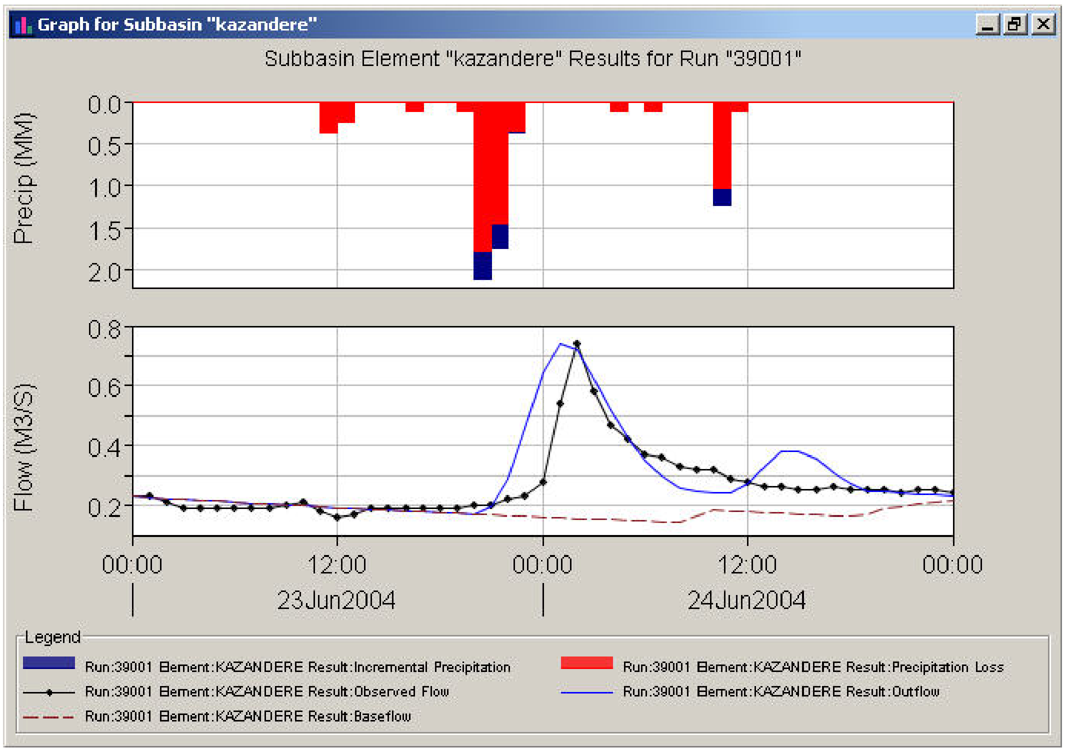

Figure A.3. Event 39 simulation graph for Kazandere

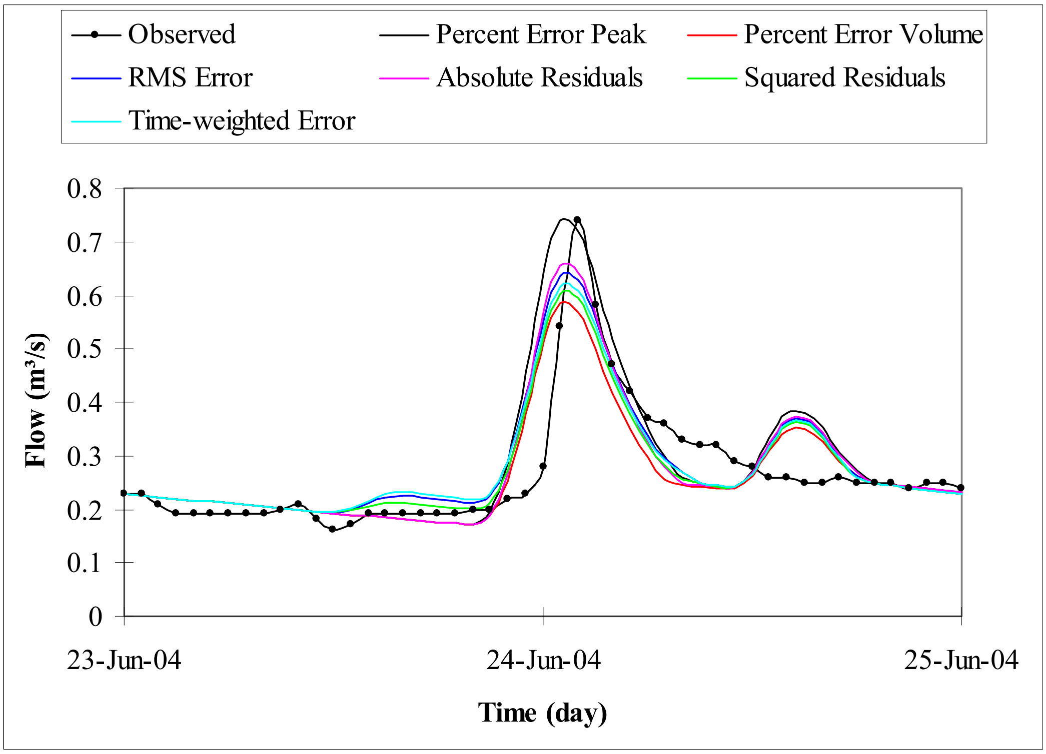

Figure A.4. Event 39 optimization graphs for Kazandere

Table A.3. Event 24 (4-6 Jan 2004) calibration results summary table for Serindere

METHOD	PARAMETER	SIMULATION	OPTIMIZATION					
			UNIVARIATE GRADIENT					
			Peak-Weighted RMS Error	Percent Error Peak	Percent Error Volume	Sum Absolute Residuals	Sum Squared Residuals	Time-Weighted Error
EXPONENTIAL LOSS	**Initial Range (mm)**	8	4.9193	7.0327	9.016	4.8209	4.9193	4.8209
	Initial Coef ((mm/hr)^(1-x))	0.94	0.93179	0.94	0.9212	0.92929	0.93226	0.93615
	Coef Ratio	1	Locked	Locked	Locked	Locked	Locked	Locked
	Exponent	0.96	0.96639	0.972	0.94942	0.98176	0.96551	0.96443
	Impervious (%)	0	0	0	0	0	0	0
RECESSION (BASEFLOW)	**Initial Discharge (m^3/s)**	4	Locked	Locked	Locked	Locked	Locked	Locked
	Recession Constant	0.8	Locked	Locked	Locked	Locked	Locked	Locked
	Threshold Flow(m^3/s)	5	Locked	Locked	Locked	Locked	Locked	Locked

Event 24			Peak-Weighted RMS Error	Percent Error Peak	Percent Error Volume	Sum Absolute Residuals	Sum Squared Residuals	Time-Weighted Error
	Observed	**Simulated**	**Computed**	**Computed**	**Computed**	**Computed**	**Computed**	**Computed**
Total Precipitation (mm)	35.72							
Total Loss (mm)		33.15	32.88	33.31	32.42	33.01	32.88	33
Total Baseflow (mm)		7.25	7.21	7.24	7.23	7.18	7.21	7.25
Peak Discharge (m^3/s)	9.57	10.33	10.52	9.57	12.33	9.7	10.54	10.36
Total Discharge (mm)	10.43	9.75	9.98	9.58	10.44	9.82	9.98	9.9
Time of Peak Discharge	01:00 (05 Jan)	04:00 (05 Jan)	04:00 (05 Jan)	04:00 (05 Jan)	04:00 (05 Jan)	04:00 (05 Jan)	04:00 (05 Jan)	04:00 (05 Jan)
Avg Abs Residual (m^3/s)		0.53	0.46	0.51	0.62	0.42	0.46	0.47
Total Residual (mm)		-0.7	-0.5	-0.8	0	-0.6	-0.5	-0.5
Peak Difference (%)		7.94	9.93	0.00	28.84	1.36	10.14	8.25
Volume Difference (%)		-6.52	-4.31	-8.15	0.10	-5.85	-4.31	-5.08

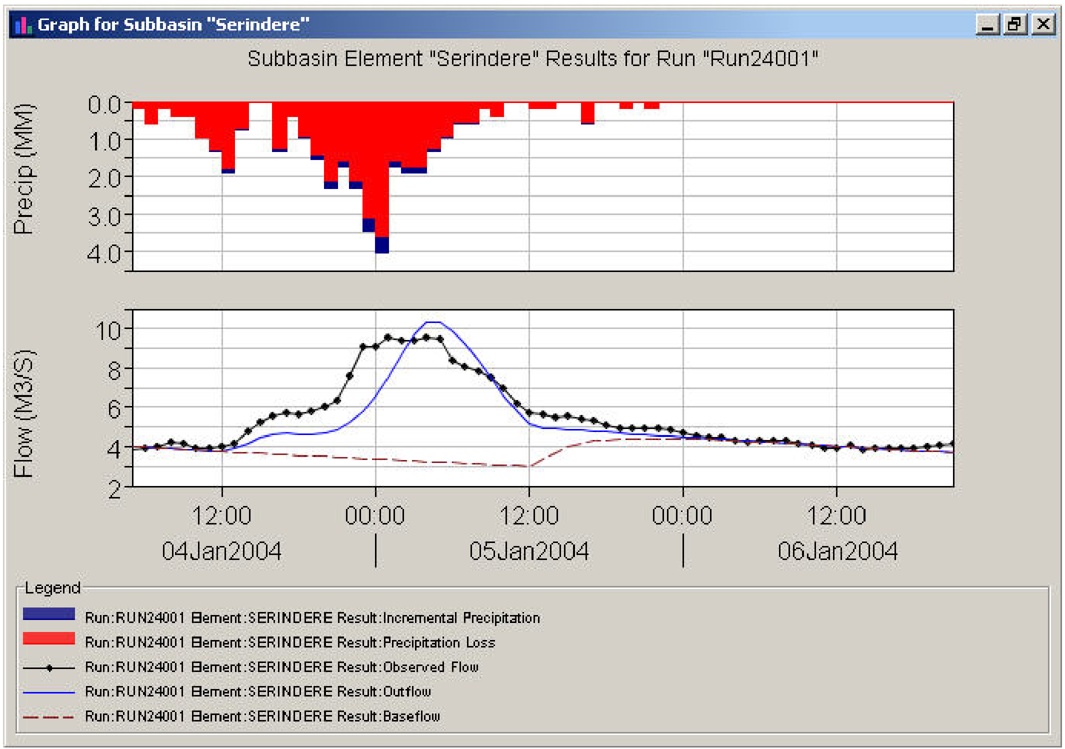

Figure A.5. Event 24 simulation graph for Serindere

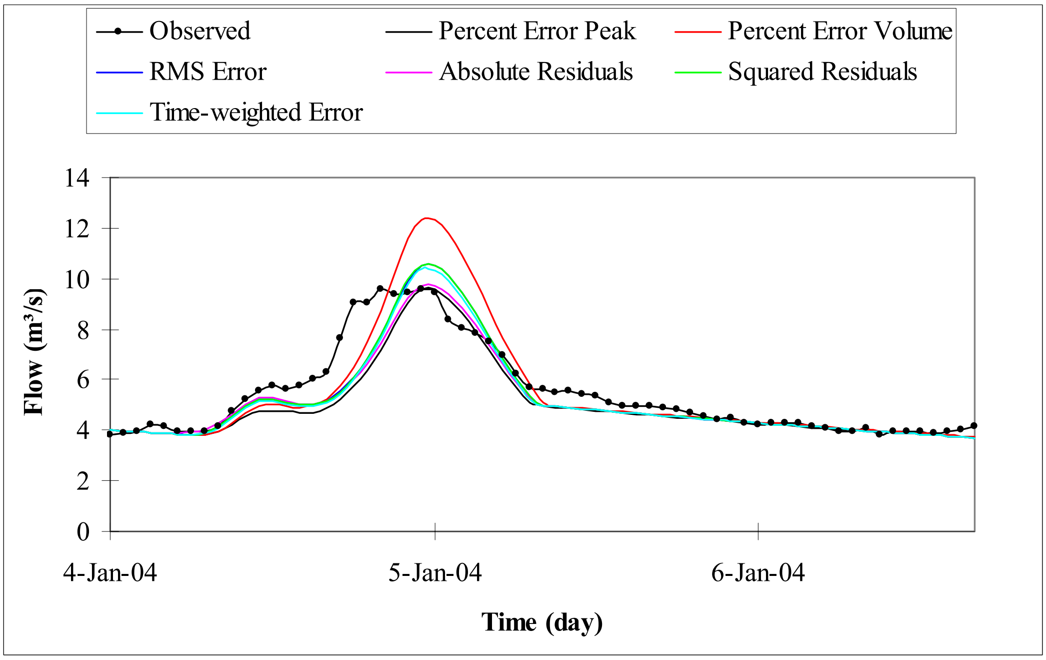

Figure A.6. Event 24 optimization graphs for Serindere

APPENDIX B. OBSERVED AND OPTIMIZED HYDROGRAPHS FOR HOURLY SIMULATIONS

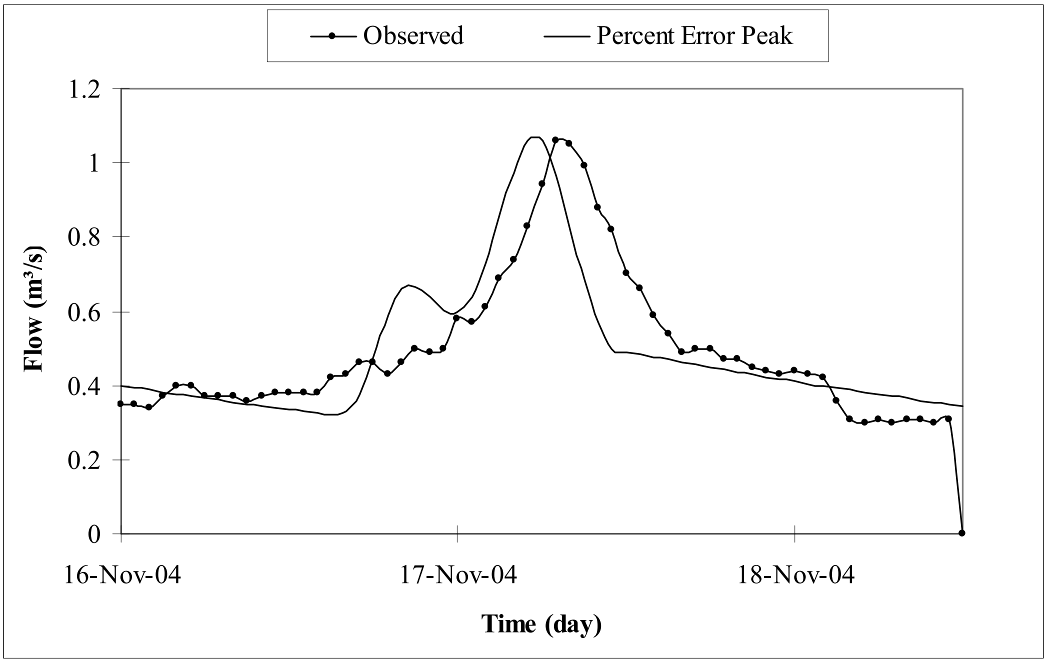

Figure B.1. Kirazdere Subbasin Event 40 Flow Hydrographs

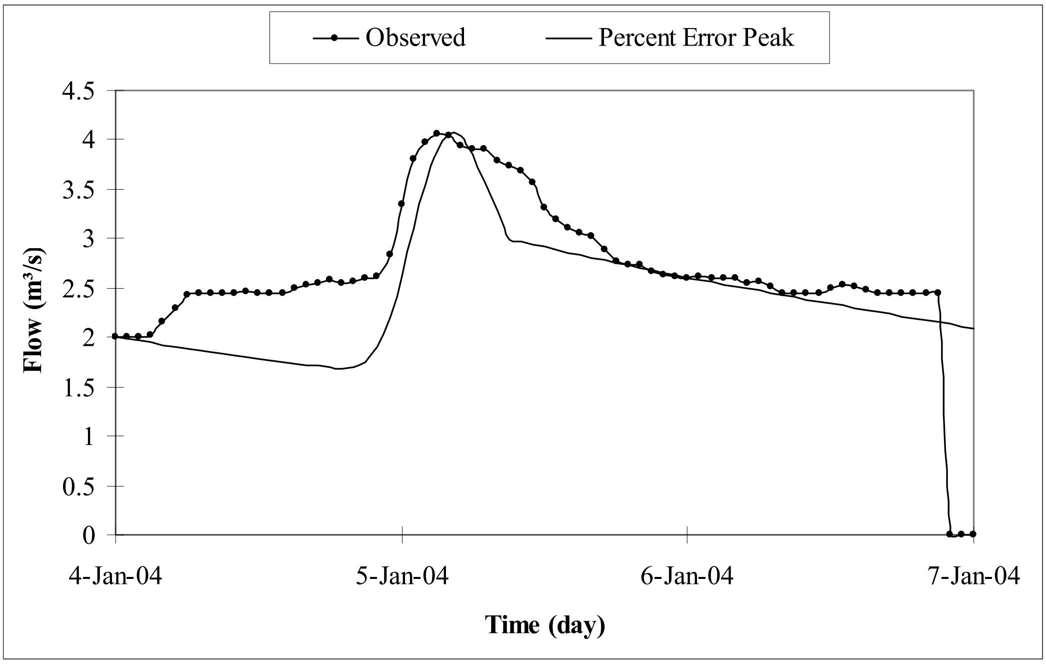

Figure B.2. Kirazdere Subbasin Event 24 Flow Hydrographs

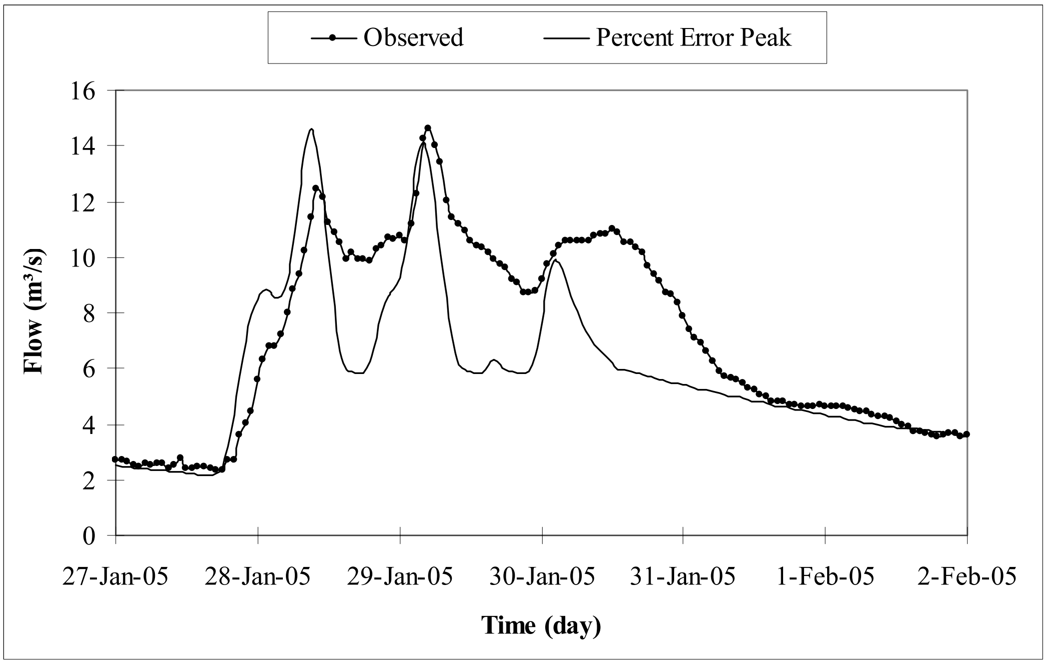

Figure B.3. Kirazdere Subbasin Event 33 Flow Hydrographs

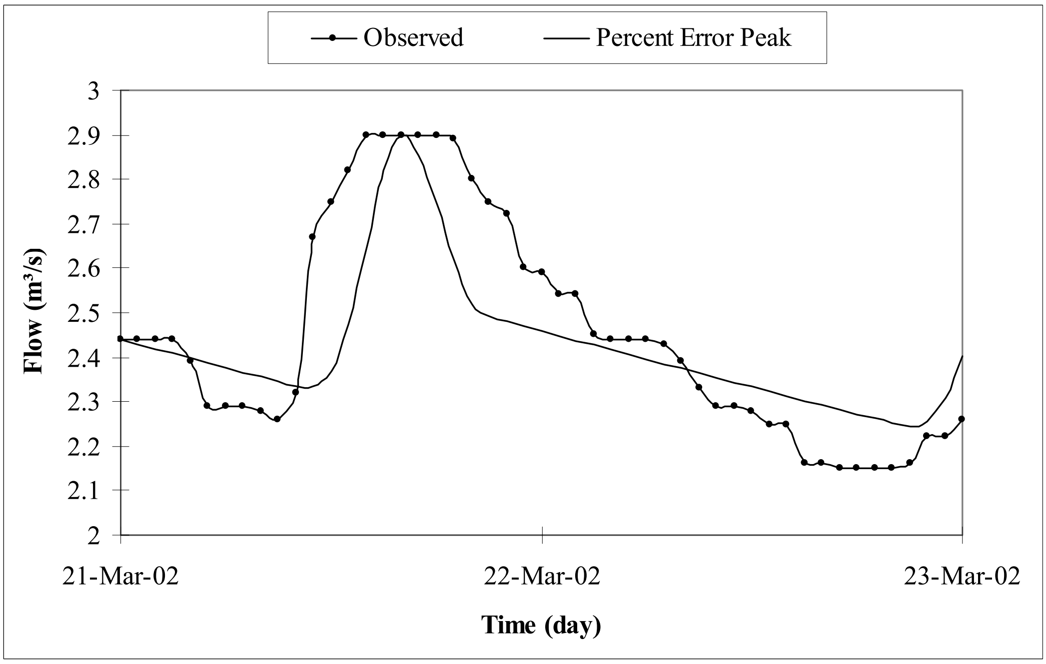

Figure B.4. Kirazdere Subbasin Event 5 Flow Hydrographs

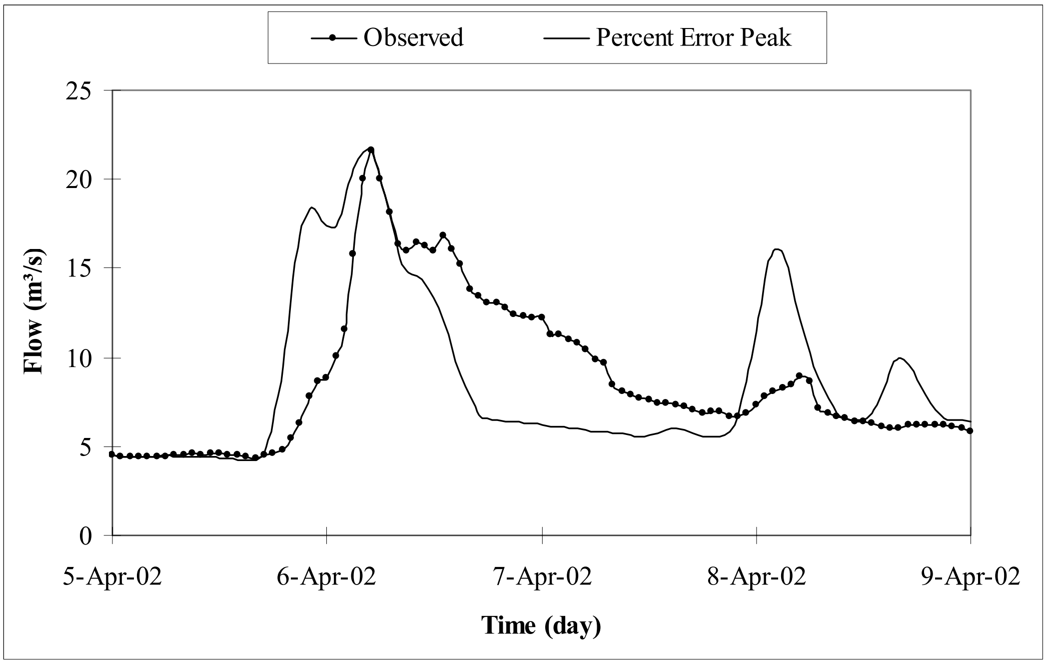

Figure B.5. Kirazdere Subbasin Event 7 Flow Hydrographs

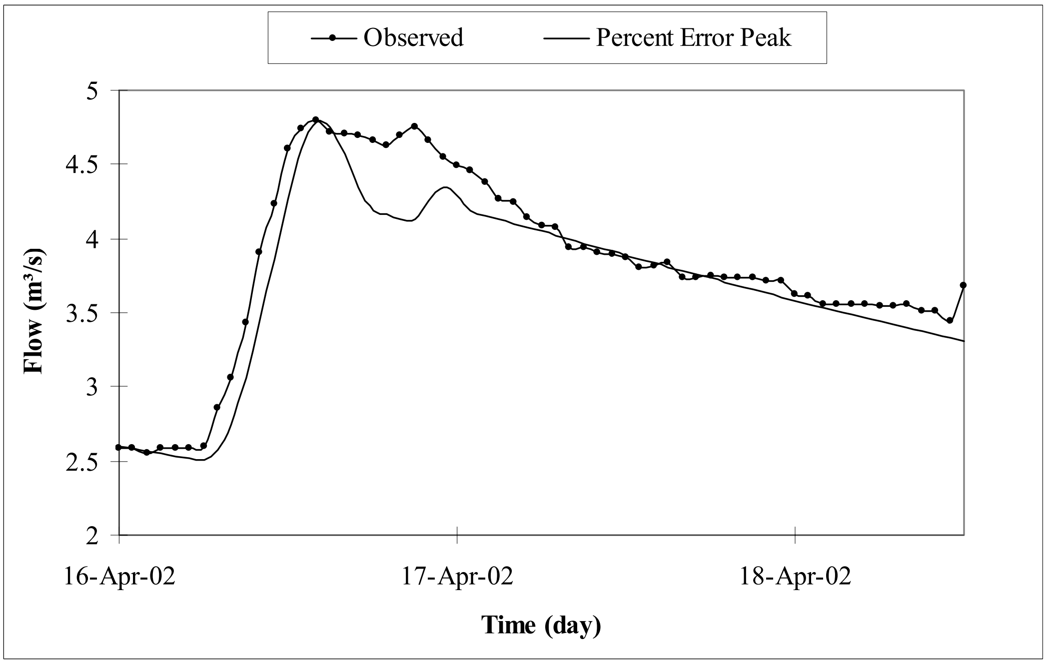

Figure B.6. Kirazdere Subbasin Event 8 Flow Hydrographs

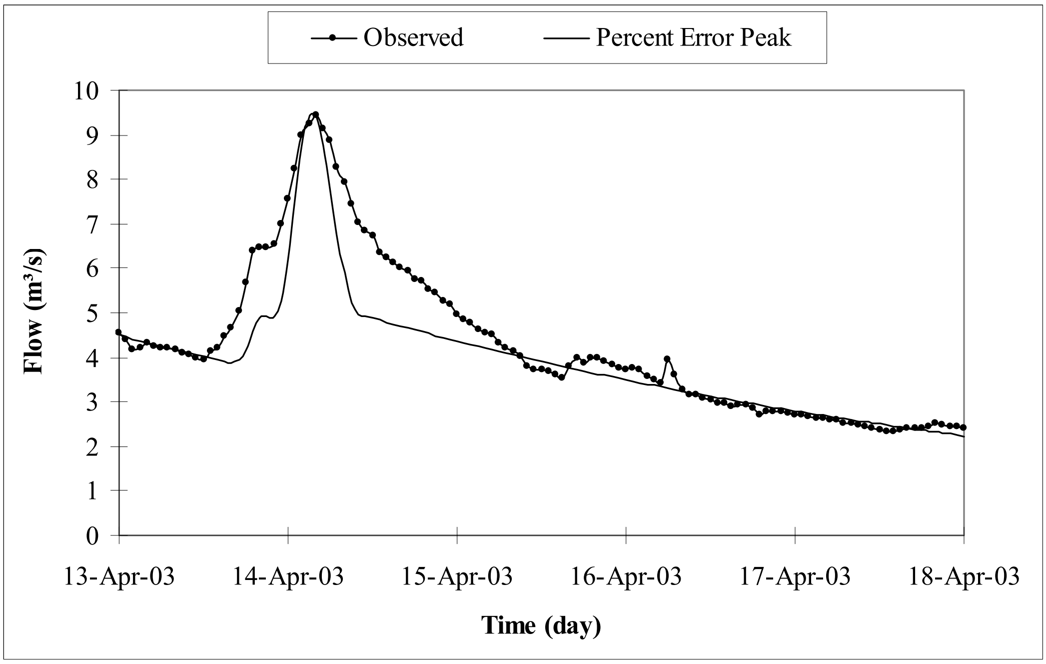

Figure B.7. Kirazdere Subbasin Event 16 Flow Hydrographs

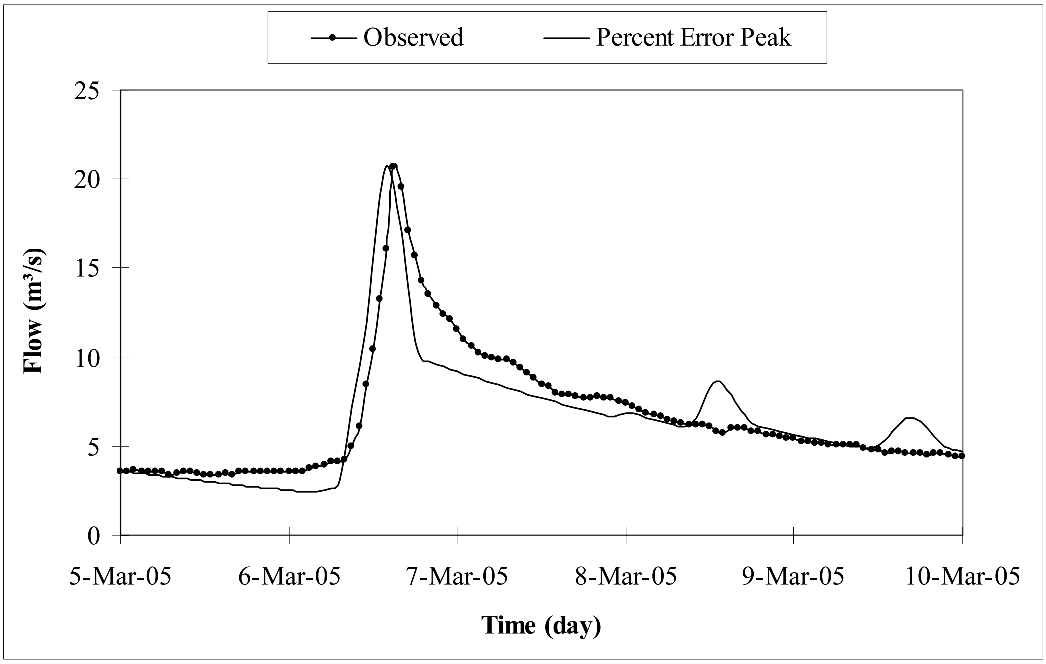

Figure B.8. Kirazdere Subbasin Event 41 Flow Hydrographs

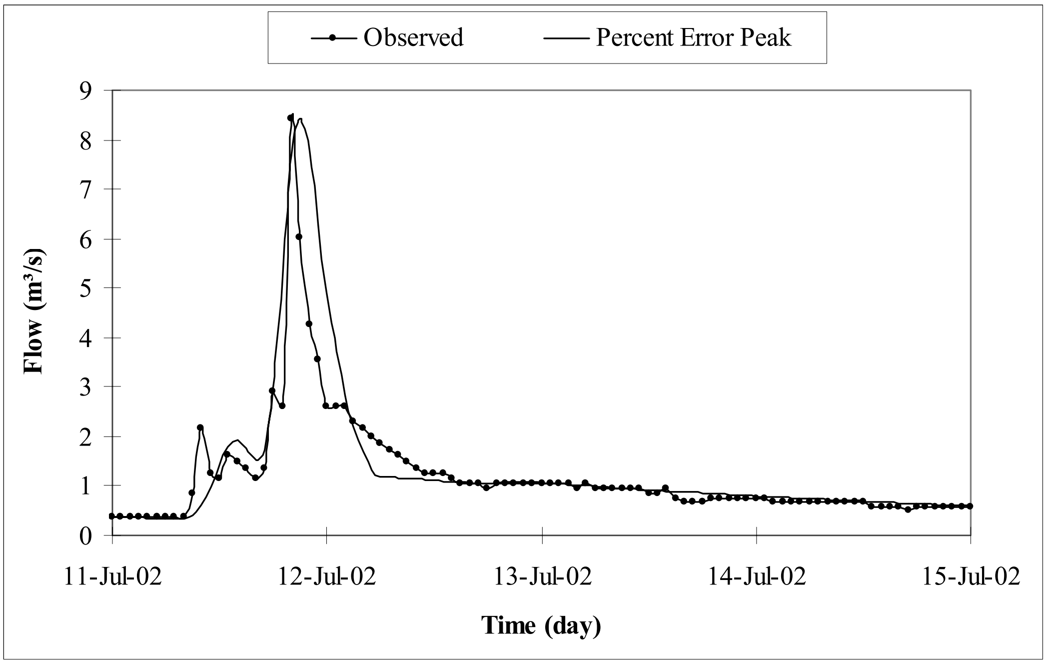

Figure B.9. Kirazdere Subbasin Event 10 Flow Hydrographs

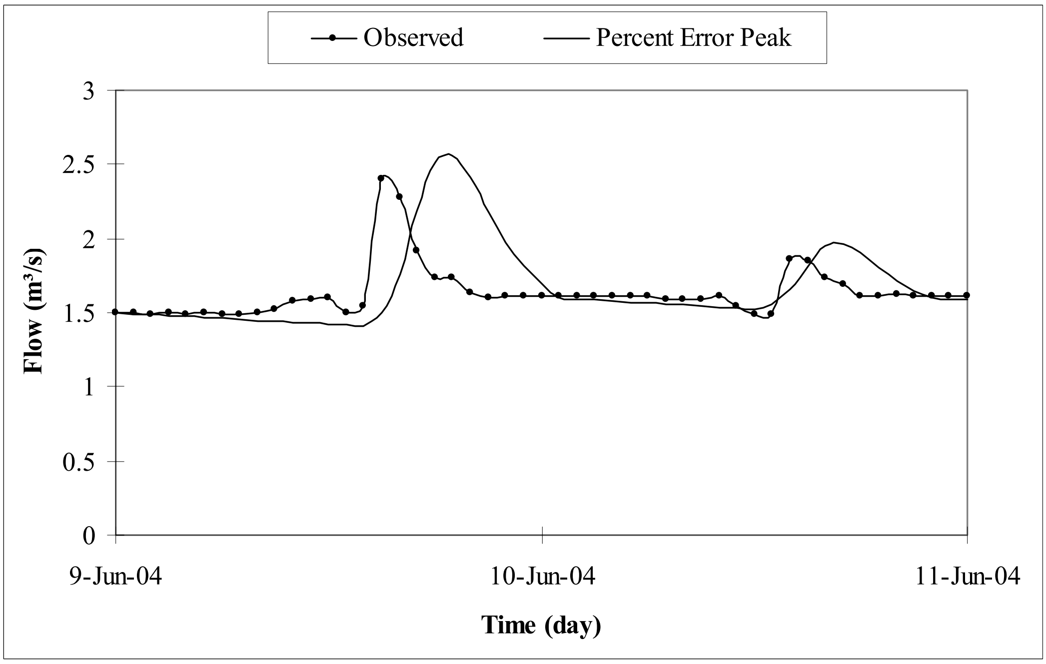

Figure B.10. Kirazdere Subbasin Event 31 Flow Hydrographs

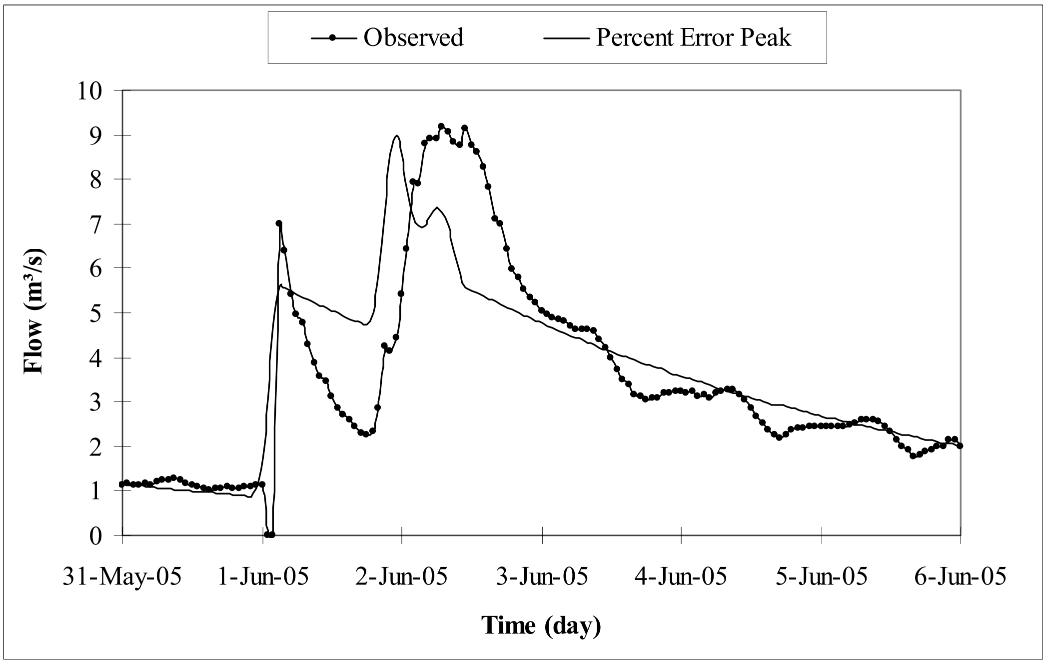

Figure B.11. Kirazdere Subbasin Event 36 Flow Hydrographs

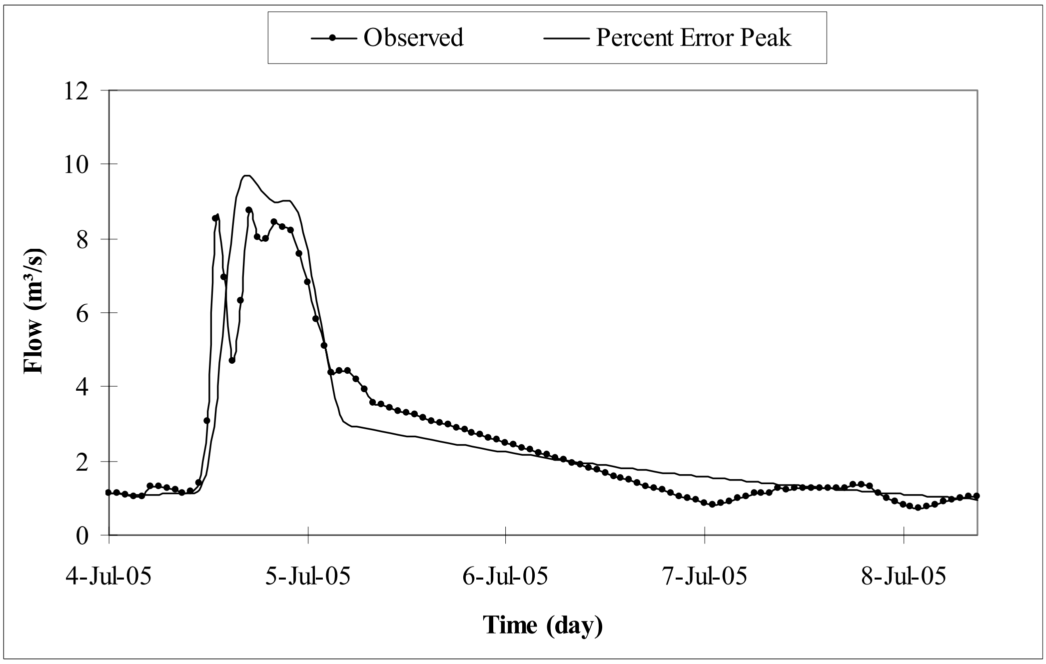

Figure B.12. Kirazdere Subbasin Event 37 Flow Hydrographs

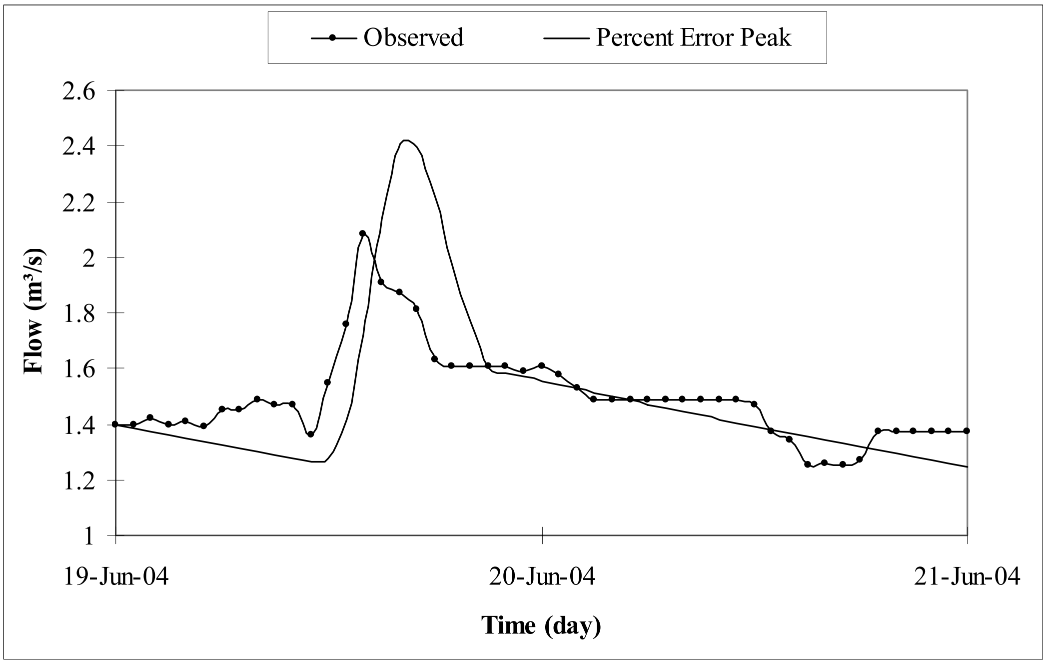

Figure B.13. Kirazdere Subbasin Event 38 Flow Hydrographs

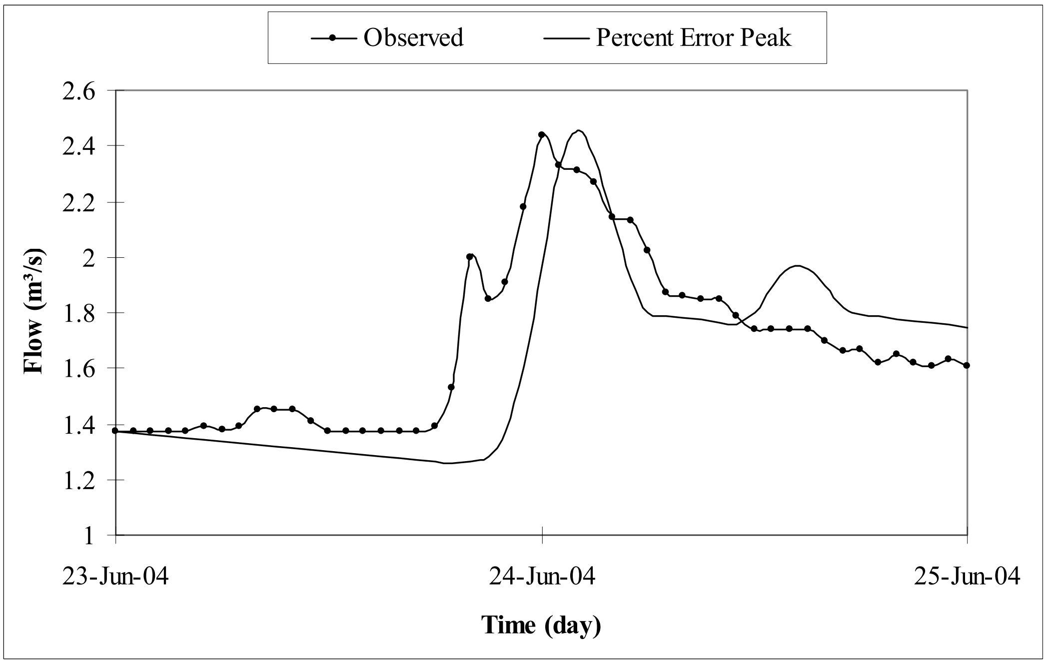

Figure B.14. Kirazdere Subbasin Event 39 Flow Hydrographs

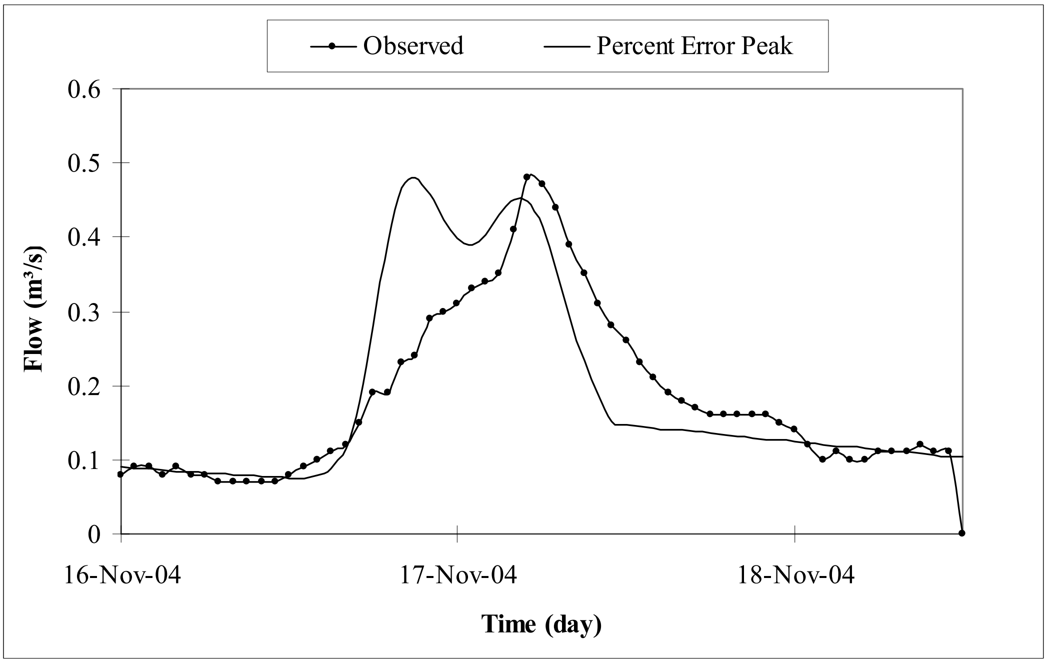

Figure B.15. Kazandere Subbasin Event 40 Flow Hydrographs

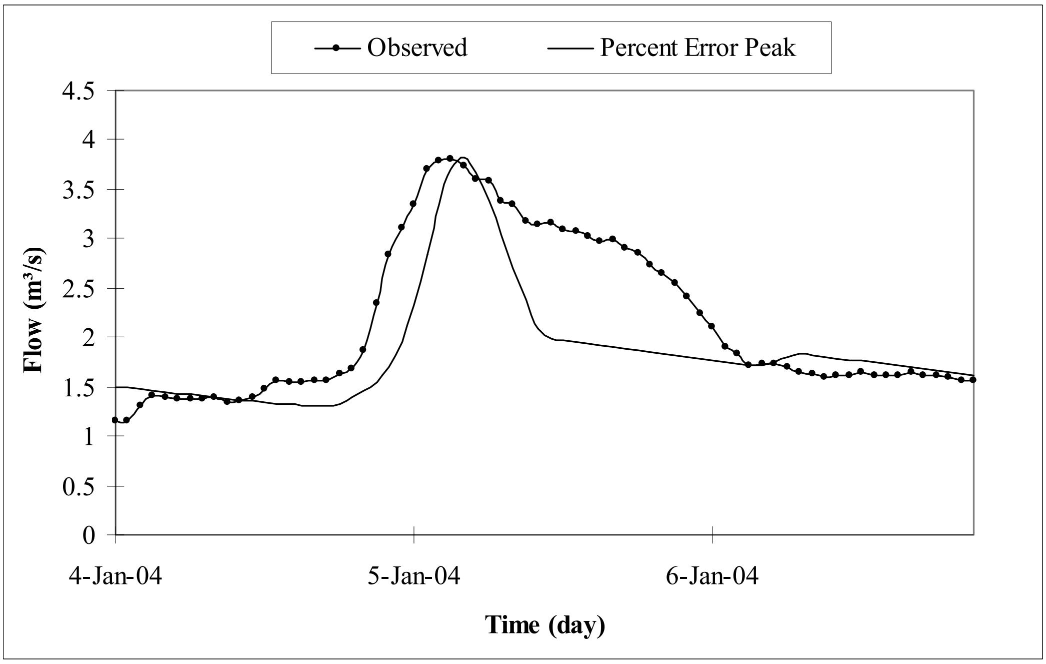

Figure B.16. Kazandere Subbasin Event 24 Flow Hydrographs

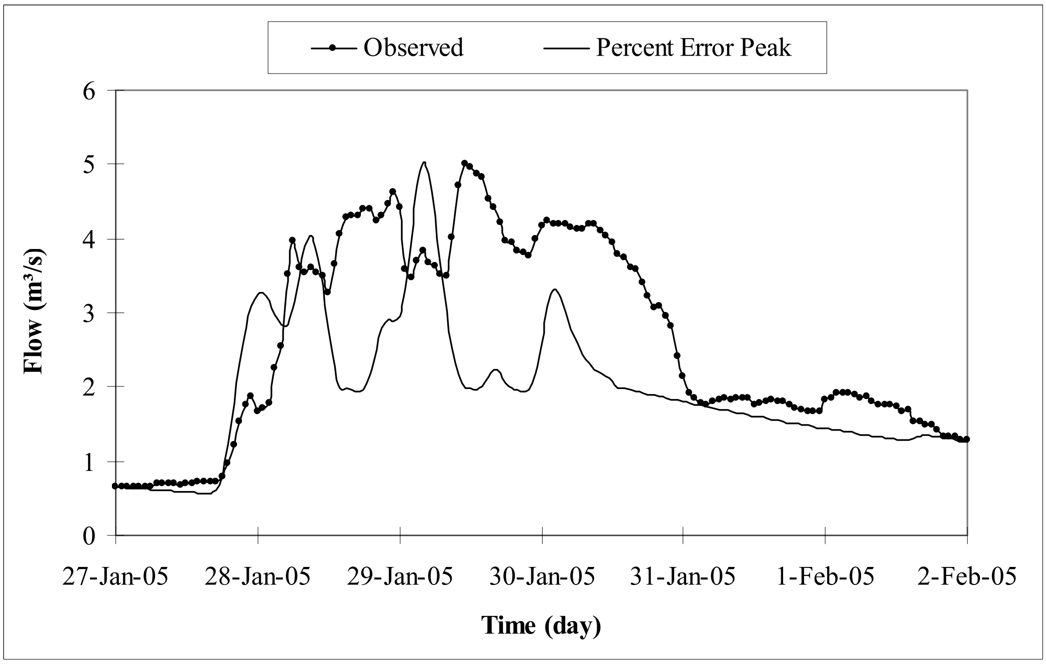

Figure B.17. Kazandere Subbasin Event 33 Flow Hydrographs

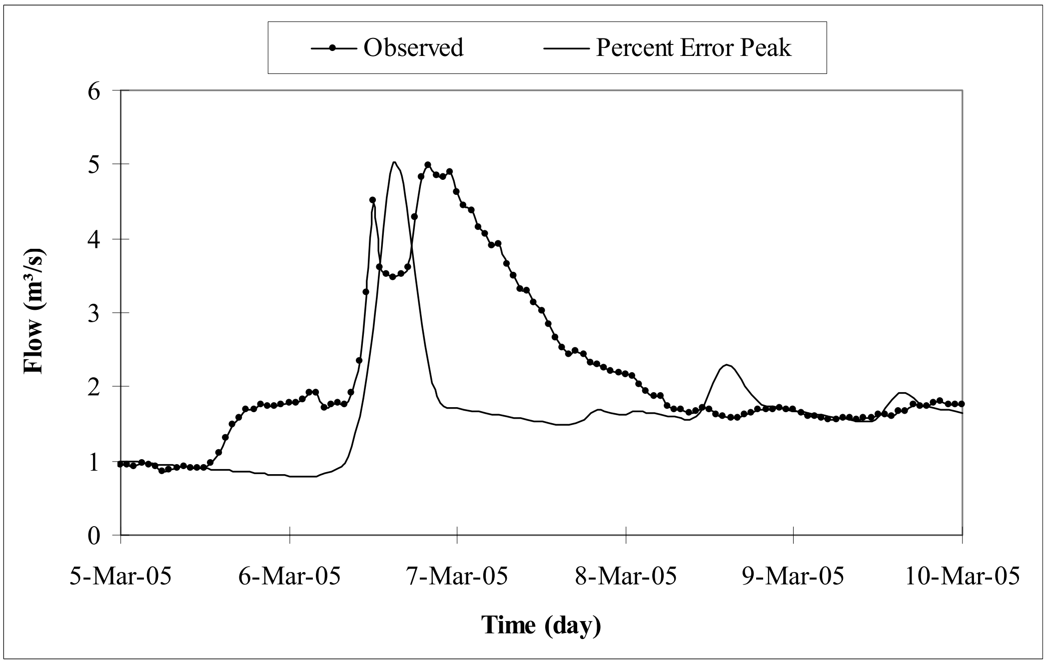

Figure B.18. Kazandere Subbasin Event 41 Flow Hydrographs

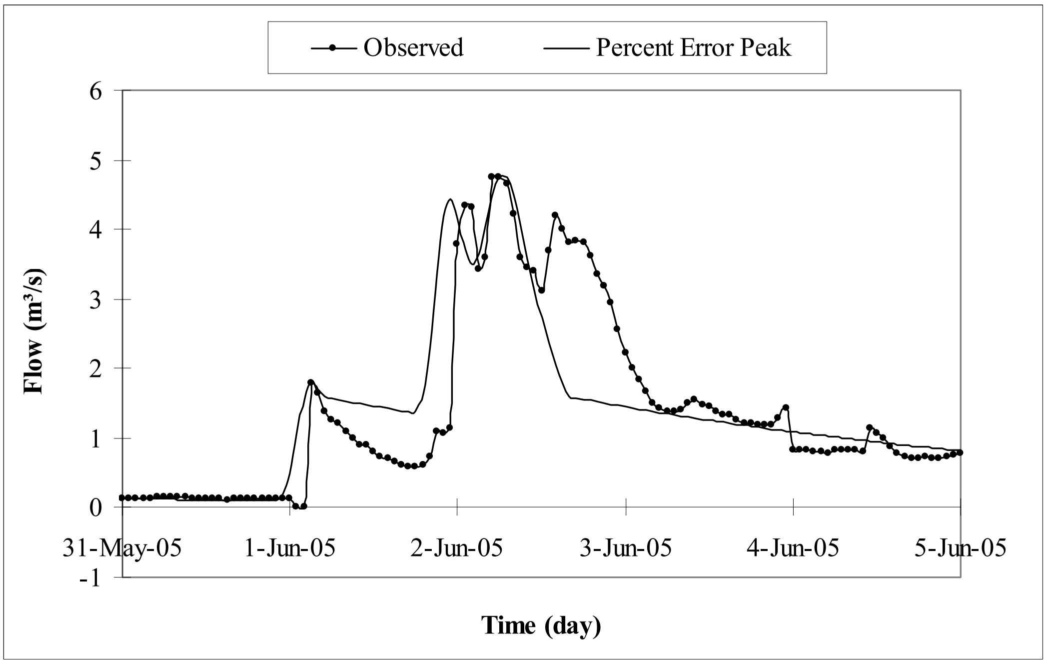

Figure B.19. Kazandere Subbasin Event 36 Flow Hydrographs

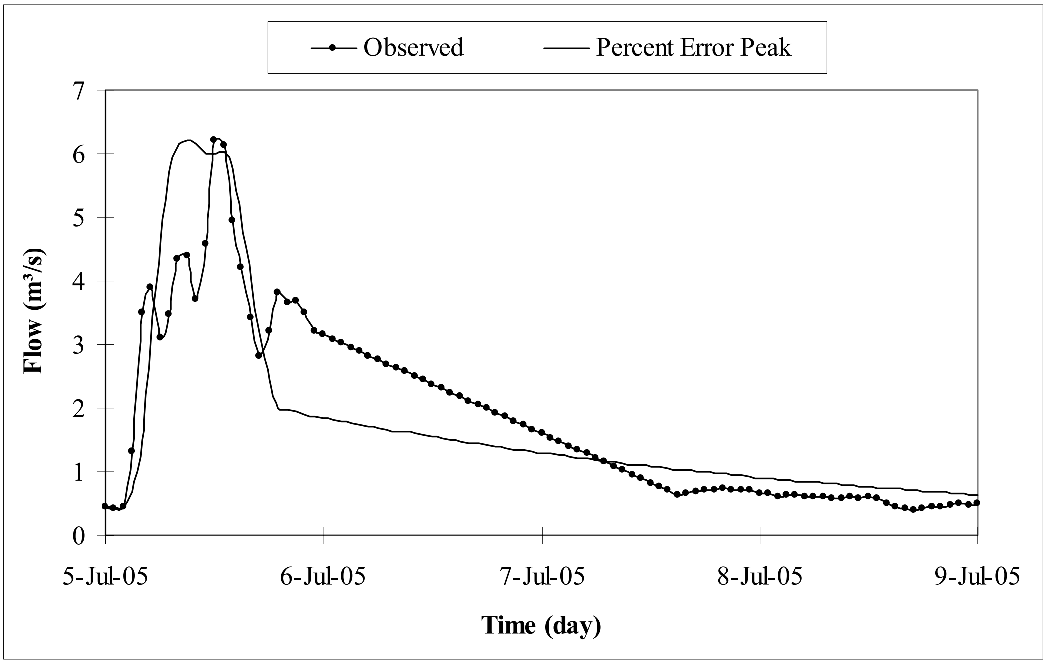

Figure B.20. Kazandere Subbasin Event 37 Flow Hydrographs

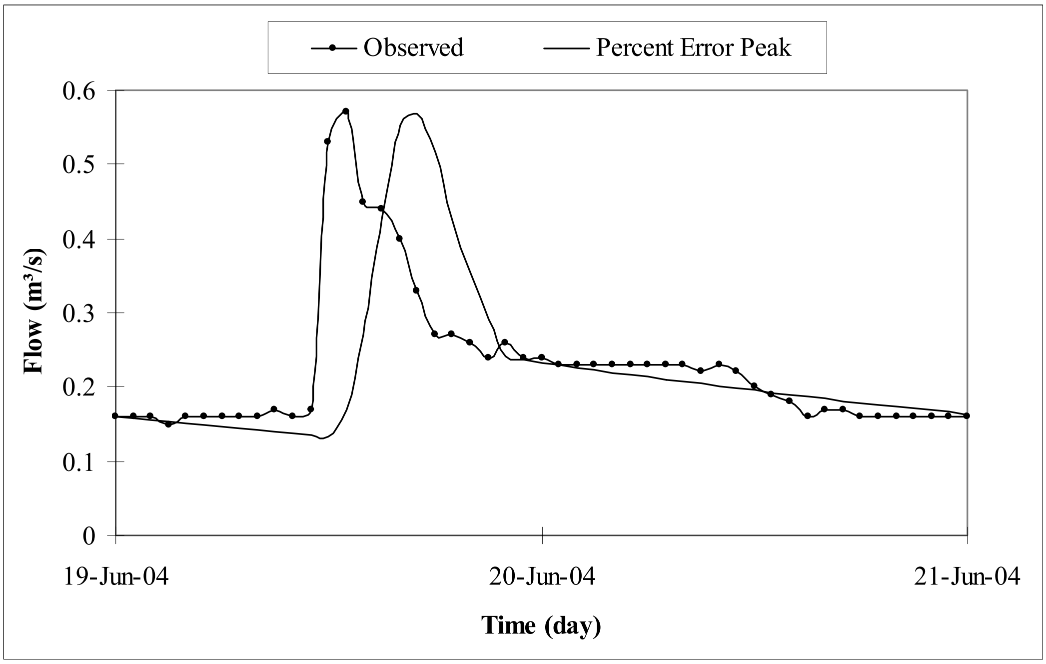

Figure B.21. Kazandere Subbasin Event 38 Flow Hydrographs

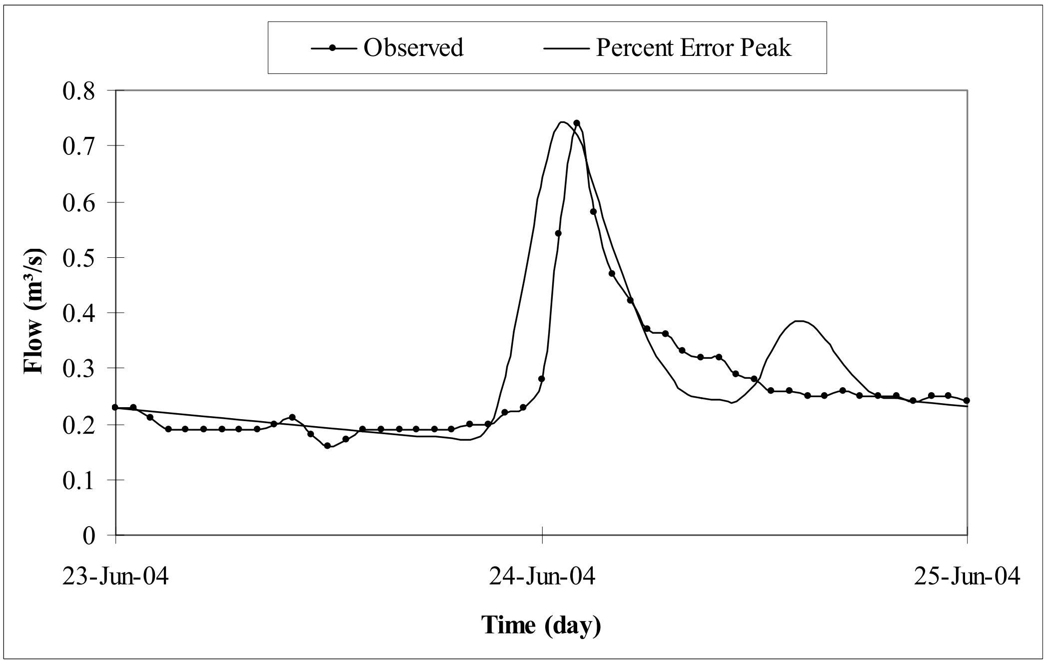

Figure B.22. Kazandere Subbasin Event 39 Flow Hydrographs

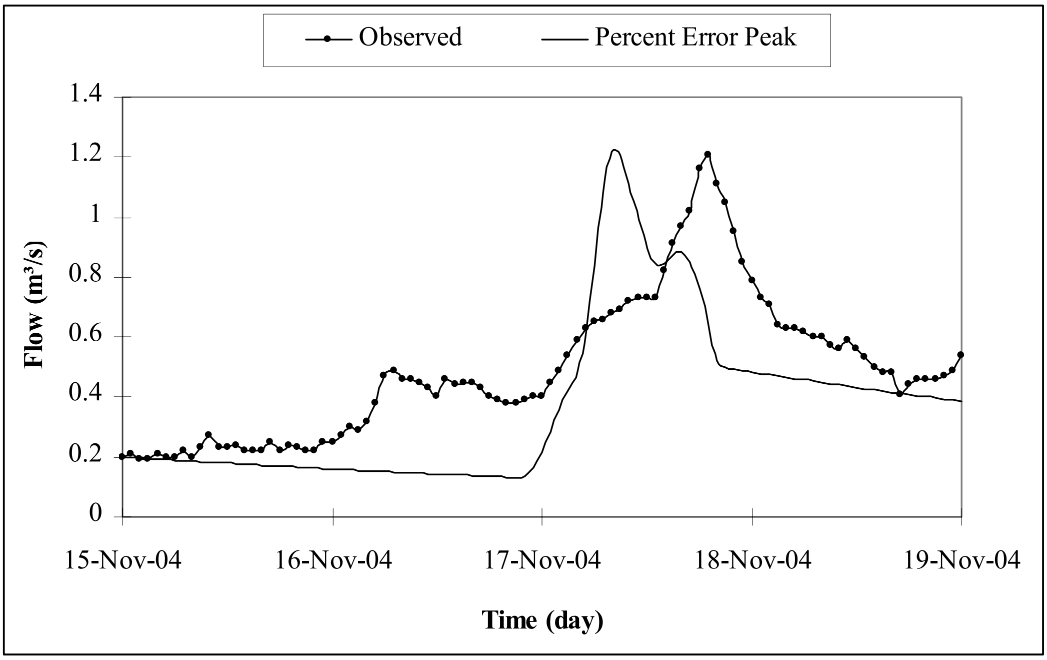

Figure B.23. Serindere Subbasin Event 40 Flow Hydrographs

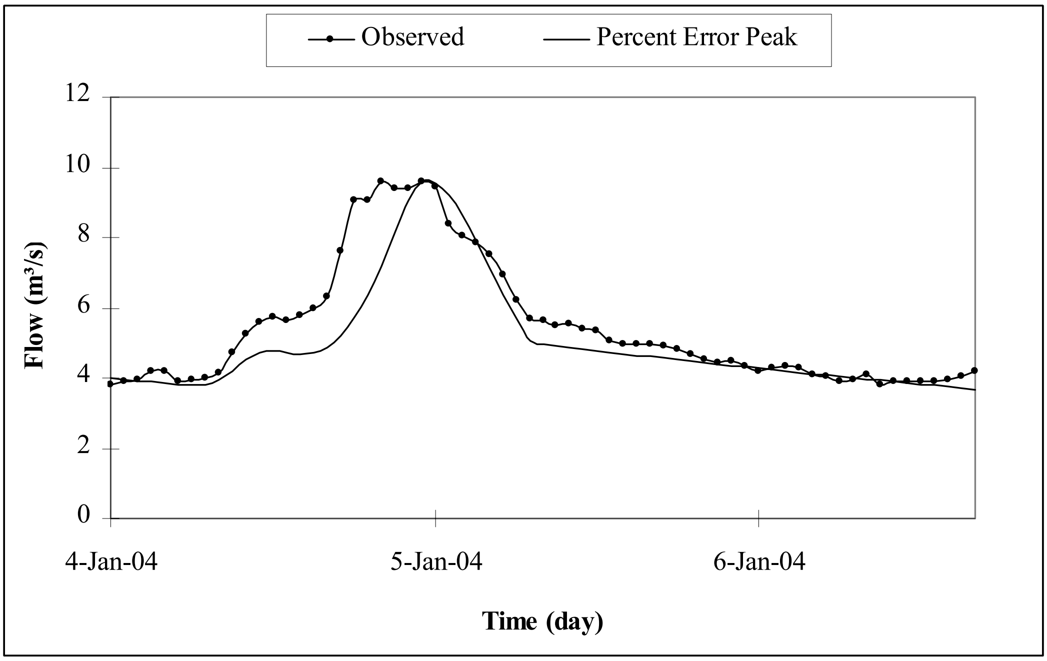

Figure B.24. Serindere Subbasin Event 24 Flow Hydrographs

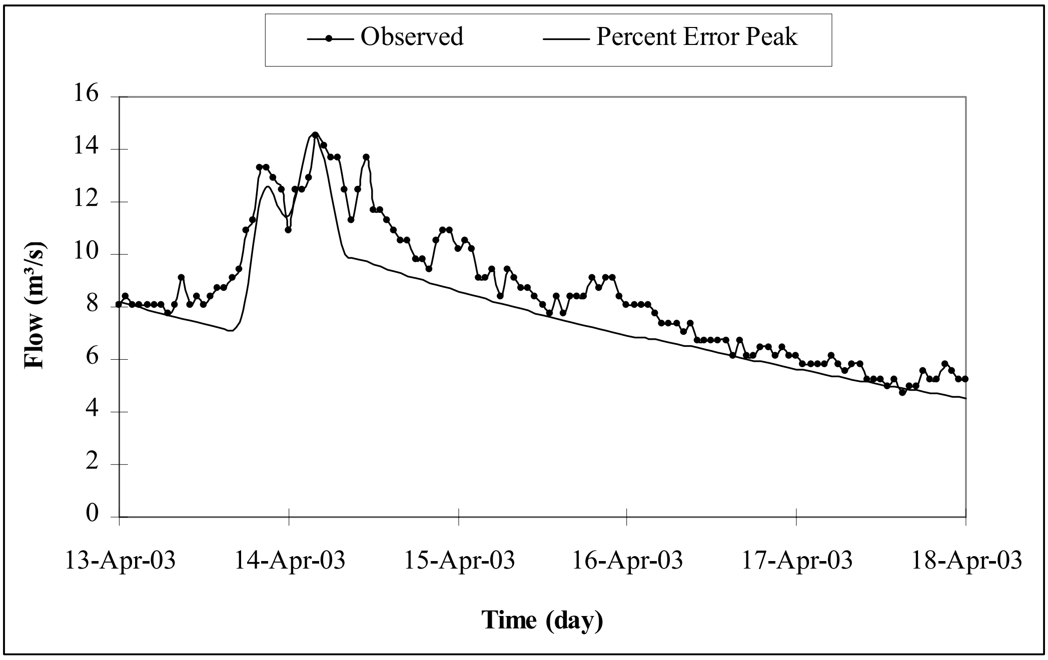

Figure B.25. Serindere Subbasin Event 16 Flow Hydrographs

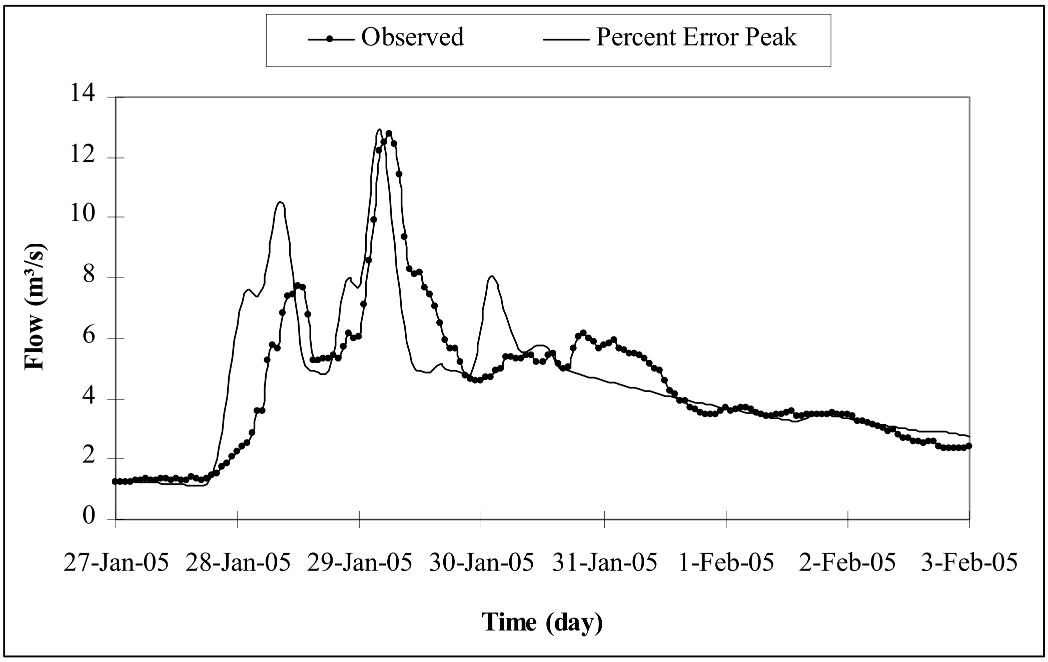

Figure B.26. Serindere Subbasin Event 33 Flow Hydrographs

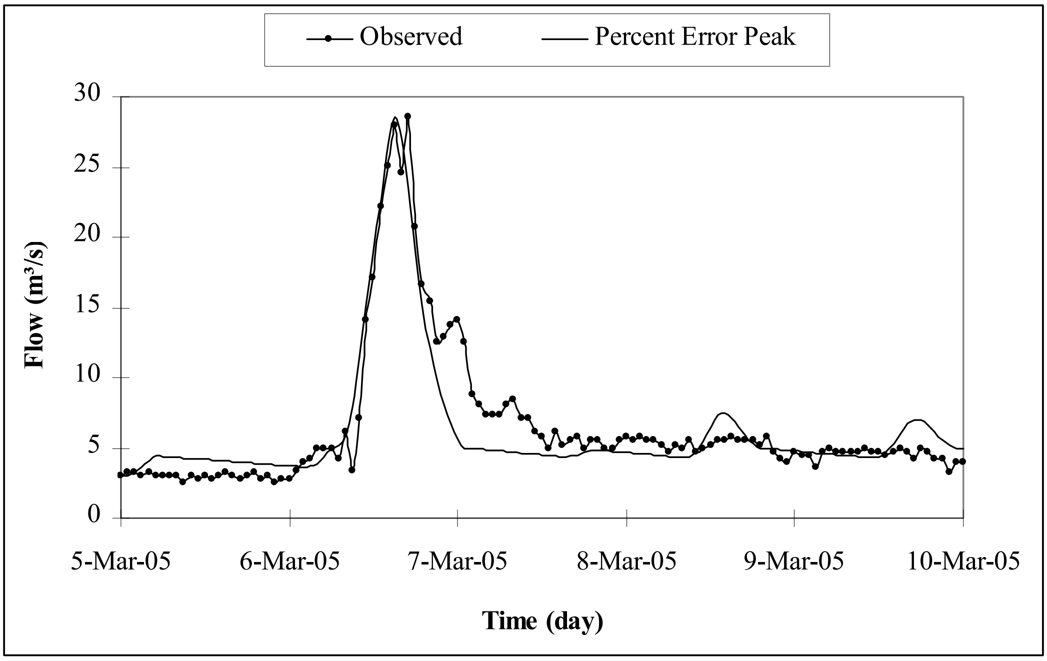

Figure B.27. Serindere Subbasin Event 41 Flow Hydrographs

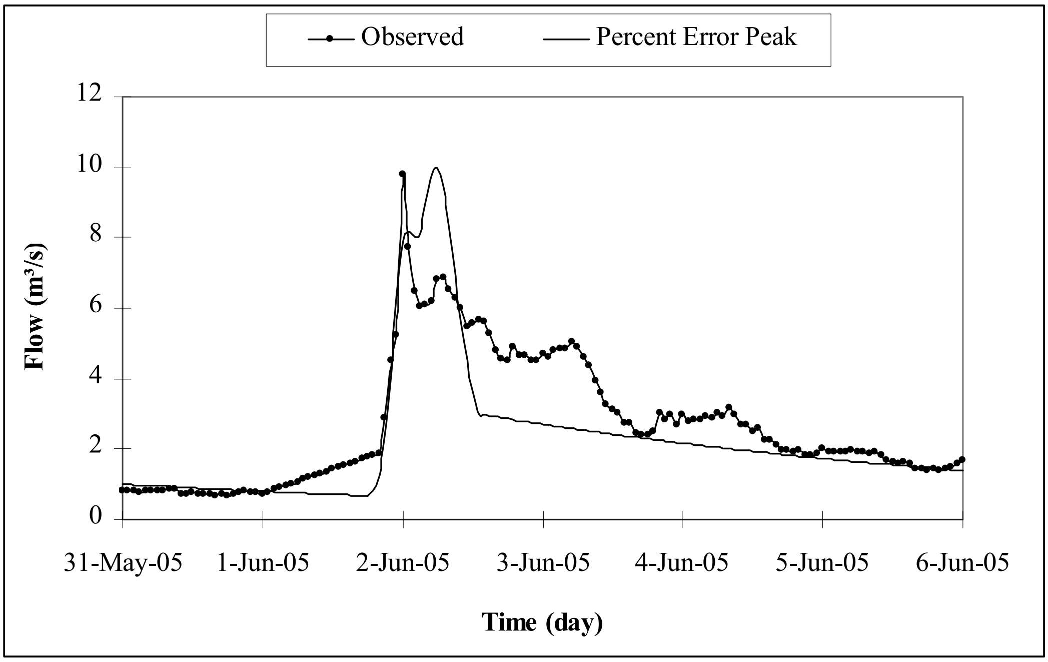

Figure B.28. Serindere Subbasin Event 36 Flow Hydrographs

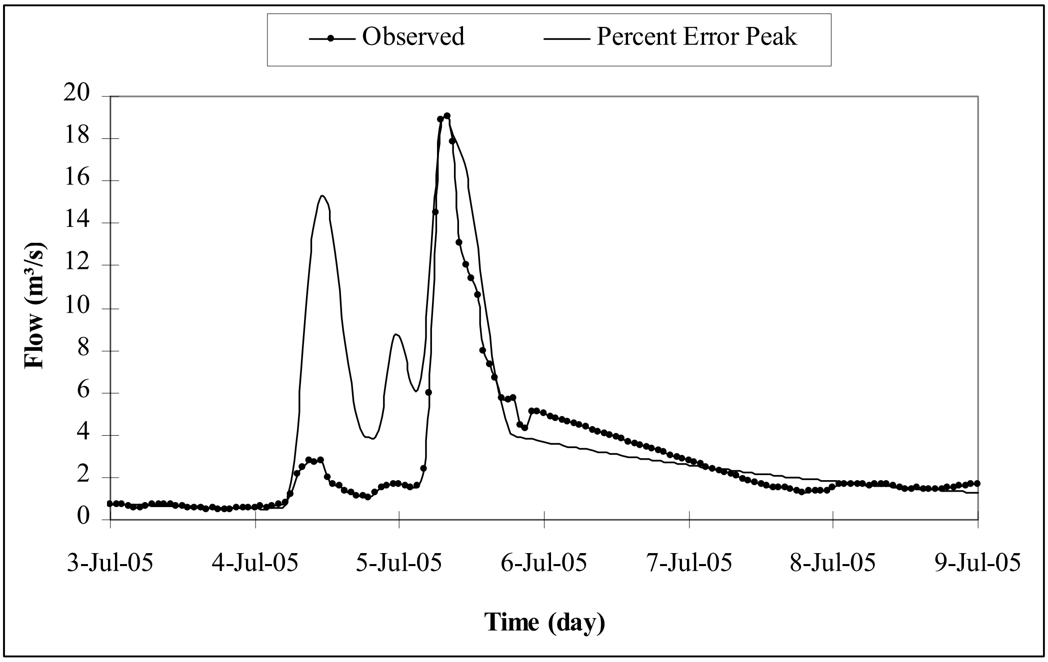

Figure B.29. Serindere Subbasin Event 37 Flow Hydrographs

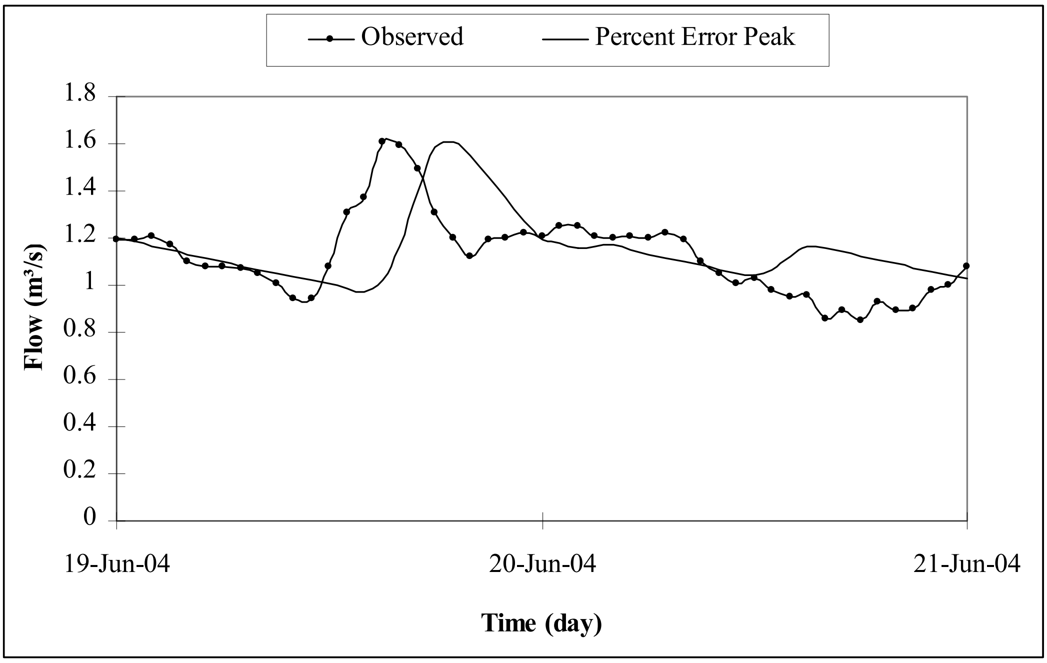

Figure B.30. Serindere Subbasin Event 38 Flow Hydrographs

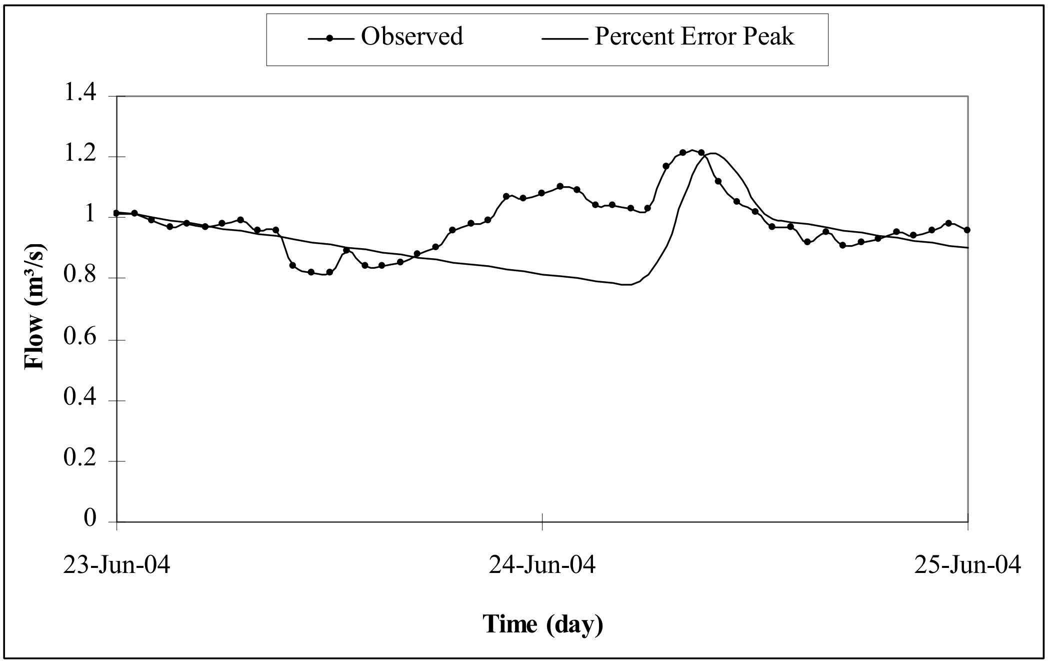

Figure B.31. Serindere Subbasin Event 39 Flow Hydrographs

APPENDIX C. OBSERVED AND FORECASTED HYDROGRAPHS FOR THE YEAR 2006

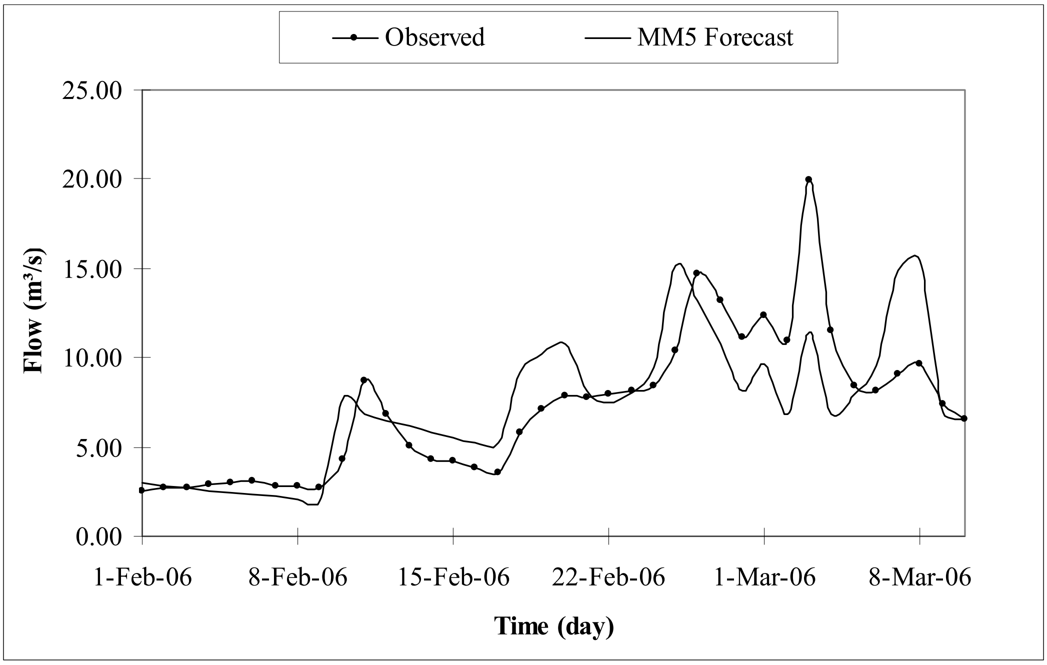

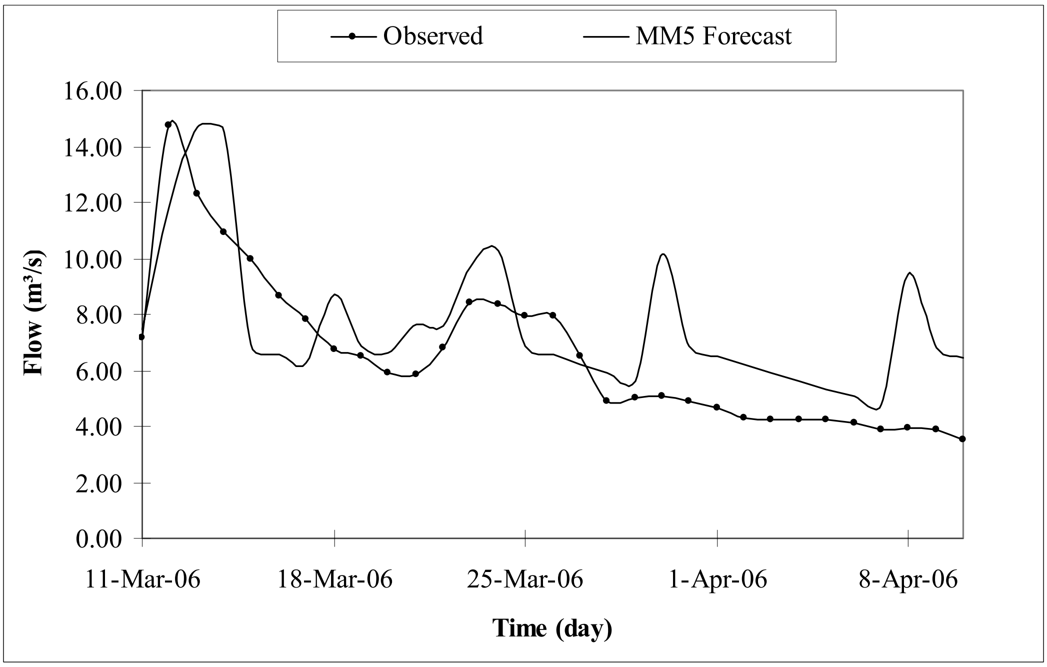

Figure C.1. Kirazdere subbasin observed and simulated hydrographs when MM5 grid data is used in the model

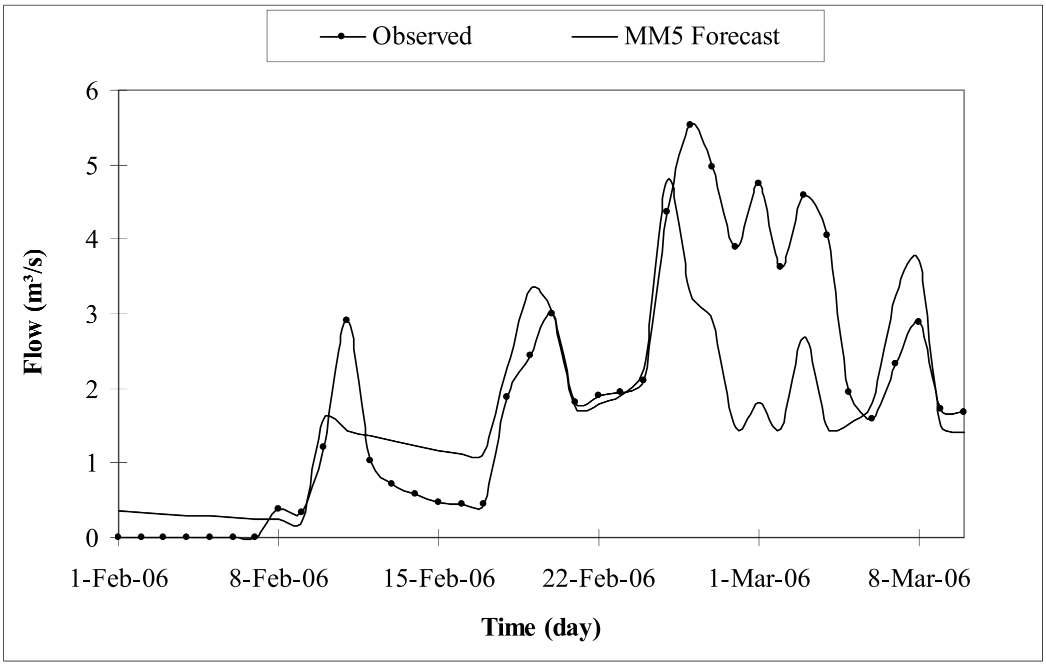

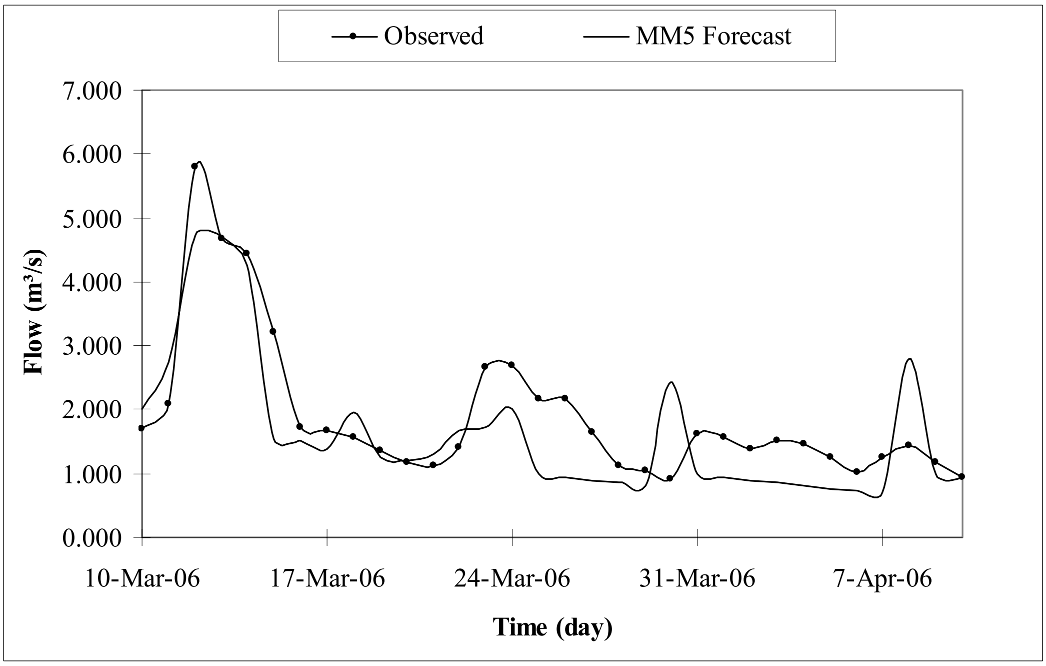

Figure C.2. Kazandere subbasin observed and simulated hydrographs when MM5 grid data is used in the model

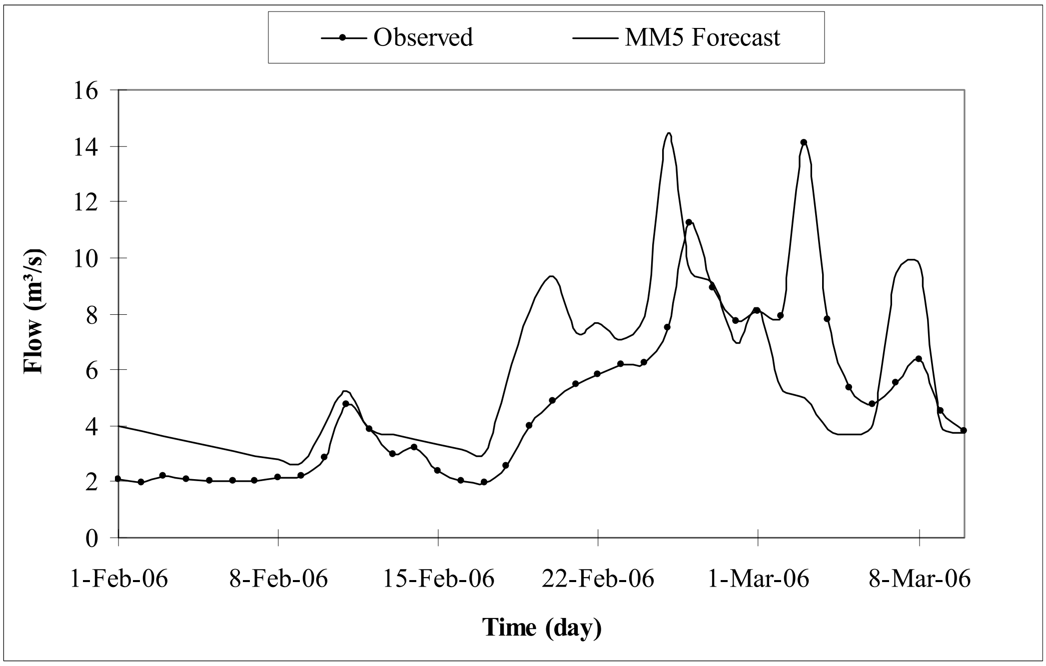

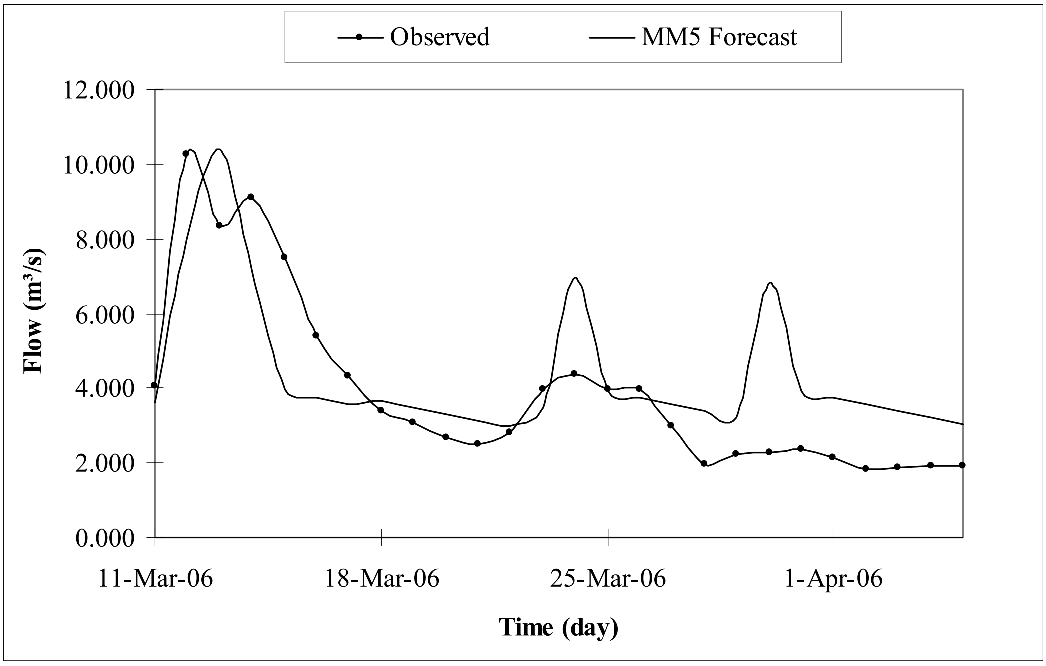

Figure C.3. Serindere subbasin observed and simulated hydrographs when MM5 grid data is used in the model